Plant hormones associated with increasing grain number and yield potential in wheat (*Triticum aestivum* L.) and their genetic regulation

Bethany Love

School of Biosciences

Sutton Bonington Campus, University of Nottingham

Thesis submitted to the University of Nottingham for the degree of

Doctor of Philosophy

September 2021

Abstract

Plant hormones are organic substances that influence specific physiological processes, such as floret fertility, and move throughout the plant. Previous studies suggest that genetic variation in grain number in cereals is associated with hormones such as cytokinin, which is crucial in controlling cell division and lateral meristem activity. This has been demonstrated in cereals when QTLs linked with reduced expression of cytokinin oxidase/dehydrogenase (*OsCKX2*) increased grain number in rice and wheat. However, how hormones regulate grain number traits such as fruiting efficiency (FE, ratio of grain number to spike dry weight at anthesis) and grain dry matter partitioning in wheat is not fully understood. The objectives of this study were, using a high biomass spring wheat panel, to identify novel grain number and partitioning traits for advancing harvest index and grain yield, and to determine how they are influenced by spike hormones. Finally, to understand the genetic regulation of these traits, using a bespoke target sequence capture strategy, to generate SNPs and establish molecular markers for the hormonal traits. A high biomass association panel (HiBAP II) of 150 CIMMYT spring wheat genotypes was phenotyped for grain number and partitioning traits in the field under irrigated conditions and spike hormone levels were sampled at anthesis in two seasons in NW Mexico. A subset of 10 genotypes representative of field variation for FE was grown in the glasshouse under well-watered conditions at the University of Nottingham, UK in three years for detailed hormonal analysis at GS49 (late booting) and 65 (anthesis). To test if certain plant components and stem internodes were competing with the spike at GS49 and GS65, destructive samples were taken where the plants were separated into their constitutive parts.

Results showed genetic variation in grain yield correlated with grain number in both the glasshouse and field experiments, and grain yield correlated with harvest index in the field experiments. The increase in grain number amongst genotypes was associated with an increase in FE. The stem internode traits which were competing for most with spike growth was stem internode 2 leaf sheath, suggesting reducing internode 2 leaf sheath length could increase allocation of assimilates to the spike at anthesis. The results also identified novel genetic variation in spike hormones and found associations between higher levels of cytokinins and increases in grain number and yield at both GS49 and GS65 in the glasshouse and field experiments. The genetic variation in spike cytokinins also correlated across the glasshouse and field experiments. Twenty-six traits were analysed in a genome-wide association study and 213 putative marker-trait associations were identified, while 53

candidate genes were suggested including one candidate gene on chromosome 1B for spike cytokinins zeatin riboside and isopentenyladenosine at anthesis, which, in *Arabidopsis*, codes for an auxin efflux carrier protein *PIN3* that is regulated by cytokinins. The next steps include validating the markers through developing KASP markers to be deployed in wider germplasm and using the genetic information from this study to improve traits in plant breeding programmes.

Acknowledgements

I would like to thank:

Dr John Foulkes for the supervision, wisdom and guidance over the past four years, and for being responsible for motivating me to finish this thesis. Also the CIMMYT wheat physiology team, and in particular Dr Matthew Reynolds and Dr Gemma Molero for sharing your knowledge and support while in Mexico. Also to Drs Carolina Rivera-Amado and Francisco Pinera-Chavez and the whole team in Obregon for assisting me in data collection in the field.

The International Wheat Yield Partnership (IWYP) for funding my PhD, in particular, the extra funding Dr Matthew Reynolds, Dr Gemma Molero and Dr John Foulkes helped to secure for the field hormonal analysis which was critical to this thesis.

Alison, if it wasn't for you first inspiring me with crop research I would never have started this journey, thank you for being my biggest support from day one and ever since, you still inspire me every day.

My fellow PhD students in Nottingham – James, Jas, Laura, Carlos, and everyone else for being on this crazy ride with me over the past four years, and to everyone yet to submit I'm always available for a cup of tea or something stronger.

Javier, Karla and Jaqui for making Mexico feel like home and Lorna, Alejandro and Amy for bringing home to Mexico.

Flat A.03, my Nottingham family, Juan, Alanna, Davide and Antonia, I'm so lucky to have randomly ended up with some of the best people I've ever met.

YAS family, Josh, Justin, Richard and Grace for always being there for me at the end of a phone and for truly understanding my excitement for plant research.

Alex for the bioinformatics, emotional support and houseplants in equal measures, I wasn't expecting you but we found each other at a time when we both needed it.

Katy, it's hard to put into words how much your friendship means to me, you've been so important to me throughout the past eight years and I know you will always have that space in my heart. Look how far we've come already.

My family for looking after me over this past year and pushing me to be the best I can be. In particular thank you to my parents, mum I'm in good company being the second Dr Love.

Table of Contents

Table of Figures

Table of Tables

Abbreviations

2iP	Isopentenyladenine, a cytokinin
6-BA	6-Benzylaminopurine, a synthetic cytokinin
A+7	Anthesis + 7 days
ABA	Abscisic acid
AGDM	Above-ground dry matter
ANOVA	Analysis of variance
BLUE	Best-linear unbiased estimates
bp	Base pairs
Chr	Chromosome
CIMMYT	International maize and wheat improvement center
CK	Cytokinin
CKX	Cytokinin oxidase/dehydrogenase, degrades cytokinins
cv.	Cultivar
DH	Doubled haploid
DM	Dry matter
DTA	Number of days to anthesis
DTM	Number of days to physiological maturity
Ent	Entry, genotype number
FE	Fruiting efficiency
FE_A/ FE_{A+7}	Fruiting efficiency calculated using the spike DM at GS65/ GS65+7d
FE_{chaff}	Fruiting efficiency calculated using the chaff DM at maturity
FL	Flag leaf
FW	Fresh weight
GA	Gibberellin
GAox	Gibberellin oxidase, a gibberellin enzyme
GEBV	Genomic estimated breeding value
GN	Grain number per m^2
GN_{MS}	Grain number per main shoot
GN_P	Grain number per plant
GS	Growth stage
GS49	Late booting (Zadoks GS)
GS65	Anthesis (Zadoks GS)
GS65+7d	7 days past anthesis (Zadoks GS)
GS89	Physiological maturity (Zadoks GS)
GWAS	Genome-wide association study
GY	Grain yield
GY_{MS}	Grain yield per MS
GY_P	Grain yield per plant
H^2	Broad-sense heritability

HI	Harvest index
HI_{MS}	Harvest index per MS
HI_{P}	Harvest index per plant
HiBAP II	High Biomass Association Panel II
IAA	Indole-3-acetic acid, an auxin
Int2	Internode 2, second stem internode
Int3	Internode 3, third stem internode
Int4+	Stem internode 4 and below
IPA	Isopentenyladenosine, a cytokinin
IPT	Isopentenyltransferase, cytokinin biosynthesis enzyme
JA	Jasmonic acid
L	Length
LS	Leaf sheath
LSD	Least significant differences
maf	Minor-allele frequency
MAS	Marker-assisted selection
MS	Main shoot
NIL	Near-isogenic line
NW	Northwest
PCA	Principal component analysis
Ped	Peduncle, first stem internode
PI	Partitioning index
PIN3	PIN-FORMED 3, auxin transport protein
PM	Physiological maturity
QTL	Quantitative trait loci
RUE	Radiation-use efficiency
SA	Salicylic acid
SHW	Synthetic hexaploid wheat
SM2	Spike number per m^2
SNP	Single nucleotide polymorphism
SPI	Spike partitioning index
SW	Specific weight
TGW	Thousand-grain weight
TGW_{MS}	Thousand-grain weight per MS
TGW_{P}	Thousand-grain weight per plant
TS	True stem
UPLC/ESI-MS/MS	Liquid chromatography coupled to electrospray ionization tandem spectrometry
Y1	2017-18
Y2	2018-19
Z	Zeatin, a cytokinin
Zr	Zeatin riboside, a cytokinin

Chapter 1: Introduction

1.1 Global wheat production

It has been predicted that agricultural crop production needs to double by 2050 to feed the growing population (FAO, 2017). With the restricted availability of agricultural land, 90 % of this growth in crop production must be a result of higher yields and/or increasing cropping density rather than increasing the land area where crops are grown (Bruinsma, 2009; Albajes et al., 2013). Wheat is a rich source of calories and a staple in most regions of the world, which contributes ~20 % of calories and a similar proportion of protein consumed by humans (Braun et al., 2010). As it is grown globally, it is adapted to a broad range of latitudes, temperatures, water availability and nutritional levels (Reynolds et al., 2012). Therefore, it is important to increase yield potential to reach the 1 billion tonnes per annum of wheat grain yield required (Bruinsma, 2009).

Wheat is the third-largest crop in terms of global production, with 771 million tonnes produced every year (FAO, 2019). The average global wheat yield per unit land area has increased linearly over the past 60 years (Figure 1.1a); from 1960 to 1980 this was partly related to an increase in the harvested area (Figure 1.1b). However, since then, the harvested area has reduced while the average yield per ha of wheat has continued to increase (FAOSTAT, 2021). Despite wheat yield increasing linearly at ca. 1 % per annum in recent decades, yields need to grow by 2-3 % each year to meet projected demand (Hawkesford et al., 2013). A study in 305 locations globally over eight seasons from 2006-2015 showed grain yield in 50 CIMMYT cultivars (Elite Spring Wheat Yield Trials, ESWYT) increased by 1.67 % per annum when compared to the check cultivar Attila (Crespo-Herrera et al., 2017), while an earlier study on the same material from 1995 to 2009 from 919 locations showed a genetic gain of 0.55 % per annum when compared to Attila (Sharma et al., 2012). When Crespo-Herrera et al. (2017) compared grain yield gains to the local checks the increase was 0.53 % per annum. Another study on CIMMYT lines from 2007 to 2016 in 360 locations grown in high- and low-rainfall environments showed a genetic gain in grain yield in terms of location checks of 1.17 % in high-rainfall and 0.73 % per annum in low-rainfall environments (Gerard et al., 2020). Even if this rate of 0.53-1.67 % per annum is maintained, this would not be enough to meet the projected demand and the required 2-3 % increase per year. On top of this, average national yields appear to plateau when they reach 70-90 % of their yield potential (Cassman et al., 2010). In addition, since 1990 climate

change in temperate climates is causing heat stress during grain filling, resulting in stagnating wheat yields in some regions, for example, France (Brisson et al., 2010). Wheat grain has different end uses depending on grain quality traits, for example, bread making, feed, distilling and bioethanol (Wrigley and Batey, 2012).

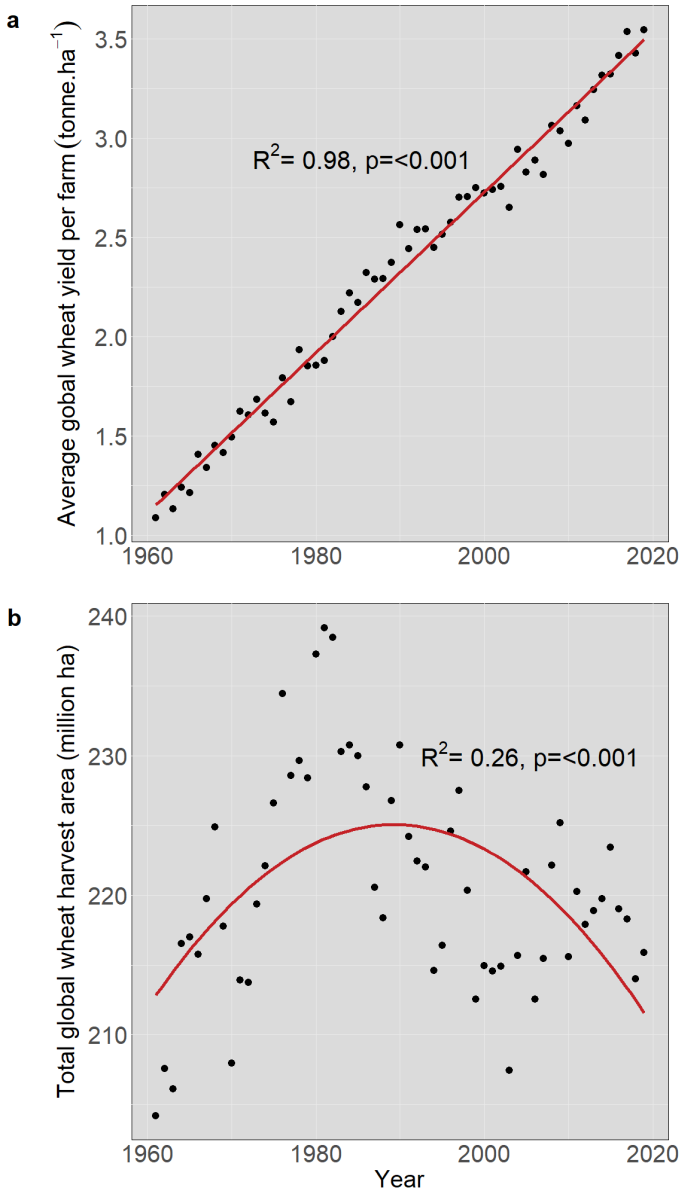

***Figure 1.1**: Linear regressions of a) average global wheat yield per farm (tonnes per hectare) and b) total global wheat harvest area (million hectares) on year from 1961 to 2019*

Data from FAOSTAT (2021), area harvested refers to the total area from which the crop is gathered, and only covers crops grown to maturity

a) $y=0.04x-78$, b) $y=-0.015x^2+60.8x-60282$

1.2 Wheat development and growth stages

Wheat development can be broadly split into three stages, the vegetative stage which is important for crop germination and leaf initiation, the reproductive stage which is important for spikelet initiation, floret development and growth and the grain filling stage which is important for grain set and grain size (Sreenivasulu and Schnurbusch, 2012). The vegetative stage occurs from germination to floral initiation, the reproductive stage from floral initiation to anthesis and the grain filling stage from anthesis to physiological maturity. The most widely used scale for wheat developmental growth stages (GS) is the Zadoks decimal scale (Zadoks et al., 1974). This scale defines the key developmental stages as GS10-19 (seedling growth), GS20-29 (tillering), GS30-39 (stem elongation), GS40-49 (booting), GS50-59 (heading), GS60-69 (flowering), GS70-79 (grain milk development), GS80-89 (grain dough development) and GS90 (ripening and physiological maturity) (Figure 1.2).

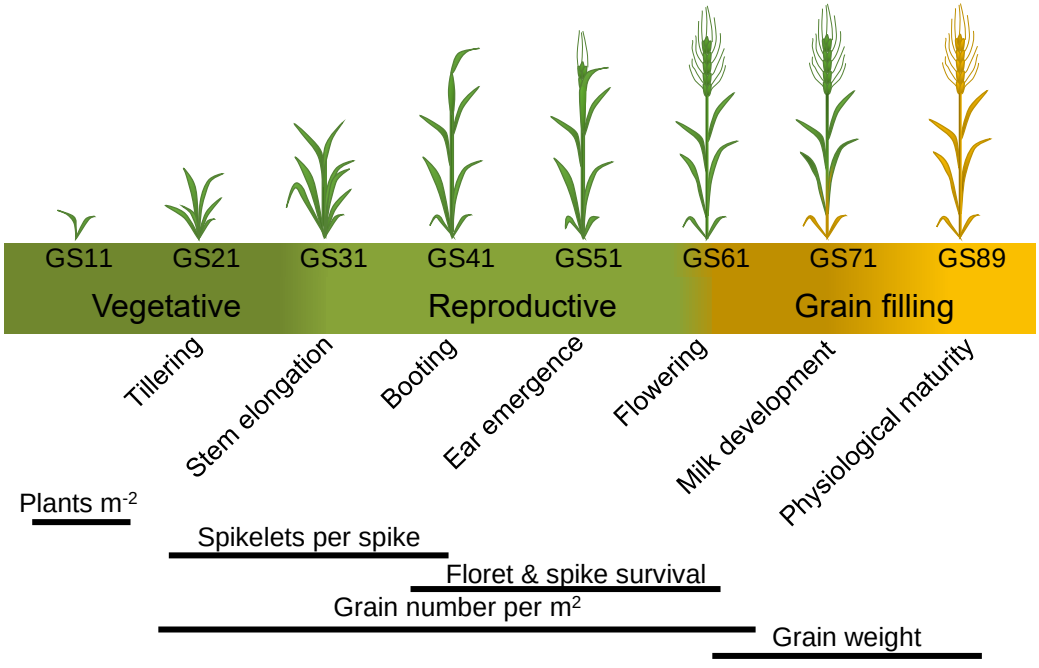

***Figure 1.2**: Wheat growth stage (GS) benchmarks*

Key general growth stages indicated as vegetative (GS10-GS31, dark green), reproductive (GS31-GS61, light green) and grain filling (GS61-GS89, yellow) (Zadoks et al., 1974; AHDB, 2021), bars represent the periods of development when different components associated with grain yield are produced, adapted from Slafer and Rawson (1994)

1.2.1 Vegetative stage: emergence (GS10) to floral initiation

During germination, the primary seminal root grows first, protected by the coleorhiza, followed by the first leaf protected by the coleoptile as it emerges (Acevedo et al., 2002). Tillers are produced by a complex developmental process, where non-elongated internodes (tiller buds) in the axil of every leaf of the main shoot emerge as tillers sequentially, with the first tiller produced after four leaves have emerged on the main shoot (Figure 1.3) (Kirby and Appleyard, 1984; Kebrom et al., 2013; Alqudah et al., 2016). The primary tillers, which are formed first, have a higher grain number per spike than later-formed tillers (Xu et al., 2015). Floral initiation at the apical meristem occurs at mid to late tillering.

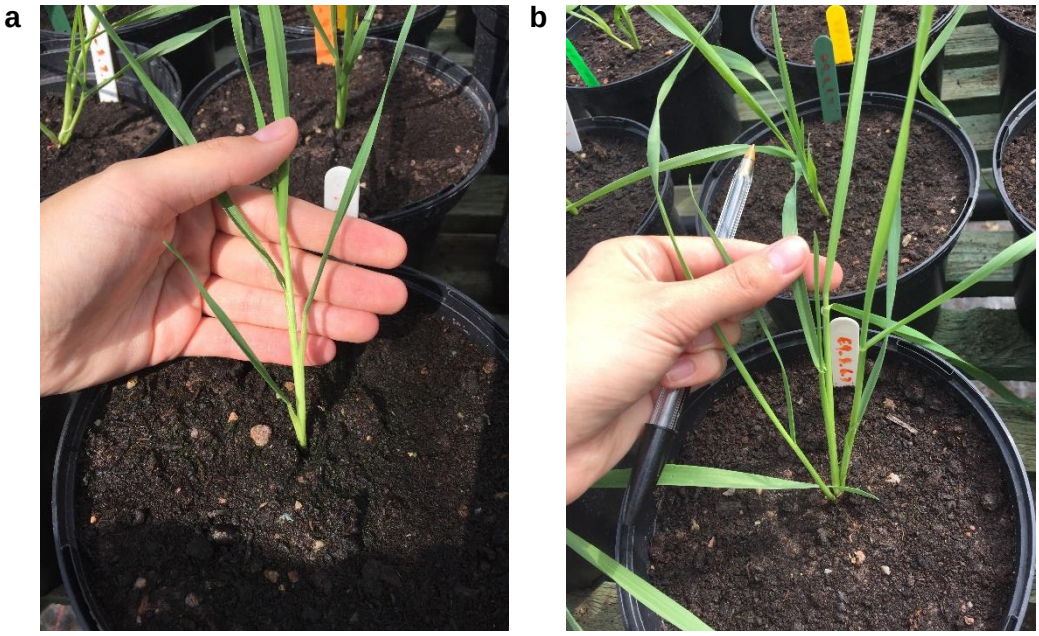

Figure 1.3*: Wheat development at the vegetative stage a) GS14 – 4 leaves unfolded and b) GS22 – main shoot and 2 tillers (Zadoks* et al*., 1974)*

1.2.2 Reproductive stage: floral initiation to anthesis (GS65)

Floral initiation occurs when the vegetative shoot apical meristem transitions to an inflorescence meristem. This inflorescence meristem generates a double-ridge structure where the upper ridges transition to spikelet meristems and form spikelets. The terminal spikelet is initiated at the shoot apex and the internodes associated with the subsequent emerging leaves elongate (Figure 1.4). At the start of stem elongation, tiller production also typically ceases (Kebrom et al., 2013). This may be induced when the red: far-red ratio drops below 0.35-0.40 (Evers et al., 2006). Some of these tillers formed die between GS31 and GS61, with the last formed dying first (AHDB, 2021). To enhance grain DM partitioning and yield

potential, the highly productive primary tillers should contribute a high proportion of the total fertile tiller number (Cai et al., 2014).

This is the rapid canopy expansion phase, and linear crop growth occurs from about mid stem elongation onwards, with maximum canopy area reached around spike emergence (AHDB, 2021). This period between the terminal spikelet formation and anthesis is of paramount importance in the yield formation of wheat, as this is when the grain number per unit area is determined (Slafer and Rawson, 1994), but also grain weight potential is partly set (Calderini et al., 2021). During this phase, floret development and differentiation starting from the white anther stage are occurring (Sreenivasulu and Schnurbusch, 2012). Towards the end of floret development from heading (GS51) to anthesis (GS61), not every developed floret remains fertile, with apical florets within each wheat spikelet aborted (Guo et al., 2018a). Typically, 9-12 floret primordia are initiated, but fewer than 50 % of the floret primordia survive to develop into fertile florets at anthesis (Guo et al., 2018b), which means a significant amount of the grain yield potential is lost during this phase. Increasing dry weight accumulation in spikes at anthesis has been linked to increasing grain number (Fischer, 2011), and the efficiency of spike growth at anthesis is reflected in the fruiting efficiency (FE, ratio of grain number to spike dry weight at anthesis) (Foulkes et al., 2011).

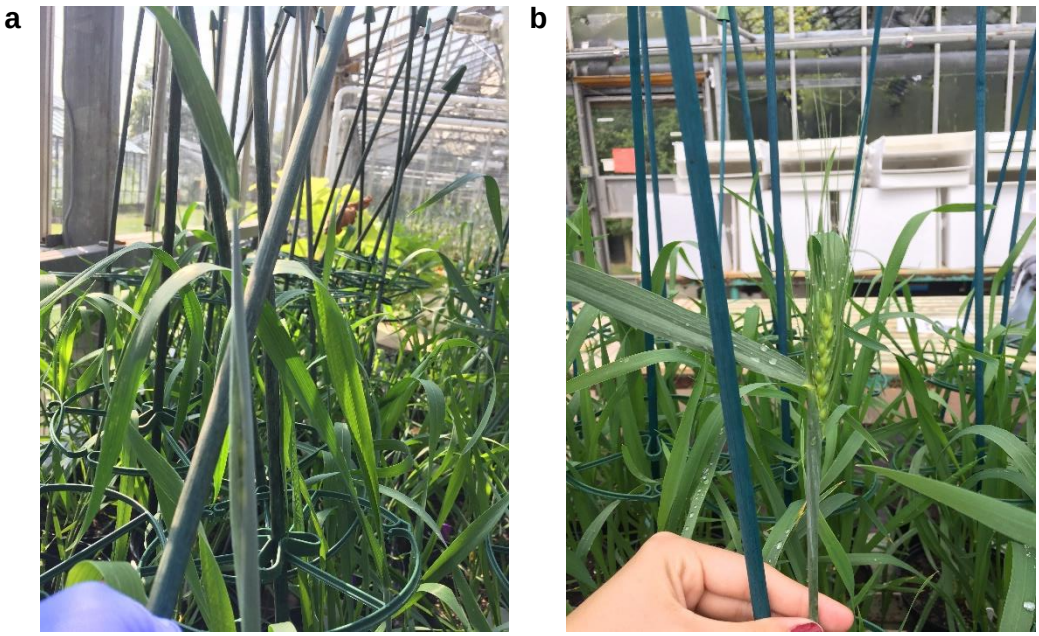

Figure 1.4*: Wheat development at the reproductive stage a) GS49 – late booting, flag leaf sheath starting to open and b) GS55 – half of the spike emerged above flag leaf ligule (Zadoks* et al*., 1974)*

1.2.3 Grain filling stage: anthesis to physiological maturity (GS89)

While the number of fertile florets determined before anthesis is extremely important for determining yield potential, grain set and potential grain weight are determined during early grain filling (Figure 1.5) (Geng et al., 2017). Grain set determines the proportion of fertile florets setting grains that grow during grain filling. The first 5-10 days after anthesis there is a multiplication of endosperm cells but negligible grain growth in terms of dry matter, by 14 days after anthesis the endosperm cells stop being meristematic, suggesting the number of endosperm cells had been fixed and potential grain size has been established (Brocklehurst, 1977). This final potential volume is then filled later during grain filling, with assimilates from both current photosynthesis and remobilisation of carbohydrates stored in plant organs such as the stem before, and shortly after, grain filling (Asseng et al., 2017). Even high yielding cultivars show an excess of photosynthetic capacity during grain filling under optimal conditions (Reynolds et al., 2005).

***Figure 1.5**: Wheat development in the grain filling stage GS89 – physiological maturity (Zadoks* et al*., 1974)*

1.3 Changes in physiological traits associated with plant breeding progress

During the Green Revolution in the 1960s and 1970s, yield progress was associated with gains in harvest index (grain dry weight as a proportion of above-ground dry weight, HI) due to *Rht* dwarfing genes which reduced biomass partitioning to the stem and increased partitioning to the spike (Hedden, 2003). Studies investigating the physiological traits responsible for yield increases in historic cultivars have identified a few key traits that increased with yield. Aisawi et al. (2015) studied CIMMYT spring wheat cultivars released from 1966 to 2009 and identified grain yield progress was associated with the increased above-ground dry matter at harvest and grain weight. Shearman et al. (2005) studied eight UK winter wheat cultivars introduced from 1972 to 1995 and identified grain yield progress was positively correlated with both above-ground dry matter at harvest and HI, with most of the increase since ca. 1985 associated with biomass. Acreche et al. (2008) reported for seven cultivars with years of release from 1940 to 1998 in Spain that HI was the main trait responsible for yield improvement. Similarly, Flohr et al. (2018) attributed yield gain in Australian cultivars of wheat released from 1901 to 2017 to HI and improved partitioning to the spikes, as well as an increase in fruiting efficiency. Grains per m^2 rather than grain weight was generally increased in these studies. Most of the studies found that rates of genetic gains in grain yield in the last 30 years have slowed down. Overall, the evidence suggests wheat breeders need simultaneously to increase biomass at maturity and grain partitioning in future cultivars.

1.4 Improving harvest index (HI) with grain partitioning traits

Harvest index (HI) is the grain dry matter divided by the above-ground dry matter (DM). Harvest index has a hypothetical limit of approximately 0.64 in wheat (Austin, 1980; Foulkes et al., 2011). However, relatively little significant genetic improvement in HI has been observed in most regions since around 1990, with present values of 0.45-0.51 in spring wheat (Reynolds et al., 2012). Further advances in HI require further gains in grain number per unit area, which could be targeted by increasing DM partitioning to, and optimising partitioning within, the spikes at anthesis while maintaining lodging resistance and grain size (Foulkes et al., 2011). It has been reported in CIMMYT spring wheat cultivars that an increase in biomass was associated with a decrease in HI in the last decades (Aisawi et al., 2015) and an increase in plant height.

Evidence suggests that under optimal conditions, grain yield is limited by grain sink size, as carbon accumulation is limited by the storage capacity of the grains both in terms of grain number and potential grain weight (Borras et al., 2004; Foulkes et al., 2011), so increasing grain number is a key target in wheat breeding. Grain sink strength could also be increased by increasing potential grain weight (Calderini et al., 2021). Key traits which have been suggested as targets potentially to increase grain number per unit area are the spike partitioning index (ratio of spike DM to above-ground DM at anthesis, SPI) and fruiting efficiency (ratio of grain number to spike DM at anthesis, FE). However, optimising the trade-offs between traits such as grain number and grain weight, or FE and SPI is key to pushing wheat closer to the limit for HI to double yield by 2050 to feed the growing population (Dreccer et al., 2009; Lazaro and Abbate, 2012; FAO, 2017). Current evidence suggests grain sink strength remains the critical yield-limiting factor, and therefore improving the balance between source and sink to increase grain sink strength, whilst maintaining sufficient photosynthetic capacity to fill the extra grain sites, is critical for further raising yield potential (Borras et al., 2004; Reynolds et al., 2005).

1.4.1 Improving HI through Spike Partitioning Index (SPI)

It is well established that plant height reduction through the introgression of semi-dwarfing genes *Rht-B1* and *Rht-D1* (formerly *Rht1* and *Rht2,* respectively) in wheat during The Green Revolution increased grain yield by reducing stem height and increasing lodging resistance and dry matter partitioning to the developing spike during stem elongation (Gale et al., 1985; Hedden, 2003; Fischer, 2011). Floret survival and therefore grain number has been shown to be associated with

increased spike weight at anthesis (Fischer, 1985), so traits associated with pre-anthesis spike growth are key targets to increase wheat yield (Gonzalez et al., 2011). The greater allocation of DM to the developing spike during stem elongation resulted in greater spike DM, grains per spikelet and higher HI in six winter wheat cultivars (Hobbit 's' and Cappelle-Desprez and their progeny) grown in the glasshouse and field conditions (Brooking and Kirby, 1981). Several investigations have shown genetic increases in grains per m^2 have been explained by a higher SPI (Siddique et al., 1989; Slafer et al., 1990). A plant with a higher SPI represents a plant with a spike that has less competition from alternative plant organs for assimilates during stem extension and therefore more assimilates are available to the spike for floret survival and grain set (Fischer and Stockman, 1980).

Therefore, reducing competition from alternative sinks (e.g., roots, leaves, stems and infertile tillers) is one strategy to increase SPI, especially during stem elongation when grain number is determined (Fischer, 1985; Foulkes et al., 2011). In particular, floret survival occurs most dramatically from booting to anthesis (Serrago et al., 2008). If spike partitioning is increased, assimilate partitioning must be reduced to alternative plant organs. However, if root partitioning is reduced, the plant may not be able to acquire enough water or nutrients to fill the additional grains, or if leaf lamina partitioning is reduced photosynthetic capacity may also be reduced. Furthermore, reducing stem partitioning could create a plant with less stem structural dry matter in basal internodes, and reduced lodging resistance or a more compacted canopy with lower radiation-use efficiency (above-ground DM per unit radiation interception, RUE) (Foulkes et al., 2011).

Reducing partitioning to infertile tillers may not have a negative effect, but as infertile tillers currently only account for 0.01 to 0.05 of the proportion of above-ground DM at anthesis the potential to raise SPI through an improved tiller economy may be small (Berry et al., 2003; Reynolds et al., 2009). When the tiller inhibition gene *tin1A* was investigated in wheat near-isogenic lines (NILs), grains per spike increased by 9 % compared to free-tillering parental genotypes, but grain yield was unaffected (Duggan et al., 2005; Gaju et al., 2009). Therefore, only small gains seem likely through reducing partitioning to infertile tillers. Overall, focusing on reducing the allocation of assimilates to the structural stem or leaf sheath, which together accounts for ~40-45 % of above-ground biomass at anthesis, may offer the greatest opportunity for increasing SPI whilst maintaining photosynthetic capacity and above-ground biomass (Foulkes et al., 2011). Evidence suggests the structural stem carbohydrate is competing more with spike growth than soluble

carbohydrate, and therefore reducing partitioning to structural stem, rather than the soluble stem reserves may be more useful for raising SPI (Foulkes et al., 2011). Further work is needed to understand fully which particular plant sub-components should be the focus within the true-stem and leaf sheath components, but previous studies investigating associations with the spike growth suggest partitioning should be reduced specifically for the true-stem internodes after the peduncle, numbered from the peduncle downwards, internodes 2 and 3 (Rivera-Amado et al., 2019; Sierra-Gonzalez et al., 2021).

Overall there may be limited scope to greatly reduce plant height, as optimum height values for modern wheat cultivars range from *ca.* 70-100 cm (Richards, 1992), and if height is reduced more than the optimal 70 cm, RUE may be reduced due to compacted canopy architecture and shading of leaves (Miralles and Slafer, 1997). There may be more scope to reduce height in CIMMYT spring wheat cultivars, as the current heights of advanced lines and cultivars in CIMMYT spring wheat panels range from 85-115 cm (Sierra-Gonzalez et al., 2021). In fact, in CIMMYT spring wheat cultivars from 1966 to 2009, plant height has increased linearly by 0.25 cm per year to *ca.* 100 cm in 2009 (Aisawi et al., 2015). Instead of reducing overall height uniformly across all stem internodes, specific internodes within the stem could be targeted as mentioned above with only minor reductions in overall plant height.

During the latter stages of the stem-elongation phase from booting to anthesis rapid spike growth and stem growth overlap (Brooking and Kirby, 1981), with internodes sequentially lengthening from the bottom to the top of the stem (Foulkes et al., 2011). Therefore, true-stem growth must compete with DM allocation to the spike differentially among the true-stem internodes (Rivera-Amado, 2016; Rivera-Amado et al., 2019). The peduncle, which is still extending after anthesis, may represent a less strong competitive sink than stem internode 2 (penultimate internode) during the rapid spike growth phase from booting to anthesis, but later it contributes to post-anthesis photosynthesis and DM remobilisation to the grain (Gebbing, 2003). Therefore, reducing the length of the peduncle may not greatly benefit spike growth at anthesis, but may have consequences for post-anthesis source capacity. Concerning lodging risk, structural stem biomass is most important in the two basal stem internodes to ensure lodging resistance and so these internodes should not be targeted for reductions in internode length (Foulkes et al., 2011; Pinera-Chavez et al., 2016a; Pinera-Chavez et al., 2016b). Rivera-Amado et al. (2019) and Sierra-Gonzalez et al. (2021) found genotypes, of the

CIMCOG and HiBAP I panels, respectively, that partitioned less DM to the true stem of internodes 2 and 3 tended to have a greater SPI at anthesis + 7 days, therefore these may be the best targets for wheat breeding to enhance SPI.

1.4.2 Improving HI through Fruiting efficiency (FE)

Previous studies have found genetic variation grain number per m^2 amongst cultivars to be positively associated with fruiting efficiency. This positive association has been identified in Mediterranean bread wheat cultivars from different eras (Acreche et al., 2008), modern Mexican spring wheat cultivars (Rivera-Amado et al., 2019) and modern Argentinian spring bread wheat cultivars (Abbate et al., 1998). However, partly because the selection of semi-dwarfing genes during The Green Revolution was so successful, FE was not actively selected as a target for increasing grain number. Therefore, despite these investigations which have indicated a positive association between FE and grain number, there are still limited studies to date which have quantified genetic variation in FE.

To increase FE, higher survival of developing florets during booting to anthesis is crucial. This can occur in two ways; either by increasing the allocation of assimilates to the developing florets, or reducing the threshold requirement of resources to the florets to maintain their development (Slafer et al., 2015). Reducing the threshold requirement of assimilate would result in higher FE genotypes but with smaller potential grain size (Dreccer et al., 2009), and therefore would be inefficient in increasing grain yield. Increasing the allocation of resources to the spikes could prolong floret development and increase the proportion which survives to form fertile florets at anthesis (Dreccer et al., 2014). Therefore, a better target for increasing FE may be through increasing DM partitioning within the spike to increase the allocation of assimilates to the florets (Slafer and Andrade, 1993). Due to the relatively few investigations reporting on genetic variation in DM partitioning in juvenile spikes pre-anthesis it is currently uncertain how this process of redistribution of DM within the spike could be optimised (Sierra-Gonzalez et al., 2021).

While FE has recently been identified as an important target to increase grain number and HI for the future, in studies comparing the year of release over the past 100 years of breeding (1920 to 1998) with changes in FE, there was generally not a consistent trend of increasing FE with newer cultivars. In Argentina (cvs. Klein Favorito, Eureka Ferrocarril Sur, Buck Manantial, Buck Pucará and ProINTA

Puntal (Slafer and Andrade, 1993; Gonzalez et al., 2003b)) and the UK (cvs. Maris Huntsman, Avalon, Norman, Galahad, Riband, Haven, Brigadier and Rialto (Shearman et al., 2005)) there was no significant positive increase of FE with the year of release, although a positive trend could be inferred in the UK study (Figure 1.6). However, in Spain (cvs. Aragon03, Pane247, Estrella, Siete Cerros, Anza, Marius, Soissons and Isengrain (Acreche et al., 2008)) there was a significant positive increase (Figure 1.6). While in these studies FE was not systematically improved through breeding, wide genetic variation between commercial cultivars has been reported (Mirabella et al., 2016), where the genetic variation was consistently larger than the genotype x environment variation. Other studies have also reported genetic variability in FE that correlates well with grains per unit area as mentioned above (Elia et al., 2016; Gonzalez-Navarro et al., 2016; Rivera-Amado et al., 2019; Sierra-Gonzalez et al., 2021), therefore in the future, there is the potential to increase FE in wheat.

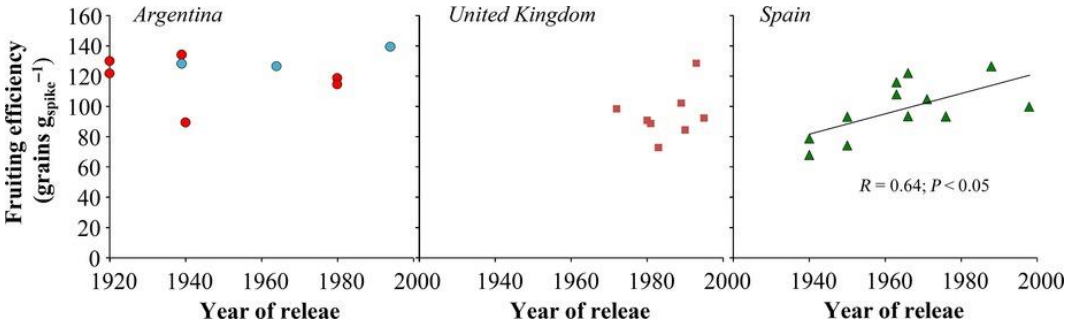

Figure 1.6: *Relationship between fruiting efficiency and year of release of cultivars. Figure taken from Slafer* et al*. (2015)*

Image licenced under CC BY 4.0. Studies conducted in Argentina (left panel, red circles from Slafer and Andrade (1993), blue circles from Gonzalez et al*. (2003b)), UK (middle panel, red squares from Shearman* et al*. (2005)) and Spain (right panel, green triangles from Acreche* et al*. (2008))*

FE is usually calculated based on spike DM at anthesis, which involves a destructive measurement of spikes at anthesis. It can also be calculated using the chaff DM at harvest. There is often growth in the non-grain parts of the spike (glumes, palea, lemma, rachis, awns) during grain filling, and previous studies have found the chaff weight at physiological maturity to be consistently higher than the spike DM at anthesis (Slafer et al., 2015). Fischer (2011) estimated the difference between spike DM at anthesis and chaff at maturity to be as much as 20-50 % greater at maturity. Abbate et al. (2013) assessed the associations between FE calculated at anthesis and maturity and found a significant association

(R^2=0.78, P<0.001), and concluded that FE can be determined accurately by sampling a small number of spikes at maturity. While FE calculated with chaff DM is an easier measurement, it is important to calculate FE both ways in exploratory studies. Nevertheless, some literature suggests FE calculated with chaff is accurate and this would allow evaluation of larger populations. As FE is not a high-throughput measurement and involves destructive sampling, the best way to select for high FE in the future would be through identifying molecular markers for deployment in marker-assisted selection.

1.4.3 Optimising trade-offs between traits

New high yield potential wheat cultivars would ideally have both increased grain weight and grain number per unit area, but a negative relationship has been frequently reported between these traits (Lazaro and Abbate, 2012; Ferrante et al., 2015). This trade-off may be because potential grain weight is related to the size of the ovary, which is in part determined by cell number pre-anthesis, the period usually associated with grain number determination (Calderini et al., 2001; Reale et al., 2017). Despite this, there have been examples where both potential grain size and grain number are both increased, so there is scope for combining high grain number with high grain weight. Bustos et al. (2013) crossed two elite parents contrasting in grain number and weight (cvs. Bacanora and Weebil) and the resultant doubled-haploid (DH) progeny had an increased grain yield of up to 31 % compared to the parents. The increase in grain yield was attributed to the reduction in the trade-off between grain number and thousand grain weight, as both were increased. Gaju et al. (2009) suggested that either altering the glume characteristics, which could physically restrict larger grain weights or increasing the rachis length which would favour spikelet photosynthesis may increase potential grain weight in larger spike phenotypes with high grains per spike. It has also been suggested that improving the vascular connections within the rachilla may minimise the trade-off, as the assimilate supply to distal florets may be limited by resistance in the vascular connections (Minchin et al., 1993; Foulkes and Reynolds, 2015) and distal florets may lack a direct connection to the vascular bundle (Hanif and Langer, 1972). This trade-off between FE and potential grain weight is likely a component of the negative relationship reported between grain number and grain weight (Lazaro and Abbate, 2012), so by reducing the trade-off, grain sink strength could be enhanced to increase yield.

Previous studies have also reported a negative association between spike PI and FE (Dreccer et al., 2009; Terrile et al., 2017; Sierra-Gonzalez, 2020). However,

this trade-off is not always observed, e.g. Bustos et al (2013), and there are several theories as to why this trade-off may exist. It could be because FE is calculated as the ratio between grain number and spike DM, and so when spike DM is increased this may tend to cause a decrease in FE due to excessive investment in non-grain chaff components of the spike. However, other investigations found no correlation between spike DM and FE (Gonzalez et al., 2011), indicating this trade-off is not constitutive and may be related to different factors. For example, spike DM and SPI may have a negative trade-off with FE because there is a limited assimilate supply to the most distal florets due to restricted vascular connections within the rachilla (Bancal and Soltani, 2002), reducing floret fertility. If this connection is not good, then developing florets at anthesis will not receive enough assimilates to be above the threshold for floret survival (Hanif and Langer, 1972). In addition, restricted vascular connections could affect grain size in terms of final grain weight, assimilates may feed back to the chaff rather than contributing to the survival of distal developing florets. Guo et al. (2017) identified a QTL on chromosome 3A associated with apical grain number per spikelet, apical grain survival and spikelet fertility, and the candidate gene was suggested to be *BRASSINOSTEROID INSENSITIVE 1 (BRI1),* indicative of the involvement of brassinosteroids in floral development of wheat. There are other potential genes and hormones which could be controlling the relationship between spike DM and FE, which need to be explored further. The effects of plant hormones on grain sink strength are discussed in the next section.

1.5 Effect of plant hormones on grain sink size

Hormones play a huge role in many aspects of plant growth and development from stress response to seed development and shoot growth (Jameson and Song, 2016). Plant hormone interactions are innovative targets for crop breeding and development, and therefore it is important to understand how hormones affect plant development, growth and dry matter partitioning to utilise them fully for potential yield increases. Improved understanding of how hormone interactions regulate source-sink relations is required so it can be applied in crop improvement. It is key to investigate these novel targets because the bottleneck for improving grain yield is grain sink strength. Furthermore, selecting directly for yield is slow and complex, so finding molecular markers for use in marker-assisted selection could accelerate yield gains (Wilkinson et al., 2012). This section will focus on the effect of six hormones: cytokinins, gibberellins, abscisic acid, auxin, jasmonic acid and salicylic acid, both endogenously and as exogenous applications pre- and post-anthesis.

1.5.1 Cytokinin (CK)

Cytokinins have been shown to be crucial in promoting cell division, cell growth and differentiation, axillary bud growth and delaying leaf senescence, all of which contribute to increasing grain number and size (Jameson and Song, 2016).

Biosynthesis pathway and structure

Cytokinins are mainly adenine derivatives that carry an isoprene-derived side chain at the N^6 position of the purine (Feng et al., 2017). They are derived from free adenine nucleosides catalysed by CK biosynthesis enzyme isopentenyltransferase (IPT) (Jablonski et al., 2020). The active forms of these CKs are nucleobases (free bases) such as isopentenyladenine (2iP) and *trans*-zeatin (Z) (Figure 1.7). The inactive forms of CK, which serve as a reservoir for CK storage, are nucleosides (added five-carbon sugar to nucleobase) such as isopentenyladenosine (IPA) and zeatin riboside (Zr) (Figure 1.7) (Feng et al., 2017). Z and Zr can be formed through hydroxylation of the side radical of 2iP and IPA, respectively (Avalbaev et al., 2012).

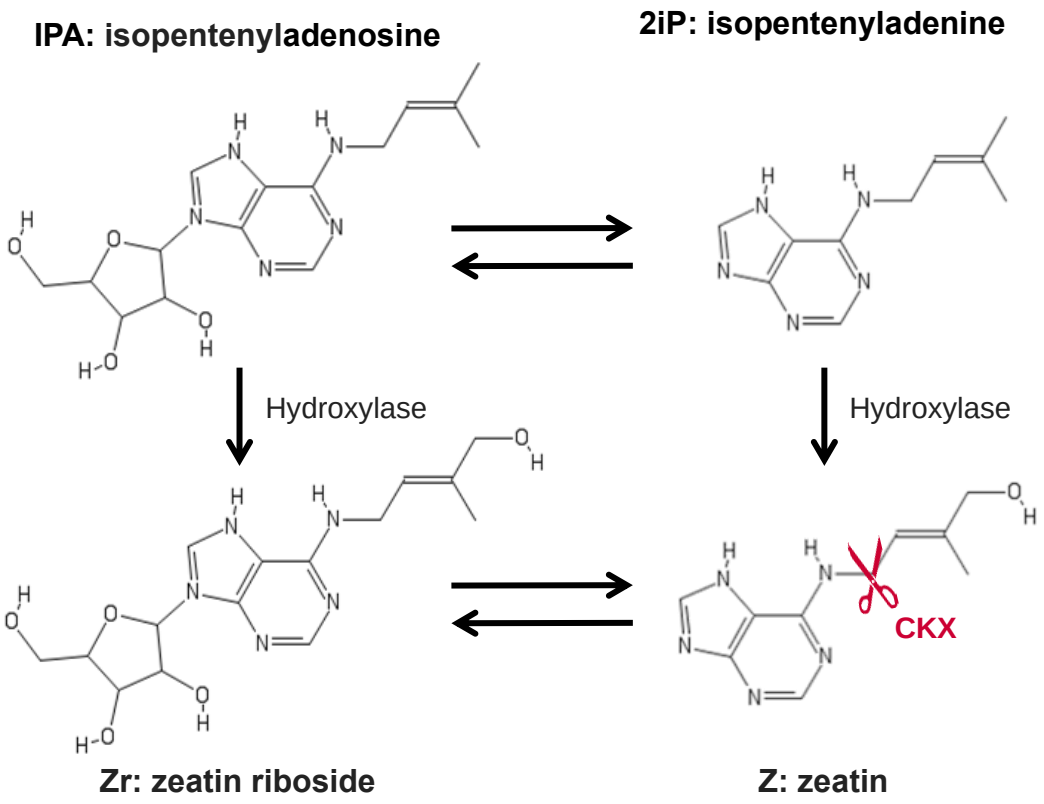

***Figure 1.7**: Simplified cytokinin biosynthesis pathway*

Isopentenyladenine (2iP) and trans-zeatin (Z) are the active forms of cytokinins and can be inactivated by purine nucleoside phosphorylase to isopentenyladenosine (IPA) and zeatin riboside (Zr) and reactivated by adenosine nucleosidase (Spichal, 2012). IPA and 2iP can be converted to Zr and Z through hydroxylase (Nordstrom et al*., 2004). Cytokinin oxidase/dehydrogenase (CKX) irreversibly degrade cytokinins by cleavage of the N^6-isoprenoid side chains, as shown on Z in this figure, although CKX will degrade all four cytokinins pictured here due to the double bond on the side chain (Jameson, 2017)*

As well as a *trans*- form of Z, there is a *cis*-isomer which is much less well documented than the *trans*- counterpart (Schmitz et al., 1972). This is reflected in the rest of this thesis by referring to the *trans*- isomer as zeatin unless specified otherwise. In barley, *cis*-Z decreases with development while *trans*-Z increases (Holubova et al., 2018), however a comprehensive analysis during spike and grain development has not yet been reported in wheat using liquid chromatography with tandem mass spectrometry (Chen et al., 2020). From the recent studies in wheat, it appears the ratios may be similar, with *cis*-Z being the dominant form early in vegetative shoots (Gajdosova et al., 2011) and *trans*-Z dominant 7 days after pollination (Jablonski et al., 2020). Studies in *Arabidopsis* have identified *cis*-Z is found mostly in the phloem, suggesting it is involved in the shoot to root translocation and may be more important in the roots (Hirose et al., 2008) , but *cis*-Z has also been detected in the xylem sap of wheat and oats (Parker et al., 1989). It was previously suggested that *cis*-Z can be converted to a *trans*- form with cis-

trans-isomerase (Bassil et al., 1993). However, subsequent studies have been unable to find conversion between the two isomers (Kudo et al., 2012; Schafer et al., 2015). While it cannot be ruled out that isomerisation may occur, it is unlikely to form a major pathway in cytokinin metabolism.

Endogenous levels of CKs are controlled by the complete irreversible inactivation through cleavage of the N^6-isoprenoid side chains by CK oxidase/dehydrogenase (CKX, Figure 1.7) (Frebort et al., 2011). CKXs are particularly active against CKs that have a double bond in their side chain, which includes 2iP, IPA, Z and Zr (Jones and Schreiber, 1997).

Effects pre-anthesis

During booting in rice, when the expression of rice cytokinin-oxidase dehydrogenase *OsCKX2* is reduced, CK accumulates in the inflorescence meristems and leads to an increase in the number of reproductive organs, resulting in an increase in the grain number per plant (Ashikari et al., 2005). The positional expression of *OsCKX2* in rice shown with a GUS construct indicated expression in the vascular tissue of developing culms, inflorescence meristems and young flowers (Ashikari et al., 2005), which is consistent with the increase in the number of reproductive organs and the resultant higher grain number. Similarly, two of the CKX genes found in wheat *TaCKX2.1* and *TaCKX2.2* were highly expressed in young spikes and culms of 12 wheat cultivars grown in the field in Beijing, China (Zhang et al., 2011). Reduction in expression of *TaCKX2.4* with transgenic wheat with RNAi gene silencing resulted in an increase in grain number per spike of 5.8-12.6 % (Li et al., 2018a), while silencing *TaCKX1* by RNAi resulted in a higher spike and grain number, but lower thousand grain weight (Jablonski et al., 2020). However, the silencing of *TaCKX1* led to an increase in expression of *TaCKX2.1* and *TaCKX2.2*, which the authors suggested may be because the other CKX genes were compensating for the reduction in *TaCKX1* (Jablonski et al., 2020). Manipulation of CKs is complex because the genes coding for their biosynthesis and degradation belong to multigene families, which are spatially and temporally differentiated, and their function does not simply affect grain number (Jameson and Song, 2016). While more research is required to understand fully the CKX gene family, investigations to date have reported an association between the reduced activity of CKX and increased grain number.

Williams and Cartwright (1980) found that when 6-Benzylaminopurine (6-BA), a synthetic CK, applied as a soil drench to pots of spring barley (*Hordeum vulgare*

cv. Ark Royal) grown in the open every 3-4 days either early or late until ear emergence, grain yield per plant increased up to 57 % with the early application, which coincided with spikelet differentiation and preceded stem-internode and rachis elongation. This increase in yield was suggested to be due to improved grain set at the basal and apical spikelet positions of secondary tillers, or increased allocation of biomass to the grains. When the CK treatment was performed later during stem elongation, the increase in yield was not detected. The authors did not report grain number, although spikelet number determined at the awn primordium stage (main shoot spike 4 mm long) was similar in the early treatment and the control. As this treatment was performed pre-anthesis, it would be expected to influence grain number rather than grain weight, so it is plausible to suggest the grain yield was increasing due to increased grain number.

Another example of grain yield increase in response to 6-BA in wheat can be seen in the investigation of Zheng et al. (2016). 6-BA was applied as a foliar spray to Chinese winter wheat (cv. Yumai 49–198) grown in the field 25 days after the initiation of stem elongation. The CK treatment resulted in an increased grain number and grain yield, as well as the number of fertile florets in basal spikelets. The mechanism by which the CK achieved this increase was suggested to be through reducing floret abortion rates of spikelets by as much as 77 % compared to the control (plants sprayed with water). Also showing positive effects of CK application, Wang et al. (2001) injected CK zeatin into the leaf sheath of winter wheat (cv. YM 158) grown in the field during five stages of floret development (floret initiation, terminal spikelet formation, anther-lobe formation, meiosis and floret degeneration). The number of fertile florets per spike and grain set per spike was significantly increased at all five stages of application, especially at anther-lobe formation. The evidence in rice, barley and wheat suggests that increasing CK concentration, whether through reducing CKX activity endogenously or exogenously applying CK increases the number of fertile florets and therefore grain number.

Effects post-anthesis

During the early stages of fruit and grain development, CK levels are elevated and correspond with cell divisions which determine final grain size and weight (Jameson and Song, 2016). High levels of CKs are generally found in the developing grains of cereals (Liu et al., 2013b) and are thought to be involved in cell division during seed development (Yang et al., 2000). In wheat (cv. Kopara) grown in the field, a sharp increase in CK occurs in the ears immediately after and

up to four days post-anthesis (Jameson et al., 1982). Hess et al. (2002) found endosperm zeatin in spring wheat (cv. PCYT-20) grown in the glasshouse was maximal at six days post-anthesis at 13 µmol kg^{-1} DM and had reduced to 0.1 µmol kg^{-1} DM nine days post-anthesis, at which point embryo differentiation is nearly complete. The endosperm in wheat is responsible for most of the volume in the mature grain, so grain size is determined mainly by endosperm cell division and expansion (Geng et al., 2017). Therefore, the effects of hormone concentrations in the endosperm are very important. While CK levels were shown to be high in the carpels of wheat (cv. Okapi) two days post-anthesis in floret positions that resulted in grain set, Lee et al. (1988) also reported high CK levels in the carpel of florets which did not result in grain set. The findings of this study suggest CK may not always be causally linked with cell division and grain development, however, transport of CK from one developing grain to another cannot be ruled out.

By either reducing CKX activity or increasing IPT activity, grain number and potential weight and hence yield could be increased. While the role of *TaCKX1* and *TaCKX2* in wheat is important in increasing grain number (Li et al., 2018a; Jablonski et al., 2020) when the natural variation of *TaCKX6-D1* was assessed, a negative correlation between the expression level of *TaCKX6-D1b* and thousand grain weight was observed (Zhang et al., 2012). However, the *TaCKX6-D1a* allele has been found to increase grain size and weight (Lu et al., 2015; Rasheed et al., 2016; Li et al., 2019b), indicating that this particular CKX allele is positively increasing yield. While the variation of *TaCKX6-D1a* in haplotypes has been found to increase grain size and weight, *TaCKX6* has yet to be validated through knockout in transgenic wheat, so the exact function has yet to be determined. A different gene identified as negatively regulating grain width and weight is *TaGW2-6A* (Jaiswal et al., 2015). When a *TaGW2-6A* allelic variant results in a loss of function to the protein it codes, IPT activity was upregulated, while CKX activity downregulated (Geng et al., 2017), which led to upregulated starch biosynthesis and larger grain size and weight. More research is required to elucidate fully the role of CK synthesis through IPT genes and degradation through CKX genes. However, it is clear both pre- and post-anthesis CK levels have a positive effect, resulting in an increased grain number and weight, which is why CKs have been suggested to be the driver of the second ‘Green Revolution’ (Jameson and Song, 2020). Many plant hormones influence other hormones, and the interaction of CK with auxin will be discussed in the auxin section below.

1.5.2 Gibberellins (GA)

Gibberellins can be generalised as stimulating organ growth through enhancement of cell elongation (Hedden and Thomas, 2012), and regulate many developmental processes such as seed germination, stem elongation and anther development (Huang et al., 2012).

Biosynthesis pathway and structure

Gibberellins are a large group of tetracyclic diterpenoid carboxylic acids, which are classified according to their structure (Hedden, 2020). Currently, 136 gibberellin structures have been identified and have been assigned names gibberellin A1 – A136, and are abbreviated to GA1 etc., which were assigned based on the order of discovery and structural characterisation (Macmillan and Takahashi, 1968). GA1 and GA4 are the most abundant forms of gibberellins in plants, which suggests they are the functionally active forms for growth promotion (Hedden and Thomas, 2012). Conversion to the biologically active forms of GA requires the 3β-hydroxylation of GA9 and GA20 to GA4 and GA1, respectively, catalysed by the 2-oxoglutarate-dependent dioxygenase named GA3-oxidase (GA3ox, Figure 1.8) (Hedden and Thomas, 2012). The main mechanism for deactivating GAs is through 2β-hydroxylation with the enzyme GA2-oxidase (GA2ox), which can occur on both GA precursors and the bioactive end products (Hedden, 2020).

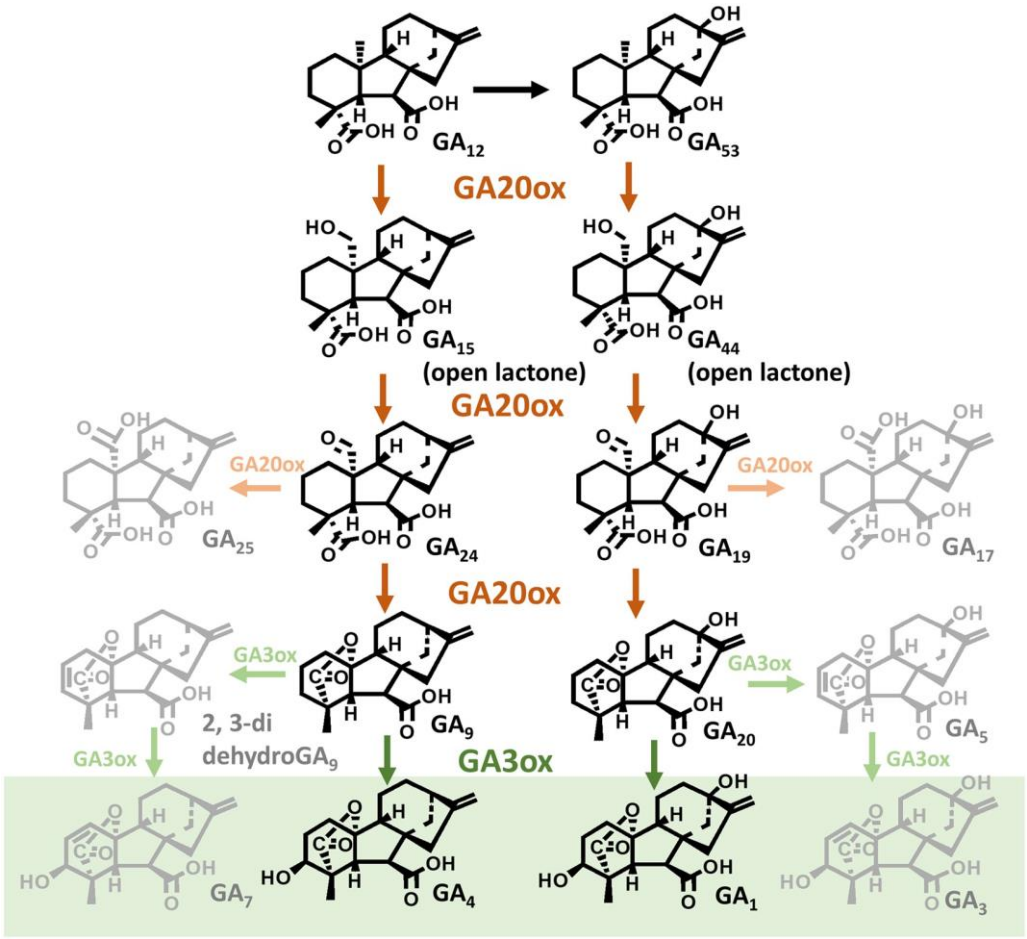

Figure 1.8: *Final stages of gibberellin biosynthesis to the biologically active end products highlighted in a green box. Figure taken from (Hedden, 2020)*

Image licenced under CC BY 4.0. Biologically active end products GA1 and GA4 are catalysed by two 2-oxoglutarate-dependent dioxygenases: GA20-oxidase (GA20ox) and GA3-oxidase (GA3ox) (Hedden and Thomas, 2012). Reactions producing minor by-products which are present in some species are indicated in grey

Effects pre-anthesis

Early work in gibberellins identified that young tissue treatment of gibberellins resulted in stem elongation, but in very high concentrations it had an inhibitory although not always toxic effect (Stowe and Yamaki, 1957). Promotion of elongation in young stems is one of the most well-documented effects of GA, which occurs through enhanced cell elongation and without a change in the number of stem internodes (Hedden and Sponsel, 2015). GA also impacts root elongation, but roots naturally contain saturating levels of GA (Tanimoto, 2012). Phinney et al. (1957) applied GA1, GA2 and GA3 to the first unfolding seedling leaf in dwarf mutants of maize, and found it rescued the growth defect in some dwarf mutants but not all.

While some dwarf maize was rescued by application of gibberellins, semi-dwarf wheat cultivars containing *Rht-B1* and *Rht-D1* do not show the same effect of stem elongation when GA3 is applied; therefore these cultivars are termed GA-insensitive (Gale and Marshall, 1973). Recently, it has been confirmed that the *Rht*-1 alleles cause dwarfism by conferring insensitivity to GA-mediated degradation of DELLA proteins through the production of N-terminal truncated proteins in the spikes and nodes but not the aleurone layers, where GA insensitivity would lead to grain dormancy (Van de Velde et al., 2021). The same response with an application of GA was seen by Colombo and Favret (1996), when both GA-sensitive and -insensitive cultivars were sprayed with GA3 but only GA-sensitive cultivars showed elongated stem internodes. In the same experiment, Colombo and Favret (1996) noted when GA3 was sprayed on the plants during floret development it induced male sterility in both the GA-sensitive and -insensitive cultivars. The critical period for the GA-sensitive cultivars was between stamen differentiation and premeiotic interphase and in GA-insensitive cultivars between glume differentiation and stamen differentiation. If GA3 was applied to the plant either before these stages in early spike development or later after the beginning of meiosis, no male sterility was induced.

Wang et al. (2001) also observed a change in response to injecting GA3 into the leaf sheath cavity depending on the timing during floral development. At the first three stages (floret initiation, terminal spikelet formation and anther-lobe formation), GA3 application increased the number of fertile florets per spike, but the grain set was decreased by as much as 29 %. However, later in floral development (meiosis and floret degeneration), the number of fertile florets did not increase with GA3 treatment, but grain set did increase. Both the results of Wang et al. (2001) and Colombo and Favret (1996) suggest that early in floral development GA has a negative effect, but later it may have either a neutral or positive effect. Despite the application of exogenous GA appearing to be deleterious in early floral development, GAs are important in stamen elongation and are also necessary for the release and germination of pollen for specific plant species (Hedden and Thomas, 2012; Marciniak and Przedniczek, 2019)

While there are indications that early in stem elongation GA increases cell elongation, the effects during floral development appear to be very dependent on the exact time point they are applied, and more research on the effects of endogenous variation in GA is required in wheat.

Effects post-anthesis

The effect of GA on flowering is complex and can be to either promote or inhibit flowering depending on the species. A single treatment of GA3 applied through spraying to a male-sterile mutant of the barley variety Maris Baldrie just before anthesis rescued fertility and resulted in the production of grain which gave male-sterile plants (Kasembe, 1967). This demonstrates that, while pre-anthesis applications of GA can be deleterious, at later floral developmental stages GA applications can rescue fertility. It also suggests GA is involved in male development of anthers and therefore pollen production (Hedden and Thomas, 2012). Furthermore, Nakajima et al. (1991) found, comparing a male-sterile mutant of rice (cv. MSM-01) to a standard japonica rice cultivar (cv. NS89), the mutant had 80-87 % lower GA than the normal cultivar, suggesting the high endogenous level of GA is important in anther development. Other studies on rice (cvs. Nihonbare, Tan-ginbozu and Tong-il) have detected the endogenous level in spikes starts low and reaches a peak after anthesis and then rapidly declines (Suzuki et al., 1981). This suggests that GA is important in affecting floral processes at anthesis but possibly not during grain filling. These studies all indicate GA has a positive effect during anthesis. However, it has been suggested that the role of GA is species dependent (Huang et al., 2003), so these results require confirmation in the case of wheat.

1.5.3 Abscisic acid (ABA)

ABA was first identified as a growth inhibitor that accumulates in abscising fruits, and most of the research identifies it as a stress hormone (Dong et al., 2015). However, ABA also plays an important role in seed maturation and dormancy, as a lack of ABA can result in precocious germination and pre-harvest sprouting (McCarty, 1995).

Biosynthesis pathway and structure

Unlike cytokinins and gibberellins, there is just one abscisic acid, which is a weak acid. The ABA biosynthetic pathway currently has more than 200 loci identified to be involved in metabolism, transport and signal transduction (Dong et al., 2015). The precursor to ABA, xanthoxin, is catalysed by ABA2, a short-chain alcohol dehydrogenase, and the final step in the pathway is the oxidation of abscisic aldehyde to ABA, catalysed by abscisic aldehyde oxidase AAO3 (Figure 1.9) (Dong et al., 2015). AAO3 requires a molybdenum cofactor (MoCo) for its catalytic activity. To regulate ABA levels through catabolism, either hydroxylation or conjugation has to occur. Hydroxylation (where a C-H bond oxidises into a C-OH

bond, Figure 1.9) that occurs at the C-8' position is commonly thought to be the major regulatory step (Nambara and Marion-Poll, 2005).

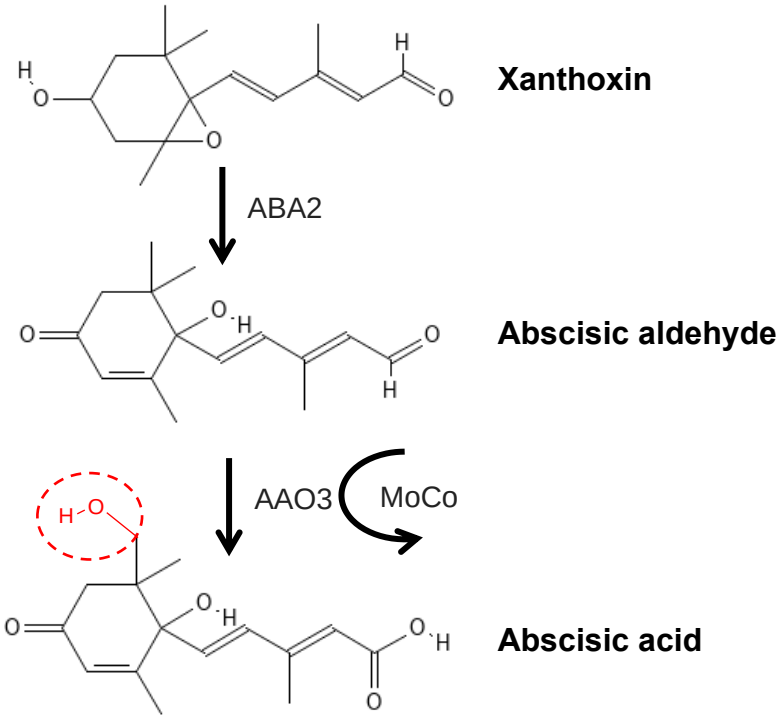

***Figure 1.9**: Last two steps in ABA biosynthetic pathway*

Xanthoxin is converted by short-chain alcohol dehydrogenase (ABA2) to abscisic aldehyde, which is then oxidised into abscisic acid by short-chain alcohol dehydrogenase (AAO3) activated by a MoCo sulfurase (Nambara and Marion-Poll, 2005). The red circle on ABA indicates what happens in the process of hydroxylation which regulates the level of ABA. Indicated here on the C-8' position

Effects pre-anthesis

Several reports suggest that the ABA content of axillary buds is related to bud dormancy (Shimizu-Sato and Mori, 2001). Knox and Wareing (1984) observed that if the bud was decapitated (stimulating growth) in 3 week-old bean plants (*Phaseolus vulgaris* L. cv. Canadian Wonder) grown in the glasshouse, ABA concentration decreased. While this is not direct evidence that the amount of ABA decreases prior to renewal of growth, it does not preclude an inhibitory role for ABA. Further evidence can be seen in the *era1* mutant of *Arabidopsis*, which is hypersensitive to ABA and has reduced branching (Pei et al., 1998; Shimizu-Sato and Mori, 2001). Other studies observed negative effects of ABA, with exogenous spraying of ABA in rice (cvs. Nanjing 44 and Yangdao 6) following panicle removal at heading. Panicle removal decreased the ABA contents of both ABA treated and control plants, while application of ABA slowed the growth rate of tiller buds (Liu et al., 2011). Because ABA did not completely inhibit growth of the tiller buds, the

authors suggested it may affect the velocity of growth rather than completely regulating growth. Emery et al. (1998) found during later stages of growth (floral bud large, flowers open, elongation of main stem and basal branches) of *Lupinus angustifolius* L. (cv. Merrit), ABA concentration showed a strong negative relationship with growth. They reported a decline in ABA level in the upper branch regions coinciding with elongation in the upper branch regions (Emery et al., 1998), suggesting further that ABA plays a role in growth inhibition.

Wang et al. (2001) also looked at the effect of ABA on floret development of winter wheat (cv. YM 158). They showed that ABA has inhibitory effects at all floret developmental stages except anther-lobe formation, where rather than inhibiting floret development and decreasing numbers of fertile florets, ABA had no significant impact. Other investigations confirm the negative effect observed for ABA on floret development. Zeng et al. (1985) found when ABA was injected between the leaf sheath and unemerged ear of spring wheat (cvs. Banks and Kalyansona) grown in the glasshouse, floret infertility was induced. This was only seen in applications during pollen meiosis, not earlier or later. The same negative association with floret fertility was also seen endogenously in wheat (cvs. 97J1, H8679 and YM158), with endogenous ABA concentration decreasing sharply from anther-lobe formation to meiosis (Cao et al., 2000).

Some studies have shown foliar sprays of ABA applied at the beginning of shoot enlargement and repeated at anthesis in wheat grown in the field (cv. Condor Relmo) promoted grain yield through the accumulation of soluble carbohydrates (Travaglia et al., 2010). However, other literature has shown NILS of pea (*Pisum sativum*) with ABA containing and ABA deficient seeds show normal growth patterns and similar growth rates (Debruijn and Vreugdenhil, 1992). The overwhelming evidence would suggest that ABA has a negative effect on floret development during stem elongation and booting, and to maximise potential grain number in spikes, ABA concentration should be maintained at low levels. However, the presence of some studies reporting positive effects of ABA applied before anthesis on soluble carbohydrate accumulation means this needs to be studied further.

Effects post-anthesis

Accumulation of ABA in developing grains of maize in response to water stress correlates with decreased endosperm cell division, indicating that higher accumulation of ABA can result in grain abortion (Ober et al., 1991; Wang et al.,

2002). The study of Hess et al. (2002) showed ABA levels in wheat decreased after anthesis and remained low in the endosperm (1.0 - 4.5 μmol kg^{-1} DM, 6-25 days post-anthesis) and embryo (3.4 - 4.8 μmol kg^{-1} DM, 13-25 days post anthesis). In an experiment where wheat plants (cvs. Brevor – high dormancy and Greer – low dormancy) were transferred to growth chambers kept at either a high temperature of 25 °C or a low temperature of 15 °C, the low temperature induced a high level of dormancy and resulted in low germination (Walker-Simmons and Sesing, 1990). When the embryos were dissected from the cultivars and ABA added to the incubation solution, the embryos from plants grown at the low temperature were blocked from germinating, but the same effect was not seen at the plants grown at higher temperatures. Therefore ABA induces embryo dormancy in wheat.

Blocking ABA synthesis in developing grains of winter wheat (cvs. Brevor and Greer), by applying fluridone to detached spikes cultured in medium, prevented dormancy by blocking ABA accumulation in the embryo (Rasmussen et al., 1997). It has been widely reported that ABA plays a major role in seed dormancy and controls the transition between dormancy and germination (Rodríguez-Gacio et al., 2009). It is important to maintain dormancy so premature germination and pre-harvest sprouting does not occur. However, if viable seeds are unable to germinate this will also cause losses in yield (Gao and Ayele, 2014). Therefore, ABA can be important during grain filling, but only in the correct concentrations.

1.5.4 Auxin

Auxin is essential in axillary meristem initiation and growth through promoting cell elongation and inflorescence branching (Gallavotti et al., 2008; Zhang and Yuan, 2014). However, most knowledge about auxin is in *Arabidopsis*, rice and maize, while less progress has been made in wheat (Li et al., 2018b).

Biosynthesis pathway and structure

Indole-3-acetic acid (IAA) is the best-studied naturally occurring active auxin (Kasahara, 2016). The indole-3-pyruvate pathway is the main contributor to free IAA, and conversion of tryptophan (trp) to IAA is a two-step process involving the Tryptophan Aminotransferase of *Arabidopsis* (TAA) family of trp aminotransferases that convert trp to indole-3-pyruvate (IPyA), and the YUCCA (YUC) family of flavin monooxygenases that convert IPyA to IAA (Figure 1.10) (Korasick et al., 2013). Many auxin storage forms can be converted back to active IAA. However, some forms comprise an IAA inactivation pathway that cannot be converted back to IAA through an IAA catabolic pathway (Korasick et al., 2013). Three types of auxin

carriers have been identified; auxin influx carriers - the AUXIN/LIKE AUXIN (AUX/LAX) family, auxin efflux carriers - the PINFORMED (PIN) family and auxin efflux carriers - the ATP-binding cassette transporters of the B class (ABCB) family (Carraro et al., 2012). ABCB and PINs work synergistically and both modulate long-range auxin transport in the stem from the apex to the base (Harrison, 2017).

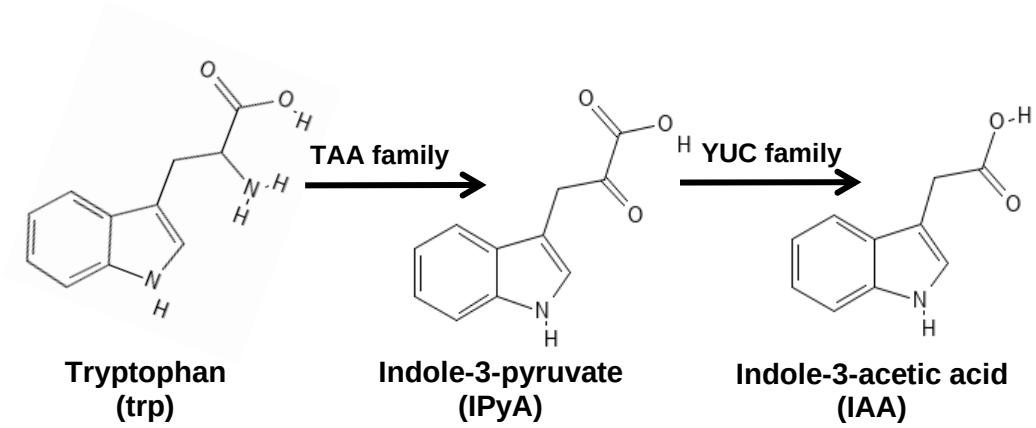

***Figure 1.10**: Biosynthesis pathway of auxin indole-3-acetic acid (IAA)*

IAA is an auxin synthesised mainly from tryptophan via indole-3-pyruvate with a two-step reaction involving the Tryptophan Aminotransferase of Arabidopsis (TAA) and YUCCA (YUC) family (Kasahara, 2016)

Effects pre-anthesis

Transgenic tobacco plants with modified genes regulating enzymes such as *iaaH* and *iaaM* (indoleacetamide hydrolase and trp monooxygenase) grown in the glasshouse had elevated levels of IAA and showed increased apical dominance and therefore reduced tillering (Sitbon et al., 1992). Larsson et al. (2017) investigated the effects of endogenous auxin concentration on ovule development pre-anthesis in *Arabidopsis*, and found that there is low auxin pre-anthesis. In wheat (cvs. 97J1, H8697 and YM158), endogenous levels of IAA were 3-fold higher in fertile florets when they began to degenerate, suggesting IAA is a factor that leads to floret degeneration (Cao et al., 2000). When Wang et al. (2001) added IAA exogenously to winter wheat (cv. YM158) grown in the field during all floret developmental stages, development of the spike was inhibited, resulting in grain loss in all spikelet positions. With both endogenous concentration being low naturally and exogenous application reducing floret fertility, these studies suggest auxin has a negative effect on floret fertility pre-anthesis.

However, auxin is essential to axillary meristem initiation in the axils of bract leaf primordia through localised auxin biosynthesis and polar auxin transport (Barazesh

and McSteen, 2008). Polar auxin transport requires the PIN family of auxin efflux proteins, and *Arabidopsis* mutants with defects in PIN1 have floral abnormalities, suggesting normal polar auxin transport is required in early floral bud formation in *Arabidopsis* (Okada et al., 1991). A systematic study of gene expression during early spike development in wheat showed increased auxin signalling as the plant moved through spike developmental stages (Li et al., 2018b). Specifically, auxin was high in the spikelet and floret differentiation stages, suggesting it is important in axillary meristem initiation. The study also reported on cytokinin signalling, and found coordinated changes in auxin and cytokinin activity, with cytokinin signalling reducing as auxin signalling increased. Cytokinins are known to regulate auxin in *Arabidopsis* through PIN-FORMED (PIN) protein accumulation (Dello Ioio et al., 2008; Ruzicka et al., 2009). It has been reported that cytokinin treatment can significantly reduce the expression of several PIN genes (Simaskova et al., 2015). Waldie and Leyser (2018) reported that cytokinin can regulate *PIN3*, *PIN4* and *PIN7* accumulation. When Li et al. (2019a) sprayed cytokinin 6-BA on the leaves of winter wheat during the abortion stage of floret development, auxin content reduced while cytokinin content increased, resulting in an increase in fertile florets and grain number by suppressing degeneration and abortion of florets. While endogenous concentrations of auxins may be low, it is clear that the low levels are necessary to floral development in some capacity. There is evidence of cross-talk with cytokinins, so mutations, for example in the PIN proteins, are detrimental for floral development.

Effects post-anthesis

In wheat (*Triticum turgidum* cv. Franshawi), injecting IAA into the peduncle during the mid-phase of grain filling (20 days post-anthesis) resulted in stimulated photoassimilate transport to developing wheat grains through grain filling (Darussalam et al., 1998), suggesting that increasing endogenous auxins during early grain filling may contribute to grain growth. In a glasshouse experiment on spring wheat (cv. PCYT-20), endogenous endosperm IAA content sharply increased from 6 to 38 μmol kg^{-1} DM 19 days post-anthesis (DPA) (Hess et al., 2002). However, while endosperm IAA increased at 19 DPA, embryo IAA content decreased from 34 μmol kg^{-1} DM at 13 DPA to 15 μmol kg^{-1} DM 6 days later. This increase in IAA may be enhancing the sink capacity of the grain and increasing grain size (Hess et al., 2002). It has also been shown that the absence of IAA causes abnormal embryo development (Naylor, 1984), possibly because auxin is

essential to establish embryo polarity (Picciarelli et al., 2001). Overall the current literature suggests that auxin during grain filling contributes to grain growth.

1.5.5 Jasmonic acid (JA)

Jasmonic acid is best known to be a plant regulator in response to abiotic and biotic stress, such as drought stress (Javadipour et al., 2019) or disease resistance to *Fusarium culmorum* (Imriz, 2020). However, JA is also important for plant growth and developmental effects (Wasternack and Hause, 2013).

Biosynthesis pathway and structure

Jasmonic acid along with its methyl ester (MeJA) and isoleucine conjugate (JA-Ile) and others are a group of fatty acids collectively known as jasmonates, which are derived from cyclopentanones and are produced either enzymatically or through autoxidation (Ali and Baek, 2020). In the cytoplasm, MeJA is produced through the activity of JA carboxyl methyltransferase (JMT) and JA-Ile is produced through a reversible conversion catalysed with jasmonate amino acid synthetase 1 (JAR1, Figure 1.11) (Ruan et al., 2019). It is suggested that JA can be irreversibly converted into the inactive and volatile *cis*-jasmone to dispose of JA (Koch et al., 1997).

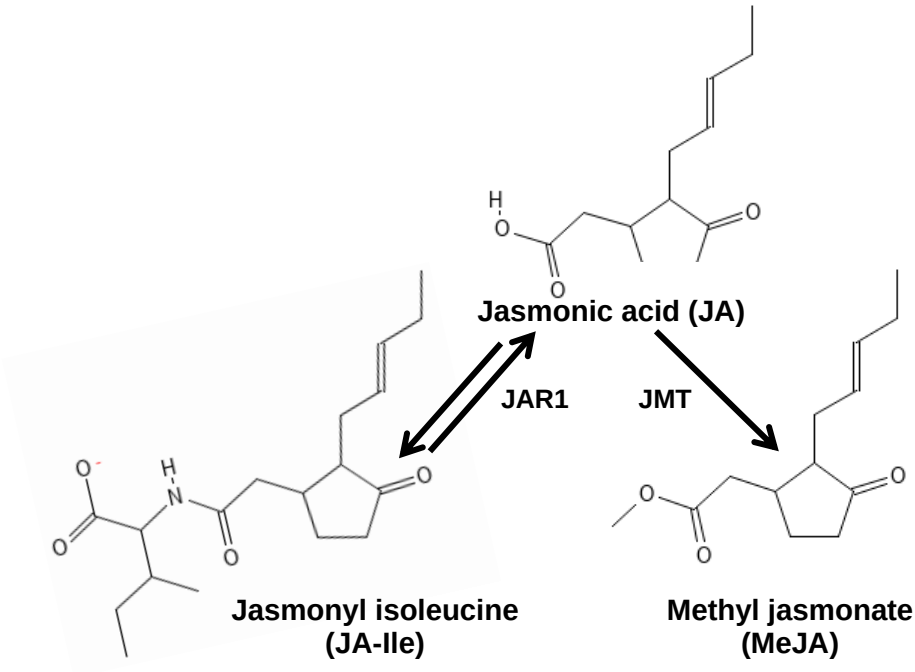

***Figure 1.11**: Key bioactive jasmonates and their conversion*

Jasmonic acid (JA) is converted to methyl-jasmonate (MeJA) through jasmonic acid carboxyl methyltransferase (JMT) and reversibly to jasmonyl isoleucine through jasmonate amino acid synthetase 1 (JAR1) (Ali and Baek, 2020)

Effects during plant development

It was previously thought that application of JA resulted in inhibition of seed germination, as applications of 10 µM of JA to alfalfa, cornflower, cress seed, maize and wheat resulted in inhibition of all species at 10 °C (Wilen et al., 1994). However, recent genetic and biochemical evidence in *Arabidopsis* has shown the inhibitory compound is the JA precursor 12-oxo-phytodienoic acid (OPDA) rather than JA itself (Dave et al., 2011). Endogenous JA detected in broad bean (*Vicia faba L.*) pericarp was found to be highest before termination of pod elongation (Dathe et al., 1981). In the same experiment, a wheat seedling bioassay reported length of seedlings was shorter with a high JA concentration, suggesting JA may have an inhibitory effect on growth.

However, in wheat, jasmonate MeJA has been shown to counteract a reduction in dormancy in grains through reducing ABA concentration (Jacobsen et al., 2013). JA has also been shown to be required for cold-induced germination in wheat (cvs. Sunstate and AC Barrie), for example, when Xu et al. (2016) inhibited jasmonate biosynthesis with acetylsalicylic acid the cold-induced germination was suppressed. The effect of the acetylsalicylic acid was rescued by adding 100 µM of MeJA, which suggested JA biosynthesis is essential for cold-induced germination in wheat. JA has also been indicated to be important in promoting seminal root formation, and therefore resource uptake in germinating seedlings (Shorinola et al., 2019). When Pigolev et al. (2021) added MeJA to Petri dishes with germinating wheat seeds (cvs. Saratovskaya-60 and Chinese Spring), while the germination rate was low, 80 % of germinated seedlings developed a sixth seminal root, while only a maximum of 20 % of control plants treated with water developed a sixth seminal root. Two wheat cultivars (cvs. Sirvan and Pishtaz) grown in the field and sprayed with 100 µM methyl jasmonate at GS39 showed an increase in grain weight of 5.4 % and 9.3 %, respectively, under fully irrigated conditions (Javadipour et al., 2019). However, the exogenous application of MeJA may be suppressing endogenous JA biosynthesis (Qiu et al., 2020). Jasmonates have yet to be studied in terms of effects on yield and yield components in high yield potential environments, but in winter wheat JA and MeJA appear to be important for germination and seminal root formation.

1.5.6 Salicylic acid (SA)

Salicylic acid plays an important role in plant defence and is involved in a number of biotic and abiotic stress responses such as pathogen infection, UV irradiation, salinity and drought (Sedaghat et al., 2017). There is also evidence that exogenous

treatments of SA increase growth and yield in wheat, if applied at the correct concentrations (Rashad, 2020).

Biosynthesis pathway and structure

Salicylic acid is derived from two independent pathways: the isochorismate synthase (ICS) pathway and the phenylalanine ammonia-lyase (PAL) pathway, both starting from chorismate (Figure 1.12). Currently, not all the enzymes catalysing these pathways have been identified in plants (Lefevere et al., 2020). Each of the two pathways contributes different amounts of SA depending on the plant species, with the ICS pathway being the most important in *Arabidopsis* and the PAL pathway more important in rice (Lefevere et al., 2020; Peng et al., 2021). SA can be modified after accumulation, by methylation that improves its mobility, or by hydroxylation or glycosylation that inactivates it (Lovelock et al., 2016; Peng et al., 2021).

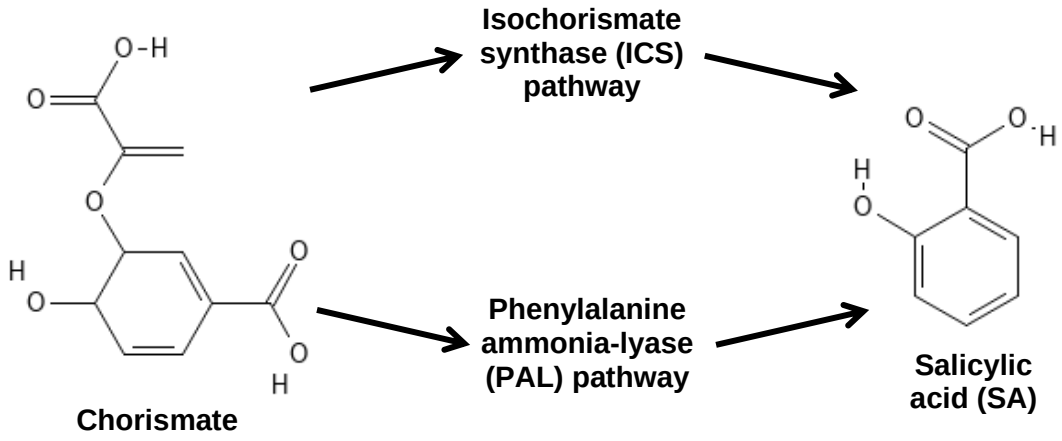

Figure 1.12: *The two pathways of salicylic acid (SA) biosynthesis*

Both pathways start with chorismate and then through conversion to isochorismate in the isochorismate synthase (ICS) pathway or through conversion to phenylalanine in the phenylalanine ammonia-lyase (PAL) pathway (Lefevere et al*., 2020; Peng* et al*., 2021)*

Effects during plant development

The vast majority of SA studies show how higher concentrations of SA decrease effects of stress (Janda et al., 2012), and there are a limited number of studies that look at SA in crops grown in optimal conditions. Treating wheat (cv. Sonalika) with a low concentration of SA (50 µM) for 7 days favoured photosynthetic activity, while a high concentration of SA (500 and 1000 µM) drastically reduced photosynthetic activity (Sahu et al., 2002). Treatment of wheat (cv. Saratovskaya 29) before sowing with 50 µM SA led to the germination of seeds and more seedling growth, which in the field led to higher yield and TGW, indicating SA promoted wheat grain

growth in optimal conditions (Shakirova et al., 2003). In a similar experiment, wheat seeds (cv. Misr 1) were soaked in SA for 12 hours before sowing in the field, and the SA treatment increased grain yield by 1.58 % compared to the control (Rashad, 2020). However, when SA was applied pre-planting (by mixing the SA solution into the top 7.6 cm of the sand in the pot), pre-emergence (by spraying on the sand surface) and post-emergence (by spraying on the plant foliage) to oats (cv. Goodfield), shoot dry weight 21 days post-emergence was reduced (Shettel and Balke, 1983). As was indicated in the study by Sahu et al. (2002), while low concentrations of SA favoured photosynthetic activity, high concentrations caused a negative effect, in this case through a reduction in shoot dry weight. This negative effect reported by Shettel and Balk (1983) may be due to SA concentrations being too high, although this paper does not report the concentration of SA, but the amount sprayed in kg ha^{-1}. Overall, the current evidence in wheat is that exogenous applications of SA at the correct concentrations may increase plant growth and yield, however currently no research has studied the effects of endogenous concentrations of SA in relation to yield traits.

1.5.7 Conclusions

As has been demonstrated in this section of the literature review, the effects of plant hormones depend on the exact growth stage and plant component that has been sampled. Plants are complex, multicellular organisms, and so the controls that govern them are also going to be complex (Leopold and Nooden, 1984). Some general trends have been seen for hormones in cereals under optimal growing conditions (Table 1.1). Cytokinins are key regulators during meristem formation, and their interactions regulate meristem differentiation and function and have a generally positive effect on yield potential traits across all growth stages in wheat. CKs are especially important in influencing tillering and floret fertility in the pre-anthesis stage. Gibberellin pre-anthesis promotes leaf and stem elongation, as indicated by some dwarf mutants being rescued by applications of GA. Despite applications of GA increasing stem elongation, at the same time, they can increase male sterility during early floral development resulting in reduced grain set. However, around anthesis GA has been shown to have the opposite effect and rescue male sterility during flowering. High auxin levels may contribute to the generation of new axillary meristems during early stem elongation but have a negative effect in wheat on floret development later during stem elongation, when it increases floret abortion, until grain filling, when auxin can help increase grain size. Similarly, abscisic acid also has negative effects during floret development,

but in grain filling, ABA could have a positive effect on dormancy, if applied at the correct time. Jasmonic acid could be important for germination and salicylic acid in low concentrations can lead to increased yield.

Not covered in detail in this section is the cross-talk between hormones. If hormones are affecting the same process, while they could be acting independently, they are likely interacting through either a non-additive effect or additive effect (Evans, 1984). Many of these previous studies have investigated exogenous applications rather than endogenous concentrations of hormones, and information on wheat is scarce. Therefore, more information on how each hormone affects grain number and size at different growth stages in wheat and studies on their genetic regulation is required to accelerate yield gains and identify genes and associated markers for marker-assisted selection.

Table 1.1 Summary table of reported investigations on how different plant hormones (cytokinins, gibberellins, abscisic acid, auxin, jasmonic acid and salicylic acid) affect yield traits in small grain cereals

Hormone	Effect	Germplasm	Environment	Papers
Cytokinin (CK)	Reduction in expression of *TaCKX2.4* resulted in an increase in grain number per spike	Transgenic wheat with RNAi gene silencing	Growth chamber under controlled conditions	Jablonski et al. (2020)
	Increase in yield and grain number through the application of CK 6-BA a) poured into pots until spikelet differentiation and b) foliar spray 25 days after the initiation of stem elongation	a) Spring barley cv. Ark Royal b) Chinese winter wheat cv. Yumai 49-198	a) Pots grown in the open b) Field trial	a) Williams and Cartwright (1980) b) Zheng et al. (2016)
	Grain CK levels were highest immediately after anthesis during embryo differentiation	a) Wheat cv. Kopara b) Spring wheat cv. PCYT-20	a) Field trial b) Grown in the glasshouse	a) Jameson et al. (1982) b) Hess et al. (2002)
	An allelic variant of *TaGW2-6A* that results in loss of function, CK biosynthesis increased, as did grain size and grain weight	Chinese spring wheat cv. NIL31	Field trial	Geng et al. (2017)
	Reduction in expression of *TaCKX2.4* resulted in an increase in grain number per spike of 5.8-12.6 %	Bread wheat cv. NB1 transformed with RNAi gene silencing	Isolated field trial for GMOs	Li et al. (2018a)

Hormone	Effect	Germplasm	Environment	Papers
Gibberellins (GA)	Spraying GA sensitive cultivars with GA3 resulted in stem elongation	Spring wheat cvs. Buck Manantial and Klein Atlas	Glasshouse and field trials	Colombo and Favret (1996)
	Injecting GA3 into the leaf sheath cavity early in floret development increased the number of fertile florets, but later did not	Winter wheat cv. YM 158	Field trial	Wang et al. (2001)
	Applying GA3 to male-sterile barley before anthesis rescued fertility	Barley cv. Maris Baldrie	Glasshouse	Kasembe (1967)
Abscisic acid (ABA)	Panicle removal decreased ABA level, while ABA application slowed the growth of tiller buds	Rice – Japonica cvs. Nanjing 44 and Indica cv. Yangdao 6	Field trial	Liu et al. (2011)
	Foliar spray of ABA at shoot enlargement and anthesis promoted grain yield	Wheat cv. Condor Relmo	Field trial	Travaglia et al. (2010)
	Blocking ABA synthesis in developing grains of wheat prevented dormancy	Winter wheat cvs. Brevor and Greer	Glasshouse	Rasmussen et al. (1997)

Hormone	Effect	Germplasm	Environment	Papers
Auxin	Adding IAA during all floret developmental stages inhibited spike development, resulting in loss of grain	Winter wheat cv. YM 158	Field trial	Wang et al. (2001)
	In early spike development, there was increased auxin signalling as the plant moved through developmental stages	Winter wheat cv. Kenong 9204	Growth room under long-day conditions	Li et al. (2018b)
	Injecting IAA into the peduncle in grain filling stimulated photoassimilate transport	*Triticum turgidum* cv. Franshawi	Glasshouse, 10 seedlings per 1.5L pot	Darussalam et al. (1998)
Jasmonic acid (JA)	MeJA counteracted a reduction in dormancy by reducing ABA concentration	Wheat cvs. Sunstate, Aus1408 and AC Barrie	Glasshouse	Jacobsen et al. (2013)
	JA required for cold-induced germination	Wheat cvs. Sunstate and AC Barrie	Phytotron glasshouse	Xu et al. (2016)
Salicylic acid (SA)	Low concentration of SA favoured photosynthetic activity, high concentration caused a negative effect	Wheat cv. Sonalika	Growth room	Sahu et al. (2002)
	Treating seeds before sowing with a low concentration of SA led to the germination of seeds and ultimately higher TGW and yield	Wheat cv. Saratovskaya 29	Field Trial	Shakirova et al. (2003)

1.6 Evolution and domestication of bread wheat

Hexaploid bread wheat (AABBDD) domestication occurred through the natural crossing of *Triticum urartu* (AA) and *Aegliops speltoides (BB)* to produce emmer wheat (AABB) 0.5 million years ago, and then 8,000 years ago a second hybridisation event which occurred between emmer wheat and *Ae. tauschii* (DD), which led to modern bread wheat *Triticum aestivum* L. (Figure 1.13) (Haas et al., 2019). These hybridisation and subsequent domestication events occurred in an initially small population of genotypes which has led to a genetic bottleneck that means there is limited genetic diversity in modern bread wheat (Winfield et al., 2016).

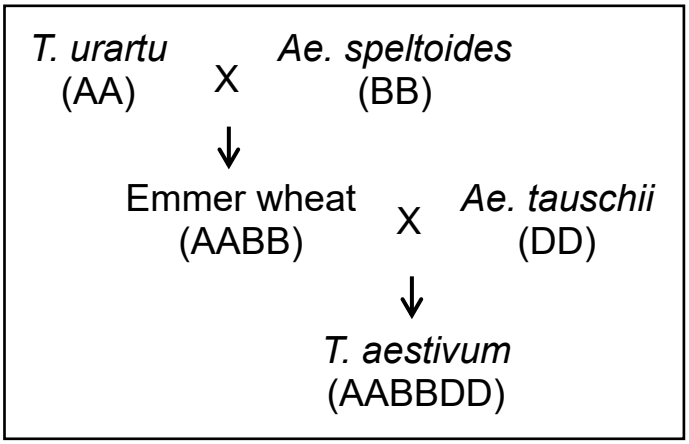

***Figure 1.13**: Summary of bread wheat (T. aestivum) genome domestication*

Methods for genetic analysis and mapping of the natural variation in crops were developed a few decades ago (Alonso-Blanco et al., 2009), and this has been mainly carried out through quantitative trait loci (QTL) linkage mapping and more recently through genome-wide association studies (GWAS), facilitated with the fully annotated wheat reference genome (IWGSC et al., 2018). Major genes identified in wheat are the vernalisation *Vrn* genes, which divide wheat into spring and winter classes, the photoperiod response *Ppd* genes, which divide wheat into photoperiod sensitive and insensitive classes and the reduced height *Rht* semi-dwarfing genes which are effective in reducing plant height (Distelfeld et al., 2009; Sukhikh et al., 2021). These genes have been key in understanding how wheat works, and subsequently increasing yield, through adapting the duration of the life cycle to specific environments, avoiding frost risk and optimising the photo-thermal quotient for grain filling and increasing grain partitioning. Identification of further QTL or SNP markers is important so more yield improving traits can be

incorporated into elite wheat varieties through marker-assisted selection (MAS). Many major genes identified to date are for qualitative traits such as disease resistance, and future application of genes should focus on quantitative traits for resource-use efficiency.

1.6.1 Quantitative trait loci (QTL) linkage mapping

The genetic variation of a complex trait is controlled by the effects of numerous genes. The genetic regions associated with a particular trait are known as quantitative trait loci. To utilise these QTLs in crop improvement, they need to be mapped using molecular markers. For QTL mapping, two diverse parents are selected that have different alleles affecting variation in a trait, before an appropriate mapping population is developed by crossing the parents. Near-isogenic lines (NILs), doubled-haploids (DH), backcrosses, recombinant inbred lines (RILs) and F_2 populations can be used (Nadeem et al., 2018). Once these lines have been phenotyped for the trait of interest and the population has been genotyped, a genetic map can be constructed and molecular markers identified and linked to the trait of interest (Sehgal et al., 2016). There are five methods used for detecting QTLs, as described in Sehgal et al. (2016) and Jansen (2007):

1. **Single-marker analysis**: phenotypic means of each marker class are compared and analysed using a t-test. When logarithm of odds (LOD) scores exceed a significance threshold this indicates a QTL is located in the vicinity of the marker
2. **Interval mapping by maximum likelihood**: test a model for the presence of a QTL at many positions between two mapped marker loci
3. **Interval mapping by regression**: A simplification of the maximum likelihood method, where phenotypes are regressed on QTL genotypes which are replaced by probabilities estimated by the nearest flanking markers
4. **Composite interval mapping**: to overcome bias from two linked QTLs, this method will perform analysis like the others, except for the variance from other QTLs is accounted for, by including regression coefficients from markers in other regions of the genome as covariates in the analysis
5. **Multiple-QTL mapping**: first, multiple genotypes are modelled with their estimated probabilities, then important markers that are not near the QTL are selected with multiple regression and backwards elimination to be used as cofactors in the mapping, using the most informative model through maximum likelihood

While single-marker analysis is the traditional method, maximum likelihood is the most common method of QTL analysis. QTL mapping is still used and has identified QTLs for key yield traits in wheat, as summarised in Table 1.2. For example, Pretini et al. (2020) used 102 doubled-haploid lines (Baguette 19 x BIOINTA 2002, with high and low fruiting efficiency, respectively) and conducted a QTL analysis using composite interval mapping. They identified 37 QTL, two of which were major for fruiting efficiency calculated with chaff dry weight (chr 3A) and anthesis spike dry weight (chr 5A). Alonso et al. (2021) developed a population of 80 RILS (derived from a cross between Baguette 10 x Klein Chajá) and conducted a QTL analysis using composite interval mapping and identified three more QTLs associated with fruiting efficiency on chromosomes 2D, 4A and 7A.

QTL mapping is useful for identifying genetic loci for traits, but the precision with which the QTL are identified depends on the genetic variation covered by a mapping population as well as the size of a mapping population (Sehgal et al., 2016). Low marker coverage and density as well as limited numbers of recombination events in a population imposed major constraints on the resolution of QTL studies in the past (Crossett et al., 2010). Therefore, it is now considered the ‘classical approach’. In comparison, genome-wide association studies (GWAS) can survey a larger gene pool and bypass the need for crossing cycles to generate populations (Neumann et al., 2011).

***Table 1.2**: Summary of past wheat QTL linkage mapping studies on a range of grain partitioning traits and their associated genomic regions*

Traits	Chromosomes	Germplasm	Environment	Genotyping	Papers
FE chaff dry weight	2D, 4A, 7A	80 RILS developed from cvs. Baguette 10 and Klein Chajá	Field trials	Axiom 35K SNP wheat breeders array	Alonso et al. (2021)
Fertile florets per spike dry weight at anthesis	1A, 2A, 5A, 5B, 6B	102 DH lines developed from cvs. Baguette 19 and BIOINTA 2002	Field trials	90 K Illumina iSelect SNP Array	Pretini et al. (2020)
FE spike dry weight	1B, 1D, 2D, 4D, 5A, 6B, 7B				
FE chaff dry weight	1A, 2D, 3A, 4D, 5A, 6A, 7A				
Grain number per spike	2B, 4A, 5A, 6B, 7A	203 DH lines developed from cvs. ND3338 and JD6	Field trials	90 K Illumina iSelect SNP Array	Guan et al. (2018)
Thousand grain weight	2A, 2D, 4A, 4B, 5A, 6A, 7A				
Grain weight per spike	2A, 2B, 2D, 4B, 7A				
Plant height	1B, 2D, 3A, 4B, 4D, 5A, 6A, 6D, 7A, 7B				
Thousand-grain weight, grain yield, grain number per spike	3A	95 recombinant inbred chromosome lines (RICLs) developed from cvs. Cheyenne and Wichita	Field and glasshouse trials	RFLP, SSR, STM and DArT molecular markers were used	Rustgi et al. (2013)

1.6.2 Genome-wide association studies

Recent advances in DNA sequencing has led to development of methods such as genotyping-by-sequencing, resulting in improvement in SNP discovery rates. In wheat, thousands of single nucleotide polymorphisms (SNPs) have been generated that cover most of the genome e.g. Walkowiak et al. (2020). A genome-wide association study is a statistical approach that was developed to identify SNPs that relate to important phenotypic traits. As advances in technology continue, the number of SNPs is increasing (Nadeem et al., 2018).

To perform a GWAS, a group of genotypes that have a wide range of genetic diversity must first be selected, the larger the population size, the more power the GWAS will have. Therefore, a minimum of 100 genotypes are required (Kumar et al., 2012). Then, the phenotypic characteristics of the population must be measured before genotyping the population with molecular markers. Using the molecular marker data, the extent of linkage disequilibrium (LD) of a population, an indicator to detect the distance between loci, must be quantified. The population structure, the level of genetic differentiation among a population, and kinship, the coefficient of relatedness between pairs of individuals, are then assessed and that information is used to test the association between the phenotypic characteristics and genotypic data (Sehgal et al., 2016).

If population structure and kinship is not correctly controlled for, it can lead to false-positive associations in GWAS studies (Kang et al., 2008). The identification of markers is also complicated by confounding effects of plant phenology, a lot of traits interact with plant height and flowering time, and these can mask the identification of minor genes, so GWAS populations must be controlled for phenology and plant height (Lopes et al., 2015). It is also important to remove SNPs that have a low minor allele frequency MAF) as they lead to a lack of resolution and power (Soto-Cerda and Cloutier, 2012). However, rare alleles have been shown to have a relatively large effect on complex traits (Youssef et al., 2017). GWAS based on SNPs also relies on the genetic reference that was used for sequencing and mapping the individuals, which means errors in the reference map can lead to errors in the GWAS (Alqudah et al., 2020b). Despite some limitations that need to be carefully considered when performing GWAS, the advantages are that no parents or crossing are required unlike in QTL mapping, historical phenotypic data can be used, and there's an unlimited number of accessions or phenotypes that can be analysed (Alqudah et al., 2020b).

Different statistical models can be used to conduct a GWAS. The general linear model (GLM) does not take population structure into account and has widely been replaced by the mixed linear model (MLM), which does consider population structure in its model (Alqudah et al., 2020b). Several methods have been developed to increase the efficiency of the MLM, and which are listed below as documented in Cortes et al. (2021):

- **Efficient mixed-model association** (EMMA) – improves speed by eliminating redundant matrix operations
- **Genome-wide efficient mixed-model analysis** (GEMMA) – improves efficiency by rewriting the likelihood function of the MLM in a form that's easier to evaluate – produces results identical to EMMA with increased speed
- **Compressed MLM** (CMLM) – improves power by using a lower-rank kinship matrix
- **Settlement of MLM under progressively exclusive relationship** (SUPER) – calculates kinship matrix more rapidly by using a reduced but carefully selected number of SNPs
- **Multi-locus mixed model** (MLMM) – improves on single-locus methods by incorporating multiple markers in the model simultaneously as covariates
- **Fixed and random model circulating probability unification** (FarmCPU) – also builds upon MLMM, a multi-locus method that uses the reduced-rank kinship matrix of SUPER to improve power and efficiency
- **Bayesian information and LD iteratively nested keyway** (BLINK) – a modified FarmCPU which enhances power by relaxing the requirement of SUPER that SNPs have to be evenly distributed in bins throughout the genome

These models have been used in a variety of genome-wide associations studies performed in wheat to produce numerous marker-trait associations and candidate genes. These GWA studies are listed in Table 1.3.

***Table 1.3**: Summary of past genome-wide association studies on a range of grain partitioning traits and their associated genomic regions*

Target trait	Traits	Chromosomes	Germplasm	Environment	Genotyping	Papers
Yield traits	Yield	2A, 2B, 3D, 4A, 5A, 5B, 6A, 6B, 7B	179 spring bread wheat cultivars	Field trial	20K Illumina iSelect SNP array	Amalova et al. (2021)
	Grains per spike	1A, 1B, 1D, 2A, 2B, 2D, 3B, 4A, 4B, 5A, 5B, 6A, 6B, 7A, 7D				
	Thousand grain weight	1B, 1D, 2A, 2B, 4B, 5A, 5D, 6A, 6B, 7A, 7B, 7D				
	Plant height	1B, 2B, 3A, 3D, 5A, 5B, 6A, 7A				
	Peduncle length	1A, 1B, 1D, 2B, 3B, 4B, 5A, 6A, 6B, 7A				
Yield traits	Yield	2A, 4B, 5A, 7A	96 wheat cultivars with high diversity in yield traits	Field trials	15K Infinium SNP array	Alqudah et al. (2020a)
	Harvest index	2B, 2D				
	Thousand-grain weight	1B, 4B, 6A				
	Grain weight per spike	2B, 5B, 6A				
	Grains per spike	1A, 2B, 2D, 3B				
	Peduncle length	2B, 3B, 4D, 5D, 6A, 7A				

Target trait	Traits	Chromosomes	Germplasm	Environment	Genotyping	Papers
Grain yield	Grain yield	1B, 2B, 4A, 5B, 6B, 7B	6,461 spring bread wheat cultivars	Field trial	192-plexing on Illumina HiSeq2000	Sehgal et al. (2020)
Radiation-use efficiency and yield traits	Grain yield	5A, 6A, 7A	High Biomass Association Spring wheat panel (150 cultivars)	Field trial	Axiom 35K SNP wheat breeders array	Molero et al. (2019)
	Harvest index	2B, 6A				
	Thousand-grain weight	2D, 6D				
	Grains per m^2	2B, 3B, 5A, 6D, 7B				
	RUE from anthesis + 7 days until physiological maturity	1A, 1D, 2A, 5A, 6A				
Yield traits	Spike weight at anthesis	2B, 7A	96 wheat cultivars including founder genotypes globally	Field trial	15K Infinium SNP array	Gerard et al. (2019)
	Grains per spike	1A, 2B, 2D				
	Thousand-grain weight	1B, 2A				
	Grain weight per spike	2A, 2B, 7A				
	FE anthesis dry weight	2A, 2D, 4D, 5A				
Yield traits	Thousand-grain weight	1A, 2A, 2B, 2D, 4A, 4B, 5B, 6A, 7A, 7B, 7D	192 bread wheat cultivars including 25 SHW, 80 landraces	Field trial	90 K Illumina iSelect SNP Array	Liu et al. (2018)
	Plant height	1A, 1B, 1D, 2A, 2B, 2D, 3B, 4A, 4B, 4D, 5A, 5B, 5D, 6A, 6B, 6D, 7A, 7B, 7D				

Target trait	Traits	Chromosomes	Germplasm	Environment	Genotyping	Papers
Yield traits	Grain yield	1A, 2A, 2B, 3B, 4A, 4B, 5A, 7A	239 cultivars of soft red winter wheat	Field trial	Illumina 9K iSelect assay	Lozada et al. (2017)
	Grains per spike	1A, 2B, 2D, 3A, 3B, 4B, 5A, 5B, 6A, 7A, 7B				
	Grain weight per spike	3A, 4A, 4B, 4D, 5A, 6B,7D				
	Peduncle length	1A,2A,2D, 3A, 3B, 7A				
Floret fertility	Apical grains per MS	1A, 1D, 3A, 3D, 7A, 7D	210 German hexaploid winter wheat cultivars	Glasshouse	90K Illumina iSelect SNP Array	Guo et al. (2017)
	Central grains per MS	6A, 6D				
	Basal grains per MS	6A, 6D				
	Grain number	2D, 3B				
	Grain weight	1B, 7A				
	FE chaff dry weight	2B, 5B, 6B				

1.6.3 Molecular plant breeding

To utilise the markers identified from GWAS analysis to improve wheat, they need to be deployed into breeding programs. Two ways this can happen are through marker-assisted selection (MAS) and genomic selection. The use of mapped genes in breeding through MAS is mainly constrained to simple monogenic traits and works best when manipulating a few major effect genes rather than many small-effect genes (Heffner et al., 2009). Genomic selection was developed to overcome the limitations of MAS, by estimating all locus, haplotype or marker effects across the entire genome to calculate genomic estimated breeding values (GEBVs). This differs from traditional MAS as there's not a defined subset of significant markers but all markers on a population are used to explain the total genetic variance (Heffner et al., 2009). Genomic selection has been indicated to outperform MAS even at low GEBV accuracies (Heffner et al., 2010).

Recently, The International maize and wheat improvement center (CIMMYT) used genomic selection for grain yield in their wheat breeding program, which highlighted the complexity of grain yield and indicated using genomic predictions and genotype x environment models was not an ideal solution, and shouldn't be used in place of multi-environment testing (Juliana et al., 2020). The genotype x environment interaction is strong in wheat and this can make it more difficult to consistently predict performance, therefore other genomic-selection studies have reported the highest prediction accuracies with genotype x environment models (Lopez-Cruz et al., 2015). It has been observed that having fewer related individuals in a population reduces the prediction accuracies for genomic selection, suggesting if a plant breeding program is applying genomic selection, it could benefit from phenotyping a smaller training population of closely related individuals (Lorenz and Smith, 2015). Further advances of genomic selection in plant breeding need to focus on how to incorporate unknown parents in a breeding program (Robertsen et al., 2019).

Due to the difficulty in understanding the genetic background of complex traits, there is value in dissecting a complex phenotype such as grain yield into several component traits. In doing this, fewer associations are detected for each component trait but with greater statistical significance.

1.7 Project objectives and hypotheses

The overall aim of the project was to identify novel grain number and partitioning traits for advancing harvest index and grain yield, and to determine how they are influenced by spike hormones using a high biomass spring wheat panel, and to understand their genetic regulation.

The specific objectives of the thesis were:

1. To identify and quantify genetic variation and heritability in new plant hormone and physiological traits that determine grain number, harvest index and yield in a set of 150 high biomass spring bread wheat cultivars in the field in NW Mexico, and perform detailed analysis on a subset of 10 lines in glasshouse experiments at the University of Nottingham, UK
2. To identify how endogenous spike hormonal levels influence genetic variation in grain number traits at growth stages key to grain number development – late booting and anthesis
3. Develop breeder-friendly molecular markers for grain partitioning traits, harvest index and grain yield and associated spike hormone traits through a genome-wide association study

The specific hypotheses of the thesis were:

1. Genetic variation in grain yield in the HiBAP II panel is correlated with both harvest index and above-ground dry matter at maturity. Grain number per m^2 and grain yield are positively correlated among genotypes in the HiBAP II panel
2. In both the glasshouse and the field experiments, increasing grain number is associated with increased spike partitioning index and fruiting efficiency among HiBAP II genotypes
3. A trade-off is observed between spike partitioning index and fruiting efficiency among HiBAP II genotypes
4. Competition for assimilates between spike growth and stem internodes 2 and 3 growth is stronger than between spike growth and the peduncle growth, so that the negative association with spike PI and grains m^{-2} is stronger for true-stem internodes 2 and 3 than the true-stem peduncle PIs
5. Genetic variation in spike hormones, in particular spike cytokinins, is associated with key grain number traits such as fruiting efficiency in both the glasshouse and field experiments among the subset of HiBAP II genotypes

6. High abscisic acid spike hormone levels pre-anthesis have a negative association with spike fertility traits determined at anthesis
7. In the glasshouse, a gradient is observed in hormonal concentrations throughout the spike (basal, central and apical spikelets) and plant (spike, flag leaf, stem) at both anthesis and booting in the HiBAP II subset
8. Marker-trait associations can be identified for spike hormonal traits and key grain partitioning traits by GWAS in the HiBAP II panel
9. Co-locating markers will be identified with fruiting efficiency and spike hormone traits
10. Candidate genes for the key SNPs associating with grain partitioning traits and spike hormonal traits can be identified and functions ascribed as reported in previous literature

1.8 Work contribution

All the work presented in this thesis is my own, except where indicated below.

Data collected in the field experiments in NW Mexico at CIMMYT were completed with the help of the physiology CIMMYT team. These data are presented in chapter 3 and chapter 5. Data collected in the glasshouse experiments at the University of Nottingham were completed with the help of John Foulkes' lab. In particular, hormonal sampling in 2019 was completed with the help of fellow PhD student James Garner. These data are presented in chapter 4. The hormonal analysis was completed in collaboration with Prof. Sergi Munné-Bosch at the University of Barcelona, and these data are presented in chapters 3, 4 and 5.

All data analysis in chapter 3 and chapter 4 is my work. The genotyping mapping data presented in chapter 5 was provided by Dr Anthony Hall's group at the Earlham Institute. Guidance on performing the genome-wide association study was given by Dr Rahul Bhosale at the University of Nottingham, but the GWAS analysis was performed by me.

Chapter 2: Overview of Materials and Methods

This chapter is a brief overview of the methodology for the experiments in this PhD project presented in chapters 3-5. For a more detailed description of the methods see each chapter's methodology.

2.1 Plant material and experimental design

2.1.1 The High Biomass Association Panel (HiBAP II)

The High Biomass Association Panel (HiBAP II) contains 150 CIMMYT spring wheat genotypes which all have an outstanding expression of high biomass and/or biomass-related traits (Table S 1). It is comprised of 8 landrace-derivatives, 32 synthetic-derivatives, 13 landrace- and synthetic-derivatives, and 97 elite cultivars. Two subsets were selected for more detailed lower-throughput physiological measurements. Subset 1 contained 30 genotypes (with 2 further lines added in the second year to make 32 lines) and within subset 1, 10 genotypes were selected which generated subset 2. Subset 1 was selected with a restricted range of anthesis date but variation for spike partitioning index, subset 2 was selected to contrast for fruiting efficiency.

Field experiments were carried out on all 150 lines of the HiBAP II in each of two field seasons, 2017-18 and 2018-19, under yield potential conditions at the Norman E. Borlaug experimental station near Ciudad Obregon, Sonora, Mexico. Glasshouse experiments were carried out on the 10 subset 2 genotypes in each of three years – 2017, 2018 and 2019, under yield potential conditions in Nottingham, UK.

2.1.2 Experimental design and growing conditions

In the field, the plants were grown in 1.6 x 4.0 m plots (2017-18) and 1.6 x 5.0 m plots (2018-19) (two beds per plot, each with two rows) with three replicates in a raised-bed planting system, randomised in an α-lattice design. The seeds were sown on 23rd November 2017 and 27th November 2018. Irrigation was supplied every 3-4 weeks using a gravity-based system, where the channels between beds were flooded. N fertiliser was applied with three irrigations with a gravity-based system.

In the glasshouse, plants (one per pot) were grown in 2 L pots filled with John Innes no. 2 soil medium, with four replicates in 2017 and 2019 and five replicates in 2018, in a randomised complete block design. The seeds were sown on 2nd August 2017, 13th June 2018 and 3rd June 2019 for the three years. Irrigation and fertiliser were

supplied throughout the cycle daily using drip irrigation. In both the glasshouse and field, herbicides, fungicides and pesticides were added as necessary to minimise the effects of weeds, diseases and pests.

2.2 Crop physiology measurements

2.2.1 Growth analysis at anthesis

In the field, anthesis measurements were taken at anthesis + 7 days (GS65+7d), to coincide with the onset of the linear grain growth phase (Zadoks et al., 1974). The lengths of the peduncle, stem internode 2 and stem internode 3 were recorded, as well as plant height (height recorded at the start of grain filling). Fresh and dry weight were recorded, and the fertile shoots were split into spike, leaf lamina and stem. Twelve stems of subset 1 (30 genotypes) were then further separated into the true stem and leaf sheath for each internode – peduncle (ped), stem internode 2 (int2), stem internode 3 (int3) and stem internode 4 and below (int4+), and then the partitioning index (PI) was calculated for the component as the proportion of above-ground biomass. In subset 2 (10 genotypes), four spikes were then separated into the rachis, glumes, awns, palea, lemma and other (small grains and anthers). PI for the spike components was calculated as the proportion of the whole spike dry matter (DM) excluding the grains and anthers. Rachis and stem specific weight was calculated as the component dry matter per unit length.

In the glasshouse at anthesis (GS65), the plants were separated into i) main shoot (MS), ii) other fertile shoots and iii) infertile shoots. Each fertile shoot was then separated into spike, leaf lamina and stem. On the MS stem, the lengths of the ped, int2 and int3 were recorded, as well as plant height, before it was separated into the true stem and leaf sheath for each internode as described above. The MS spike was also separated into the rachis, glumes, awns, palea, lemma and other (small grains and anthers, not included in the partitioning analysis). PI was calculated for both the leaf lamina, true stem, leaf sheath and spike and the spike components in the same way as in the field experiments. Flag-leaf photosynthesis rate measurements were taken in all three years with a Licor 6400 photosynthesis system, in both the pre- and post-anthesis phases, as described in chapter 4.2.

2.2.2 Growth analysis at physiological maturity

At physiological maturity, 50 fertile shoots in the field and all fertile shoots in the glasshouse were cut at ground level and separated into the spike and straw (stem and leaves), before the ears were threshed to obtain the dry weight of grains and chaff, as well as grain number. These data were then used to calculate harvest

index (HI, proportion of above-ground DM in the grain), above-ground DM ($AGDM_{PM}$) and fruiting efficiency (FE, ratio of grain number to spike DM at anthesis or to chaff DM at maturity). In the field, after physiological maturity, grain yield was measured in each plot by machine harvesting, and values were further adjusted to moisture percentage measured in each plot.

2.3 Plant hormone analysis

2.3.1 Field

In the field experiments, spikes were sampled for plant hormone analysis only in 2018-19. At late booting (GS49) subset 2 was sampled in 3 replicates, and at anthesis (GS65) spikes were sampled in 2 replicates for all 150 genotypes. Two spikes per plot, one from each inner row of each of the two beds, both at similar heights and growth stages were sampled and frozen in liquid nitrogen immediately in the field.

2.3.2 Glasshouse

In 2017, 2018 and 2019 the MS spike of each genotype in subset 2 was sampled for plant hormones at GS49 and GS65. Additionally, in 2019 genotypes 1 and 9 (Table 4.1) were selected to show low (genotype 1) and high (genotype 9) fruiting efficiency values from 2017 and 2018 glasshouse data. These two genotypes were sampled at GS49 and GS65 for the flag leaf and peduncle, and at GS65 the spike was split into three sections (basal central and apical spikelets). Each plant component was sampled in the glasshouse and immediately frozen in liquid nitrogen.

2.3.3 Laboratory analysis

In the laboratory, 100 mg of frozen material was subsampled. The sub-samples were then sent to the Department of Evolutionary Biology, Ecology and Environmental Sciences at the University of Barcelona, for plant hormone profiling analysis performed by Prof. Sergi Munné-Bosch using liquid chromatography coupled to electrospray ionization tandem spectrometry (UPLC/ESI-MS/MS) (Müller and Munné-Bosch, 2011).

2.4 Statistical analysis

2.4.1 Field and glasshouse experiments

The genotype best-linear unbiased estimates (BLUEs) were estimated from the cross-year Analysis of Variance (ANOVA) using META-R 6.0 (Alvarado et al., 2015) for the field data, and Genstat 19th edition (VSN International, 2021) for the

glasshouse data. Days to anthesis was added as a covariate when it had a significant effect. Genstat 19th edition (VSN International, 2021) was used for calculating Pearson's correlation coefficients and linear regressions using the BLUEs calculated previously from the ANOVAs. Principal component analysis (PCA) was used to examine associations between plant hormones and key grain yield traits and grain yield and was performed using the R package FactoMineR (Lê et al., 2008).

2.4.2 Genome-wide association analysis

A detailed GWAS methodology can be found in chapter 5.2. It was performed using the 2-year field BLUEs and genotyping data obtained at the Earlham Institute by Anthony Hall's research group, as described by Joynson et al. (2021). The panel was genotyped using enrichment capture sequencing and de novo SNP discovery, and mapped to the RefSeq-v 1.0 reference sequence (IWGSC et al., 2018). Single nucleotide polymorphisms (SNPs) that had ≥10 % missing data and a minor allele frequency of ≤5 % were removed. Population structure was inferred using both STRUCTURE 2.3.4 (Pritchard et al., 2000) and principal component analysis with the PCA data produced in FarmCPU (Liu et al., 2016), and drawn using R v.4.0.3 (R Core Team, 2020) package ggplot2 (Wickham, 2016).

Genome-wide association analysis was carried out using FarmCPU (Liu et al., 2016) through GAPIT3 (Wang and Zhang, 2021) in R v.4.0.3 (R Core Team, 2020). The model was adjusted using the first two PCs suggested from the PCA for most traits, 0 PC were added for traits where two PCs were adding confounding data and making the QQ plots deviate from the diagonal line. To identify possible candidate genes, intervals +/- 500,000 bp were submitted to Knetminer (Hassani-Pak et al., 2021).

Chapter 3: Field Experiments on the High Biomass Association Panel (HiBAP II)

3.1 Introduction

Yield potential is the maximum attainable yield per unit land area achieved by a crop cultivar in an environment that it is adapted to when water and nutrients are non-limiting, and diseases and other stresses are controlled (Evans and Fischer, 1999). In some environments, improving agronomic practices could help to increase grain yield (GY) by closing the gap with yield potential. However, implementation of improved agronomic practices can be much less straightforward and more expensive than developing new cultivars (Foulkes and Reynolds, 2015), and there is evidence that plant breeding is becoming a proportionally larger component of yield improvement than crop management (Fischer and Edmeades, 2010; Mackay et al., 2011).

There have been continuous improvements in grain yield of ca. 1 % per annum through wheat breeding since the Green Revolution associated with increased resistance to disease, adaptation to abiotic stress and genetic improvements in yield potential (Shearman et al., 2005; Reynolds et al., 2009). Although a lot of breeding to date has been based on direct selection for yield, there is strong evidence that the breeding process could be accelerated by an improved understanding of traits at the physiological level (Foulkes et al., 2011). One such trait that has been strongly associated with grain yield is grain number per unit area (Peltonen-Sainio et al., 2007; Fischer et al., 2014). In the past, wheat yield improvement was the result of increased partitioning of dry matter to the grain, in large part through the introgression of *Rht* semi-dwarfing genes during the Green Revolution (Miralles and Slafer, 2007). Despite this, evidence suggests that during grain filling wheat yield potential is still limited by the grain sink strength under favourable environments and, therefore, to increase grain yield, strategies that improve the sink capacity are crucial (Acreche and Slafer, 2009). Not only this but when the source/sink ratio is manipulated to increase sink strength, leaf photosynthesis rate post-anthesis and crop radiation-use efficiency appear to be responsive (Reynolds et al., 2005). As a result, for future improvements in the photosynthetic capacity to result in additional yield, these assimilates need to be partitioned to the developing spikes and florets during stem elongation to increase grain number. Potential grain size must also be increased to accommodate the extra assimilate (Foulkes et al., 2011).

During stem elongation, spike and stem growth overlap (Brooking and Kirby, 1981), which means the stem and the spike are competing for assimilates. This competition impacts floret survival and consequently the final grain number (Fischer, 1985; Slafer and Rawson, 1994). Therefore, if the plant decreases partitioning to the stem growth, this may favour the assimilate partitioning to the spike, resulting in increased grain number (Foulkes et al., 2011). Reducing leaf lamina partitioning may not be beneficial here because of the effect on post-anthesis photosynthetic capacity. In wheat, it has been suggested that the leaf sheaths, which are the lower leaf component that attaches to the stem node, are important for storing and later transporting assimilates to the developing grain (Araus and Tapia, 1987). In addition, it is important to take into account that reducing stem partitioning could affect translocation of stored assimilates during grain filling, or affect lodging resistance by reducing stem strength. Qin et al. (2009) reported in the wheat cultivar Shirane that the top internode of the stem – the peduncle – had a higher photosynthetic rate per unit area than the flag leaf, so reducing peduncle growth may affect the photosynthetic rate, and also later translocation of stored assimilates to the spike. On the other hand, it has previously been reported in spring wheat in field experiments in NW Mexico that true-stem internodes 2 and 3 were competing more strongly with the spike for assimilates than the peduncle, and so specifically reducing these internodes increased HI and spike partitioning index (Rivera-Amado et al., 2019; Sierra-Gonzalez et al., 2021). However, these stem internode traits need to be studied in more germplasm in order to investigate their effects further.

Another trait that could be a target to increase grain number is the fruiting efficiency (ratio of grain number to spike DM at anthesis, FE). A positive association with grains per m^2 has been identified in Mediterranean wheat cultivars (Acreche et al., 2008), Mexican spring wheat cultivars (Rivera-Amado et al., 2019) and Argentinian spring wheat cultivars (Abbate et al., 1998). An increased FE may occur through increasing the allocation of assimilates from the plant and spike to the developing florets (Slafer et al., 2015). Another trait that may be affecting both FE and grain number is spike hormone content, as plant hormones play a huge role in plant growth and development (Jameson and Song, 2016). A detailed review of the effect of hormones on plant growth both pre- and post-anthesis was set out in chapter 1.5, but in summary, cytokinins are especially important in influencing floret fertility pre-anthesis (Jameson and Song, 2016), while gibberellin can rescue male sterility during flowering (Kasembe, 1967) and auxin can help increase grain size

during early grain filling (Darussalam et al., 1998). It is important therefore to fully understand how endogenous hormone levels interact with key growth traits so they can be applied in crop improvement.

3.1.1 Chapter hypotheses

- Genetic variation in grain yield in the HiBAP II panel is correlated with both harvest index and above-ground dry matter at maturity. Grain number per m^2 and grain yield are positively correlated among genotypes in the HiBAP II panel
- In the field experiments, increasing grain number is associated with increased spike partitioning index and fruiting efficiency among HiBAP II genotypes
- A trade-off is observed between spike partitioning index and fruiting efficiency among HiBAP II genotypes
- Competition for assimilates between spike growth and stem internodes 2 and 3 growth is stronger than between spike growth and the peduncle growth, so that the negative association with spike PI and grains m^{-2} is stronger for true-stem internodes 2 and 3 than the true-stem peduncle PIs
- Genetic variation in spike hormones, in particular spike cytokinins, is associated with key grain number traits such as fruiting efficiency in the field experiments among the HiBAP II genotypes
- High abscisic acid spike hormone levels pre-anthesis have a negative association with spike fertility traits determined at anthesis in the field experiments among the subset of HiBAP II genotypes

3.2 Materials and methods

3.2.1 Plant materials and experimental design

Two field experiments were carried out, one in each of 2017-18 and 2018-19, under fully irrigated yield potential conditions at the Norman E. Borlaug experimental station near Ciudad Obregon, Sonora, Mexico (27.33°N, 109.09°W, 38 m above sea level). The soil is a coarse sandy clay, mixed montmorillonitic typic caliciorthid, low in organic matter and with a slightly alkaline pH of 7.7, as described in Sayre et al. (1997). The High Biomass Association Panel (HiBAP II) was used which contains 150 spring wheat genotypes that all have an outstanding expression of high biomass and/or biomass-related traits. It is comprised of 8 landrace-derivatives, 32 synthetic-derivatives, 13 landrace and synthetic-derivatives, and 97 elite cultivars or advanced lines (Table S 1).

In the field, the plants were grown in 1.6 x 4.0 m plots in 2017-18 and 1.6 x 5.0 m plots in 2018-19 (two beds and four rows per plot) with three replicates in a raised-bed planting system, randomised in an α-lattice design. Each bed had a 24 cm gap between rows and there was a 56 cm gap between beds (Figure 3.1). In 2017, the seeds were sown on November 23 and the emergence date was November 29, while in 2018 the seeds were sown on November 27 and the emergence date was December 3. The seed rate was 10.17 g m^{-2} in 2017-18 and 10.25 g m^{-2} in 2018-19, with plant establishment ranging from 139 to 249 plants per m^2 in 2017-18 and 132 to 214 plants per m^2 in 2018-19. Herbicides, fungicides, and pesticides were added to minimise the effects of weeds, diseases and pests (Table S 2). Irrigation was supplied throughout the cycle every 3-4 weeks using a gravity-based system where the channels between beds were flooded (Table S 3). In each season an application of N fertiliser was applied as urea to prepare the land (50 kg N ha^{-1}), and then an application of triple superphosphate at sowing (50 kg P ha^{-1}). A second and third N application (200, 150 kg N ha^{-1}, respectively) were applied with the second and third irrigations. No plant hormones were applied.

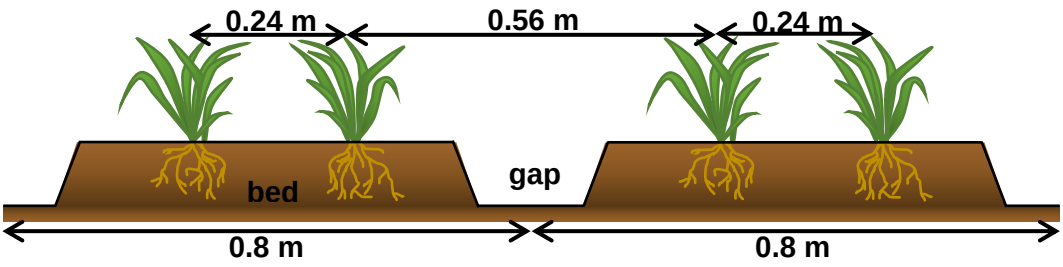

***Figure 3.1**: Transverse view of raised-bed field plot for the HiBAP II field trials*

Unless stated otherwise, crop measurements were carried out on all 150 genotypes. Two subsets were selected for more detailed crop measurements; medium intensity measurements such as stem-internode dry matter partitioning were carried out for subset 1 of 30 genotypes in 2017-18, with two further genotypes added in 2018-19. These lines were selected to contrast for high and low spike partitioning index and selected at anthesis in the first year using the present data. For the lowest throughput measurements, such as spike morphological dry matter partitioning, 10 genotypes in 2017-18 and 12 genotypes in 2018-19 of subset 1 were selected (subset 2), to contrast for fruiting efficiency using previous data sets. Both subset lists can be found in Table S 1. Subset 2 includes the 10 genotypes that were grown in the glasshouse experiments detailed in chapter 4.

3.2.2 Crop measurements

Samples were collected at late booting (GS49), seven days after anthesis (GS65+7d) and physiological maturity (GS89) (Zadoks et al., 1974). The growth stages were taken when 50 % of the fertile shoots in the plot had reached that stage (Pask et al., 2012).

Growth analysis at anthesis + 7 days

Seven days after anthesis was selected to coincide with the onset of the linear grain growth phase.

In all 150 genotypes in three replicates, sampling was carried out by cutting shoots at ground level in a quadrat of 0.8 m^2 (0.5 m in length, 1.6 m in width), leaving at least 0.25 m from the end of the plot. The fresh weight of the total sample was recorded, before a representative 50-shoot sub-sample was selected and fresh weight recorded and then dried at 70°C for 48 hours and weighed. From the remainder of the sampled material, 12 fertile shoots (spike fully emerged, <10 cm difference in height between shoots) were randomly selected for plant dry matter (DM) partitioning analysis. Each shoot was separated into the spike, leaf lamina and stem (true stem and leaf sheath attached). Each plant component was then dried for 48 hours at 70°C before dry weight was recorded. Also, the lengths of stem internode 2 and internode 3 were recorded.

In subset 1 (32 genotypes) the 12 shoots were further separated into the true-stem and leaf-sheath for each stem internode – peduncle (ped), internode 2 (int2) and internode 3 (int3) (Figure 3.2). For internode 4 and below (int4+), the leaf sheath and true stem were not separated. The dry matter (DM) weight was recorded after

drying for 48 hours at 70°C, and the partitioning index (PI) was calculated for the component as the proportion of above-ground biomass. True-stem specific weight (SW) was calculated as true-stem DM per unit length.

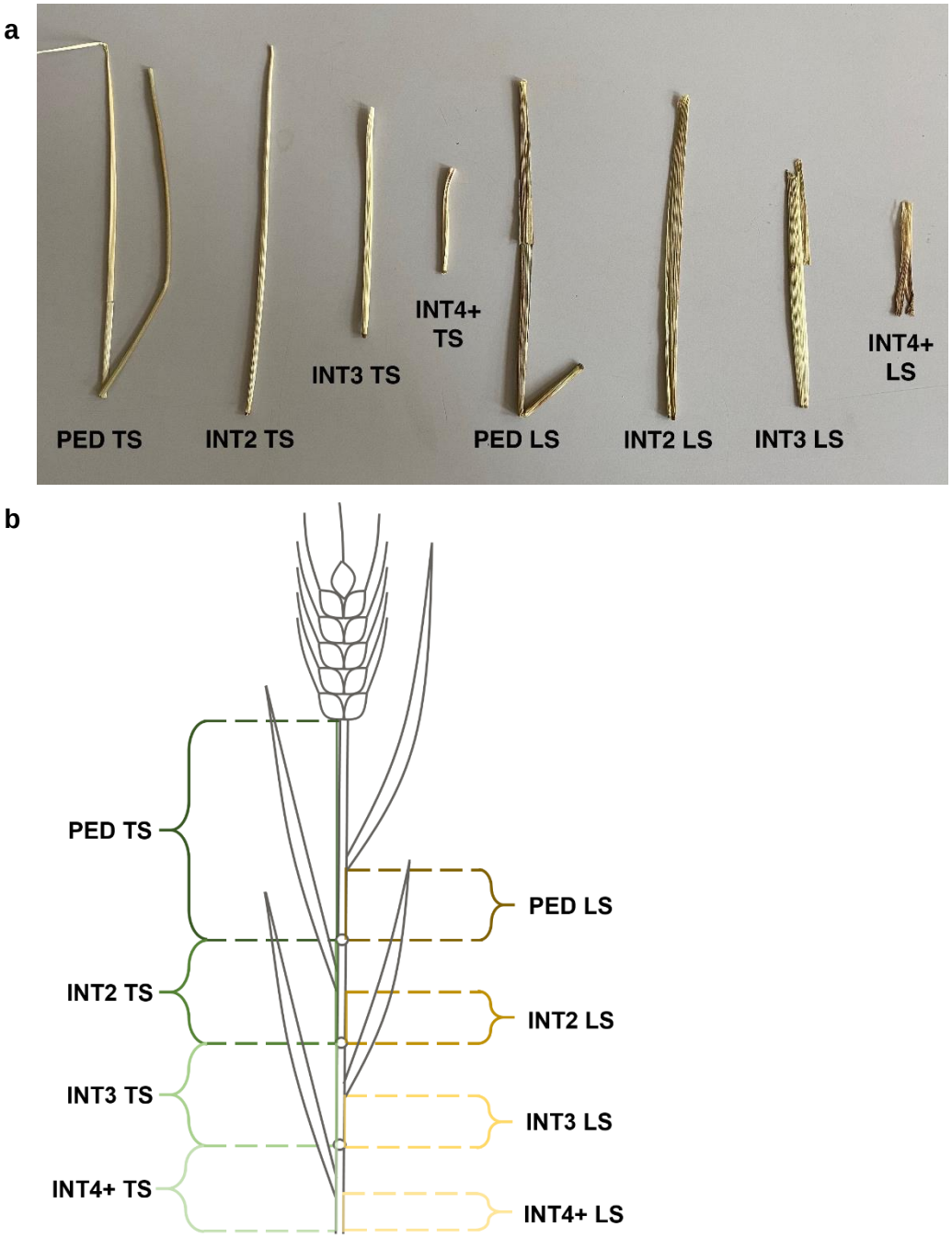

***Figure 3.2**: Stem-internode true stem and leaf sheath partitioning at GS65+7d*

a) Photograph of shoot components, b) diagram illustrating partitioning components

***PED**: peduncle, **INT2**: stem internode 2, **INT3**: stem internode 3, **INT4**+: stem internode 4 and below, **TS**: true stem, **LS**: leaf sheath*

In subset 2 (12 genotypes), four spikes from the 12 sampled at GS65+7d were selected and dissected into rachis, glumes, awns, palea, lemma and other components (small grains and anthers, not included in the analysis) (Figure 3.3). The DM weight for each component was recorded after drying for 48 hours at 70°C. Dry matter partitioning index (PI) was calculated for the spike component as the proportion of the whole spike DM excluding the small grains and anthers (other components, Figure 3.3a). Rachis length was measured and the rachis specific weight (SW) was calculated as the rachis DM per unit length.

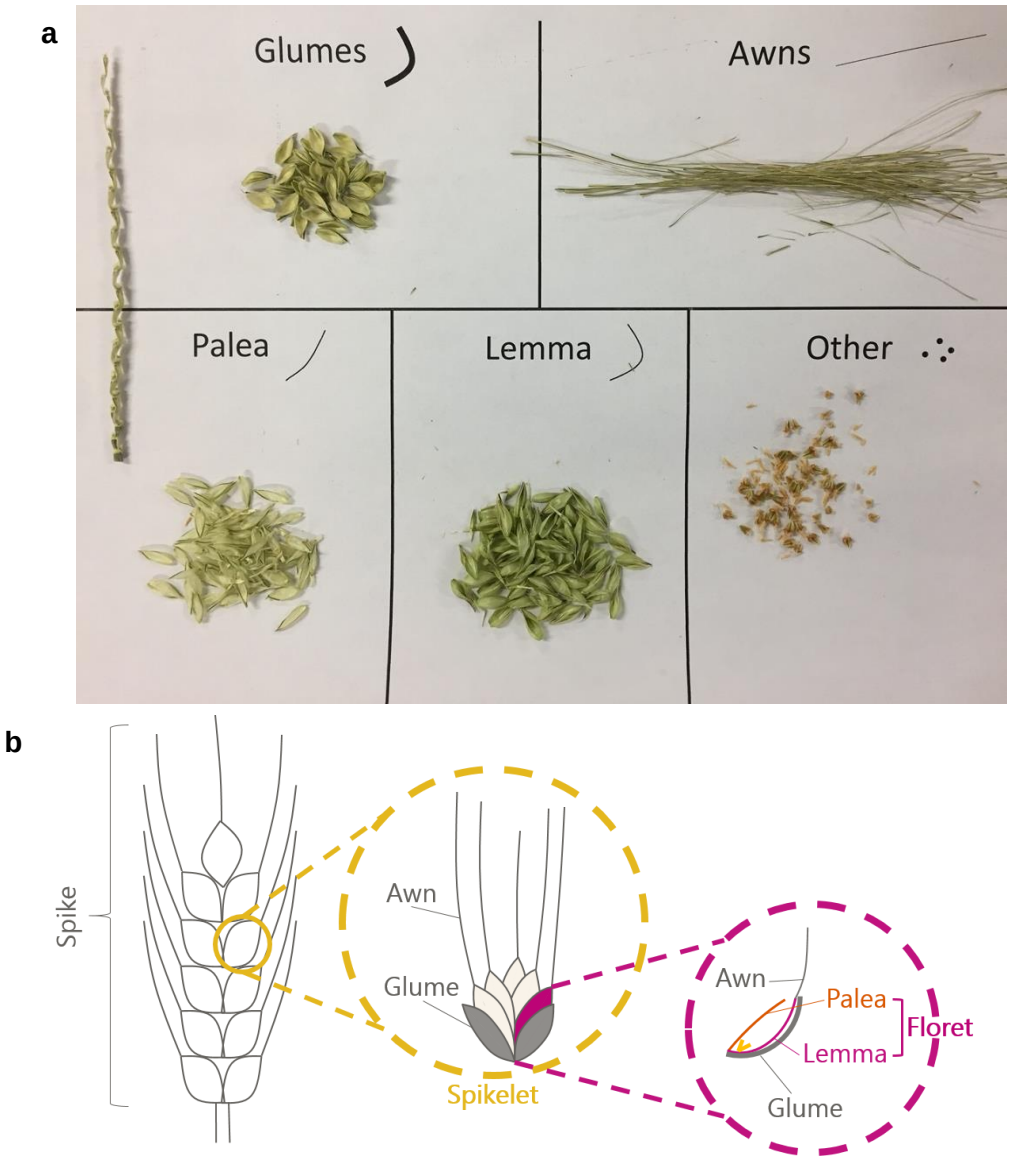

***Figure 3.3**: Spike component partitioning at GS65+7d*

a) Photograph of a spike separated into rachis, glumes, awns, palea, lemma and other components (grains and anthers, not included in the analysis), b) Diagram showing the position of spike components within the spike

Plant height and spike length

Plant height, peduncle length, spike length and awn length were measured on six fertile shoots per plot for all 150 lines at the start of grain filling. Plant height was measured from soil surface to tip of the spike and spike length from spike collar to tip of the spike, both excluded the awns from measurement.

Growth analysis at physiological maturity and combine harvest

At physiological maturity, 50 fertile shoots (those with a spike) were randomly selected and cut at ground level throughout the whole plot for all 150 genotypes in three replicates. The spike was separated from the straw (stem and leaves), and DM weight was recorded separately after drying for 48 hours at 70°C. These spikes were then threshed using a mechanical thresher to obtain the DM weight of grains and chaff, and 200 grains were counted and weighed. After the growth analysis samples were taken, each plot was machine-harvested in an area ranging from 2.6 to 4.0 m^2 in 2017-18, and 3.2 to 5.6 m^2 in 2018-19, and values were further adjusted to moisture percentage measured in each plot (ca. 10 %). These data were then used to calculate harvest index (HI, proportion of above-ground DM in the grain), above-ground DM ($AGDM_{PM}$, GY/HI), grain number per m^2 (GN, GY/TGW), and fruiting efficiency (FE_{A+7}, ratio of grain number to spike DM at anthesis + 7 days or FE_{chaff}, ratio of grain number to chaff DM at maturity).

Plant hormone sampling and analysis

In 2018-19 subset 2 was sampled in three replicates at late booting (GS49), and all 150 lines were sampled in two replicates at anthesis (GS65).

Two spikes per plot, one from each inner row of the two beds, both at similar heights and growth stages were sampled and frozen in liquid nitrogen immediately in the field. Then in the laboratory, while keeping the two spikes frozen on dry ice, central spikelets from both spikes were combined to make a 100 mg fresh weight sample of frozen material, which was stored at -80 °C. The sub-samples were then sent to the Department of Evolutionary Biology, Ecology and Environmental Sciences at the University of Barcelona for plant hormone profiling analysis performed by Prof. Sergi Munné-Bosch using liquid chromatography coupled to electrospray ionization tandem spectrometry (UPLC/ESI-MS/MS) (Müller and Munné-Bosch, 2011). The frozen plant material was ground in liquid nitrogen, then extracted with extraction solvent using ultrasonication, before centrifugation and re-extraction of the pellet was performed three times. The supernatants from each extraction were combined and filtered before analysis with UPLC/ESI-MS/MS.

3.2.3 Statistical analysis

The genotype best-linear unbiased estimates (BLUEs) were estimated from the cross-year Analysis of Variance (ANOVA) using META-R 6.0 (Alvarado et al., 2015), a windows R code-based platform. Replicates and years were considered as a random effect and genotypes as a fixed effect. A covariate for days to anthesis was included in the ANOVA when it had a significant effect. Broad-sense heritability (H^2) was estimated using META-R, and calculated as described in Equation 3.1, where $\sigma^2 g$ and $\sigma^2 e$ are the genotypic and environment variance, respectively, and $\sigma^2 ge$ is the cultivar x environment interaction. The number of environments and number of replicates are represented by *e* and *r*.

$$H^2 = \frac{\sigma^2 g}{\sigma^2 g + \frac{\sigma^2 ge}{e} + \frac{\sigma^2 e}{re}}$$

Equation 3.1

Genstat 19th edition (VSN International, 2021) was used for calculating Pearson's correlation coefficients and linear regressions using the BLUEs calculated in META-R. Principal component analysis (PCA) was performed to examine associations between plant hormones and key grain yield traits using the R package FactoMineR (Lê et al., 2008).

3.3 Results

3.3.1 Crop traits at physiological maturity

Averaging over all 150 genotypes of the HiBAP II in the two seasons - 2017-18 (Y1) and 2018-19 (Y2), it took longer to reach both anthesis (4 days) and maturity (6 days) in Y2 than Y1 (Figure 3.4, Table 3.1), although GY was similar in the two years (622 g m^{-2} in Y1 vs. 640 g m^{-2} in Y2, data not shown). Both daily mean temperature and solar radiation were similar for the two seasons, an earlier sowing date and increase in temperature in 2017-18 may explain the shorter time to reach anthesis and maturity (Figure 3.4). Averaging over both years, harvest index (HI) ranged from 0.40 to 0.53 ($P<0.001$) amongst the 150 genotypes (Table 3.1), and there was wide genetic variation in the above-ground dry matter at both anthesis+7 days (733-1177 g m^{-2}, $P<0.001$) and physiological maturity (1043-1522 g m^{-2}, $P<0.001$). Grouping the genotypes into their genetic origin, synthetic + landrace derived genotypes had over 1000 grains per m^2 (GN) fewer than the other genotypes (Table S 4), although this did not translate through to GY, which was no higher for the synthetic + landrace genotypes as the elite and synthetic genotypes (631 and 632 g m^{-2}, respectively, Table S 4). High values of heritability were observed for most traits (0.711-0.934) based on the combined analysis across years. The cross-year analysis showed a significant effect of genotype and also a genotype by year interaction for all traits at anthesis + 7 days and physiological maturity (Table 3.1).

Considering linear relationships between the traits at harvest and anthesis + 7 days, GY showed a positive linear association with $AGDM_{PM}$ (R^2= 0.39, $P<0.001$, Figure 3.5a, Table 3.2), harvest index (R^2=0.28, $P<0.001$, Figure 3.5b) and thousand-grain weight (R^2= 0.10, $P<0.001$, Figure 3.5c). Whereas, grains per m^2 was negatively associated with thousand-grain weight (R^2=0.54, $P<0.001$, Figure 3.5d). There was also a trade-off between $AGDM_{PM}$ and HI (R^2=0.11, $P<0.001$, Table 3.2). Plant height was not correlated with GY (R^2=0.006, ns, Table 3.2), but was negatively associated with HI (R^2=0.15, $P<0.001$) and GN (R^2=0.157, $P<0.01$, Figure 3.5f), and positively associated with $AGDM_{PM}$ (R^2=0.19, $P<0.001$, Table 3.2).

Spike PI was positively associated with spike DM_{A+7} ($r=0.60$, $P<0.001$), HI ($r=0.55$, $P<0.001$) and GY ($r=0.21$, $P<0.05$, Table 3.2) but not associated with grains per m^2 ($r=-0.001$, ns, Table 3.2). Fruiting efficiency was strongly positively associated with grains per m^2 ($r=0.63$, $P<0.001$, Table 3.2). FE_{A+7} was also positively associated with both the lamina and stem PI ($r=0.40$, $P<0.001$ and $r=0.27$,

P<0.001, respectively, Table 3.2). However, FE_{A+7} was negatively associated with each of the spike PI (r=-0.45, P<0.001), spike DM_{A+7} (r=-0.65, P<0.001) and TGW (r=-0.60, P<0.001). Spike PI was also negatively associated with $AGDM_{PM}$ (r=-0.28, P<0.001, Table 3.2).

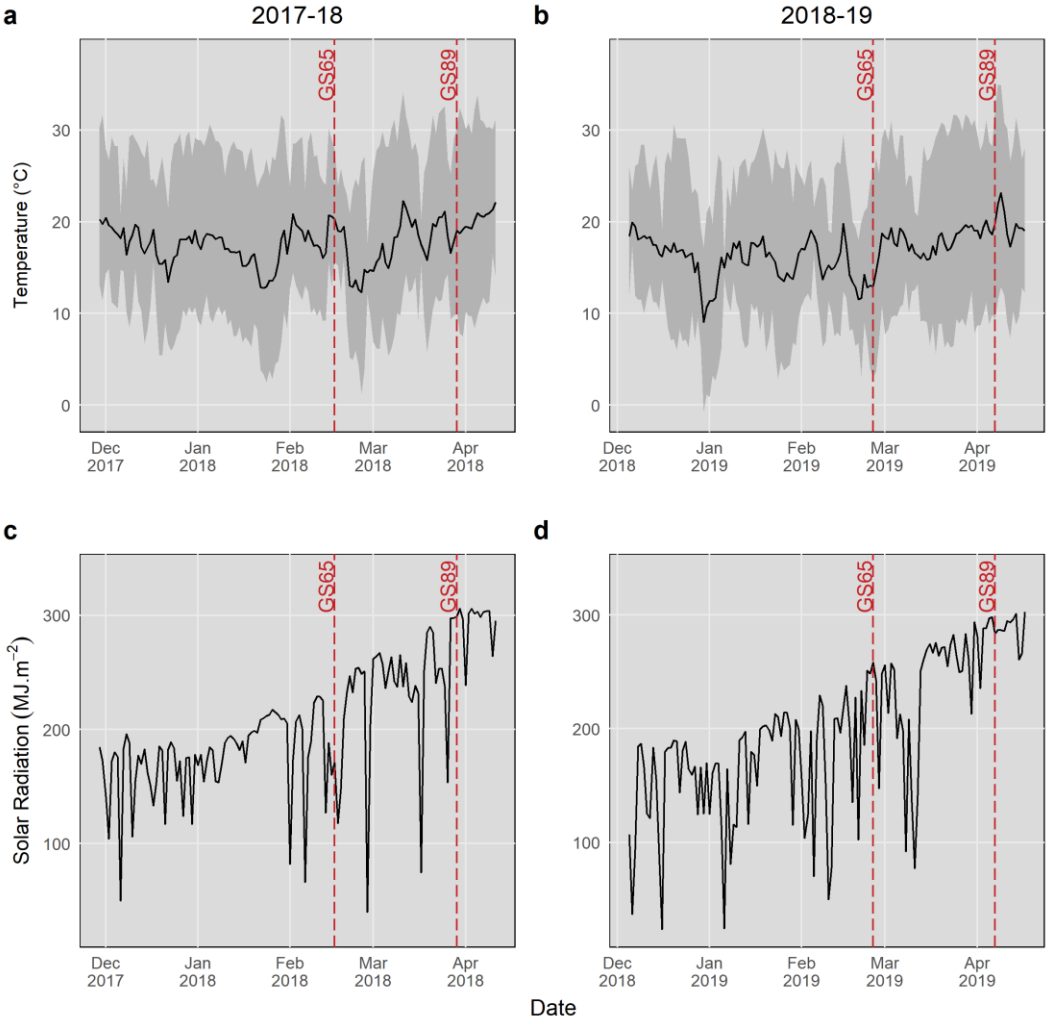

Figure 3.4: *Meteorological data for daily mean temperature in a) 2017-18 and b) 2018-19 and solar radiation in c) 2017-18 and d) 2018-19 with key growth stages*

Red dotted lines indicate the average date of key growth stages – anthesis (GS65) and physiological maturity (GS89). Means taken per 24 hour period, grey shading indicates the minimum and maximum temperature values for each day. Months indicated on the x-axis indicate the start of the month

Table 3.1: *Phenotypic ranges, least significant differences (LSD, P=0.05), heritability and significance (p-values) for 150 HiBAP II genotypes at anthesis +7 days and physiological maturity*

The combined range is combined means for 2017-18 and 2018-19, †: DTA added as a covariate if P<0.05, sig: significance, ***DTA****: days from emergence to anthesis,* ***$AGDM_{A+7}$****: above-ground dry matter (DM) at anthesis + 7 days,* ***Stem PI****: stem partitioning index,* ***Spike PI****: spike partitioning index,* ***Lamina PI****: Lamina partitioning index,* ***Spike DM****: DM spike per unit area,* ***FE_{A+7}****: fruiting efficiency (calculated using spike DM at anthesis + 7 days),* ***DTM****: days from emergence to physiological maturity,* ***$AGDM_{PM}$****: above ground DM at physiological maturity,* ***GY****: grain yield per m^2,* ***TGW****: thousand-grain weight,* ***HI****: harvest index,* ***SM2****: spikes per m^2,* ***GN****: grain number per m^2*

		Range 17-18	Range 18-19	Genetic range combined and ANOVA treatment effects					
		(Min-Max)	(Min-Max)	(Min-Max)	Heritability	LSD (5 %)	Genotype sig	Year sig	GenxYear sig
Anthesis + 7 days (GS65+7d)	**DTA**	70-91	76-92	73-91	0.933	2.890	<0.001	<0.001	<0.001
	$AGDM_{A+7}$ (g m^{-2})	779-1255†	701-1199†	733-1177†	0.501	125.6	<0.001	<0.001	0.017
	Stem PI	0.487-0.592	0.601-0.690†	0.550-0.641†	0.788	0.021	<0.001	<0.001	<0.001
	Spike PI	0.182-0.296†	0.131-0.255†	0.169-0.269†	0.768	0.024	<0.001	<0.001	<0.001
	Lamina PI	0.157-0.255†	0.127-0.181	0.143-0.214†	0.343	0.022	<0.001	<0.001	0.017
	SpikeDM (g m^{-2})	127-388†	152-363†	165-354†	0.322	68.20	<0.001	0.002	0.006
	FE_{A+7} (grns g^{-1})	34.9-84.1†	33.8-86.1†	36.0-76.8†	0.582	14.38	<0.001	0.007	<0.001
Physiological Maturity (GS89)	**DTM**	115-126†	121-130†	119-127†	0.711	1.990	<0.001	0.001	<0.001
	$AGDM_{PM}$ (g m^{-2})	959-1516†	1115-1666†	1043-1522†	0.732	112.6	<0.001	0.002	0.021
	GY (g m^{-2})	476-722	494-743	485-716	0.832	45.87	<0.001	0.062	<0.001
	TGW (g)	29.9-55.5†	31.9-54.9	32.2-53.5†	0.934	2.659	<0.001	0.108	<0.001
	HI	0.40-0.55†	0.40-0.51†	0.40-0.53	0.831	0.028	<0.001	<0.001	<0.001
	SM2 (spikes m^{-2})	210-394	211-393	212-363	0.827	33.89	<0.001	0.215	<0.001
	GN (grains m^{-2})	10912-17695	11974-17991	11389-17368†	0.889	1188.9	<0.001	1.000	<0.001

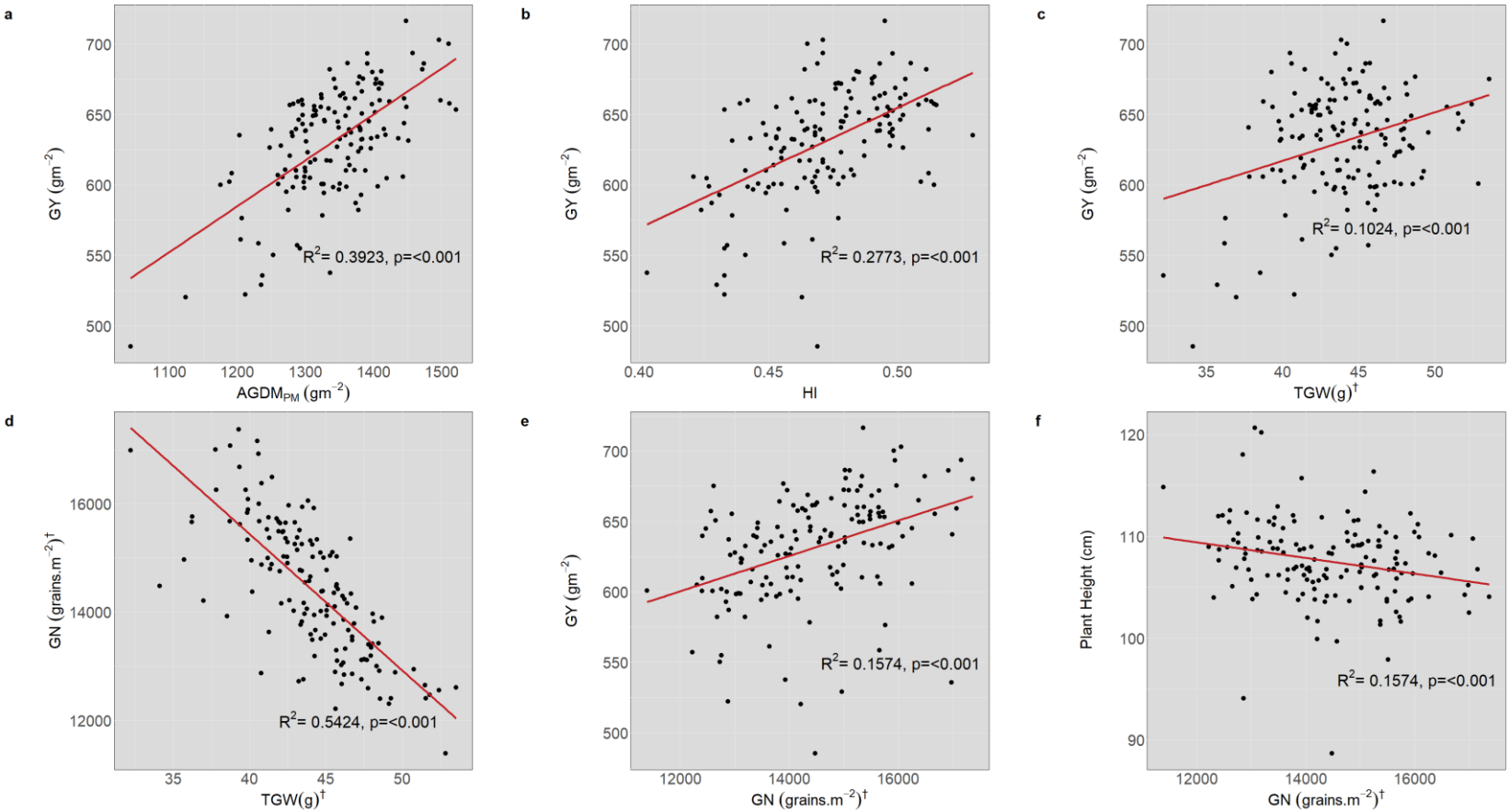

Figure 3.5: *Linear regressions of traits measured at physiological maturity among 150 HiBAP II genotypes*

†: DTA added as a covariate if P<0.05, cross-year means 2017-18 and 2018-19, a) Grain yield (GY) vs. above-ground dry matter at physiological maturity (AGDM$_{PM}$) y=0.33x+194.2, b) Grain yield vs. harvest index (HI) y=852.5x+228.6, c) Grain yield vs. thousand-grain weight (TGW) y=3.45x+479.1, d) Grain number per m^2 (GN) vs. thousand-grain weight y=-251.2x+25490, e) Grain yield vs. grain number per meter squared y=0.013x+450, f) Plant height vs. grain number per m^2 y=-0.0008x+118.6

Table 3.2: *Pearson's correlation coefficients between traits measured at GS65+7d and physiological maturity among 150 HiBAP II genotypes*

*†: DTA added as covariate if P<0.05, based on cross-year means 2017-18 and 2018-19, ‡P<0.10, *P<0.05, **P<0.01, ***P<0.001*

***GN**: grain number per m², **GY**: grain yield per m², **TGW**: thousand-grain weight, **HI**: harvest index, **AGDM$_{PM}$**: above-ground dry matter (DM) at physiological maturity, **FE$_{A+7}$**: fruiting efficiency (calculated using spike DM at anthesis + 7 days), **Height**: plant height from the base of plant to tip of the spike, **L Ped**: stem peduncle length, **L Int2**: stem internode 2 length, **L Int3**: stem internode 3 length, **LaminaPI**: Lamina partitioning index, **Spike PI**: spike partitioning index, **Stem PI**: stem partitioning index, **AGDM$_{A+7}$**: above ground DM at anthesis + 7 days, **SpikeDM$_{A+7}$**: DM spike per unit area at anthesis + 7 days*

Traits	GN†	GY	TGW†	HI	AG DM_{PM}	FE_{A+7}†	Height	L Ped	L Int2	L Int3†	Lamina PI†	Spike PI†	Stem PI†	AG DM_{A+7}†	Spike DM_{A+7}†
GN†	-														
GY	**0.40*** **	-													
TGW†	**-0.74*** **	**0.32*** **	-												
HI	**0.19***	**0.53*** **	**0.17***	-											
AG DM_{PM}	**0.26****	**0.63*** **	**0.21***	**-0.33*** **	-										
FE_{A+7}†	**0.63*** **	0.07	**-0.60*** **	-0.02	0.10	-									
Height	**-0.23****	0.08	**0.30*** **	**-0.39*** **	**0.44*** **	-0.08	-								
L Ped	**-0.46*** **	**-0.16***	**0.35*** **	**-0.20***	0.003	**-0.19***	**0.42*** **	-							
L Int2	-0.02	0.12	0.13	-0.06	**0.19***	0.08	**0.40*** **	**-0.15‡**	-						
L Int3†	-0.01	0.09	0.08	**-0.17***	**0.24****	-0.02	**0.46*** **	**-0.18***	**0.39*** **	-					
Lamina PI†	0.10	-0.11	**-0.17***	**-0.15‡**	0.02	**0.40*** **	-0.03	0.05	-0.07	**-0.22****	-				
Spike PI†	-0.001	**0.21***	0.13	**0.55*** **	**-0.28*** **	**-0.45*** **	**-0.43*** **	**-0.18***	**-0.29*** **	-0.13	**-0.51*** **	-			
Stem PI†	-0.06	**-0.16***	-0.04	**-0.54*** **	**0.31*** **	**0.27*** **	**0.52*** **	**0.17***	**0.39*** **	**0.30*** **	-0.06	**-0.83*** **	-		
AG DM_{A+7}†	**-0.15‡**	**0.24****	**0.32*** **	-0.13	**0.37*** **	**-0.30*** **	**0.42*** **	0.05	**0.28*** **	**0.33*** **	**-0.28*** **	-0.05	**0.24****	-	
Spike DM_{A+7}†	**-0.29*** **	**0.33*** **	**0.53*** **	**0.28*** **	0.12	**-0.65*** **	0.11	-0.02	-0.10	0.05	**-0.49*** **	**0.60*** **	**-0.38*** **	**0.26****	-

3.3.2 Crop dry matter partitioning traits at anthesis + 7 days

Above-ground DM at GS65+7d ranged from 733-1177 gm^{-2} (P<0.001, Table 3.1), and the stem (true stem and leaf sheath combined) accounted for the highest amount of $AGDM_{A+7}$, ranging amongst genotypes from 1.19-2.24 g per shoot (P<0.001, Figure 3.6), followed by the spike at 0.33-1.10 g (P<0.001, Figure 3.6), and finally the lamina ranging from 0.47-0.84 g (P<.001, Figure 3.6). As a proportion of $AGDM_{A+7}$, the stem PI ranged from 0.550 to 0.641 (P<0.001, Table 3.1). Concerning the stem internode lengths, top-down the peduncle was the longest component (31.9-43.5 cm, P<0.001), followed by internode 2 (17.5-26.3 cm, P<0.001) and then internode 3 (9.5-15.6 cm. P<0.001) (Figure 3.6). A strong negative relationship was found between stem PI and spike PI (R^2=0.68, P<0.001, Figure 3.7a), as well as between stem PI and spike DM_{A+7} (r=-0.38, P<0.001, Table 3.2). Along with a significant genetic variation for all the above traits, the genotype x year interaction was also significant (P<0.05, Table 3.1).

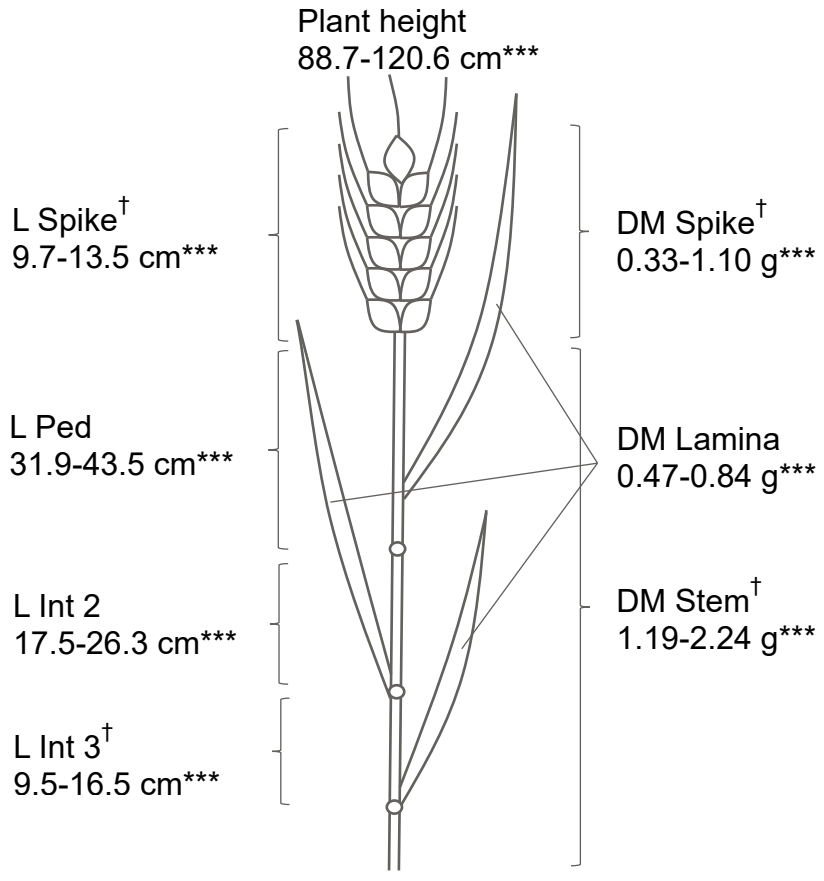

Figure 3.6: *Genetic ranges for 150 HiBAP II genotypes at GS65+7d for dry matter (DM) per shoot (right) and spike and stem internode length (left)*

*†: DTA added as covariate if P<0.05, cross-year means 2017-18 and 2018-19, genotype significance values: *P<0.05, **P<0.01, ***P<0.001*

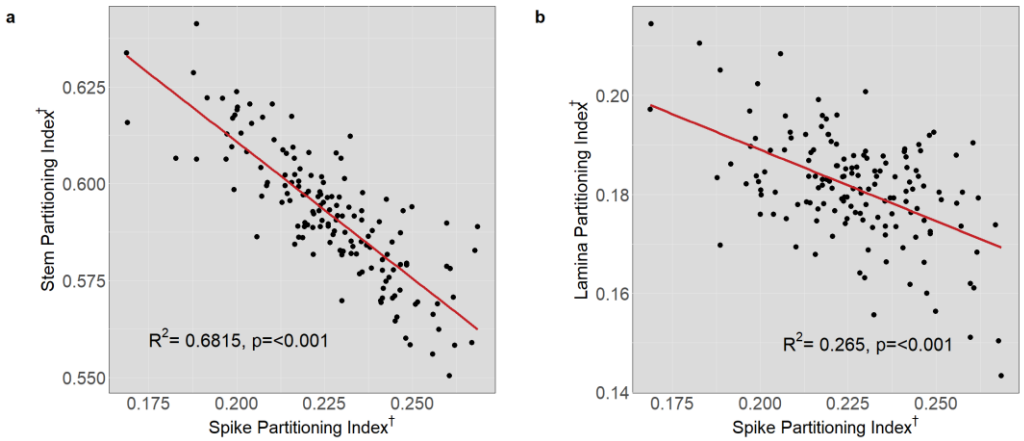

***Figure 3.7**: Linear regressions for 150 HiBAP II genotypes of spike partitioning index on a) Stem partitioning index and b) Lamina partitioning index*

†: DTA added as a covariate if P<0.05, cross-year means 2017-18 and 2018-19, a) y=-0.71x+0.75, b) y=-0.29x+0.25

Amongst the 150 genotypes, there was a negative association between spike PI and stem-internode 2 length (R^2=0.08, P<0.001, Figure 3.8a) and spike PI and the peduncle length (R^2=0.03, P=0.03, Figure 3.8a). Stem-internode 3 length was also negatively associated with lamina PI (R^2=0.05, P=0.007, Figure 3.8c). Conversely, stem-internode length was positively associated with stem PI for each internode (P<0.05, Figure 3.8b).

For the subset of 32 genotypes, there were large differences in DM partitioning to the plant components between genotypes (Figure 3.9). Spike PI showed a negative correlation with all the leaf sheath PIs (Table 3.3). Thus, there were negative linear regressions of spike PI with the leaf sheath PIs (ped: R^2=0.16, P=0.025, int2: R^2=0.32, P<0.001, int3: R^2=0.12, P=0.049, Figure 3.10b). The only stem internode traits that correlated with FE_{A+7} were int3 leaf sheath PI (r=0.58, P<0.001, Table 3.3), and ped true stem specific weight (SW, r=-0.43, P<0.05, Table 3.3) and int2 true stem SW (r=-0.33, P<0.1, Table 3.3). There was a general trend that varieties with less spike DM and more stem DM tended to have a higher FE_{A+7} (Figure 3.9), with a negative relationship between FE_{A+7} and spike PI (r=-0.45, P<0.001, Table 3.2).

Both leaf sheath and true stem int2 PI were correlated with GY, although the true stem PI was weakly positively correlated (r=0.33, P<0.1, Table 3.3) and leaf sheath PI was negatively correlated (r=-0.46, P<0.01, Table 3.3). Ped, int2 and int3 true stem SWs were all positively correlated with GY, TGW and spike DM (P<0.01, Table 3.3), although this could be an indirect effect of the negative associations observed between SWs and spikes per m^2 (P<0.001, Table 3.3).

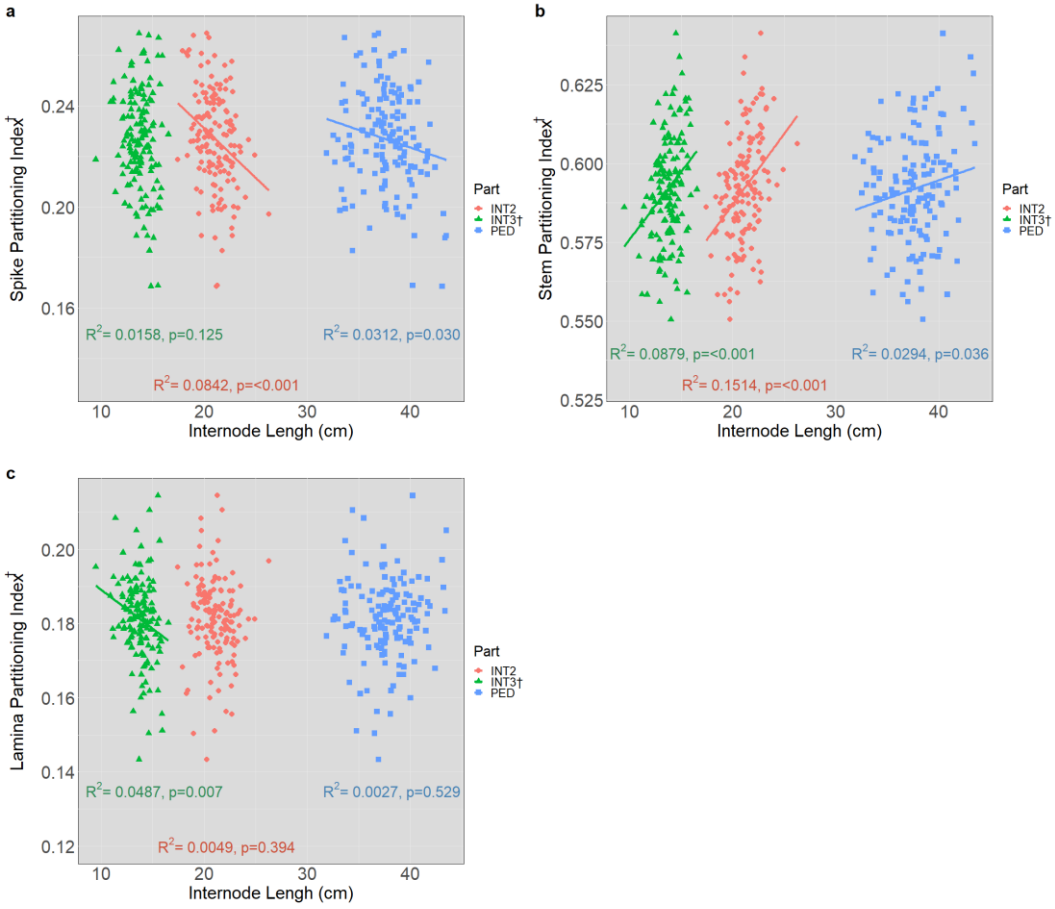

***Figure 3.8**: Linear regressions for 150 HiBAP II genotypes of internode lengths on a) Spike partitioning index b) Stem partitioning index, c) Lamina partitioning index*

*†: DTA added as a covariate if P<0.05, cross-year means 2017-18 and 2018-19, ns=not significant, **INT**: stem internode, **PED**: peduncle, a) Int3: y=-0.002x+0.26, Int2: y=-0.004x+0.31, Ped: y=-0.001x+0.28, b) Int3: y=0.004x+0.53, Int2: y=0.005x+0.50, Ped: y=0.001x+0.55, c) Int3: y=-0.002x+0.21, Int2: y=-0.0005x+0.19, Ped: y=0.0002x+0.17*

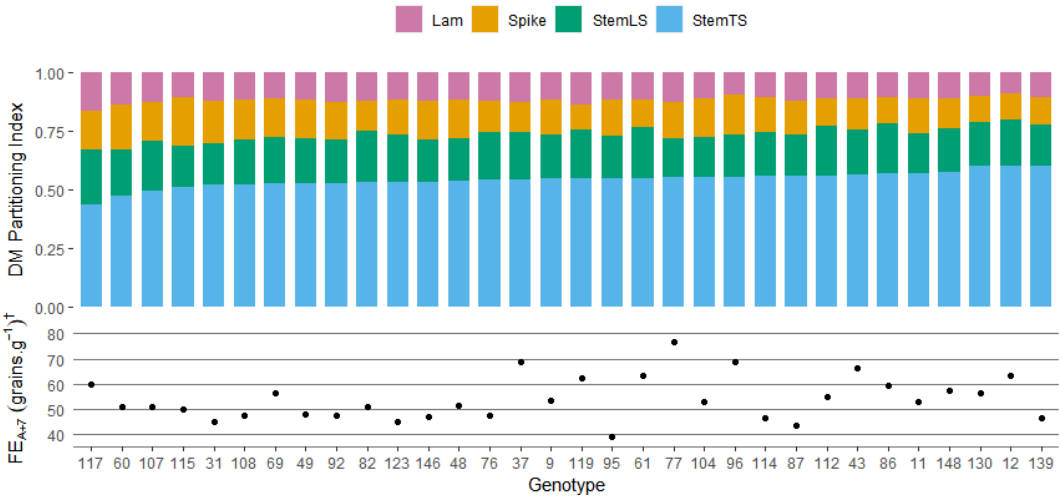

***Figure 3.9**: Dry matter partitioning indices for each plant component in 32 HiBAP II genotypes (subset 1) at GS65+7d*

Partitioning indices calculated as a component of DM from ANOVA genotypes means in 2017-18 and 2018-19, FE_{A+7}: calculated using spike DM at anthesis + 7 days

Table 3.3: *Pearson's correlation coefficients between traits measured at GS65+7d and physiological maturity and stem-internode partitioning traits among 32 HiBAP II genotypes (subset 1)*

*†: DTA added as covariate if P<0.05, cross-year means 2017-18 and 2018-19, correlation significance: ‡P<0.10, *P<0.05, **P<0.01, ***P<0.001*

***GY**: grain yield per m², **GN**: grain number per m², **SM2**: spikes per m² at physiological maturity **TGW**: thousand-grain weight, **HI**: harvest index, **FE$_{A+7}$**: fruiting efficiency (calculated using spike dry matter (DM) at GS65+7d), **SPI**: spike partitioning index, **SpikeDM$_{A+7}$**: spike DM per unit area at GS65+7d, **PED**: peduncle, **INT2**: stem internode 2, **INT3**: stem internode 3, **INT4+:** stem internode 4 and below (TS+LS), **TS**: true stem, **LS**: leaf sheath, **PI**: partitioning index (calculated as a proportion of above-ground biomass), **SW**: specific weight (proportion of the DM with length)*

Traits	GY	GN†	SM2	TGW†	HI	FE$_{A+7}$†	SPI†	Spike DM$_{A+7}$†
PED TSPI	-0.11	-0.19	0.18	0.07	0.25	-0.23	0.24	-0.02
INT2 TSPI†	**0.33‡**	0.05	0.01	0.18	0.30	0.04	0.25	0.12
INT3 TSPI	0.09	0.08	0.19	0.04	-0.22	0.17	-0.11	-0.15
PED LSPI	**-0.31‡**	-0.22	0.16	-0.02	-0.22	0.25	**-0.39***	**-0.44***
INT2 LSPI†	**-0.46****	-0.04	0.36	-0.28	**-0.37***	0.29	**-0.56*****	**-0.62*****
INT3 LSPI	-0.27	0.17	0.27	**-0.35***	-0.19	**0.58*****	**-0.35***	**-0.55****
INT4+ PI	0.19	0.07	-0.2	0.10	**-0.44***	0.14	**-0.43***	0.05
PED TSSW†	**0.50****	-0.12	**-0.67*****	**0.45****	**0.39***	**-0.43***	0.27	**0.78*****
INT2 TSSW†	**0.48****	-0.12	**-0.66*****	**0.46****	0.27	**-0.33‡**	0.22	**0.76*****
INT3 TSSW†	**0.43***	-0.16	**-0.62*****	**0.47****	0.25	-0.25	0.26	**0.71*****

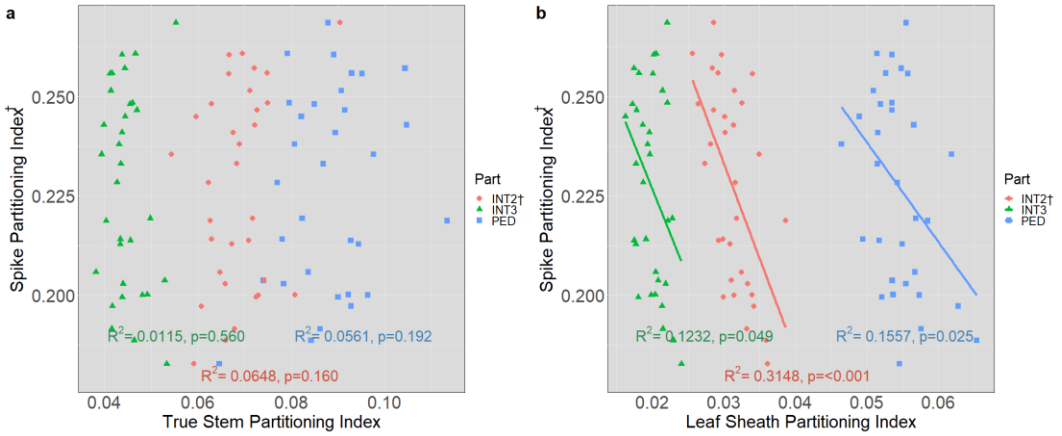

***Figure 3.10**: Linear regression of spike partitioning index on a) true-stem internode partitioning index and b) leaf-sheath internode partitioning index for HiBAP II subset 1 at GS65+7d*

*†: DTA added as a covariate if P<0.05, cross-year means 2017-18 and 2018-19, ns=not significant, **INT**: stem internode, **PED**: peduncle*

a) Int3: y=-0.66x+0.26, Int2: y=0.94x+0.16, Ped: y=0.61x+0.17, b) Int3: y=-4.5x+0.32, Int2: y=-4.8x+0.38, Ped: y=-2.5x+0.36

When regressing the true stem DM per shoot on internode length, for int 2 and 3, there was a positive linear association (R^2=0.44, P<0.001 and R^2=0.59, P<0.001, respectively, Figure 3.11a), but no association for the peduncle (R^2=0.07, ns, Figure 3.11a). True stem DM per shoot and specific weight were positively linearly associated for each of the internodes (P<0.001, Figure 3.11b). Relating internode length to specific weight, only internode 2 (R^2=0.15, P=0.026, Figure 3.11c) and internode 3 (R^2=0.11, P=0.065, Figure 3.11c) were significantly associated.

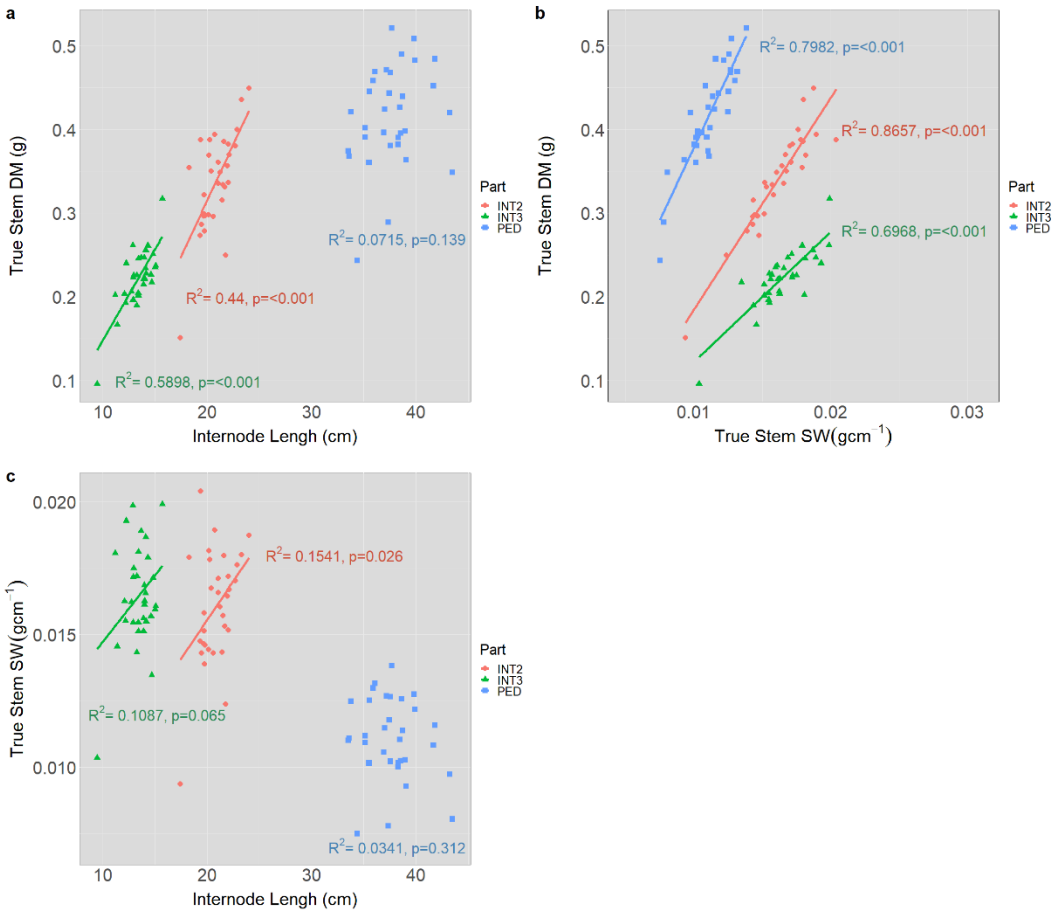

***Figure 3.11**: Linear regressions of HiBAP II subset 1 genotypes between stem internode traits at GS65+7d*

*All traits except Ped and Int2 length estimated with DTA as a covariate (P<0.05), cross-year means 2017-18 and 2018-19, ns=not significant, **INT:** stem internode, **PED:** peduncle, **DM:** dry matter, **SW:** specific weight*

a) True stem dry matter per shoot vs. Internode length, Int3: y=0.02x-0.07, Int2: y=0.03-0.22, Ped: y=0.006x+1, b) True stem dry matter per shoot vs. true stem specific weight, Ped: y=34.8x+0.03, Int2: y=25.3x-0.07, Int3: 15.5x-0.03, c) True stem specific weight vs. internode length, Int3: y=0.0005x+0.0097, Int2: y=0.0006x+0.004, Ped: y=-0.0001x+0.0153

3.3.3 Spike morphological partitioning at anthesis + 7 days

For the detailed spike morphology partitioning traits on the subset of 13 genotypes, there were fewer significant correlations with FE and HI compared to the stem internode partitioning traits. There was no association between any of the spike morphology partitioning indices or rachis specific weight and fruiting efficiency calculated using the spike DM at anthesis + 7 days (Figure 3.12a). However, when fruiting efficiency was calculated using chaff DM at physiological maturity, rachis specific weight was negatively associated (R^2=0.30, P=0.063, Figure 3.12b), and lemma PI was positively associated with FE_{chaff} (R^2=0.28, P=0.077, Figure 3.12b).

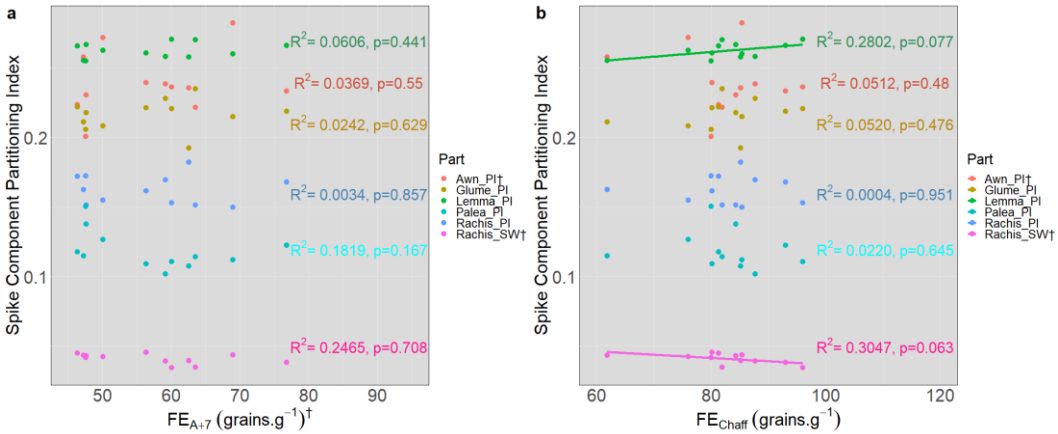

***Figure 3.12**: Linear regressions for the subset of 12 lines (subset 2) in the HiBAP II, of spike component partitioning index on fruiting efficiency calculated using 2 methods*

†: DTA added as a covariate if P<0.05, cross-year means 2017-18 and 2018-19

a) Fruiting efficiency calculated using the spike dry matter (DM) at anthesis + 7 days, b) Fruiting efficiency calculated using the chaff DM at physiological maturity

***PI**: partitioning index (calculated as a proportion of spike), **SW**: specific weight (proportion of the DM with length)*

Also, there was a positive correlation between TGW and each of palea PI (r=0.5, P<0.1, Table 3.4) and rachis specific weight (r=0.65, P<0.05, Table 3.4). Spike PI was positively correlated with awn PI (r=0.51, P<0.1, Table 3.4), but negatively with rachis specific weight (r=-0.57, P<0.1, Table 3.4). Finally, spike DM per unit area at anthesis was positively associated with rachis specific weight (r=0.68, P<0.05, Table 3.4).

***Table 3.4**: Pearson's correlation coefficients between traits measured at GS65+7d and physiological maturity and spike component partitioning among HiBAP II subset 2*

*†: DTA added as covariate if P<0.05, cross-year means 2017-18 and 2018-19, correlation significance: ‡P<0.10, *P<0.05, **P<0.01, ***P<0.001*

***GY**: grain yield per m², **GN**: grain number per m², **TGW**: thousand-grain weight, **HI**: harvest index, **FE_{A+7}**: fruiting efficiency (calculated using spike dry matter (DM) at anthesis), **SPI**: spike partitioning index, **$SpikeDM_{A+7}$**: DM spike per unit area at anthesis+7d, **PI**: partitioning index (calculated as a proportion of spike), **SW**: specific weight (proportion of the DM with length)*

Traits	GY	GN†	TGW†	HI	FE_{A+7}†	SPI†	Spike DM_{A+7}†
Glume PI	0.23	0.22	0.001	0.36	0.16	0.06	0.13
Awn PI†	-0.2	0.01	-0.21	0.15	0.19	**0.51‡**	0.08
Palea PI	0.14	-0.46	**0.5‡**	0.24	-0.43	0.33	0.45
Lemma PI	0.06	0.24	-0.15	0.5	0.25	0.18	-0.05
Rachis PI	0.13	-0.01	0.16	-0.37	-0.06	**-0.57‡**	-0.2
Rachis SW†	0.30	-0.47	**0.65***	0.33	-0.5	0.41	**0.68***

3.3.4 Spike hormone associations

Spike hormone analyte levels at both late booting and anthesis for the subset of 10 genotypes are shown in Figure 3.13. Some plant hormones showed a large change between stages, e.g. salicylic acid had a much lower level at late booting (GS49) than GS65, whereas ABA showed a lower concentration at anthesis. When correlating the spike hormones sampled in all 150 genotypes at anthesis to FE_{chaff}, the cytokinins (CKs) zeatin riboside (Zr, r=0.33, P<0.001), zeatin (Z, r=0.15, P<0.10), isopentenyladenosine (IPA, r=0.24, P<0.01) and isopentenyladenine (2iP, r=0.15, P<0.10) were all positively correlated (Table 3.5). Similarly, with FE_{A+7}, cytokinins Zr and 2iP were positively correlated (r=0.17, P<0.10 and 0.35, P<0.001, respectively). As well as the CKs, jasmonic acid (JA) was positively correlated with FE_{A+7} (r=0.18, P<0.10, Table 3.5). The cytokinins which were positively associated with FE_{A+7} were negatively associated with TGW (Zr; r=-0.25, P<0.01, 2iP; r=-0.24, P<0.01, Table 3.5). The same associations can be seen in the biplot in Figure 3.14, where the CKs were positively associated with FE_{chaff} and GN, but negatively with TGW. The linear regression of CKs with FE_{chaff} also shows Zr had a positive association (R^2=0.08, P<0.001, Figure 3.15a), and IPA had a slightly weaker association (R^2=0.04, P=0.01, Figure 3.15b). Gibberellins were associated with some grain yield traits, e.g. GA1 was negatively correlated with grain number per m² (r=-0.14, P<0.10, Table 3.5).

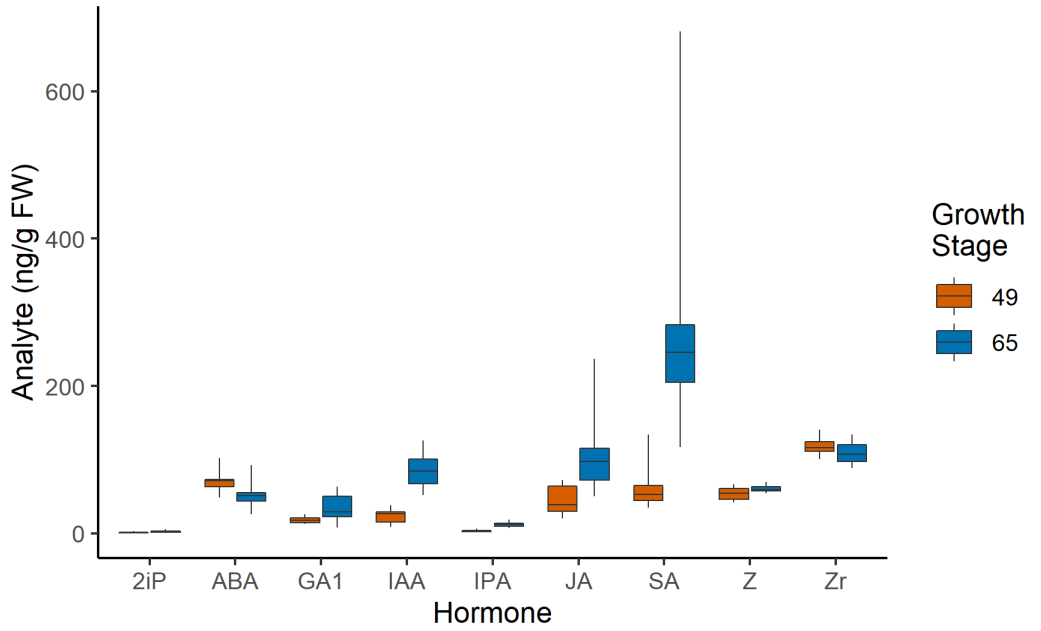

***Figure 3.13**: Boxplots showing genetic ranges for HiBAP II in 10 genotypes of subset 2 in spike hormonal analyte levels at late booting (GS49) and anthesis (GS65) in a field experiment in 2018-19*

Values represent means of fresh weight (FW) samples from 2018-2019

***2iP:** isopentenyladenine, **ABA**: abscisic acid, **GA1**: gibberellin 1, **IAA**: indole-3-acetic acid, **IPA**: isopentenyladenosine, **JA**: jasmonic acid, **SA**: salicylic acid, **Z**: zeatin, **Zr**: zeatin riboside*

***Table 3.5**: Pearson's correlation coefficients between traits measured at GS65+7d and physiological maturity and spike hormones at GS65 among 150 HiBAP II genotypes*

*†: DTA added as covariate if P<0.05, hormone levels (ng/g FW) calculated as the means of 2 reps, other traits 3 reps, both in 2018-19, correlation significance: ‡P<0.10, *P<0.05, **P<0.01, ***P<0.001*

***AGDM$_{PM}$**: above-ground dry matter (DM) at physiological maturity**, **GY**: grain yield per m^2, **GN**: grain number per m^2, **TGW**: thousand-grain weight, **HI**: harvest index, **FE$_{A+7}$**: fruiting efficiency (calculated using spike DM at anthesis + 7 days), **FE$_{chaff}$**: fruiting efficiency (calculated using chaff DM at physiological maturity), **SPI**: spike partitioning index, **SpikeDM$_{A+7}$**: DM spike per unit area at anthesis + 7 days, **ABA**: abscisic acid, **GA1**: gibberellin 1, **IAA**: indole-3-acetic acid, **JA**: jasmonic acid, **SA**: salicylic acid, **Z**: zeatin, **Zr**: zeatin riboside, **IPA**: isopentenyladenosine, **2iP:** isopentenyladenine*

	AG DM$_{PM}$	GY	GN	TGW	HI†	FE$_{A+7}$†	FE$_{chaff}$	SPI†	Spike DM$_{A+7}$†
ABA	-0.01	0.09	-0.05	0.08	0.07	-0.03	-0.03	0.08	0.07
GA1	-0.04	-0.07	**-0.16‡**	0.05	-0.06	**-0.17‡**	-0.10	0.01	0.11
IAA	0.11	0.09	0.12	-0.11	0.02	0.08	0.09	-0.14	-0.04
JA	-0.02	-0.08	0.00	-0.06	-0.07	**0.18‡**	0.09	**-0.20***	-0.10
SA	-0.04	**-0.22***	-0.10	-0.09	**-0.22***	0.02	-0.10	-0.08	-0.12
Z	**-0.18‡**	0.04	0.11	-0.11	**0.20***	-0.01	**0.15‡**	**0.19***	-0.01
Zr	-0.15	-0.02	**0.19***	**-0.25****	0.12	**0.17‡**	**0.33*****	-0.03	-0.15
IPA	0.04	**0.18***	**0.19***	-0.11	**0.16‡**	0.12	**0.24****	0.00	0.03
2iP†	0.07	**-0.16‡**	**0.21***	**-0.24****	-0.09	**0.35*****	**0.15‡**	**-0.42*****	**-0.29****

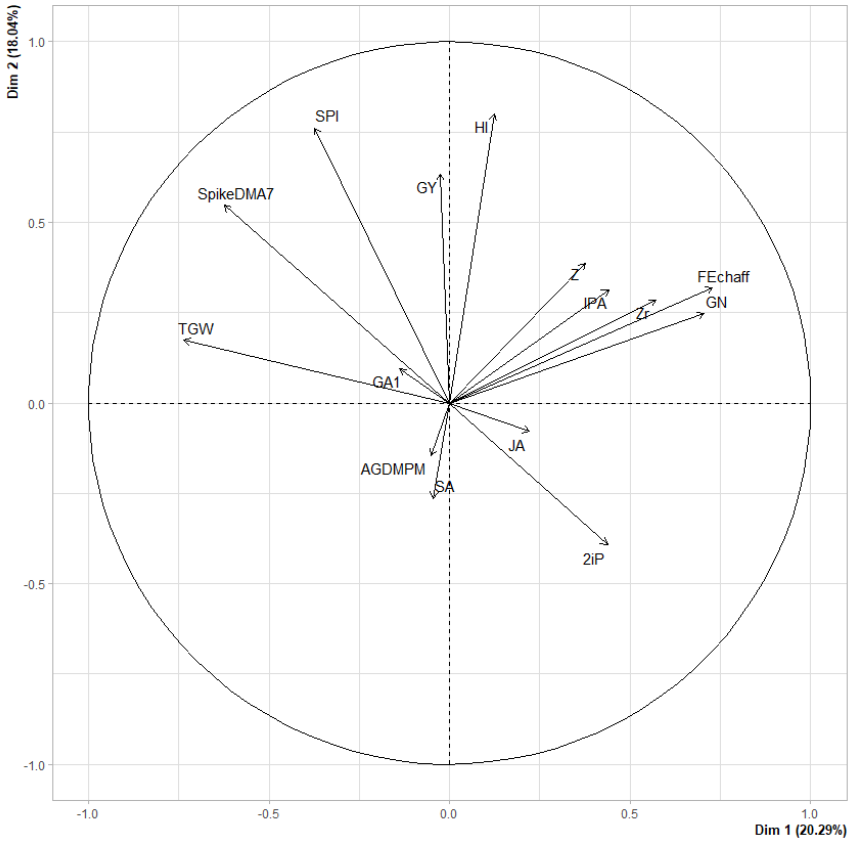

***Figure 3.14**: Principal component analysis (PCA) for traits measured at GS65+7d and physiological maturity and spike hormones at GS65 among 150 HiBAP II genotypes in 2018-19*

*Hormone levels (ng/g FW) calculated as the means of 2 reps, other traits 3 reps, both in 2018-19, **GY**: grain yield per m^2, **GN**: grain number per m^2, **TGW**: thousand-grain weight, **AGDMPM**: above-ground dry matter (DM) at physiological maturity, **HI**: harvest index, **FEA7**: fruiting efficiency (calculated using spike dry matter (DM) at anthesis + 7 days) **FEchaff** fruiting efficiency (calculated using chaff weight at physiological maturity), **SPI**: spike partitioning index, **SpikeDMA7**: DM spike per unit area at anthesis+7d, **Z:** zeatin, **Zr**: zeatin riboside, **IPA**: isopentenyladenosine, **2iP:** isopentenyladenine, **JA**: jasmonic acid, **SA:** salicylic acid, **GA1:** gibberellin 1*

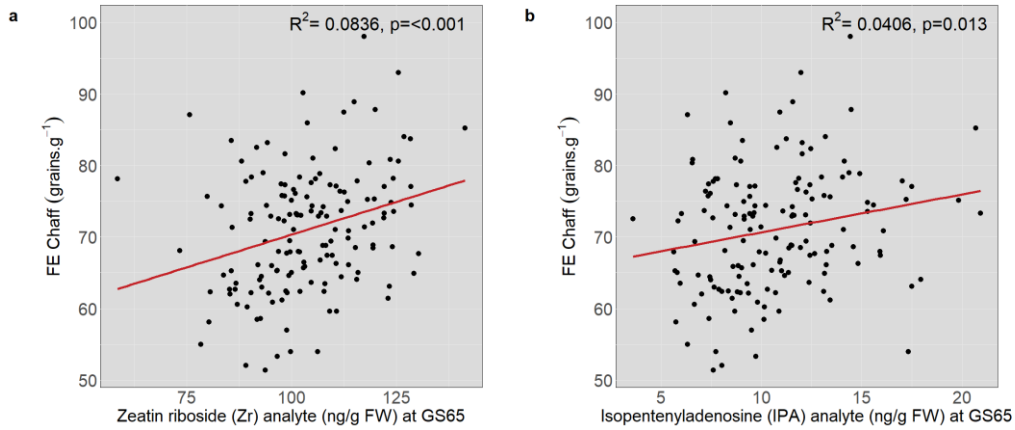

***Figure 3.15**: Linear regressions of 150 HiBAP II genotypes between spike cytokinins at GS65 and fruiting efficiency calculated with chaff DM*

Hormones calculated as the means of 2 reps, FE as 3 reps, both in 2018-19, a) Zr, y=0.16x+54.6, b) IPA, y=-0.13x+72.4, fruiting efficiency calculated using the chaff DM at physiological maturity

For the subset of 10 lines, at GS49 the spike hormones correlating with key grain partitioning traits were different from the hormones at GS65. Spike abscisic acid (ABA) level was negatively correlated with $AGDM_{A+7}$ (r=-0.58, P<0.10) and $AGDM_{PM}$ (r=-64, P<0.05) (Table 3.6), while it was not correlated with any trait at anthesis. In contrast, salicylic acid (SA) was negatively correlated with GY when sampled at both GS49 (r=-0.69, P<0.05, Table 3.6) and GS65 (r=-0.22, P<0.001, Table 3.5). SA at GS49 was also negatively associated with above-ground DM at both anthesis (r=-0.76, P<0.05) and physiological maturity (r=-0.71, P<0.05), and had a very strong negative association with plant height (r=-0.88, P<0.001) (Table 3.6). Regarding the spike cytokinins at GS49, Z was positively correlated with GY (r=0.68, P<0.05), as was IPA (r=0.56, P<0.10), while 2iP was positively correlated with $AGDM_{PM}$ (r=0.78, P<0.01) and GY (r=0.70, P<0.05) but negatively correlated with SPI (r=-0.72, P<0.05) (Table 3.6).

Table 3.6*: Pearson's correlation coefficients between traits measured at GS65+7d and physiological maturity and spike hormones at GS49 among HiBAP II subset 2*

*†: DTA added as covariate if P<0.05, means of 3 reps in 2018-19, correlation significance: ‡P<0.10, *P<0.05, **P<0.01, ***P<0.001*

GY*: grain yield per m^2,* ***GN****: grain number per m^2,* ***TGW****: thousand-grain weight,* ***HI****: harvest index,* ***Height****: plant height from the base of plant to tip of the spike,* ***$AGDM_{PM}$****: above-ground dry matter (DM) at physiological maturity,* ***$AGDM_{A+7}$****: above ground DM at anthesis +7 days,* ***FE_{Chaff}****: fruiting efficiency (calculated using chaff DM at physiological maturity),* ***SPI****: spike partitioning index,* ***$SpikeDM_{A+7}$****: DM spike per unit area at anthesis+7d,* ***ABA****: abscisic acid,* ***GA1****: gibberellin 1,* ***IAA****: indole-3-acetic acid,* ***JA****: jasmonic acid,* ***SA****: salicylic acid,* ***Z****: zeatin,* ***Zr****: zeatin riboside,* ***IPA****: isopentenyladenosine,* ***2iP:*** *isopentenyladenine*

	GY	GN	TGW	HI†	Height	AG DM_{PM}	AG DM_{A+7}†	FE_{chaff}	SPI†
ABA†	-0.36	0.35	-0.42	0.21	-0.3	**-0.64***	**-0.58‡**	0.55	0.3
GA1	-0.17	-0.11	0.35	**-0.62‡**	**0.59‡**	0.26	0.41	**-0.62‡**	-0.09
IAA	0.30	0.01	-0.16	0.22	0.46	0.29	0.05	-0.23	-0.22
JA	-0.04	0.30	-0.26	-0.09	0.02	-0.04	0.08	-0.09	0.22
SA	**-0.69***	0.10	**-0.84****	0.1	**-0.88*****	**-0.71***	**-0.76***	0.49	-0.16
Z	**0.68***	-0.15	0.38	0.34	0.27	0.54	0.37	-0.01	-0.1
Zr	0.27	0.43	0.07	-0.13	0.13	0.48	0.15	0.3	-0.37
IPA	**0.56‡**	-0.08	0.34	**0.60‡**	0.09	0.08	-0.08	0.44	0.29
2iP	0.25	**0.70***	-0.13	-0.49	0.43	**0.78****	0.2	0.12	**-0.72***

3.4 Discussion

3.4.1 Association between harvest index, biomass and grain yield

During the Green Revolution in the 1960s and 1970s, biomass partitioning to the grain was increased to raise yields, mainly through introgression of the *RhtB1b* and *RhtD1b* semi-dwarfing genes (Miralles and Slafer, 2007). The harvest index has, in many countries, had relatively little improvement since about 1990. Instead, in the last 30 years mainly above-ground biomass has increased with plant breeding, e.g. in NW Mexico (Aisawi et al., 2015), in the UK (Shearman et al., 2005), and in Australia (Sadras and Lawson, 2011). Nevertheless, in Argentinean wheat cultivars released from 1999 to 2011, yield gains were still associated with an increase of HI with no association with above-ground DM (Lo Valvo et al., 2018). In the HiBAP II, GY was strongly correlated with above-ground DM at physiological maturity ($AGDM_{PM}$) and slightly less strongly with harvest index. However, there was a trade-off between $AGDM_{PM}$ and HI, so the potential of the genotypes which had the highest biomass was not fully exploited (Foulkes et al., 2011). HI in the HiBAP II was at a maximum of 0.53, which is still significantly below the hypothetical limit of ca. 0.64 (Austin, 1980; Foulkes et al., 2011). In recent decades, genetic progress in CIMMYT spring wheat has slowed and HI has decreased (Aisawi et al., 2015), suggesting there is further scope to increasing HI in high biomass genotypes.

Many earlier studies have found a positive association between genetic variation in GN and GY, reflecting that breeders have increased grain sink strength through increasing GN or potential grain weight or both (Fischer, 1985; Slafer and Savin, 1994). GN was also associated with GY in the HiBAP II. The trade-off between GN and TGW (Figure 3.5) could be due to increased grain set in distal floret positions within spikelets that have a smaller potential size, or because of a source limitation to grain growth (Slafer and Savin, 1994; Acreche et al., 2008). Grain growth involves the expansion of pericarp and seed endosperm cells before grain filling, which determines the capacity of the grain for the storage of starch (Calderini et al., 2021). Therefore, manipulating grain expansion could increase both grain potential weight and final realised weight. This trade-off suggests that further increases in GN would be partially offset by decreases in grain weight, so the potential grain weight in distal grains needs to be increased, potentially through understanding hormonal or genetic controls (Gaju et al., 2009; Bustos et al., 2013). For example in barley, *Vrs2* is involved in inflorescence and shoot development by

maintaining hormonal homeostasis during spike development (Youssef et al., 2017).

A higher GN was observed in shorter plants (Figure 3.5), which was partly explained because there was increased partitioning to the spike with shorter plants, as observed by Miralles and Slafer (2007). However, no association was found between GY and plant height, likely due to the trade-off with TGW. A positive correlation was reported between plant height and $AGDM_{A+7}$ and $AGDM_{PM}$, which has been previously observed in modern CIMMYT spring wheat germplasm (Aisawi et al., 2015; Rivera-Amado et al., 2019). This effect on higher biomass with taller plants could be partly because taller plants achieve earlier canopy closure and greater fractional radiation interception during the first half of the stem-extension phase (Song et al., 2013).

In addition, planting in a raised bed system, where there is a relatively large gap between the beds (56 cm between beds in these experiments), may favour taller genotypes, as the taller genotypes achieve earlier canopy closure in the gap between the beds. This, therefore, increases the interception of photosynthetically active radiation (Fischer et al., 2005; Fischer et al., 2019). CIMMYT currently plants in raised beds as it saves water, supplemental nitrogen application and reduces the risk of lodging. Therefore, despite the potential favouring of tall genotypes with reduced HI in the CIMMYT breeding program, this may be offset by the increased biomass and the agronomic benefits (Sayre and Hobbs, 2004). Consequently, wheat breeders should take account of the planting system when optimising plant height for HI and biomass in their programs.

Plant height was negatively associated with HI, and in the past reducing height was the target that subsequently increased HI (Acreche et al., 2008). The HiBAP II ranged in height from 88.7 cm to 120.6 cm, slightly taller than the upper range of optimum height of 70-100 cm reported by Richards (1992). Aisawi et al. (2015) reported the plant height of CIMMYT spring wheat cultivars to have increased from 94 to 104 cm from 1966 to 2009 in a set of 12 historic cultivars. Therefore, small targeted reductions in specific internode lengths of the plant height in CIMMYT spring wheat cultivars may help to increase HI further through increasing spike growth, and may not negatively impact yield by reducing plant height below the optimal range.

3.4.2 Strategies to increase spike partitioning index

As mentioned above, and observed in recent investigations, HI is decreasing or a least stagnant with plant breeding in many countries such as Mexico (Reynolds et al., 2017). Further advances in HI require further gains in GN, which could be targeted by increasing partitioning to, and optimising partitioning within the spikes, while maintaining lodging resistance and grain size (Foulkes et al., 2011). Grain sink size could also be increased by increasing potential grain weight, but this assumes that grain growth is still sink limited (Duan et al., 2018). Currently, most evidence suggests that wheat is still sink limited (Fischer et al., 2014). Two traits that have been suggested to potentially increase HI but have not been actively selected for in wheat breeding programmes are spike partitioning index (ratio of spike DM to above-ground DM at anthesis) and fruiting efficiency (ratio of grain number to spike DM at anthesis). In the HiBAP II, there was a trade-off between SPI and FE (Table 3.2), which will be discussed in the next section.

Grain number was not associated with spike partitioning index, which was not expected, as grain number is known to be fixed in the pre-anthesis period and is previously reported to be correlated with spike growth (Foulkes et al., 2011). Previous work in the HiBAP I, a panel that shares 50 lines with HiBAP II and was developed under the same principles, found a positive association between SPI and GN (Sierra-Gonzalez, 2020). The lack of association of SPI with GN amongst the lines of the HiBAP II has been observed before in CIMMYT germplasm, Rivera-Amado et al. (2019) found no association in a panel of 26 spring wheat cultivars. In the HiBAP II, this may be partially explained by a negative association between spike DM_{A+7} and GN, which has been reported before in recombinant inbred lines from the Seri/Babax population (Dreccer et al., 2009). This could be because relatively more DM is allocated to the chaff in larger spikes, rather than the biomass being allocated to fertile florets. However, spike PI was positively associated with both GY and HI, and also spike DM_{A+7}, so even though no association was seen when comparing GN and SPI, SPI may have been associated with an increase in grain sink size (GN x potential grain weight), even though we saw no association with GN or TGW. Both SPI and spike DM_{A+7} were negatively associated with FE_{A+7}, as has been reported in previous literature, (Dreccer et al., 2009; Terrile et al., 2017; Sierra-Gonzalez, 2020), suggesting that reducing spike DM_{A+7} may be increasing FE. If reducing spike PI or spike DM_{A+7} increases FE, it may be that plants are unable to allocate enough resources from the rest of the spike to the florets.

3.4.3 Optimising partitioning pre-anthesis for spike growth

It is important to understand how biomass within the plant is competing with the spike growth in the pre-anthesis period, to know what plant component can be reduced to allocate more biomass to the spike and increase grain number. There was a negative relationship between stem PI and spike PI, and also a negative but less strong association between lamina PI and spike PI. Reducing stem partitioning could be addressed by reducing the plant height, however, further reduction in plant height below the optimum range may mean a reduced radiation-use efficiency due to increased shading of leaves and sub-optimal light distribution (Miralles and Slafer, 1997). Similarly, while there's a negative association between SPI and lamina PI, there's likely a trade-off between reduced lamina partitioning and post-anthesis photosynthetic capacity (Cruz-Aguado et al., 1999), so this might not be the best target to increase SPI, HI and GY.

Since stem and spike growth overlaps during stem elongation from booting to anthesis (Brooking and Kirby, 1981), the extent to which the stem is competing with the spike will differ between stem internodes. Therefore reducing competition with the stem by selectively reducing specific stem internodes may help increase translocation of carbohydrates to the spike whilst broadly maintaining plant height (Rivera-Amado et al., 2019). In the present study, spike PI was negatively associated with all leaf-sheath internode PIs, but no association was seen with true-stem internode PIs. This is in contrast to what was reported in the HiBAP I, where true-stem internode 2 and 3 PI were negatively associated with spike PI (Sierra-Gonzalez, 2020). The seasons were slightly longer in the HiBAP II experiments rather than HiBAP I experiments (68-85 days to anthesis in HiBAP I vs. 73-91 days to anthesis in HiBAP II), so perhaps the longer growth period changed canopy size and structure and allowed for more leaf sheath growth in the HiBAP II. However, the leaf sheath PI in the HiBAP I ranged from 0.16 to 0.20 (Sierra-Gonzalez et al., 2021) and in the HiBAP II ranged from 0.16 to 0.21, so the leaf sheath growth was not much higher in the HiBAP II. When relating overall leaf sheath PI and true-stem PI to days to anthesis, only leaf sheath PI saw a positive trend with days to anthesis (R^2=0.07, P= 0.140, data not shown). When looking within the stem, the strongest association for leaf sheath PI with spike PI was internode 2, which concerning priority phytomers is consistent with HiBAP I, suggesting the timing effects of competition with the spike growth were similar, but an alternative plant organ was responsible. Leaf-sheath internode 2 PI also had a strong negative association with GY, HI and spike DM_{A+7}.

Previously, Rivera-Amado et al. (2019) suggested one way to increase SPI and hence HI may be to decrease DM partitioning to true-stem internode 2 as mentioned above, so in the case of the HiBAP II, where leaf sheath was the plant component that appeared to be competing most strongly with the spike, can leaf sheath DM partitioning be reduced? In practice, decreasing leaf sheath without decreasing true stem may be difficult, but potentially this could help increase HI whilst keeping plant height within the optimum range (Miralles and Slafer, 1997). The leaf sheath has a photosynthetic role, particularly after the flag leaf senesces and is important for grain growth during late grain filling (Rivera-Amado, 2016). This means reducing the leaf sheath may have negative effects for TGW, although this will depend on the source-sink balance of the genotype. While the peduncle was also negatively associated with spike PI, it contributes to post-anthesis photosynthesis and DM remobilisation to the grain relatively more than internode 2 (Gebbing, 2003). As expected from photosynthetic organs like leaves, sucrose concentration in the peduncle increases during the light as temporary storage before the export of sugars to sinks or respiration in the dark (Gebbing, 2003). In addition, internode 4+ PI (true stem + leaf sheath) was negatively associated with the spike PI and HI. However, these lower internodes are important for lodging resistance so may not be the optimum target to be reduced (Foulkes et al., 2011).

While internode 2 leaf sheath PI appears to be an important trait, measurement is time-consuming and could not be easily scaled up to thousands of plots in breeders' trials. Therefore, high throughput phenotyping methods need to be established for these target traits, and internode length is a good proxy for internode 2 and 3 true-stem PI (Figure 3.11). However, individual internode lengths did not correlate with their corresponding internode leaf sheath PIs. Alternatively, molecular markers may be developed for these traits. Peduncle length did not show the same association with ped true-stem PI, potentially because the peduncle still extends post-anthesis + 7 days (Gebbing, 2003), and the peduncle length measurement was taken at the start of grain filling rather than anthesis +7 days to reduce demand on measurements required at anthesis +7 days.

3.4.4 Strategies to increase fruiting efficiency

FE_{A+7} showed a positive association with GN amongst genotypes, as observed previously in other wheat field studies (Gonzalez et al., 2011; Garcia et al., 2014), but there was no association with HI or GY (Table 3.2). The lack of association with GY and HI could be because of the negative association observed between FE_{A+7} and TGW. Increased FE could be because of an increased proportion of

distal grains within the spikelets reducing the average potential weight of the grain and therefore the TGW (Ferrante et al., 2015). For example, this could be explained by larger ovaries in more proximal florets within the spikelet, leading to heavier grains (Bustos et al., 2013). Alternatively, it could be associated with a lower threshold for floret survival. (Slafer et al., 2015). Despite this relationship in the HiBAP II, it is possible to increase both TGW and grain number, as demonstrated by Bustos et al. (2013) in a Bacanora x Weebil DH population in field experiments in Chile. Therefore, if breeding is aimed at improving FE, breeders must be aware of the possible, though not mandatory, trade-off with TGW, and should check that the trade-off is not emerging from the progeny being selected.

As well as looking at the resource threshold for floret development, one avenue to improve FE could be to optimise intra-spike partitioning, so that assimilate is delivered to developing florets rather than spike structural components (Garcia et al., 2014). In the subset of 10 lines in the HiBAP II, there were no associations between spike component PIs and FE_{A+7}, but there were with FE_{chaff}. This could be partly because the spike morphological components were measured at anthesis +7 days rather than anthesis. Whilst the extra grain growth was not included in the PI calculations, there were small differences in the amounts of growth between lines, which could potentially affect the grain set. FE_{chaff} could also be more precise because there is remobilisation of soluble carbohydrate from the chaff components post-anthesis, and therefore the chaff may represent a more precise estimate of the structural DM of the spike components, which competes with the florets for assimilate pre-anthesis. Rachis PI had a negative association with spike PI, suggesting the rachis was competing for assimilates with florets during spike development and growth.

Rachis specific weight and FE_{chaff} were negatively associated, which could be explained by associations with the vascular connections within the rachis (Bancal and Soltani, 2002). This association between rachis SW and FE has been reported previously in Mexican spring wheat germplasm (Rivera-Amado et al., 2019). Rachis SW was also positively associated with TGW and spike DM_{A+7}. This would suggest that more compact spikes, which had smaller investment in the rachis, may reduce TGW, potentially through reduced spike photosynthesis or reduced transport of assimilates to the grain through vascular architecture effects. There are also more physical restrictions to grain growth in compact spikes (Millet, 1986; Foulkes et al., 2011). If the rachis, and more importantly the vascular connections within the rachis, are important for increasing FE, then it's important we understand

more about how this process is working, including the signalling occurring in the spike with plant hormones.

In the present experiments, measurements of spike DM were taken at anthesis + 7 days rather than anthesis. This stage was selected to coincide with the onset of rapid linear grain growth. However, this is not always consistent between genotypes, particularly with changing weather conditions, and so a more accurate growth stage to sample at may have been GS65. Sampling plants at anthesis + 7 days could also lead to underestimation of FE values, as some of the spike dry weight at anthesis + 7 days is grain growth, not chaff (Elia et al, 2016).

3.4.5 Spike hormone effect on key yield traits

It is important to understand how hormones play a role during the period immediately before and after anthesis, as grain number and potential grain weight are determined during this period (Geng et al., 2017). At GS65 across all 150 genotypes, the cytokinins Zr and IPA were positively associated with both FE_{A+7} and FE_{chaff} and negatively associated with TGW (Table 3.5, Figure 3.14). Zr, IPA and 2iP were also positively associated with GN. Previous studies have found high levels of cytokinins in the developing grains of cereals (Liu et al., 2013a). However, cytokinin levels have also been found to be high in florets where grain filling does not occur (Lee et al., 1988). Considering the trade-off between FE and TGW is being reflected in the cytokinin associations, it's possible that in the HiBAP II the reported effect of cytokinin decreasing TGW at anthesis may be an indirect effect on the GN. Cytokinins have also been shown to be key in promoting cell division, growth and differentiation, axiliary bud growth and delaying leaf senescence, all of which could contribute to increasing grain number and hence fruiting efficiency (Jameson and Song, 2016).

The period between the terminal spikelet formation, when the stem begins to elongate, and anthesis is of paramount importance in the yield formation of wheat as this is when the grain number per unit area is determined (Slafer and Rawson, 1994). Evidence suggests that hormones may mediate the impact of environmental conditions during stem elongation and booting (Reynolds et al., 2012), and so the subset of 10 genotypes was selected to additionally assess spike hormones at GS49. In the present experiments, cytokinins IPA and Z at GS49 were positively associated with GY, while cytokinin 2iP was positively correlated with GN. In previous studies, exogenous applications of Z to winter wheat (cv. YM 158) during floret development increased the number of fertile florets per spike and grain set

per ear (Wang et al., 2001). Adding 6-BA, a synthetic cytokinin, to spring barley during the glume primordium stage increased GY by up to 57 % (Williams and Cartwright, 1980). While these studies have looked at exogenous applications of cytokinins, evidence on endogenous effects is provided by the *Gn1a* QTL in rice, which is a gene for cytokinin oxidase/dehydrogenase (*OsCKX2*), an enzyme that degrades cytokinin. When the expression of *OsCKX2* is reduced, cytokinin accumulates in the inflorescence meristems and increases the number of reproductive organs resulting in enhanced GY (Ashikari et al., 2005). This is also seen in wheat grown in the greenhouse, where reducing expression of *TaCKX2.4* increased grain number (Li et al., 2018a). This positive association was also seen in the HiBAP II at late booting with 2iP and anthesis with Zr, 2iP and IPA positively correlating with GN.

Previous literature suggests that applications of gibberellins rescue the fertility of male-sterile mutants of barley (Kasembe, 1967; Huang et al., 2003), as they are involved in the development of anthers and pollen. Furthermore, Nakajima et al. (1991) found a male-sterile mutant of rice had 80-87 % lower GA than the standard japonica rice cultivar. This suggests GA is important in floral processes at anthesis. However, in the current study GA1 at GS65 was negatively associated with GN and FE_{A+7}. The previous studies that reported GA having a positive effect were not in wheat, and so, as suggested by Huang et al. (2003), the role of GA could be species dependent. Other studies have reported a negative effect of applying GA in wheat when added early in floret development (Colombo and Favret, 1996), and for GA1 at late booting, there was not only a negative association with HI but also with FE_{chaff}.

Spike ABA levels at GS49 had a negative relationship with both AGDM at physiological maturity and anthesis + 7 days. In other plants, studies have found that ABA is related to slowing or inhibiting growth. For example in *Lupinus angustifolius,* ABA concentration showed a negative relationship with growth (Emery et al., 1998). In two wheat cultivars, exogenous applications of ABA reduced total biomass under both well-watered and water-stressed conditions (Zhang et al., 2005). This suggests that the negative relationship seen with both DM at anthesis and maturity was due to higher concentrations of ABA acting as a growth inhibitor. Literature has also reported that ABA impacts grain number, with applications of ABA on winter wheat inhibiting floret development (Wang et al., 2001). However, in the HiBAP II, there was no association between ABA at either GS49 or GS65 and GN. This may be because ABA levels stayed low enough to

not have the inhibitory effect, compared to other studies reported in the literature, e.g. McWha (1975) reported a range of 100-125ng/g FW in two genotypes, while the 150 lines of the HiBAP II ranged from 23-109 ng/g FW at GS65.

One hormone that had a consistent effect at both GS49 and GS65 was salicylic acid, a hormone that is reported to be involved in several stress responses such as pathogen infection, UV irradiation, salinity and drought (Sedaghat et al., 2017). In the present experiment, SA was negatively associated with GY at both GS49 and GS65, and at GS65 SA was also negatively associated with HI. The vast majority of SA studies show how higher concentrations of SA effect stress conditions (Janda et al., 2012). However, in optimal conditions, exogenous applications of SA can be toxic and inhibit dry matter accumulation in several crops (Shettel and Balke, 1983) and decrease the thickness of leaves in barley (Uzunova and Popova, 2000). Some literature indicates exogenous applications of low concentrations of SA may be beneficial, but higher concentrations can be detrimental to photosynthetic capacity (Sahu et al., 2002), and the present results showed excess SA either directly or indirectly may have a deleterious effect.

3.4.6 Conclusions

It is likely that the spike hormone traits are highly influenced by the environment, which resulted in R^2 values for trait associations which were not always very high. Spike hormonal samples for the 150 genotypes were sampled over 3 hours around midday to control for the environment but there was also a certain amount of spatial variation across the field experiment and within replicates. For genetic studies to take these spike hormone traits forward, they might need to be measured in a more controlled environment such as a glasshouse. Nevertheless, it is still encouraging that highly significant P values were reported in the field environment between spike cytokinins and grain number traits despite the large environmental variation.

Chapter 4: Glasshouse Experiments on a Subset of 10 HiBAP II Genotypes

4.1 Introduction

Previously, grain yield was increased during the Green Revolution through the introgression of *Rht* dwarfing genes that resulted in height reduction and changed assimilate partitioning, favouring the spike during stem elongation, increasing spike growth and grain number (Hedden, 2003). Thus *Rht* dwarfing genes increased grain number per m^2 (GN) by increasing the spike partitioning index (ratio of spike dry matter to above-ground dry matter, SPI). Despite this major advancement in the 1960s and 1970s, with a growing population and a slowing rate of increase in grain yield, we presently need to double wheat production by 2050 in new and novel ways (Bruinsma, 2009; Reynolds et al., 2021). The grain yield of modern cultivars is still limited by grain sink strength and grain number (Rivera-Amado et al., 2020).

There is evidence in recent investigations in wheat that genetic variation in fruiting efficiency (the ratio of grain number to spike dry matter at anthesis, FE) is associated with GN (Gonzalez et al., 2011; Garcia et al., 2014), and could therefore be used as a proxy in selection in wheat breeding to increase GN. However, FE has not been actively selected as a target to increase GN, and so there are limited investigations that have quantified the genetic basis of FE. As FE is a medium-throughput destructive measurement, to deploy it into breeding an understanding of the basis of the genetic variation could lead towards identifying mechanisms and molecular markers that will help breeders screen material in marker-assisted selection. One way to increase FE could be by improving assimilate partitioning within the spike to the developing florets (Ferrante et al., 2013), as FE reflects the outcome of floret development (Slafer et al., 2015). Ferrante et al. (2017) showed previously that the difference in yield between a contemporary and traditional Spanish wheat cultivar was due to differences in FE. However, there are still unknowns on how to manipulate the partitioning to and within the spike to increase FE, due to the limited research.

Previous work has shown a trade-off between FE and SPI (Dreccer et al., 2009; Terrile et al., 2017; Sierra-Gonzalez, 2020), suggesting that increasing spike growth may decrease FE. This may be because the plants are unable to allocate enough resources from the rest of the spike to the florets in larger spikes, or that restricted vascular connections within the rachilla are limiting assimilate supply

(Bancal and Soltani, 2002). Other investigations have found no correlation between spike dry matter (DM) and FE, e.g. Gonzalez et al. (2011), so if this trade-off is not constitutive, it may be related to different factors. The interaction between FE and SPI is yet to be fully explained, and this could be because it is linked to plant hormone signalling.

There is evidence that genetic variation in FE is influenced by levels of spike hormones. Plant hormones have a role in more than just the relationship with FE and SPI, they are important throughout the plant life cycle from growth to stress responses (Jameson and Song, 2016). In particular, cytokinins (CK) are important at multiple growth stages. In Chinese winter wheat, when synthetic CK 6-benzylaminopurine (6-BA) was added 25 days after stem elongation initiation, floret abortion rates were reduced as much as 77 % compared to the control sprayed with water (Zheng et al., 2016). Later in wheat growth, a sharp increase in endogenous CK has been reported in the spikes immediately after anthesis (Jameson et al., 1982). One gene currently identified for CK degradation is CK oxidase/dehydrogenase (*OsCKX2*), found in the QTL *Gn1a* in rice. When the expression of *OsCKX2* is reduced, CK accumulates in the inflorescence meristems of rice (Ashikari et al., 2005). *OsCKX2* was found to be expressed in developing culms, inflorescence meristems and young flowers, and reduced expression was found to increase grain number (Ashikari et al., 2005), suggesting more CK increases grain number in rice. The CK oxidase/dehydrogenase genes found in wheat *TaCKX2* and *TaCKX6* were negatively correlated with grain number per spike and grain weight, respectively, suggesting that CKs can increase both grain number and weight in wheat (Zhang et al., 2011; Zhang et al., 2012). CKs are also known to regulate plant development through cross talk with other plant hormones. For example, auxin cytokinin cross talk is well documented. CKs are known to regulate the expression and accumulation of auxin efflux carriers PINFORMED (PIN) family, which results in increased auxin efflux (Waldie and Leyser, 2018). Auxin added exogenously post-anthesis has been shown to increase grain size (Darussalam et al., 1998), while ABA controls the transition between dormancy and germination (Rodríguez-Gacio et al., 2009).

A systematic study of gene expression during early spike development in wheat showed increased auxin signalling as the plant moved through spike developmental stages (Li et al., 2018b). Specifically, auxin was high in the spikelet and floret differentiation stages, suggesting it is important in axillary meristem initiation. The study also reported on cytokinin signalling, and found coordinated

changes in auxin and cytokinin activity, with cytokinin signalling reducing as auxin signalling increased. Cytokinins are known to regulate auxin in *Arabidopsis* through PIN-FORMED (PIN) protein accumulation (Dello Ioio et al., 2008; Ruzicka et al., 2009). Previous literature has reported cytokinin treatments can significantly reduce the expression of several PIN genes, such as *PIN3*, *PIN4* and *PIN7* (Waldie and Leyser, 2018). When Li et al. (2019a) sprayed cytokinin 6-BA on the leaves of winter wheat during the abortion stage of floret development, auxin content reduced while cytokinin content increased, resulting in an increase in fertile florets and grain number by suppressing degeneration and abortion of florets. While endogenous concentrations of auxins may be low, it is clear that the low levels are necessary to floral development in some capacity. There is evidence of cross-talk with cytokinins, so mutations, for example in the PIN proteins, are detrimental for floral development.

If these novel targets such as spike cytokinins determining FE are identified, then molecular markers can be found and used in marker-assisted selection to accelerate yield gains (Wilkinson et al., 2012). Therefore, a glasshouse experiment was carried out over three years to quantify genetic variation in spike hormone traits on 10 spring wheat cultivars (selected to contrast for fruiting efficiency), to understand in more detail how key spike hormones influence FE, GN and other key yield-related traits.

4.1.1 Chapter hypotheses

- Grain number and grain yield per plant and main shoot are positively correlated among genotypes among the subset of HiBAP II genotypes
- Increasing grain number is associated with increased spike partitioning index and fruiting efficiency among the subset of HiBAP II genotypes
- A trade-off is observed between spike partitioning index and fruiting efficiency among the subset of HiBAP II genotypes
- Competition for assimilates between spike growth and stem internodes 2 and 3 growth is stronger than between spike growth and the peduncle growth, so that the negative association with spike PI and grains m^{-2} is stronger for true-stem internodes 2 and 3 than the true-stem peduncle PIs
- Genetic variation in spike hormones, in particular spike cytokinins, is associated with key grain number traits such as fruiting efficiency in the glasshouse experiments among the subset of HiBAP II genotypes
- High abscisic acid spike hormone levels pre-anthesis has a negative association with spike fertility traits determined at anthesis

- In the glasshouse, a gradient is observed in hormonal concentrations throughout the spike (basal, central and apical spikelets) and plant (spike, flag leaf, stem) at both anthesis and booting in the HiBAP II subset

4.2 Materials and methods

4.2.1 Plant materials and experimental design

The experiments were carried out over three years, in 2017, 2018 and 2019 under fully irrigated conditions in the glasshouse at Nottingham University, Sutton Bonington Campus, UK. A subset of 10 lines from the High Biomass Association Panel (HiBAP II, Table 4.1) was used, which contains spring wheat genotypes that all have an outstanding expression of high biomass and/or biomass-related traits. The 10 genotypes were part of subset 2 in the field experiments, and are comprised of nine elite cultivars and one synthetic-derived cultivar. The 10 lines were selected based on contrasting field expressions of fruiting efficiency using previous CIMMYT data. One plant per 2 L pot was grown in John Innes no. 2 soil medium, with four replicates in 2017 and 2019 and five replicates in 2018 in a randomised complete block design (Figure 4.1). Four different sets of plants were grown per replicate to allow for sampling of destructive measurements at different stages on different plant organs throughout the growth cycle – spike hormones at late booting and anthesis and growth analysis at anthesis and maturity. All non-destructive measurements such as flag-leaf photosynthesis rate were taken on the set of plants that went through to maturity.

In 2017, the plants were sown on 2nd August, in 2018 on 13th June and in 2019 on 3rd June. Herbicides, fungicides, and pesticides were added as required to minimise the effect of weeds, diseases and pests (Table S 5). Irrigation was supplied throughout the whole cycle every day using a mixture of water and complete nutrient fertiliser applied through drip irrigation. Supplementary lighting was added in 2017 from October onwards to provide a 16 hour day length.

Table 4.1*: List of spring wheat HiBAP II genotypes in the glasshouse experiments and field experiments in subset 2*

FE_A MS: fruting efficiency calculated using spike DM at anthesis on the main shoot, calculated using 3 year means, low values are under 100 grns g^{-1} and high values are over 100 grns g^{-1}

Ent	GID	Cross Name	Origin	FE_A MS
1	5551750	CHEWINK #1	Elite	Low
2	6676541	PASTOR//HXL7573/2*BAU/3/WBLL1	Elite	Low
3	7025958	DPW 621-50	Elite	High
4	3825355	SOKOLL	Synthetic derivative	Low
5	6171902	F2SR2-69//YANGLING SHAANXI/PASTOR	Elite	High
6	7806808	BORLAUG100 F2014	Elite	High
7	6415761	FRET2*2/BRAMBLING//BECARD/3/WBLL1*2/ BRAMBLING	Elite	High
8	6415882	KIDEA	Elite	Low
9	4982242	JANZ	Elite	High
10	6489593	BCN/RIALTO//ROLF07	Elite	Low

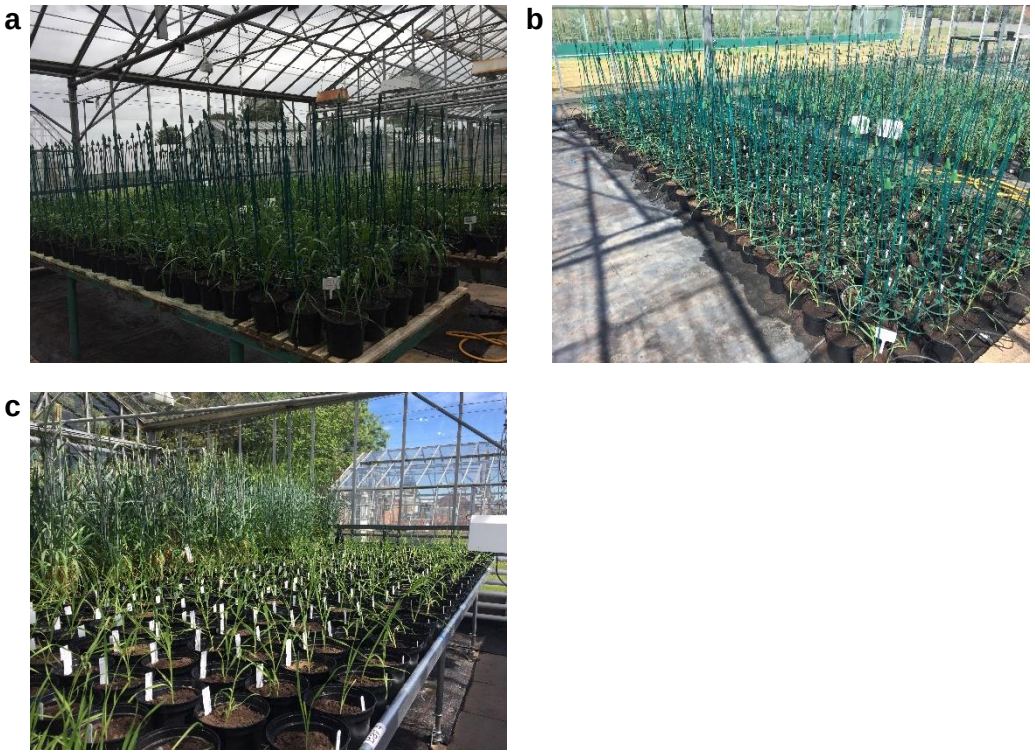

***Figure 4.1**: Photographs of glasshouse experiments of the HiBAP II in a) 2017, b) 2018 and c) 2019*

4.2.2 Plant measurements

Samples were collected at late booting (GS49), anthesis (GS65) and physiological maturity (GS89). Growth stage was taken on the main shoot (MS) of each plant by assessment twice a week according to the Zadoks growth stages (Zadoks et al., 1974).

Growth analysis at anthesis

Plants were separated into MS, other fertile shoots and infertile shoots. Each fertile shoot was then separated into the spike, leaf lamina and stem (true stem and leaf sheath attached, MS separately). The lengths of the peduncle, stem internode 2 and stem internode 3 were recorded for the MS, as well as the plant height (measured from soil surface to tip of the spike, excluding awns). Each plant component was then dried for 48 hours at 70 °C before the MS was further separated into the true stem and leaf sheath for each internode – peduncle (ped), internode 2 (int2), internode 3 (int3) and internode 4 and below (int4+) (Figure 3.2). The dry weight of each component was then recorded, and the partitioning index (PI) was calculated for the component as the proportion of above-ground biomass. True-stem specific weight (SW) was calculated as internode true-stem DM per unit internode length.

The number of fertile florets per MS spike was assessed according to the Waddington scale, where any floret over a developmental score of W9.5 (styles and stigmatic branches spreading outward, stigmatic hairs well developed, Figure 4.2) or above was considered a fertile floret (Waddington et al., 1983). The MS spike was then dissected into rachis, glumes, awns, palea, lemma and other components (small grains and anthers, not included in the partitioning analysis), as described in chapter 3, Figure 3.3. The DM for each component was recorded after drying for 48 hours at 70 °C. Dry matter partitioning index (PI) was calculated for the spike component as the proportion of the whole spike DM excluding the grains and anthers (other, Figure 3.3a). Rachis specific weight (SW) was calculated as the rachis DM per unit length.

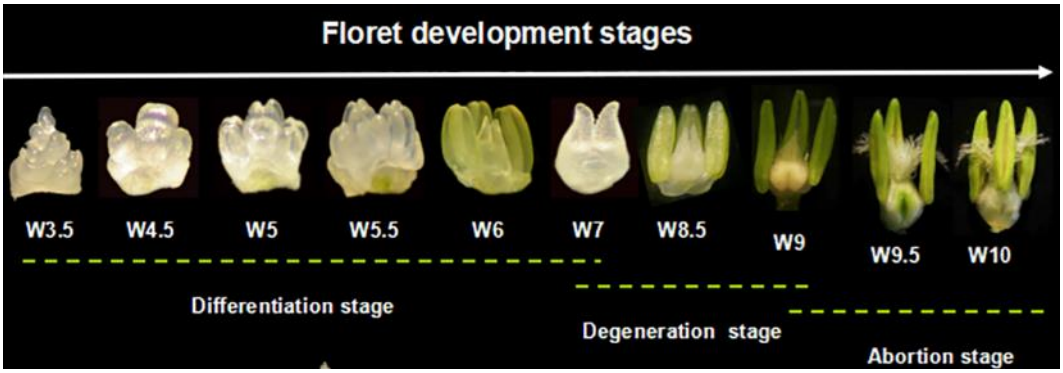

Figure 4.2*: Floret developmental stages of wheat determined with the Waddington scale (Waddington* et al*., 1983). Figure taken from Zheng* et al*. (2016)*

Image licenced under CC BY 4.0. W9.5 and over - styles and stigmatic branches spreading outward, stigmatic hairs well developed considered as a fertile floret

Growth analysis at physiological maturity

At physiological maturity, for all fertile shoots, the spike was separated from the straw (stem and leaves), and DM of the straw and spike was recorded separately after drying for 48 hours at 70 °C (MS separately). The number of spikes was counted and then threshed by hand to obtain the DM weight of grains and chaff, and grain number (MS separately). These data were then used to calculate harvest index (HI, proportion of above-ground DM in the grain), above-ground DM ($AGDM_{PM}$) and fruiting efficiency (FE, calculated two ways as a ratio of grain number to spike DM at anthesis, FE_A, or as a ratio of grain number to chaff DM at maturity, FE_{chaff}).

Flag-leaf photosynthesis rate measurements

Flag-leaf (FL) photosynthesis rate measurements were taken at 2-4 assessment dates in all three years, and split into pre- and post-anthesis measurements, as detailed in Table 4.2. Flag-leaf photosynthesis rate was measured as net CO_2 uptake using a LI-6400XT portable gas-exchange photosynthesis system (LICOR, Inc., Lincoln NE, USA).

Table 4.2: *Dates of photosynthesis rate measurements in the 3-year glasshouse experiments*

Average growth stage indicated in brackets

Year	Pre-anthesis	Post-anthesis
2017	5th October (GS 52)	1st November (GS 69)
	27th October (GS 68)	8th November (GS 75)
2018	30th July (GS 55)	9th August (GS 69)
	2nd August (61)	14th August (GS 75)
2019	N/A	14th August (GS69)
	N/A	20th August (GS 74)

The flag-leaf photosynthesis rate was measured at a saturating photosynthetic photon flux density (PPFD) of 1800 µmol m^{-2} s^{-1}, a CO_2 concentration of 400 µmol mol^{-1}, relative humidity between 50 to 70 % and temperature at 22 °C. Leaves were left to stabilise in the IRGA chamber for 5-10 minutes before readings were taken, and leaf area was used to adjust the calculation of leaf photosynthesis rate. Measurements were taken around midday to ensure the plants were still transpiring.

Plant hormone sampling and analysis

In 2017, 2018 and 2019 the MS spike of each genotype was sampled for plant hormones at GS49 and GS65. Additionally, in 2019,two genotypes (entries 1 and 9) were selected to show low (ent 1) and high (ent 9) fruiting efficiency values from 2017 and 2018 glasshouse data. For these two genotypes at GS49, the FL and ped were sampled, and at GS65 for the same two genotypes the FL, ped, and three spike sections (basal, central and apical spikelets, dividing total spikelet number by three) were sampled. Each plant component was sampled and frozen in liquid nitrogen immediately in the glasshouse and analysed for plant hormone levels as described in chapter 3.2.

4.2.3 Statistical analysis

The genotype means were estimated from the cross-year Analysis of Variance (ANOVA) using Genstat 19th edition (VSN International, 2021), where the genotypes were considered as fixed effects and replicate and years as random effects. A covariate for days to anthesis was included in the ANOVA when it had a significant effect. Broad-sense heritability (H^2) was calculated as described in Equation 4.1, where $\sigma^2 g$ and $\sigma^2 e$ are the genotypic and environment variance, respectively, and $\sigma^2 ge$ is the genotype x environment interaction. The number of environments and number of replicates are represented by *e* and *r,* respectively.

$$H^2 = \frac{\sigma^2 g}{\sigma^2 g + \frac{\sigma^2 ge}{e} + \frac{\sigma^2 e}{re}}$$

Equation 4.1

Genstat was used for calculating Pearson's correlation coefficients and linear regressions using the genotype means from the ANOVA calculated previously.

4.3 Results

4.3.1 Plant traits at anthesis and physiological maturity

The mean daily temperatures in the glasshouse experiments are shown in Figure 4.3, in 2017 the experiment was sown later than the two other years (02/08/17 vs 13/06/18 and 03/06/19). This resulted in lower temperatures during grain filling and a longer growing season, as anthesis was reached 13 days later in 2017 than 2018 and 2019 (66 DTA in 2017 vs. 51 in 2018 and 53 in 2019, Table 4.3).

Comparing between years, mean values for most anthesis traits were similar, except for peduncle length and plant height, which was longer in 2017 than other years and above-ground dry matter at anthesis ($AGDM_A$) per plant, which was greater in 2017 than in 2018 and 2019 (Table 4.3). Cross-year analysis of variance of plant height, internode length, biomass and partitioning traits showed the genotype by year interaction was not significant. The effect of genotype and genotype by year interaction was significant for all other traits (Table 4.3). Averaging over all years, there was wide genetic variation in above-ground dry matter per plant at both anthesis (5.45-9.24 g, $P<0.001$, Table 4.3) and physiological maturity (11.05-22.01 g, $P<0.001$, Table 4.4). At physiological maturity, fruiting efficiency calculated based on main shoot (MS) spike DM at anthesis (FE_A) ranged among varieties from 78.7-115.8 grns g^{-1} ($P=0.015$), and based on chaff DM (FE_{chaff}) from 73.3-116.9 grns g^{-1} ($P=0.004$) (Table 4.4). Grain number per MS (GN_{MS}) ranged from 29-48 grains ($P=0.004$) and grain number per plant (GN_P) ranged from 136-275 ($P<0.001$). Moderate heritability (0.5-0.7) was observed for most traits at anthesis such as stem internode 2 and 3 lengths, and lamina PI. A few traits at anthesis had high heritability (>0.7) such as stem PI and peduncle length. At maturity, high heritability was seen for the majority of traits except for MS $AGDM_{PM}$ and HI per MS (HI_{MS}) (0.51 and 0.46, respectively).

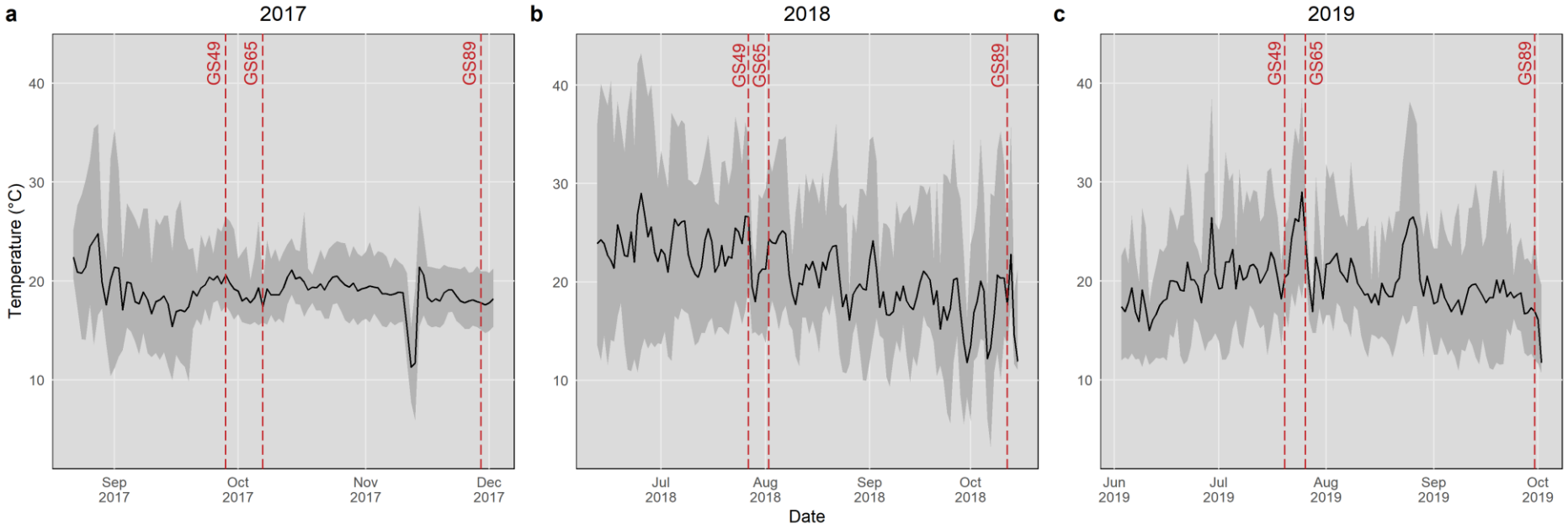

***Figure 4.3**: Meteorological data for daily mean temperature in a) 2017, b) 2018 and c) 2019 with key growth stages indicated*

Red dotted lines indicate the average date of key growth stages – late booting (GS49), anthesis (GS65) and physiological maturity (GS89). Means taken per 24 hour period, grey shading indicates the minimum and maximum values for each day. Months labelled on the x-axis indicate the start of the month

***Table 4.3**: Phenotypic ranges, least significant differences (LSD, P=0.05), heritability and significance (p-values) for 10 spring wheat HiBAP II genotypes at anthesis in the glasshouse experiments*

†: DTA added as a covariate if P<0.05

***DTA**: days from emergence to anthesis, **AGDM$_A$**: above-ground dry matter (DM) at anthesis, **Stem PI**: stem partitioning index, **Spike PI**: spike partitioning index, **Lamina PI**: Lamina partitioning index, **Int**: stem internode*

		Range 2017	Range 2018	Range 2019	Genetic range combined and ANOVA treatments effect				
		(Min-Max)	(Min-Max)	(Min-Max)	(Min-Max)	Heritability	LSD (5 %)	Genotype significance	GenxYear significance
Main Shoot	DTA	55-76	49-54	50-55	51-60	0.34	2.45	<0.001	<0.001
	Plant Height cm	65.28-101.19	55.66-70.30	60.50-72.10	60.11-80.29	0.44	6.54	<0.001	0.388
	AGDM$_A$ g	1.71-2.70	0.88-1.68	1.09-1.60	1.20-1.91	0.26	0.21	<0.001	0.131
	Fertile florets per spike	38.46-58.00	24.73-42.00	31.00-51.00	32.74-45.38	0.54	6.17	<0.001	0.026
	Spike DM g	0.33-0.51	0.25-0.40	0.26-0.49	0.31-0.43	0.55	0.06	0.001	0.097
	Spike PI	0.14-0.21	0.21-0.32	0.22-0.38	0.21-0.30	0.48	0.03	<0.001	0.004
	Lamina PI	0.21-0.36	0.17-0.28	0.16-0.28	0.18-0.29	0.67	0.03	<0.001	0.003
	Stem PI	0.46-0.58	0.47-0.54	0.46-0.53	0.48-0.54	0.79	0.02	<0.001	<0.001
	Ped length cm	23.80-32.25	17.72-29.61	19.45-32.50	21.62-29.69	0.79	4.31	<0.001	0.502
	Int 2 length cm	15.60-25.65	12.42-18.37	12.40-18.47	13.39-19.86	0.69	2.14	<0.001	0.097
	Int 3 length cm	8.83-17.25	4.81-10.98	7.27-12.30	6.80-12.30	0.60	1.42	<0.001	<0.001
Plant	AGDM$_A$ g†	7.56-12.67	4.29-8.25	3.13-7.04	5.45-9.24	0.64	1.21	<0.001	0.043

***Table 4.4**: Phenotypic ranges, least significant differences (LSD, P=0.05), heritability and significance (p-values) for 10 spring wheat HiBAP II genotypes at physiological maturity in the glasshouse experiments*

***$AGDM_{PM}$**: above-ground dry matter (DM) at physiological maturity, **TGW**: thousand-grain weight, **HI**: harvest index, **FE_A**: fruiting efficiency calculated using spike DM at anthesis, **FE_{chaff}**: fruiting efficiency calculated using chaff DM at maturity*

		Range 2017	Range 2018	Range 2019	Genetic range combined and ANOVA treatment effects				
		(Min-Max)	(Min-Max)	(Min-Max)	(Min-Max)	Heritability	LSD (5 %)	Genotype significance	GenxYear significance
Main Shoot	**$AGDM_{PM}$ g**	2.83-4.32	1.76-3.05	1.96-4.02	2.15-3.42	0.51	0.46	<0.001	0.023
	Grain yield g	1.07-1.83	0.83-1.52	0.81-2.09	0.91-1.51	0.81	0.28	0.005	0.005
	TGW g	21.36-35.90	26.15-46.40	27.30-50.34	25.03-43.72	0.74	5.36	<0.001	0.049
	HI	0.34-0.42	0.43-0.51	0.33-0.56	0.40-0.47	0.46	0.05	0.05	0.048
	FE_A grns g^{-1}	85.7-116.6	80.5-144.5	65.6-128.3	78.7-115.8	0.72	24.18	0.015	0.081
	FE_{chaff} grns g^{-1}	76.9-153.1	72.8-98.8	50.8-111.3	73.3-116.9	0.76	20.64	0.004	0.328
	Grain no.	34.20-69.40	27.80-37.20	16.50-42.00	29.20-48.00	0.52	9.11	0.004	0.429
Plant	**No. fertile shoots**	4-9	6-12	4-9	6-9	0.72	1.26	<0.001	0.010
	No. Infertile shoots	1-11	0-5	0-3	1-6	0.63	1.46	<0.001	<0.001
	$AGDM_{PM}$ g	13.61-21.31	8.85-24.60	7.69-19.48	11.05-22.01	0.77	2.80	<0.001	0.005
	Grain yield g	3.96-6.96	4.24-9.76	2.35-8.33	4.75-8.29	0.83	1.48	<0.001	0.001
	TGW g	28.17-36.55	23.09-41.47	25.84-42.81	25.96-34.94	0.71	5.45	0.044	0.091
	HI	0.22-0.38	0.37-0.48	0.31-0.55	0.32-0.46	0.64	0.04	<0.001	0.018
	FE_{chaff} grns g^{-1}	70.6-134.3	79.5-95.5	61.3-111.6	73.0-112.0	0.92	14.77	<0.001	0.464
	Grain no.	135.6-232.7	134.8-329.9	78.3-263.5	136.3-275.3	0.84	39.60	<0.001	0.002

Correlations between stem-internode traits and other key traits amongst genotypes measured at anthesis and physiological maturity are shown in Table 4.5. Both true stem (TS) and leaf sheath (LS) ped PI were negatively correlated with the MS spike DM (r=-0.73, P<0.05 and r=-0.63, P<0.10, Table 4.5). MS spike DM was also correlated with MS int3 TS PI (r=0.55, P<0.10), ped TS specific weight (SW, r=0.62, P<0.10) and int2 TS SW (r=0.66, P<0.05, Table 4.5). MS ped TS PI was negatively correlated with grain yield per MS (GY_{MS}) (r=-0.68, P<0.05), while MS int3 LS PI and MS ped, int2 and int3 TS SWs were all positively correlated to GY_{MS} (P<0.05, Table 4.5). FE_{chaff} was also negatively correlated with int2 LS PI (r=-0.62, P<0.10).

When looking at how FE_A and FE_{chaff} MS were related to GN_{MS}, only FE_{chaff} was positively correlated to GN_{MS} (R^2=0.56, P=0.013, Figure 4.4), while FE_A did not correlate with GN_{MS} (R^2=0.12, ns, Figure 4.4). The linear regressions between other traits at physiological maturity are shown in Figure 4.5. GN_P and grain yield per plant (GY_P) were positively correlated (R^2=0.73, P=0.002 Figure 4.5b), and there was a trend for an association between GN_{MS} and GY_{MS} (R^2=0.05, Figure 4.5a). GY_{MS} and $AGDM_A$ per MS were also positively correlated (R^2=0.50, P=0.023, Figure 4.5e), as was GY_P and $AGDM_A$ per plant (R^2=0.65, P=0.005, Figure 4.5f). There was no association between GY and thousand-grain weight (TGW) or GY vs. harvest index (HI) on either a per MS or per plant basis.

Table 4.5: *Pearson's correlation coefficients between traits measured at anthesis and physiological maturity and stem internode partitioning among 10 HiBAP II genotypes in glasshouse experiments*

*Cross year means of 2017, 2018 and 2019, correlation significance: ‡P<0.10, *P<0.05, **P<0.01, ***P<0.001*

***GY**: grain yield, **GN**: grain number, **TGW**: thousand-grain weight, **HI**: harvest index, **FE_A**: fruiting efficiency calculated using spike DM at anthesis, **FE_{chaff}**: fruiting efficiency calculated using chaff DM at maturity, **Spike PI**: spike partitioning index, **Spike DM**: dry weight spike per unit area at anthesis, **MS**: Main shoot, **PED**: peduncle, **INT2**: stem internode 2, **INT3**: stem internode 3, **TS**: true stem, **LS**: leaf sheath, **PI**: partitioning index (calculated as a proportion of above-ground biomass), **SW**: specific weight (proportion of the DM with length)*

Traits	GY MS	GN MS	TGW MS	HI MS	FE_A MS	FE_{chaff} MS	Spike PI MS	Spike DM MS
PED TSPI	**-0.68***	-0.17	-0.38	-0.28	0.46	0.26	0.20	**-0.73***
INT2 TSPI	-0.02	0.41	-0.28	0.13	-0.16	0.41	0.45	0.37
INT3 TSPI	0.16	0.23	0.08	0.08	-0.50	0.04	0.15	**0.55‡**
PED LSPI	-0.38	-0.51	0.03	-0.01	0.34	-0.05	0.15	**-0.63‡**
INT2 LSPI	0.16	**-0.82****	**0.74***	0.04	-0.11	**-0.62‡**	-0.31	-0.20
INT3 LSPI	**0.70***	0.04	**0.64***	-0.04	-0.35	-0.28	-0.52	0.50
PED TSSW	**0.76***	0.13	0.48	-0.04	-0.34	-0.39	**-0.58‡**	**0.62‡**
INT2 TSSW	**0.73***	0.01	0.54	0.14	-0.44	-0.33	-0.34	**0.66***
INT3 TSSW	**0.61‡**	-0.07	0.55	0.01	-0.35	-0.35	-0.45	0.43

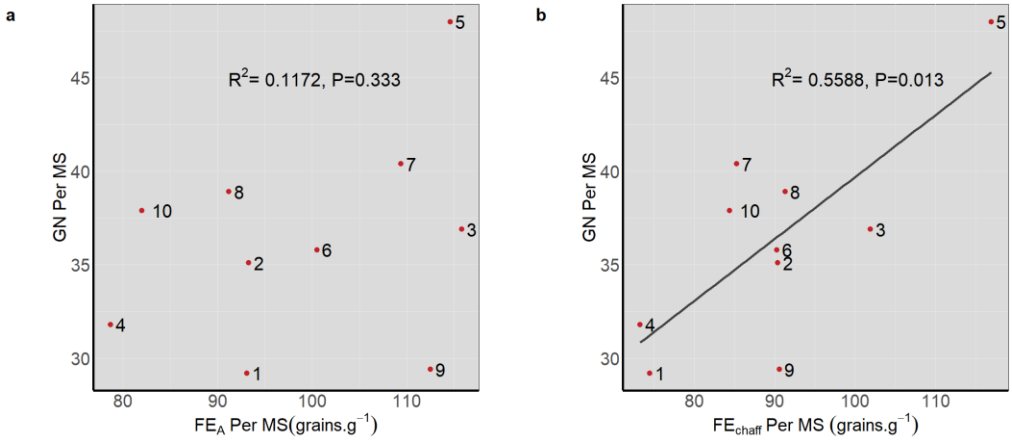

***Figure 4.4**: Linear regressions of a) fruiting efficiency calculated using spike DM at anthesis (FE_A) and b) fruiting efficiency calculated using chaff DM (FE_{chaff}) per MS on grain number (GN) per main shoot (MS) for 10 HiBAP II genotypes in glasshouse experiments*

Values represent means across 2017, 2018 and 2019, Numbered points are each genotype, b) y=0.33x+6.53

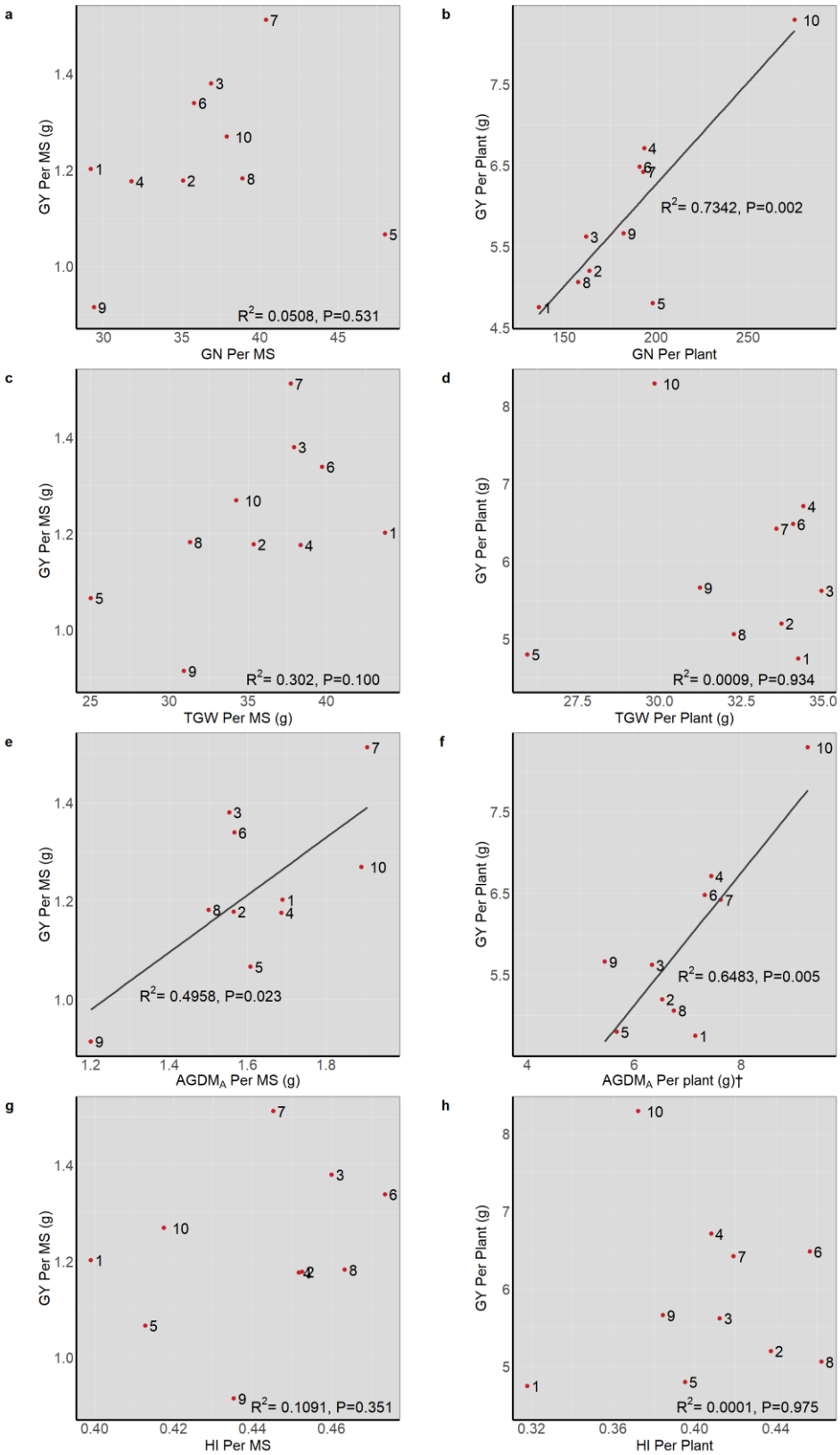

***Figure 4.5**: Linear regressions of traits measured at physiological maturity on the main shoot (MS) and plant for 10 HiBAP II genotypes in glasshouse experiments*

*Values represent means across 2017, 2018 and 2019, †: Days to anthesis (DTA) added as a covariate if P<0.05. Numbered points are with each genotype. **GY**: grain yield, **GN**: grain number, **TGW**: thousand-grain weight, **AGDM$_A$**: above-ground dry matter (DM) at anthesis, **HI**: harvest index. b) y=0.02x+1.24, e) y=0.58x+0.28, f) y=0.81x+0.25*

4.3.2 Flag-leaf photosynthetic rate

Flag-leaf pre-anthesis photosynthetic rate (A_{max}) was positively correlated amongst genotypes with GY_{MS} (R^2=0.50, P=0.023, Figure 4.6e), while post-anthesis A_{max} was positively correlated with GN_{MS} (R^2=0.36, P=0.066, Figure 4.6d) and GY_{MS} (R^2=0.52, P=0.018, Figure 4.6f). No correlations were observed between either pre- or post-anthesis A_{max} and $AGDM_A$ per MS or pre-anthesis A_{max} and GN_{MS}.

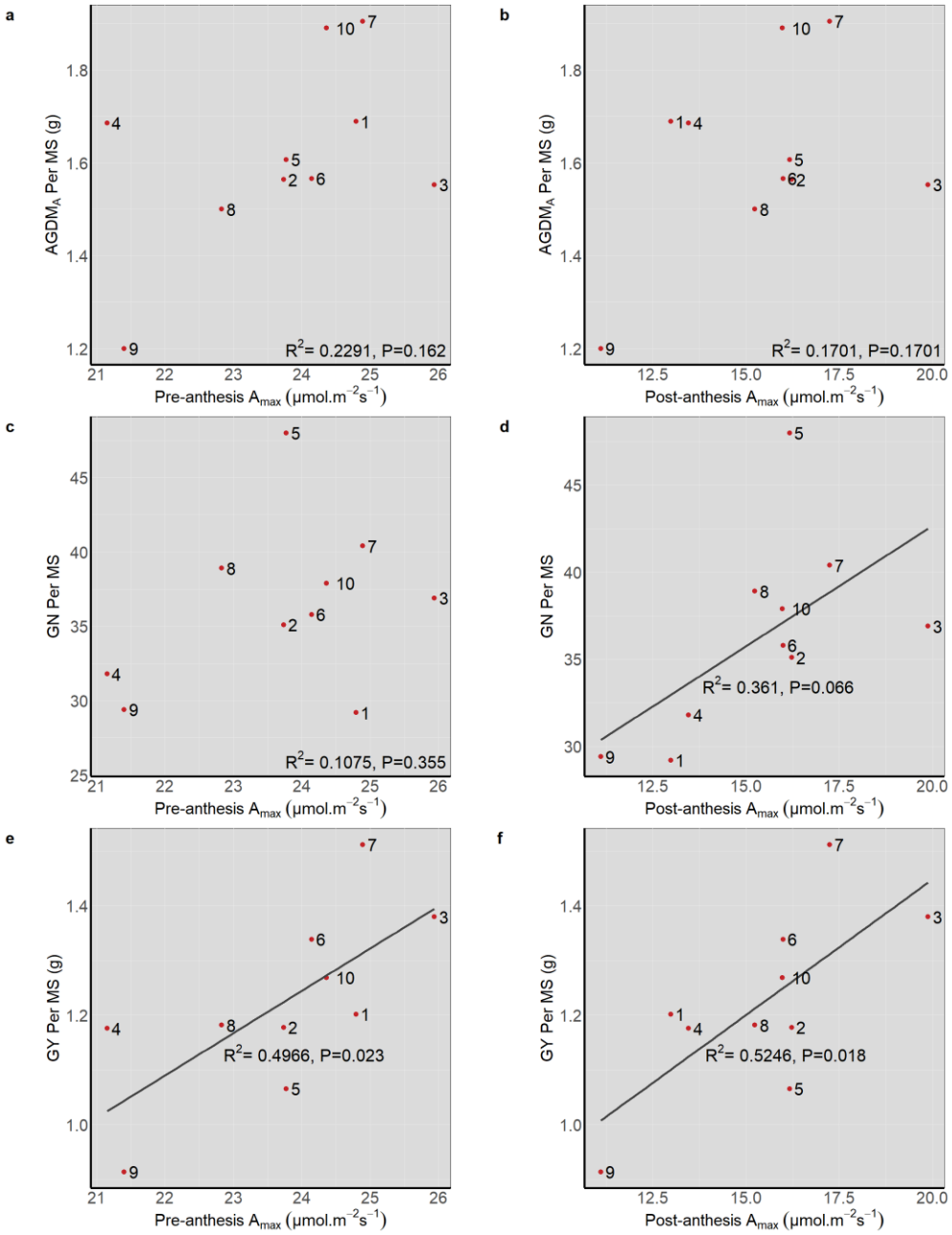

***Figure 4.6**: Pre- and post-anthesis flag-leaf photosynthesis rate (A_{max}) linear regressions with $AGDM_A$ (a, b), GN (c, d) and GY (e, f) for 10 HiBAP II genotypes in glasshouse experiments*

*Values represent means across 2017, 2018 and 2019, numbered points are with each genotype. **GY**: grain yield, **GN**: grain number, **$AGDM_A$**: above-ground dry matter (DM) at anthesis, d) y=1.39x+15.0, e) y=0.078x-0.61, f) y=0.05x+0.46*

4.3.3 Genetic variation in spike hormone levels and association with physiological traits

Spike hormone analyte levels averaging across the three years at late booting (GS49) and anthesis (GS65) are shown in Figure 4.7. Some plant hormones showed a large change between stages, e.g. auxin indole-3-acetic acid (IAA) had a much lower level at GS49 than GS65, as did salicylic acid (SA). The distribution of analyte levels per year is shown in the boxplots in Figure 4.8. For most hormones, the pattern followed between GS49 and GS65 is similar in the individual years. For example, abscisic acid (ABA) levels are consistently higher at GS49 by approximately 100 % compared to at GS65 (Figure 4.8b). Similarly, for both cytokinins zeatin (Z) and zeatin riboside (Zr), levels were lower at GS49 than at GS65 (Figure 4.8 h, i).

For most spike hormones, genetic variation was normally distributed, but there were a few cases such as IAA at both GS49 and GS65 in 2018 for which variation was very skewed (Figure 4.8d). Concerning the significance of the growth stage on hormone level, all hormones apart from IPA and JA showed a significant difference from GS49 to 65 (Table 4.6). The linear regressions among genotypes of each hormone analyte level from GS49 to GS65 indicate only ABA was positively correlated between growth stages (R^2=0.55, P=0.014, Table S 6). Cross-year analysis of the hormones showed genotype had a significant effect on all hormones at GS49 except ABA and isopentenyladenine (2iP). However, at GS65, genotype was only significant for 2iP, ABA, IAA and SA (Table 4.7). When considering the genotype effect in each year, not all years showed a significant effect of genotype on hormones, particularly in 2019 where only 2iP and ABA had a significant effect at GS65 (Table S 7). The genotype x year interaction was significant for all hormones at GS49 except ABA and JA, and for all at GS65 except GA1, IPA and SA (Table 4.7).

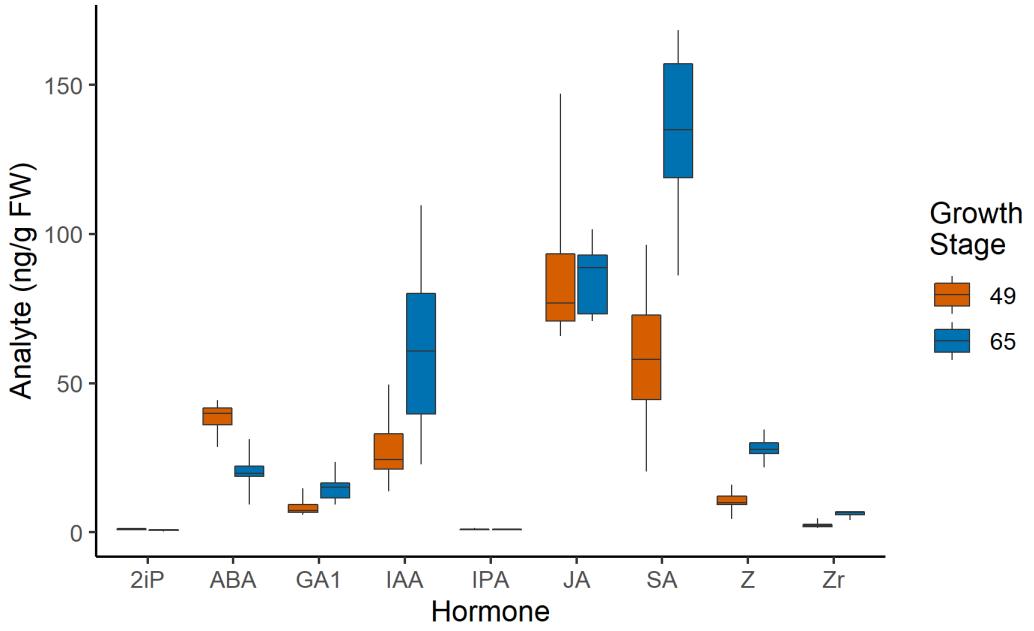

***Figure 4.7**: Boxplots showing genetic ranges for 10 HiBAP II genotypes in spike hormonal analyte levels at late booting (GS49) and anthesis (GS65) in glasshouse experiments*

Values represent means of fresh weight (FW) samples across 2017, 2018 and 2019

***2iP:** isopentenyladenine, **ABA**: abscisic acid, **GA1**: gibberellin 1, **IAA**: indole-3-acetic acid, **IPA**: isopentenyladenosine, **JA**: jasmonic acid, **SA**: salicylic acid, **Z**: zeatin, **Zr**: zeatin riboside*

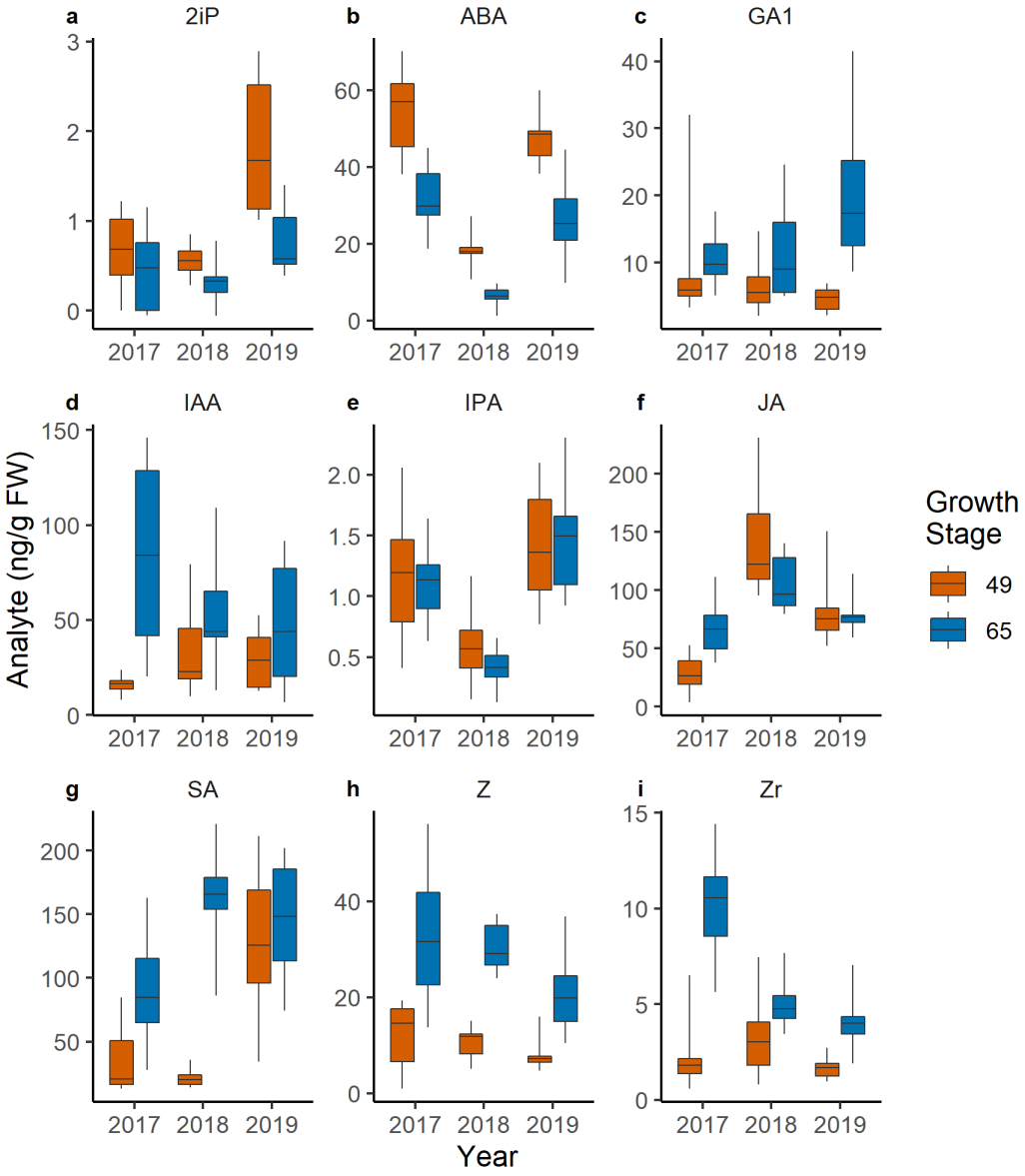

***Figure 4.8**: Boxplots of spike hormonal analyte levels at late booting (GS49) and anthesis (GS65) for 10 HiBAP II genotypes in the glasshouse experiments over 3 years*

***2iP:** isopentenyladenine, **ABA**: abscisic acid, **GA1**: gibberellin 1, **IAA**: indole-3-acetic acid, **IPA**: isopentenyladenosine, **JA**: jasmonic acid, **SA**: salicylic acid, **Z**: zeatin, **Zr**: zeatin riboside*

Table 4.6: *Significance (p-values) of growth stage (GS) on hormonal analyte levels for 10 spring wheat HiBAP II genotypes in the glasshouse experiments from cross-year ANOVA 2017-2019*

ABA*: abscisic acid,* ***GA1****: gibberellin 1,* ***IAA****: indole-3-acetic acid,* ***JA****: jasmonic acid,* ***SA****: salicylic acid,* ***Z****: zeatin,* ***Zr****: zeatin riboside,* ***IPA****: isopentenyladenosine,* ***2iP:*** *isopentenyladenine*

Hormone	GS Significance	Genotype x GS significance
ABA	<0.001	1.000
GA1	0.001	0.701
IAA	<0.001	0.065
JA	0.955	0.959
SA	<0.001	0.869
Z	<0.001	0.599
Zr	<0.001	0.970
IPA	0.787	0.996
2iP	0.066	0.837

Table 4.7*: Significance (p-values) of hormonal analyte levels for 10 HiBAP II genotypes in the glasshouse experiments from cross-year ANOVA 2017-2019 and least significant differences (LSD, P=0.05) for genotype*

†: DTA added as a covariate if P<0.05

ABA*: abscisic acid,* ***GA1****: gibberellin 1,* ***IAA****: indole-3-acetic acid,* ***JA****: jasmonic acid,* ***SA****: salicylic acid,* ***Z****: zeatin,* ***Zr****: zeatin riboside,* ***IPA****: isopentenyladenosine,* ***2iP:*** *isopentenyladenine*

Hormone		LSD	Year Significance	Genotype Significance	GenxYear Significance
GS49	ABA	10.21	<0.001	0.098	0.259
	GA1	3.12	0.387	<0.001	<0.001
	IAA	12.39	0.021	<0.001	<0.001
	JA	34.89	<0.001	<0.001	0.272
	SA	37.52	<0.001	0.006	0.020
	Z	2.75	0.003	<0.001	<0.001
	Zr	1.08	0.007	<0.001	<0.001
	IPA	0.44	<0.001	0.038	0.005
	2iP	0.57	<0.001	0.100	0.027
GS65	ABA†	6.76	<0.001	<0.001	0.051
	GA1	11.52	0.102	0.417	0.208
	IAA	31.46	0.005	<0.001	0.040
	JA	24.51	0.003	0.117	0.013
	SA	54.35	<0.001	0.082	0.170
	Z	11.92	0.008	0.556	0.034
	Zr	2.37	<0.001	0.263	0.081
	IPA	0.73	<0.001	0.997	0.796
	2iP	0.35	0.001	<0.001	<0.001

At GS49, spike cytokinin zeatin was positively correlated with GN_{MS} (r=0.77, P<0.01), FE_{chaff} (r=0.60, P<0.10) and negatively with TGW_{MS} (TGW_{MS}) (r=-0.66, P<0.05), while zeatin riboside was positively correlated with HI_{MS} (r=0.61, P<0.10) and negatively with peduncle length (r=-0.66, P<0.05). (Table 4.8). Cytokinin isopentenyladenine (2iP) at GS49 was positively correlated with fertile florets per spike at anthesis (r=0.62, P<0.10) (Table 4.8). Jasmonic (JA) at GS49 was positively associated with both spike DM and fertile florets per spike (r=0.59 and 0.62, respectively, P<0.10), but negatively with peduncle length (r=-0.59, P<0.10) (Table 4.8). ABA correlated positively with peduncle length measured at both GS49 (r=0.66, P<0.05) and GS65 (r=0.66, P<0.05).Similarly to zeatin at GS49, zeatin riboside at GS65 was positively associated with FE_{chaff} (r=0.56, P<0.10).

***Table 4.8**: Pearson's correlation coefficients between traits measured at anthesis and physiological maturity and spike hormone analyte levels for 10 spring wheat HiBAP II genotypes in the glasshouse experiments combined over 3 years*

*Combined means for 2017, 2018 and 2019, †: DTA (days to anthesis) added as a covariate if P<0.05, correlation significance: ‡P<0.10, *P<0.05, **P<0.01, ***P<0.001*

***ABA**: abscisic acid, **GA1**: gibberellin 1, **IAA**: indole-3-acetic acid, **JA**: jasmonic acid, **SA**: salicylic acid, **Z**: zeatin, **Zr**: zeatin riboside, **IPA**: isopentenyladenosine, **2iP:** isopentenyladenine, **$AGDM_A$**: above-ground dry matter (DM) at anthesis, **Ped Length:** peduncle length in cm, **Int2 Length**: internode 2 length in cm, **Int3 Length**: internode 3 length in cm, **$AGDM_{PM}$**: above ground DM at physiological maturity, **GN**: grain number, **GY**: grain yield (g), **HI**: harvest index, **FE_A**: fruiting efficiency calculated using spike DM at anthesis, **FE_{chaff}**: fruiting efficiency calculated using chaff DM at maturity, **TGW**: thousand-grain weight (g)*

	Hormone	$AGDM_A$ MS	Spike DM MS	Fertile Florets/Spike	Ped Length	Int2 Length	Int3 Length	$AGDM_{PM}$ MS	GN MS	GY MS	HI MS	FE_A MS	FF_{chaff} MS	TGW MS
GS49	ABA	0.20	-0.42	-0.02	**0.66***	-0.05	-0.07	0.13	0.15	0.04	-0.26	0.26	0.13	0.08
	GA1	-0.10	-0.23	0.26	0.28	-0.36	-0.34	0.07	-0.09	0.18	0.38	0.17	0.06	0.17
	IAA	-0.23	0.03	0.37	-0.53	-0.34	-0.24	0.04	-0.20	0.21	0.53	0.04	-0.18	0.23
	JA	0.41	**0.59‡**	**0.62‡**	**-0.59‡**	0.46	0.52	0.18	0.20	0.20	0.00	-0.50	-0.10	-0.05
	SA	0.16	0.07	0.31	0.20	-0.33	-0.28	0.31	-0.45	0.25	-0.07	-0.17	-0.48	0.50
	Z	0.03	0.07	-0.22	-0.21	0.42	0.24	-0.03	**0.77****	0.03	0.15	0.39	**0.60‡**	**-0.66***
	Zr	-0.24	-0.13	0.19	**-0.66***	-0.26	-0.11	0.17	-0.17	0.37	**0.61‡**	0.22	0.06	0.40
	IPA	-0.07	-0.05	0.26	-0.10	0.02	0.15	0.15	-0.07	0.20	0.20	0.01	-0.04	0.39
	2iP	0.53	0.42	**0.62‡**	-0.47	0.47	0.50	0.46	0.36	0.44	-0.05	-0.19	-0.02	0.09
GS65	ABA†	0.28	-0.29	-0.30	**0.66***	0.20	0.10	0.03	0.28	-0.14	-0.52	0.17	0.21	-0.20
	GA1	-0.47	0.18	-0.10	-0.40	-0.01	-0.06	-0.33	-0.02	-0.19	0.37	-0.03	0.19	-0.28
	IAA	-0.03	-0.23	-0.29	0.08	0.26	0.24	-0.09	0.08	-0.27	**-0.60‡**	0.11	0.13	-0.04
	JA	-0.19	0.05	-0.24	-0.17	0.37	0.31	-0.50	0.30	-0.52	-0.21	-0.11	0.29	**-0.59‡**
	SA	-0.09	0.11	0.08	0.29	-0.12	-0.08	-0.10	0.04	0.04	0.50	-0.08	-0.11	-0.01
	Z	-0.04	0.11	0.09	0.29	-0.03	0.10	0.01	-0.15	0.10	0.36	-0.22	-0.14	0.29
	Zr	-0.32	-0.26	-0.12	-0.16	0.00	-0.14	-0.16	0.24	-0.11	0.05	0.39	**0.56‡**	-0.37
	IPA	0.26	0.39	0.23	-0.18	**0.79****	**0.80****	0.09	**0.59‡**	0.10	0.00	-0.22	0.41	-0.23
	2iP	-0.31	0.18	-0.32	0.03	0.47	0.45	**-0.57‡**	0.31	-0.50	0.09	-0.22	0.43	**-0.56‡**

In 2017, 2018 and 2019, the whole spike was sampled for hormonal analysis. However, in 2019, in addition for two genotypes, the flag leaf and peduncle were also sampled at both GS49 and GS65, and at GS65 the central spikelets of the spike were also sampled as normal, and the basal and apical spikelets for the same spike were sampled. At GS49, plant organ position had a significant effect on each of hormones 2iP, ABA and SA (Figure 4.9). For Z, 2iP and ABA hormone level at GS49 was higher in the spike and flag leaf than in the peduncle. At GS65, the plant organ position effect was significant for ABA, IPA, SA, Z and Zr (Figure 4.10). IPA had much higher hormone levels in the peduncle than the flag leaf or spike, while ABA showed the opposite effect, with lower hormone levels in the peduncle. Concerning the hormones sampled at different locations within the spike, there were no significant differences among the spike positions (Table S 8).

Comparison of spike cytokinins sampled in the glasshouse experiments (3 year means) and field experiments in 2018-19 showed a positive association amongst the 10 genotypes for 2iP at GS49 (R^2=0.20, P=0.19), IPA at GS49 (R^2=0.76, P<0.001) and Zr at anthesis (R^2= 0.45, P=0.034) (Figure 4.11). Some spike hormones had a similar range in both glasshouse and field experiments such as 2iP at GS65 (glasshouse 0.235-0.764 ng/g FW vs field 1.06-5.18 ng/g FW, Figure 4.11e), whereas other hormones had very different analyte ranges such as Zr at GS49 (glasshouse 1.32-4.78 ng/g FW vs. field 42.1-65.6 ng/g FW, Figure 4.11d).

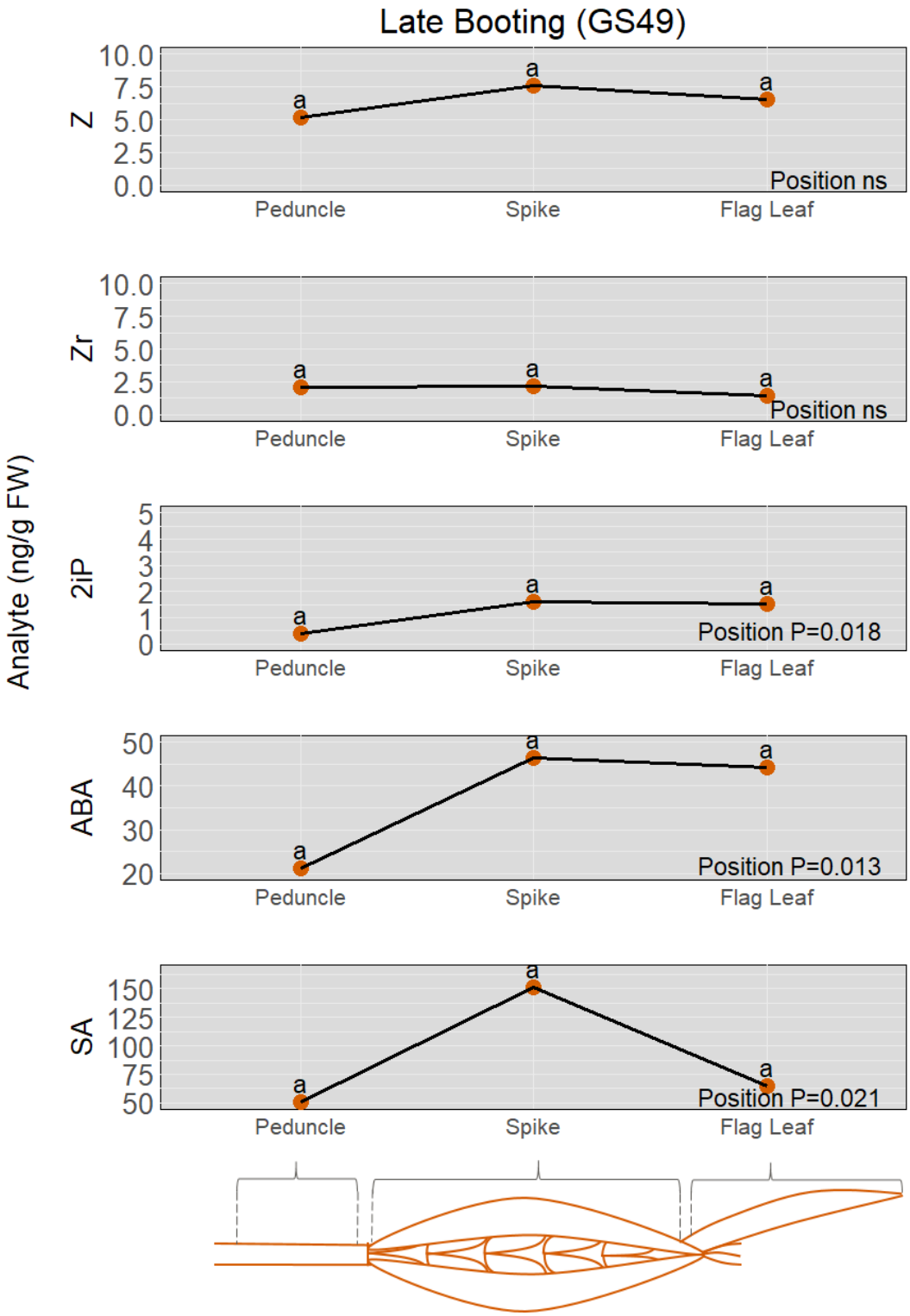

***Figure 4.9**: Average hormone analyte levels in different plant organs at late booting (GS49) for two HiBAP II genotypes in the glasshouse experiments in 2019*

***Z**: zeatin, **Zr**: zeatin riboside, **2iP**: isopentenyladenine, **ABA**: abscisic acid, **SA**: salicylic acid, position significance calculated from 2-way ANOVA, letters indicate if the plant organs are significantly different based on LSD (5%), different letters indicate those plant organs are significantly different*

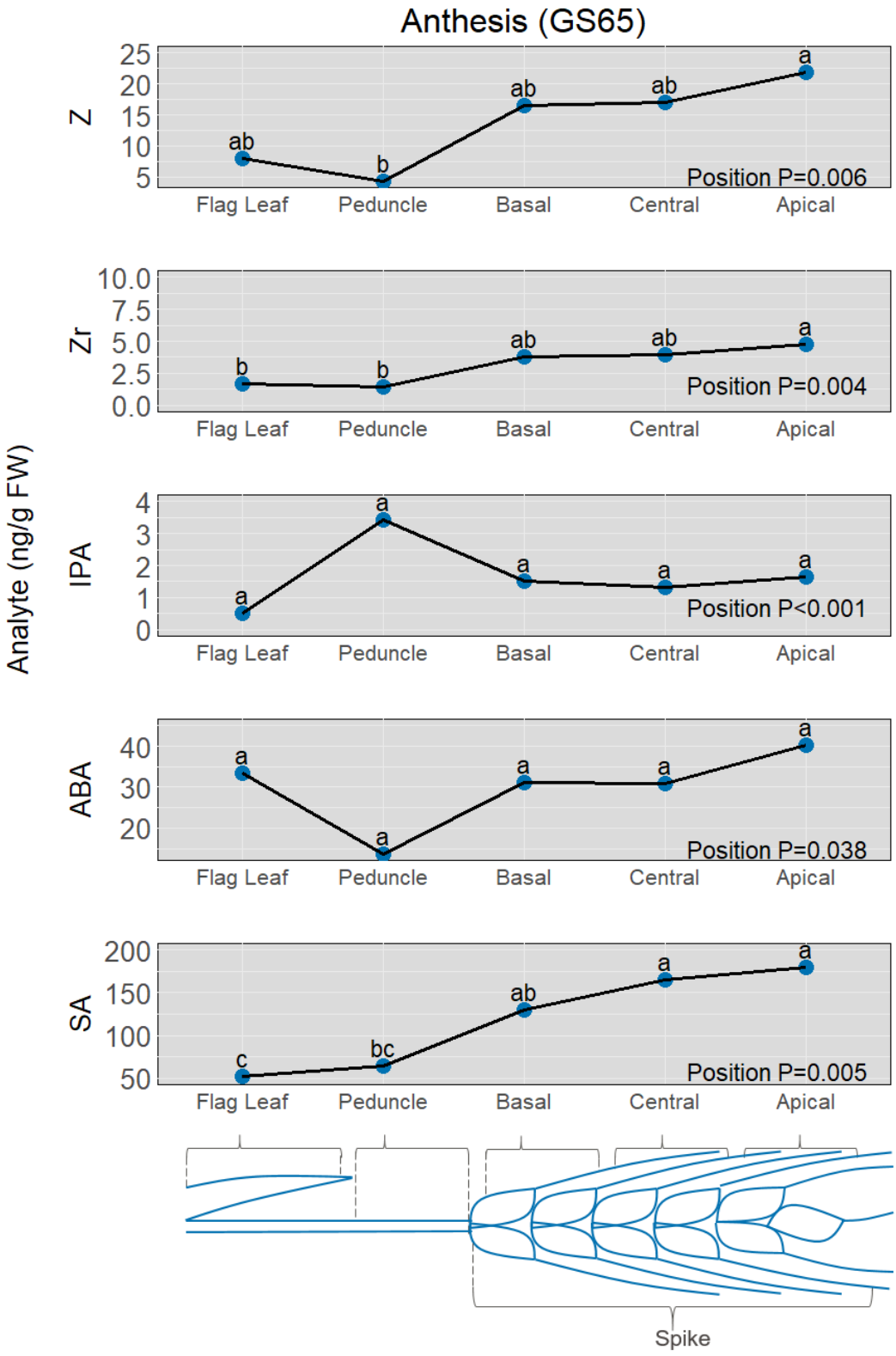

***Figure 4.10**: Average hormone analyte levels in different plant organs at anthesis (GS65) for two HiBAP II genotypes in the glasshouse experiments in 2019*

***Z**: zeatin, **Zr**: zeatin riboside, **IPA**: isopentenyladenosine, **ABA**: abscisic acid, **SA**: salicylic acid, position significance calculated from 2-way ANOVA, letters indicate if the plant organs are significantly different based on LSD (5%), different letters indicate those plant organs are significantly different*

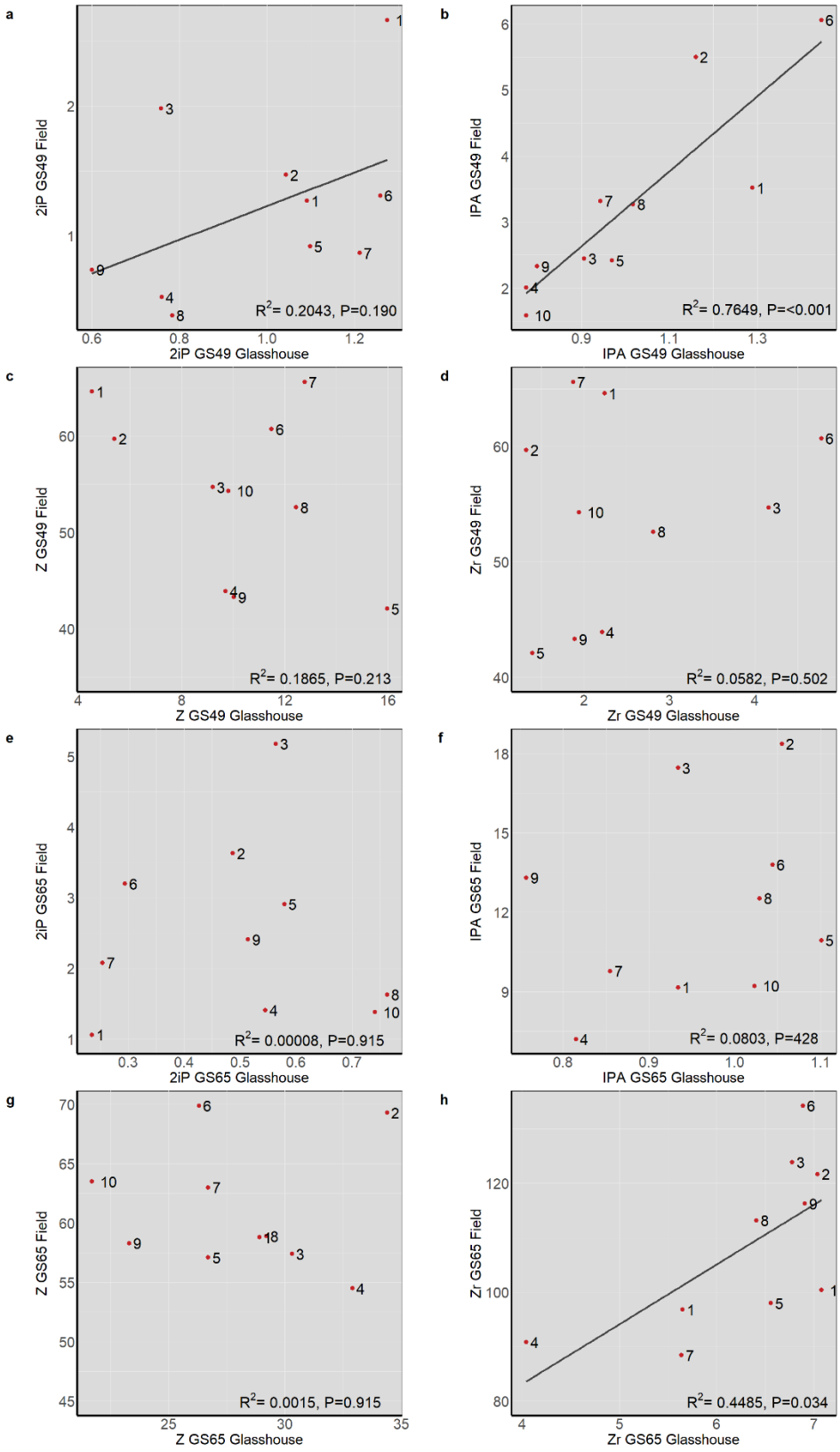

Figure 4.11: *Linear regressions among 10 HiBAP II genotypes of four cytokinin analyte levels (ng/g FW) at GS49 and GS65 in the glasshouse experiments for 3 years (2017, 2018, 2019) and on levels in the field experiment for 1 year (2018-19)*

Glasshouse: combined means for 2017, 2018, 2019, Field: means from 2018-19, Numbered points are with each genotype. ***2iP:*** *isopentenyladenine,* ***IPA****: isopentenyladenosine,* ***Z****: zeatin,* ***Zr****: zeatin riboside, a) y=1.29x-0.06, b) y=5.67x-2.47, h) y=10.98x+39.23*

4.4 Discussion

Later sowing in August in 2017 than other years caused a lower temperature throughout the growth cycle in this year, causing a longer growing season with anthesis being reached 10 days later than other seasons. This resulted in increased plant height and more biomass at anthesis in 2017. However, this did not affect the relative cultivar performance for the grain partitioning traits. For the three years, the genotype by year interaction was not significant for most traits at anthesis, e.g. plant height, internode lengths or biomass per plant, and for key traits at maturity e.g. fruiting efficiency and grain number per MS. The 'moderately high' and high values of heritability observed for most traits also indicated they were genetically inherited and not influenced strongly by genotype x environment.

4.4.1 Optimising pre-anthesis partitioning for spike growth

Previously, both in the HiBAP I (Sierra-Gonzalez, 2020) and HiBAP II (chapter 3) in field experiments true-stem internode 2 and 3 PIs were negatively associated with spike PI and spike DM per unit area. However, in the HiBAP II subset in the glasshouse experiments, internode TS Pis were not associated with spike PI. Furthermore, in contrast to the field results, peduncle TS PI was negatively associated with spike DM per MS at anthesis, internode 3 TS PI was positively correlated with spike DM at anthesis and internode 3 LS PI was positively correlated with grain yield. These correlations differ with those in the field experiments, perhaps because of the different environmental conditions in the UK glasshouse experiments compared to the Mexico field experiments affecting tillering. There may have been effects on inter-shoot competition for assimilates according to the differences between single plants grown in the glasshouse and populations of plants in the field experiments. In the glasshouse, light interception per shoot is likely much greater than in the field, so competition between spike and stem for assimilates due to mutual shading may occur at a relatively later stage during stem extension, i.e. during peduncle extension rather than stem internode 2 and 3 extension.

There were also differences in the phenology between the glasshouse and field experiments. In the glasshouse experiments, the average number of days from sowing to anthesis (DTA) was 51-60 days, whereas in the field it was 73-91 (Table 3.1). It has previously been reported that in photoperiod sensitive cultivars, a longer duration of stem elongation (from the terminal spikelet stage to anthesis), through both changing the length of vernalisation and by adding supplementary lighting to extend day length, would result in increased spike dry weight at anthesis and

increased yield (Miralles et al., 2000; Gonzalez et al., 2003b). This is because the onset of maximum stem growth rate was delayed, and therefore there was delayed competition between spike growth and stem growth. Gonzalez et al. (2003a) suggested that among cultivars with similar sowing and flowering date, those induced earlier from the vegetative to the reproductive stage will favour increased spike dry weight. This is because the stem elongation phase will be longer resulting in increased spike dry weight and yield. This may explain the increased spike DM in 2017 compared to other years, as it took 10 days longer for anthesis to be reached. However this did not translate to increased spike PI in 2017, in fact, spike PI was lower in 2017, suggesting while spike DM was increased, the DM of other plant organs were also increased. SPI was also higher in the glasshouse experiments (0.21-0.30) than in the field experiments (0.17-0.27).

Elongation of stem internode 3 occurs shortly after the terminal spikelet stage, after which no more spikelets are initiated and this is when floret initiation occurs and floret primordia number is determined (Guo et al., 2018a). Elongation of stem internode 2 occurs later in floret development, at anther development, coinciding approximately with booting, when floret abortion occurs (Dixon et al., 2020). The floret survival phase from booting to anthesis is important for determining grain number. In contrast, the peduncle continues to elongate past anthesis and may contribute more to post-anthesis photosynthesis through both current photosynthesis and accumulation and remobilisation of stem carbohydrate reserves (Dodig et al., 2017). It was suggested by Reynolds et al. (2009) that reducing peduncle length might increase the spike partitioning index. However, the peduncle is important for post-anthesis photosynthesis and DM remobilisation to the grain (Gebbing, 2003), so reducing peduncle biomass may have other negative effects on the source-sink balance. On the other hand, Ehdaie et al. (2006a) found 27 % of remobilised dry matter came from internode 2, while only 18 % was remobilised from the peduncle. In addition, requirements for stem soluble carbohydrate depend on the environment and source-sink balance. Generally, the requirement for stem soluble carbohydrates to contribute to grain yield is less in irrigated CIMMYT spring wheat than UK winter wheat because there is less source limitation in Mexico wheat crops (Rivera-Amado et al., 2020). In the field trials, internode 2 true stem PI had the strongest negative association with spike PI, HI and GY (chapter 3.4.3). Therefore, overall internode 2 still seems be the better target for reductions in length of specific internodes in the HiBAP II. Moreover, in the glasshouse there was a much higher source to sink balance, as there was less

mutual shading of shoots than in the field, so results on relationships between stem-internode traits and GY in the glasshouse conditions should be interpreted cautiously.

Unlike in previous literature and the HiBAP II field experiments in chapter 3, there were no correlations between any TS internode partitioning traits and spike PI or HI, although there was a correlation with spike DM at anthesis as observed previously (Sierra-Gonzalez, 2020). The glasshouse experiment was a subset of just 10 lines, so it's possible with more genotypes similar associations to those reported in chapter 3 and in the CIMMYT spring wheat HiBAP I panel would have been observed. All true-stem specific weights were positively correlated to GY_{MS}. This may be because greater stem specific is associated with greater stem reserve storage capacity and therefore the stem can provide a greater source of assimilates to the spike during grain filling (Blum et al., 1994; Ehdaie et al., 2006b). Also, larger shoots with increased TS specific weights would be associated with larger grain yield since there were no significant genotype differences in HI in these experiments.

4.4.2 Optimising source-sink balance for grain yield potential

Like many earlier studies, a positive association between genetic variation in grain number and grain yield per plant was found in the present study (Shearman et al., 2005; Peltonen-Sainio et al., 2007). This is likely due to breeders increasing grain sink strength through increasing grain number, potential grain weight or both, and grain growth being predominantly sink limited (Fischer, 1985; Slafer and Savin, 1994). While there was no significant association between grain yield and thousand-grain weight, there was a positive trend, as expected as both may relate to potential grain weight. There was also no association between grain yield and harvest index per MS or per plant. Whilst during the past decade in some regions, for example Argentina, wheat yield genetic gains were associated with an increase of HI and not above ground DM (Lo Valvo et al., 2018), in many other countries there was no improvement in HI in the last 30 years, e.g. in spring wheat in NW Mexico (Aisawi et al., 2015). In the case of the HiBAP II genotypes in the glasshouse, rather than an association between grain yield and HI, there was an association between grain yield and above ground DM at anthesis and physiological maturity, both per the MS and per plant. In the field, HiBAP II genotypes showed a stronger correlation between grain yield and HI than above ground DM at anthesis, so environmental conditions could be changing the associations seen. In particular, tiller number could be influencing the associations

seen in the glasshouse, as there was a positive association seen between fertile tiller number and GY_P (R^2=0.51, P=0.02, Data not shown). Therefore, the genetic variation in biomass traits may not correlate from the glasshouse to the field because of the tillering effect as mentioned above.

The flag-leaf pre-anthesis photosynthetic rate was correlated with GY_{MS}, and post-anthesis photosynthesis rate was correlated positively with both GN_{MS} and GY_{MS}. Grain number is determined partly by spike growth from booting to anthesis (Gonzalez et al., 2011), while grain weight is determined by post-anthesis growth, so it is surprising that the pre-anthesis leaf photosynthesis rate is not correlating with grain number, but with grain yield, the association with grain yield would be expected to be via increased grain number and grain sink strength. Pre-anthesis photosynthesis would be expected to be associated with above-ground DM at anthesis, and while it was not significant there was a tendency for a positive association. Grain sink strength may be upregulating post-anthesis photosynthesis, which in the glasshouse may partly explain the positive association between post-anthesis photosynthesis rate and both grain yield and grain number. A positive association between genetic variation in post-anthesis photosynthesis and yield has been reported previously in wheat (Reynolds et al., 2005; Gaju et al., 2016; Tang et al., 2017). However, other studies found no correlation between post-anthesis gas exchange and grain yield (Xue et al., 2002; Yildirim et al., 2013). As environmental effects on gas exchange can be large (Reynolds et al., 2000), it has been suggested that more time points of leaf photosynthesis rate measurements may increase the association.

Genetic variation in FE_{chaff} correlated with GN_{MS}, suggesting FE is an important trait explaining GN. There were more trait correlations with FE_{chaff} than FE_A, which may be because FE_A is measured using one set of plants from anthesis, and one from maturity, so there can be more plant to plant variation. Relating grain number at maturity to spike biomass at anthesis (on different plants) will result in more variation than the chaff at maturity (on the same plants). Therefore, it is not a surprise that there were more associations with the maturity traits and the FE calculated from chaff DM. FE_A calculated per plant was not included in the glasshouse analysis due to differing numbers of tillers in anthesis and maturity for the genotypes.

4.4.3 Spike hormone effects on physiological traits

Genetic variation in hormone analyte levels were consistent across years, with levels also reliably changing between one growth stage and the other. Considering cytokinins Z and Zr, for both analyte levels were always lower at GS49 than at GS65, indicating as the plants approached anthesis the concentrations of cytokinins increased. Previous literature is consistent with this as a sharp increase in CK has been reported immediately after anthesis (Jameson et al., 1982).

Levels of 2iP at GS49 were positively correlated with fertile florets per spike, which is consistent with results in winter wheat (cv. YM 158), when Z was exogenously added during floret development and the number of fertile florets per spike was increased (Wang et al., 2001). Floret abortion occurs from the onset of booting (GS41) onwards (Guo et al., 2018a), so the correlation of hormones at GS49 with fertile floret number may be more related to either an increase in floret numbers as floret initiation is maximal at around onset of booting, or related to an effect on floret survival throughout booting from GS41 to GS49. Levels of Z at GS49 were positively correlated with both GN_{MS} and MS FE_{chaff}. Previous research in Chinese winter wheat found an exogenous application of synthetic CK 6-BA during booting reduced floret abortion rates by as much as 77 % (Zheng et al., 2016), therefore increasing grain number. The positive association seen between Zr at GS49 and HI_{MS} is likely related to the increase in grain number. Z levels at GS49 were also found to be negatively associated with TGW_{MS}; this could be an indirect association, as there is frequently a negative association observed between FE and TGW (Ferrante et al., 2015; Slafer et al., 2015). Similarly to Z at GS49, analyte levels of Zr at anthesis were positively correlated to FE_{chaff} per MS. At anthesis, cytokinins are crucial in promoting cell division, growth and differentiation, all of which contribute to increasing grain number, and therefore FE (Jameson and Song, 2016).

Cytokinin levels differ between plant organs at both booting and anthesis. At GS49, there was a significant effect of plant organ position for 2iP, and at GS65 for both Z and Zr. At GS49, 2iP levels were increased 4-fold from the peduncle to the spike and flag leaf. As spike 2iP levels at GS49 were positively correlated with fertile florets per spike (Wang et al., 2001), this indicates that at booting high levels of cytokinins are not required in the peduncle to promote fertile florets. At anthesis, Z was 4 fold higher in the spike than the peduncle, and Zr was 2.8 fold higher. Again this suggests that high levels of CKs are more important in the spike at anthesis than in the stem. The hypothesis was that there would be a gradient in CK

concentrations throughout the plant, as reported by Youssef et al. (2017) in barley (cv. Bowman) where the lowest levels of CKs were reported in the basal spikelets and highest in the apical during spike differentiation. However, in the HiBAP II, there was no effect of hormone levels concerning the spike positions. The only cytokinin to have a significant effect for the genotype x position interaction was IPA at GS65. This may not be because genotypes do not show relative differences in the spike positions for the hormones, but instead because the positional hormones were only measured in two genotypes. Despite position effect being significant for IPA at GS65 in a 2-way ANOVA, the LSD value, which indicates if the pairwise difference between two positions was significantly different, showed no difference. This may be because the main effect position difference is more complicated than an individual pairwise test, and ANOVAs test for all combinations of interactions.

Out of all the hormones measured, the only one to have a consistently higher analyte level at GS49 than at GS65 was ABA. Endogenous ABA concentration has been reported to decrease sharply from anther-lobe formation to meiosis in wheat (Cao et al., 2000), and it has been suggested that ABA concentration should be maintained at low levels to maximise potential grain number (Wang et al., 2001). Perhaps because of the lower levels of ABA at anthesis, there were no effects of ABA on grain number. However, ABA was positively associated with peduncle length at both GS49 and GS65. ABA was half as low in the peduncle compared to the other organs at both GS49 and GS65. This correlates with literature suggesting ABA can have a negative effect at all stages of development as a growth inhibitor (Emery et al., 1998), and perhaps lack of ABA is important for increasing stem length.

Other hormonal associations of note are that at GS49 spike jasmonic acid level was positively associated with spike DM and fertile florets per spike. Current literature in wheat has not reported the effects of JA on yield, but JA has been shown to counteract dormancy in wheat (Jacobsen et al., 2013). While the relation between JA and spike DM is unclear, it could be having a positive effect on yield and yield components. Unlike in the HiBAP II in the field experiment (chapter 3), spike gibberellins had no associations with any key physiological traits. Colombo and Favret (1996) found when wheat with a developing spike was sprayed with GA3 it was ineffective at inducing male sterility, so the lack of interactions with gibberellins could be because they were measured at later growth stages and they’re most influential early in plant growth. Despite spike SA level also having no associations with the key physiological traits, there was a significant effect of plant

organ at both booting and anthesis, with the highest level in the spike rather than the flag leaf or peduncle. As high levels of SA are mainly associated with stress response (Sedaghat et al., 2017), the lack of correlations might be expected as the plants in the glasshouse were not significantly stressed. Spike auxin IAA level at GS65 showed a positive association with the main shoot HI. Previous literature has shown endogenous applications of IAA during grain filling resulted in more photoassimilate transport to the grains (Darussalam et al., 1998), therefore the increased translocation of assimilates to grains due to auxin could be improving the HI.

No hormones at GS65 showed an effect of spike position, which differs from the hypothesis that hormones are translocated differently through the spike. The lack of statistical difference observed could be related to the small sample size or perhaps indicate more detailed distribution data are required for the mapping of the spikelets along the rachis. When comparing genetic variation for spike cytokinins sampled in the glasshouse and field experiments, there was a positive association for 2iP at GS49, IPA at GS49 and Zr at anthesis. Plants grown in the field tend to show more variation from plot to plot due to greater spatial variation, so it's promising when looking at a small subset of lines the same trends are shown. Despite correlations amongst genotypes, for some spike hormones such as Zr at anthesis, in the field, the average analyte level was 108 ng/g FW, while in the glasshouse the level was much lower at 6.3 ng/g FW. A study by Liu et al. (2013b) identified Z and Zr levels at anthesis in winter wheat (cv. Zhoumai 18) grown in the field were at ~6 ng/g FW, which suggests the levels reported in the glasshouse at anthesis may be more representative, although that study was performed in winter wheat rather than spring wheat. In the same study, IAA levels were reported to be ~45 ng/g FW, which would also be more similar to the glasshouse levels at 62 ng/g FW rather than the field levels of 84 ng/g FW. The higher spike hormone levels in the field may be partly because of the higher incident radiation the plants received in the field than in the glasshouse. Higher incident radiation may increase spike hormone levels due to increased photosynthesis and assimilates.

4.4.4 Conclusions

In the glasshouse, many of the same associations reported in the field experiments in chapter 3 were observed for the spike hormones, demonstrating the scope for deploying spike cytokinins as a selection trait for raising grain number in wheat breeding programs. The association between pre-anthesis photosynthesis rate

and grain yield over three years also highlighted the potential importance of this trait in raising yields in future wheat breeding. Despite the spike hormonal levels across the plant only being performed in two genotypes in one year, these results are interesting and future work could investigate plant-wide hormonal distribution to understand the effects more clearly in wheat.

Chapter 5: Genetic Analysis of Physiological Traits in the HiBAP II

5.1 Introduction

Bread wheat is a hexaploid genome (denoted AABBDD), which developed through the natural hybridisation of *Aegilops tauschii* (DD) and emmer wheat (AABB) (Haas et al., 2019). The hybridisation, domestication and subsequent inbreeding of an initially small population in wheat breeding programmes has produced a genetic bottleneck, decreasing the available genetic diversity for bread wheat (Winfield et al., 2016). Therefore, it is important to create new varieties which exploit novel genetic variation through the creation of synthetic hexaploid wheat (SHW) lines, which are the result of crosses between *Ae. tauschii* and durum or emmer wheat, or wide crosses with landraces. Since the 1980s, CIMMYT has developed 1200 SHW lines (Jafarzadeh et al., 2016), 32 derivatives of which are in the HiBAP II panel, with a further 13 lines a landrace and synthetic derivative mix. Landrace accessions may also provide novel genetic diversity as they originated in abiotically stressed environments that were isolated from mainstream gene pools (Reynolds et al., 2007). While creating more diversity is the first step in increasing yields, the diversity within germplasm needs to be evaluated, and its genetic basis understood so this information can be applied to improve complex yield traits.

Grain sink strength is the main factor limiting yield in high yield potential conditions (Miralles and Slafer, 2007), in particular, the rapid spike growth phase from booting to anthesis is critical for grain number determination. Therefore, to further advance grain number, traits that may increase grain number such as spike partitioning index (SPI), determining spike dry matter at anthesis, and fruiting efficiency (FE) must be optimised (Slafer et al., 1990; Slafer et al., 2015). However, a trade-off between SPI and FE has been previously reported (Dreccer et al., 2009; Gaju et al., 2014), although cultivars that have both high FE and SPI have been identified (Bustos et al., 2013; Garcia et al., 2014). As there are examples of these traits not negatively influencing each other, it is necessary to understand to what extent these traits are additive. Since some studies show it is possible to increase both, it may be possible for the underlying genes determining the traits to be pyramided (Reynolds et al., 2017). Fruiting efficiency can be affected by intra-spike partitioning (Ferrante et al., 2013), but also through plant hormonal signalling. For example, cytokinins are key regulators of cell division during meristem formation,

cell growth and leaf senescence, all of which determine grain number and/or size (Jameson and Song, 2016).

It is known that plant hormones play a key role in influencing growth and yield. However, many studies have looked at exogenous applications of hormones, e.g. Wang et al. (2001), or plant signalling in model crop species such as *Arabidopsis*, e.g. Larsson et al. (2017). Therefore, improved understanding is needed of how endogenous hormone concentrations affect key yield traits in wheat in the field. Endogenous spike concentrations and FE were measured in both the field and glasshouse experiments and these results are detailed in chapter 3 and chapter 4. However, phenotyping methods for traits such as FE and spike hormonal concentrations are low-throughput and can be expensive, so there is a need to develop molecular markers linking to these traits that can be deployed in marker-assisted breeding instead.

Previously, molecular markers and candidate genes have been identified in wheat through genome-wide association studies (GWAS), where the association between a marker and a trait are tested. Guo et al. (2017) conducted a GWAS experiment on winter wheat cultivars grown in the glasshouse and found putative associations between floret fertility, assimilate partitioning and spike morphology through shared SNP markers. They reported candidate genes involved in carbohydrate metabolism and signalling by plant hormones such as brassinosteroids that might be genetically regulating these complex grain number traits. Alqudah et al. (2020a) not only identified candidate genes on chromosome 1B for fertile spikelet per spike and thousand-grain weight from their GWAS, but also for the first time identified the same SNPs were marker-trait associations (MTAs) for spikelet sterility, with a candidate gene for Gibberellin 2-oxidases (GA2oxs). While most genome-wide association studies are conducted with 100-500 individuals (Alqudah et al., 2020a), recently a GWAS was conducted on a much larger population of 6,461 advanced breeding lines (Sehgal et al., 2020), where seven hotspots on chromosomes 1A, 2B, 4A, 5B, 6B and 7B were associated with grain yield.

Despite previous studies, the genetic basis of these complex grain partitioning traits is still unclear. While some genetic studies have been conducted for FE (Gerard et al., 2019; Pretini et al., 2020), these are still limited and as a result, the potential yield increases associated with these traits have yet to be exploited. In this chapter, key grain partitioning traits at both maturity and anthesis, along with

spike hormonal concentrations at anthesis were combined with genotypic data in a genome-wide association study to identify MTAs. This will allow the identification of genomic regions of interest that will help elucidate the genetic basis of these complex grain partitioning and spike hormonal traits determining yield potential.

5.1.1 Chapter hypotheses

- Marker-trait associations can be identified for spike hormonal traits and key grain partitioning traits by GWAS in the HiBAP II panel
- Co-locating markers will be identified with fruiting efficiency and spike hormone traits
- Candidate genes for the key SNPs associating with grain partitioning traits and spike hormonal traits can be identified and functions ascribed as reported in previous literature

5.2 Materials and methods

5.2.1 Plant materials and experimental design

The field experiments were carried out over two seasons, one in each of 2017-18 and 2018-19 under fully irrigated yield potential conditions at the Norman E. Borlaug experimental station near Ciudad Obregon, Sonora, Mexico (27.33°N, 109.09°W, 38 m above sea level). The High Biomass Association Panel (HiBAP II) was used, which contains 150 spring wheat genotypes with an outstanding expression of high biomass and/or biomass-related traits. It is comprised of landrace-derivatives, synthetic-derivatives, landrace and synthetic-derivatives, and elite cultivars. In the GWAS analysis, data for 146 lines were used. Agronomic details such as sowing dates, fertiliser, herbicide and fungicide inputs and the details of the crop measurements can be found in chapter 3.2, and all traits were measured in both years apart from the spike hormonal traits which were only measured in 2018-19 at anthesis.

5.2.2 DNA extraction and genotyping

DNA extraction and genotyping were performed at the Earlham Institute by Anthony Hall's research group, and are described in detail in Joynson et al. (2021). Flag-leaf tissue was obtained from 10 individuals per line were extracted using a standard CTAB based method and the DNA pooler per line. DNA purity was assessed using a NanoDrop 2000 (Thermofisher Scientific) and quantified fluorometrically using the Quant-iTTM assay kit (Life Technologies). The panel was genotyped using enrichment capture sequencing and de novo SNP discovery (Joynson et al., 2021). A 12-Mb target sequence was developed using the MyBaits system (Arbor Bioscience) based on that described by Gardiner et al. (2018), and mapped to the RefSeq-v 1.0 reference sequence (IWGSC et al., 2018). SNPs that had ≥10 % missing data and/or a minor allele frequency of ≤5 % were removed, leaving 154,365 SNPs.

5.2.3 Population structure analysis

Inference of the population structure of the panel was made using STRUCTURE 2.3.4 (Pritchard et al., 2000) using 50,000 burn-in iterations and 50,000 repetitions of the Markov Chain Monte Carlo (MCMC) model for the assumed subpopulations of K 1-8, for 9 independent, randomly seeded iterations of the analysis per assumed subpopulation. To identify the statistically most likely number of definable subpopulations, ΔK was calculated from the rate of change in the probability of likelihood [LnP(D)] value between each K value. This was implemented with STRUCTURE HARVESTER Python3.8 (Python Core Team, 2020) script (Earl and

Vonholdt, 2012). Population structure was also analysed using principal component analysis, with the PCA data produced in FarmCPU (Liu et al., 2016) and drawn using R v.4.0.3 (R Core Team, 2020) package ggplot2 (Wickham, 2016), and confirmed using R v.4.0.3 (R Core Team, 2020) package ggfortify (Tang et al., 2016).

5.2.4 Genome-wide association analysis

Genome-wide association analysis was carried out using GAPIT3 (Wang and Zhang, 2021) in R v.4.0.3 (R Core Team, 2020). Five statistical models were tested – Blink, CMLM, FarmCPU, GLM and MLM – to compare their strength and power of association detection. The QQ plot was used for assessing how strong each model was, and FarmCPU (Liu et al., 2016) was selected. FarmCPU iteratively uses a mixed linear model (fixed effect) and stepwise regression (random effect), which improves statistical power (Liu et al., 2016). This multi-locus approach is particularly powerful for complex traits controlled by large-effect loci (Cortes et al., 2021).

The model was adjusted using the two PCs suggested from the PCA for most traits, no PCs were added for traits where two PCs were adding confounding data and making the QQ plots deviate from the diagonal line. FarmCPU produces two thresholds, the green dashed line is the false discovery rate (FDR) cutoff, calculated using the Benjamini–Hochberg procedure (Benjamini and Yekutieli, 2001), and the green solid line is the Bonferroni cutoff (Sidak, 1967). Any markers for the same trait that were within 10,000 bp of each other were removed. Markers were visualised in an ideogram using a custom Python3.8 (Python Core Team, 2020) and Matplotlib v.3.4.1 (Hunter, 2007) script. To identify possible candidate genes, intervals +/- 500,000 bp were submitted to KnetMiner (Hassani-Pak et al.), and the resultant networks were assessed by reading supporting literature to test if there was adequate evidence to suggest the gene was linked to the associated trait.

5.3 Results

5.3.1 Population structure

A total of 154,365 single nucleotide polymorphisms (SNPs) were mapped to the IWGSC RefSeq-v1.0 reference sequence (IWGSC et al., 2018). STRUCTURE software (Pritchard et al., 2000) (Figure 5.1) indicated the panel formed two groups, as indicated by a high ΔK value at K=2, with a reducing ΔK for subsequent K values. The principal component analysis (Figure 5.2a) also indicated that the genotypes of the HiBAP II panel were split into two groups, which corresponded with the panel pedigrees – one group being the elite lines and the other the landrace-derived, synthetic-derived and landrace + synthetic-derived lines. When all four origins of the HiBAP II panel were highlighted, however, the landrace, synthetic and landrace-synthetic derived groups were not segregating further into separate groups (Figure 5.2b).

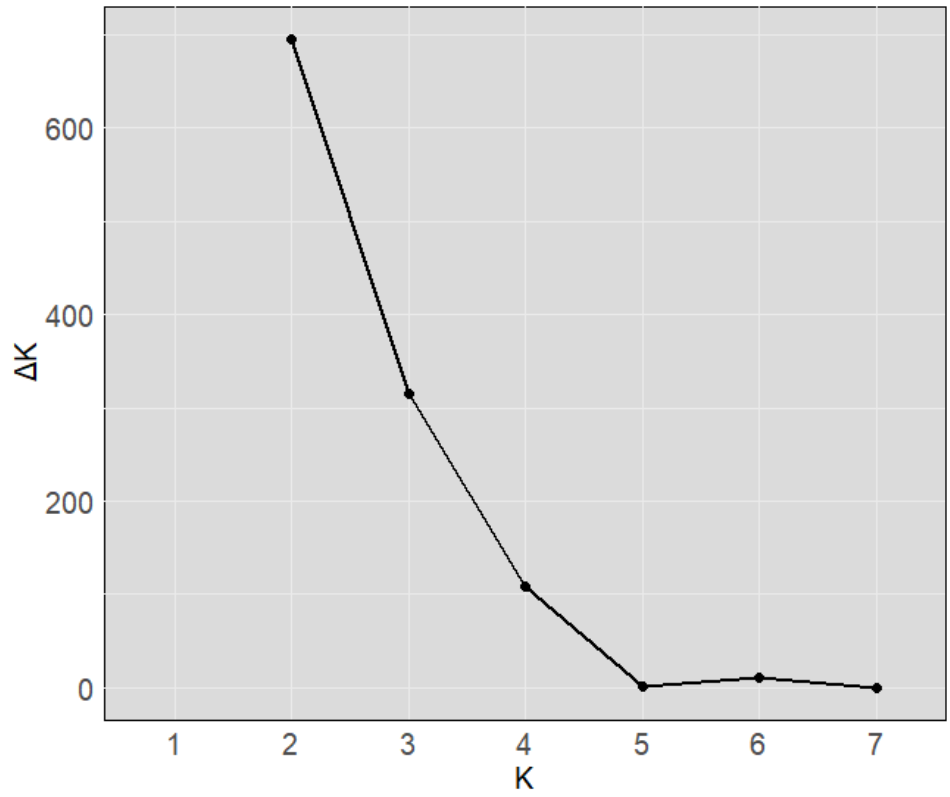

***Figure 5.1**: HiBAP II panel structure, showing the number of groups (K) against the second derivative (ΔK)*

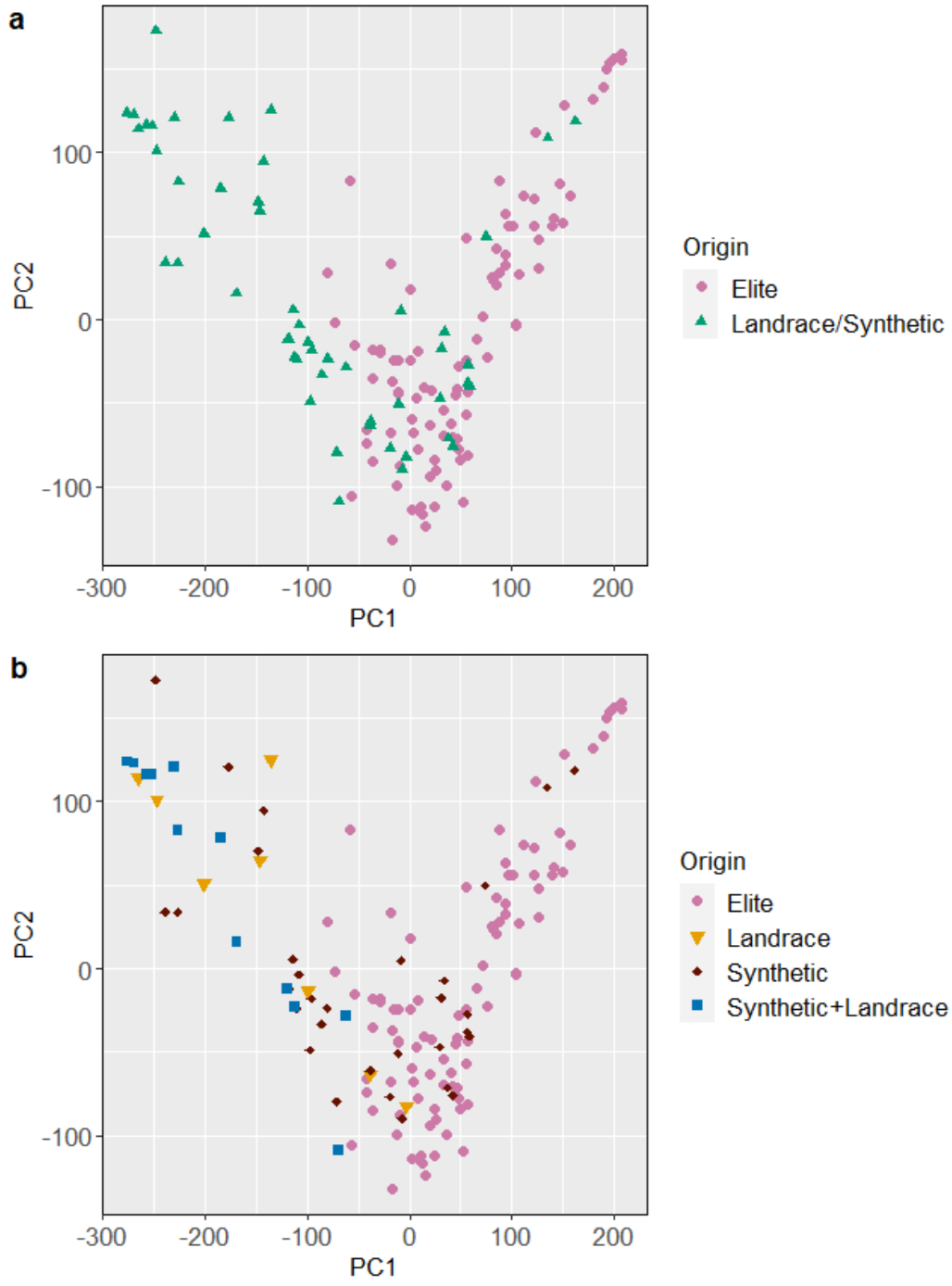

***Figure 5.2**: Principal component analysis of the first two principal components (PC) considering the HiBAP II panel pedigree background a) 2 main groups (elite and landrace/synthetic derivatives) and b) 4 groups (elite, landrace, synthetic and synthetic and landrace derivatives)*

5.3.2 Genome-wide association analysis

Marker-trait association analysis was carried out using best-linear unbiased estimates for all the crop traits measured at anthesis + 7 days and physiological maturity based on means across the two seasons 2017-18 and 2018-19. However, for the spike hormone analyte levels measured at anthesis, BLUEs based on only one year were used. For the 26 traits analysed, 213 MTAs were identified with a $-\log_{10}$ P value of >4 (putative MTAs), while 46 were identified with a $-\log_{10}$ P value of >6 (significant MTAs) (Table 5.1, Table 5.2). Thirty-nine of these MTAs passed the Bonferroni threshold determined in FarmCPU (Liu et al., 2016) ($-\log_{10}(P)>6.5$, Figure 5.3). The full list of significant MTAs is shown in Table S 9.

Considering specifically the significant MTAs ($-\log_{10}(P)>6$), the majority of the points on the QQ plots were along the expected straight line, with just a small number of SNPs with the highest P values deviating from the QQ plot towards the y-axis (Figure 5.3). These deviated SNPs were most likely associated with the trait in the study, and the lack of deviation for the rest of the QQ plot suggested the GWAS accounted for population structure and familial relatedness. For some traits, two PCs were added as covariates to account for the two groups observed in Figure 5.1 and Figure 5.2. However, for some traits, the QQ plots when two PCs were added deviated from the straight line for many SNPs, suggesting confounding data and that the population structure was not being properly accounted for. When the GWAS was re-run with 0 PC, the QQ plots looked much more as expected with only a few high P-value SNPs deviating from the straight line and so, in these cases, no covariate was used (Figure 5.3 d, e, f, I, j).

Looking at the Manhattan plots (Figure 5.3), a range of yield traits had MTAs above the Bonferroni and FDR thresholds. Grain yield (GY), thousand-grain weight (TGW), harvest index (HI), grain number per m^2 (GN) and fruiting efficiency calculated using the spike dry weight at anthesis (FE) all had at least 5 MTAs above $-\log_{10}(P)>6$. For example, GY had 9 markers above the threshold spread over 2B, 3A, 4A, 5A, 5B, 6B, 7B (P values ranging from $3.1\text{x}10^{-11}$ to $3.1\text{x}10^{-7}$ Figure 5.3a, Table 5.1), while FE had 5 markers spread over 1A, 2B, 4A and 7A (P values ranging from $9.9\text{x}10^{-12}$, $2.7\text{x}10^{-7}$, Figure 5.3e, Table 5.1). Some traits had $-\log_{10}(P)$ values much higher than the threshold, for instance, GN had a marker on 3D located at 17.6 (Figure 5.3d). Other traits such as the spike hormone levels had fewer markers spread across all the chromosomes, but still had markers far above the thresholds, for example, spike cytokinin zeatin riboside had markers above the threshold of 6 on 1B, 2B, 7A and 7B (Table 5.2), with the marker on 1B co-locating

with cytokinin IPA. Spike cytokinin zeatin had significant markers above the threshold on chromosomes 3D, 4B and 6B. Hormone ABA has just two markers above the significance threshold on 6A and 6B, but they are still highly significant (P values $3.2x10^{-10}$ and $7.8x10^{-8}$, respectively, Table 5.2).

A wheat chromosomal ideogram with the results of the GWAS is shown in Figure 5.4. It shows some chromosomes have very good coverage of SNPs, such as 7A and 7B, while others are sparser such as 1A and 5D. Significant and putative MTAs were located on nearly all chromosomes, with 98 on sub-genome A, 132 on sub-genome B and 29 on sub-genome D. Chromosome 5B contained the highest individual number of MTAs with 56, while chromosome 4D had 0 MTAs. Some chromosomes such as 3A had a high concentration of markers for specific traits such as GY, GN and HI, while chromosome 5B had a range of markers associated with spike hormonal concentrations such as GA1, GA3, JA and IAA.

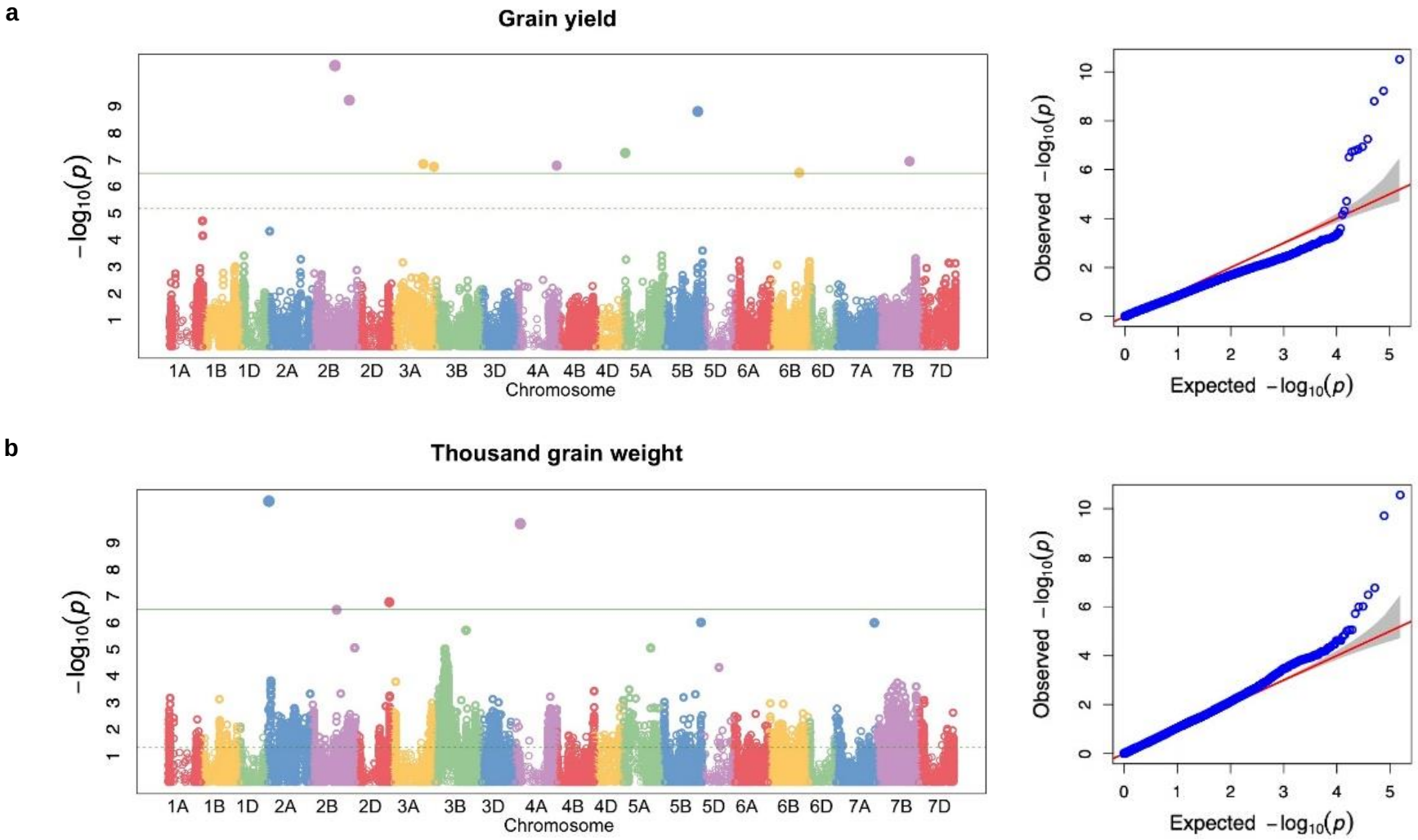
a
Grain yield
$-\log_{10}(p)$
1 2 3 4 5 6 7 8 9
1A 1B 1D 2A 2B 2D 3A 3B 3D 4A 4B 4D 5A 5B 5D 6A 6B 6D 7A 7B 7D
Chromosome
Observed $-\log_{10}(p)$
0 2 4 6 8 10
0 1 2 3 4 5
Expected $-\log_{10}(p)$
b
Thousand grain weight
$-\log_{10}(p)$
1 2 3 4 5 6 7 8 9
1A 1B 1D 2A 2B 2D 3A 3B 3D 4A 4B 4D 5A 5B 5D 6A 6B 6D 7A 7B 7D
Chromosome
Observed $-\log_{10}(p)$
0 2 4 6 8 10
0 1 2 3 4 5
Expected $-\log_{10}(p)$

c

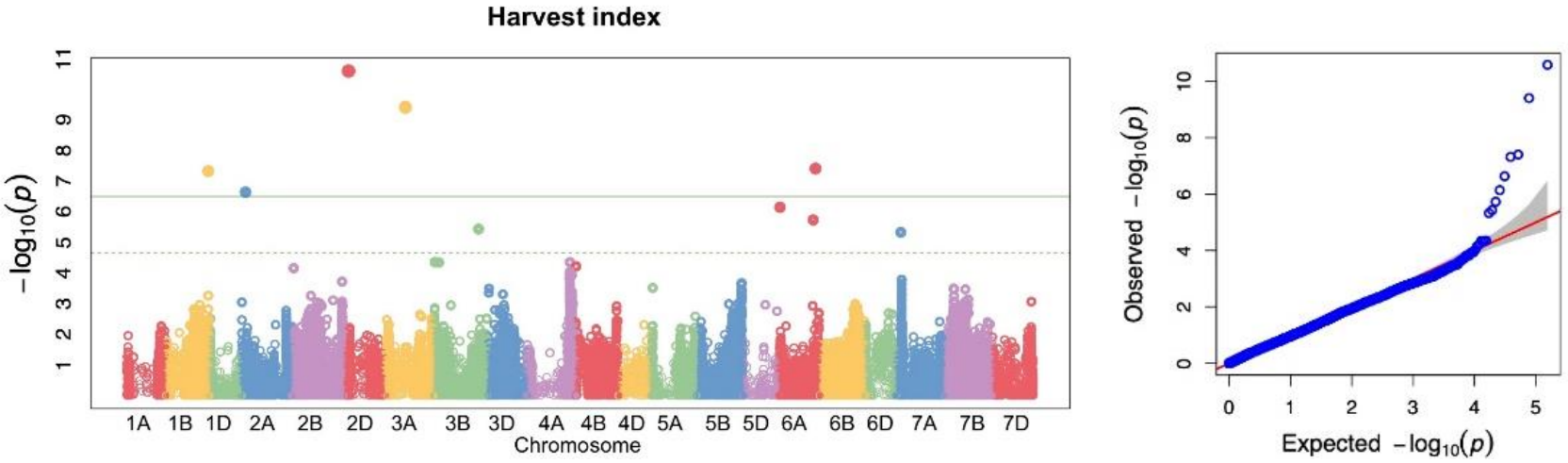
Harvest index
$-\log_{10}(p)$
1 2 3 4 5 6 7 8 9 11
1A 1B 1D 2A 2B 2D 3A 3B 3D 4A 4B 4D 5A 5B 5D 6A 6B 6D 7A 7B 7D
Chromosome
Observed $-\log_{10}(p)$
0 2 4 6 8 10
0 1 2 3 4 5
Expected $-\log_{10}(p)$

d

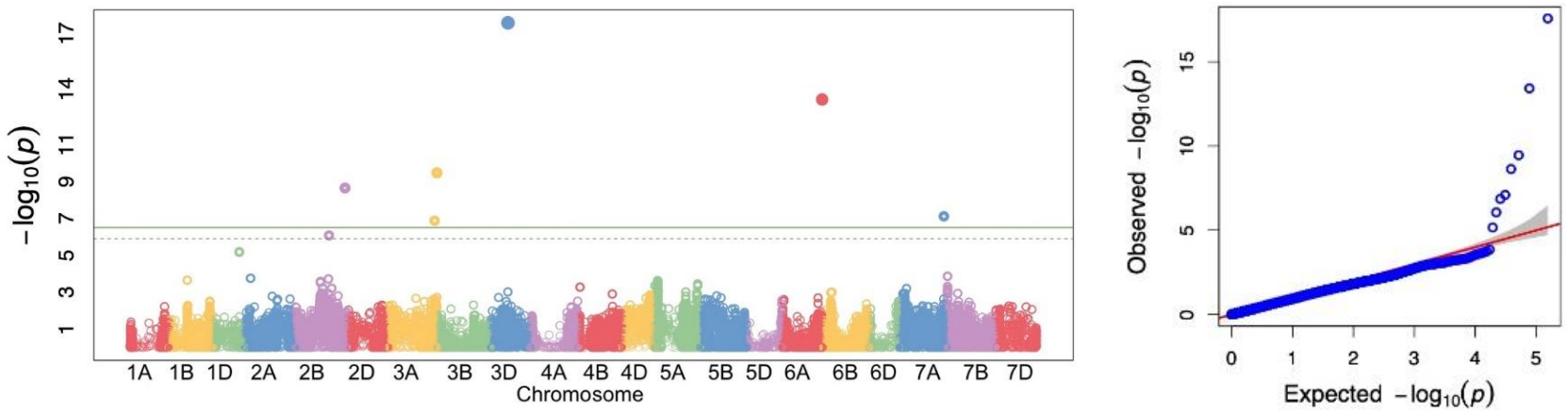
Grain number per m²
$-\log_{10}(p)$
1 3 5 7 9 11 14 17
1A 1B 1D 2A 2B 2D 3A 3B 3D 4A 4B 4D 5A 5B 5D 6A 6B 6D 7A 7B 7D
Chromosome
Observed $-\log_{10}(p)$
0 5 10 15
0 1 2 3 4 5
Expected $-\log_{10}(p)$

e

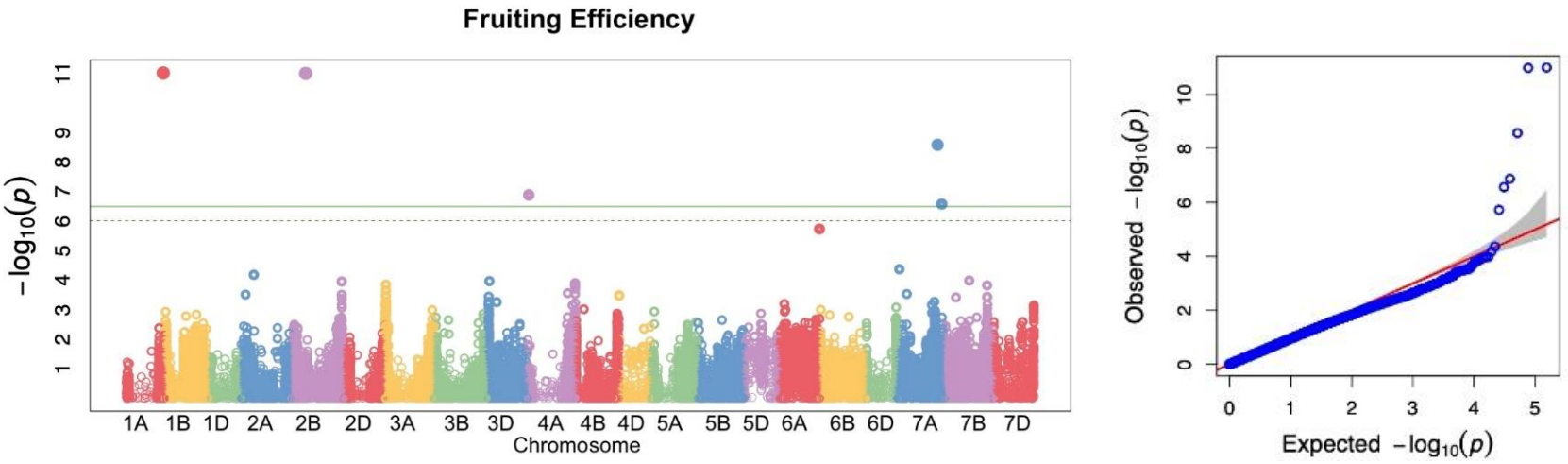
Fruiting Efficiency
$-\log_{10}(p)$
1 2 3 4 5 6 7 8 9 11
1A 1B 1D 2A 2B 2D 3A 3B 3D 4A 4B 4D 5A 5B 5D 6A 6B 6D 7A 7B 7D
Chromosome
Observed $-\log_{10}(p)$
0 2 4 6 8 10
0 1 2 3 4 5
Expected $-\log_{10}(p)$

f

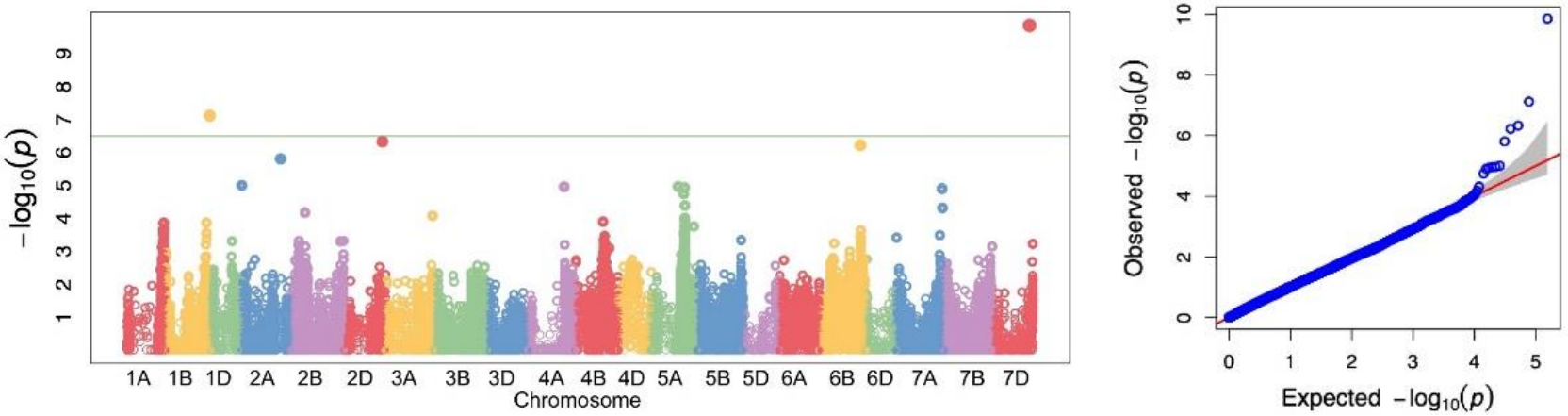
Peduncle length
$-\log_{10}(p)$
1 2 3 4 5 6 7 8 9
1A 1B 1D 2A 2B 2D 3A 3B 3D 4A 4B 4D 5A 5B 5D 6A 6B 6D 7A 7B 7D
Chromosome
Observed $-\log_{10}(p)$
0 2 4 6 8 10
0 1 2 3 4 5
Expected $-\log_{10}(p)$

g

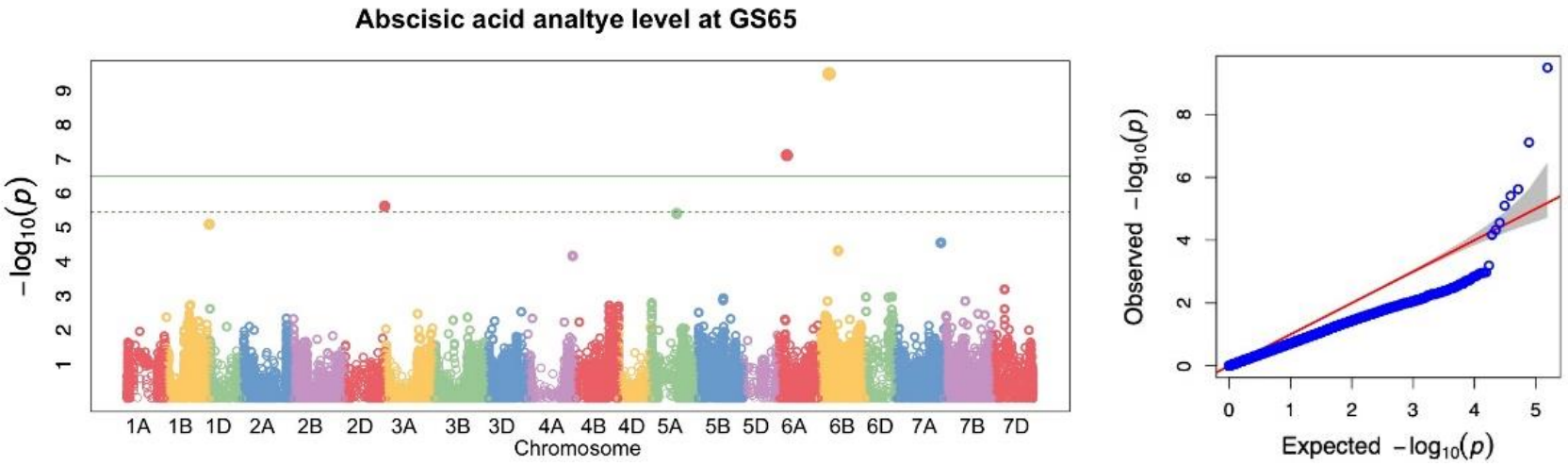
Abscisic acid analtye level at GS65
$-\log_{10}(p)$
1 2 3 4 5 6 7 8 9
1A 1B 1D 2A 2B 2D 3A 3B 3D 4A 4B 4D 5A 5B 5D 6A 6B 6D 7A 7B 7D
Chromosome
Observed $-\log_{10}(p)$
0 2 4 6 8
0 1 2 3 4 5
Expected $-\log_{10}(p)$

i

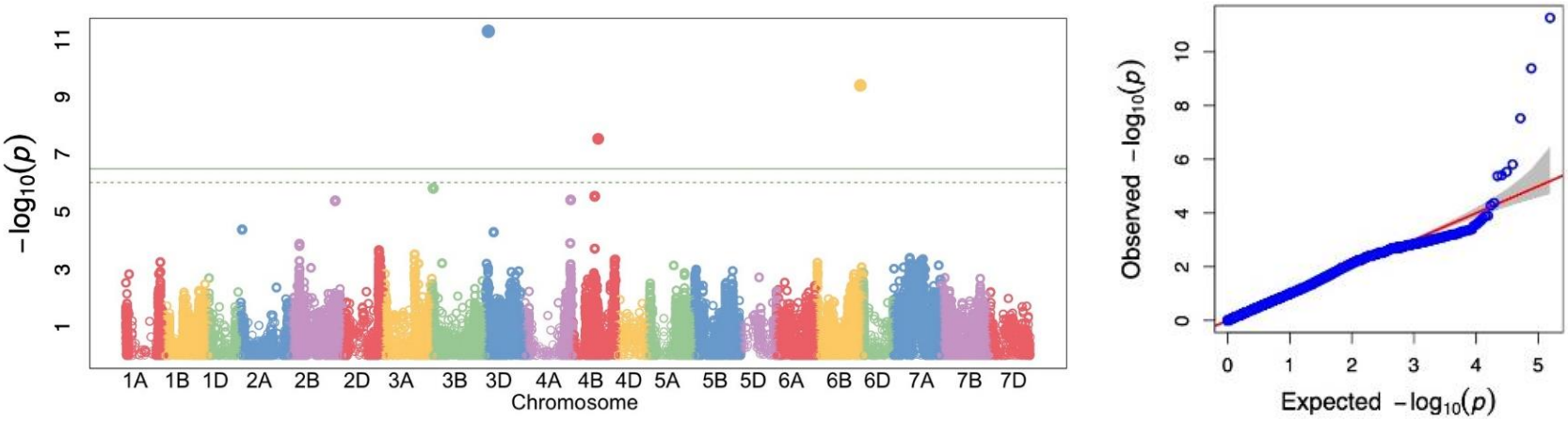
Zeatin analyte level at GS65
$-\log_{10}(p)$
1 3 5 7 9 11
1A 1B 1D 2A 2B 2D 3A 3B 3D 4A 4B 4D 5A 5B 5D 6A 6B 6D 7A 7B 7D
Chromosome
Observed $-\log_{10}(p)$
0 2 4 6 8 10
0 1 2 3 4 5
Expected $-\log_{10}(p)$

j

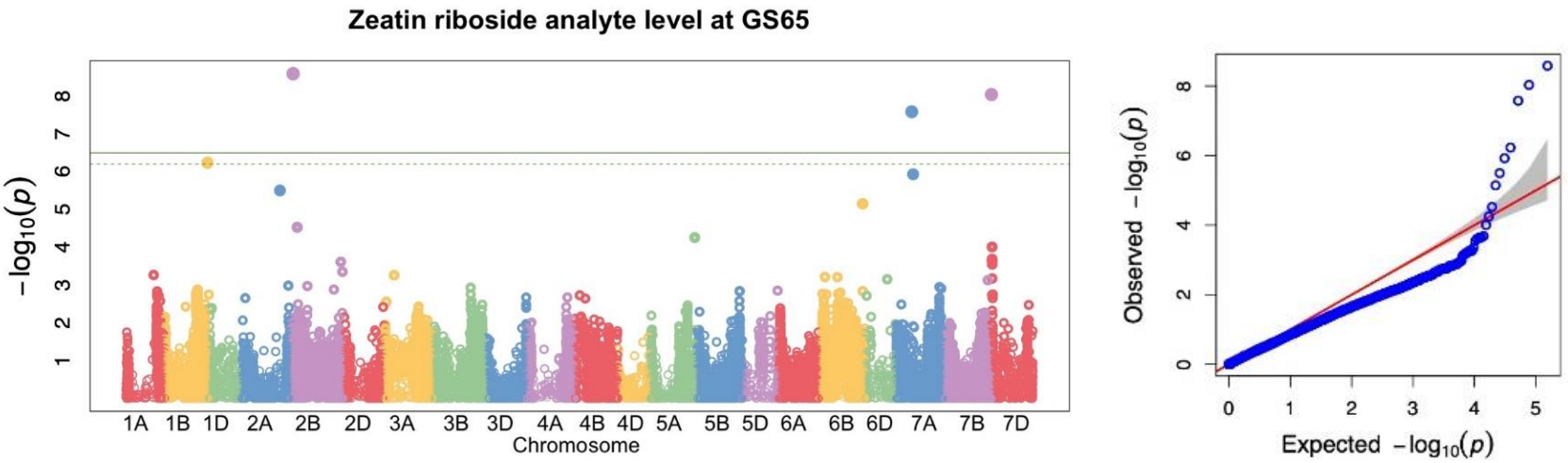
Zeatin riboside analyte level at GS65
$-\log_{10}(p)$
1 2 3 4 5 6 7 8
1A 1B 1D 2A 2B 2D 3A 3B 3D 4A 4B 4D 5A 5B 5D 6A 6B 6D 7A 7B 7D
Chromosome
Observed $-\log_{10}(p)$
0 2 4 6 8
0 1 2 3 4 5
Expected $-\log_{10}(p)$

k

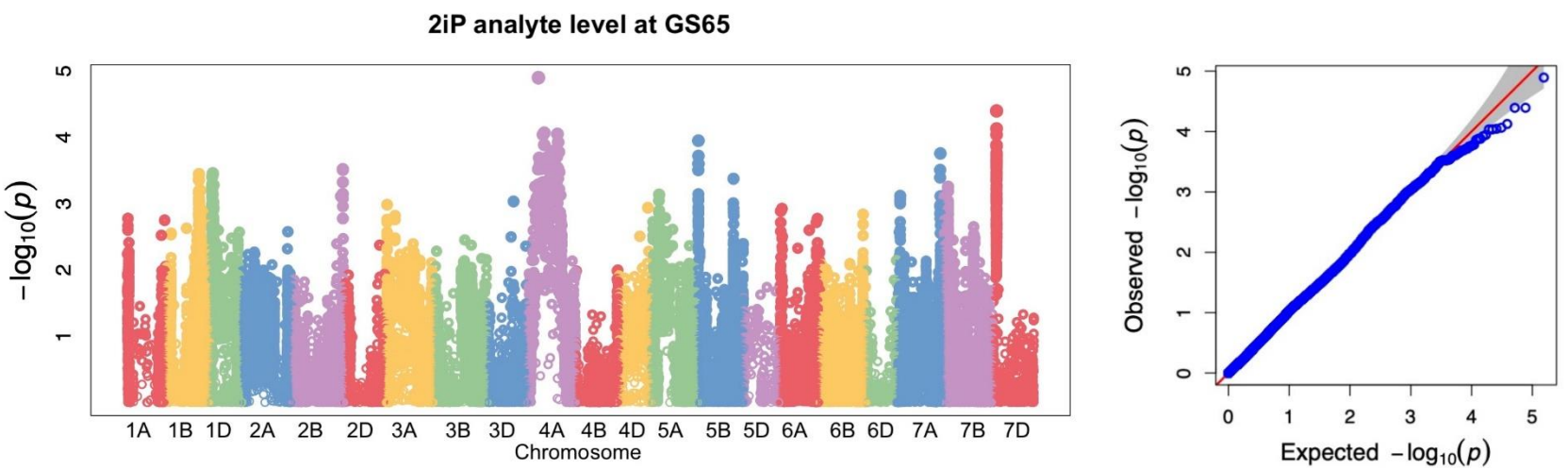
2iP analyte level at GS65
$-\log_{10}(p)$
1 2 3 4 5
1A 1B 1D 2A 2B 2D 3A 3B 3D 4A 4B 4D 5A 5B 5D 6A 6B 6D 7A 7B 7D
Chromosome
Observed $-\log_{10}(p)$
0 1 2 3 4 5
0 1 2 3 4 5
Expected $-\log_{10}(p)$

I

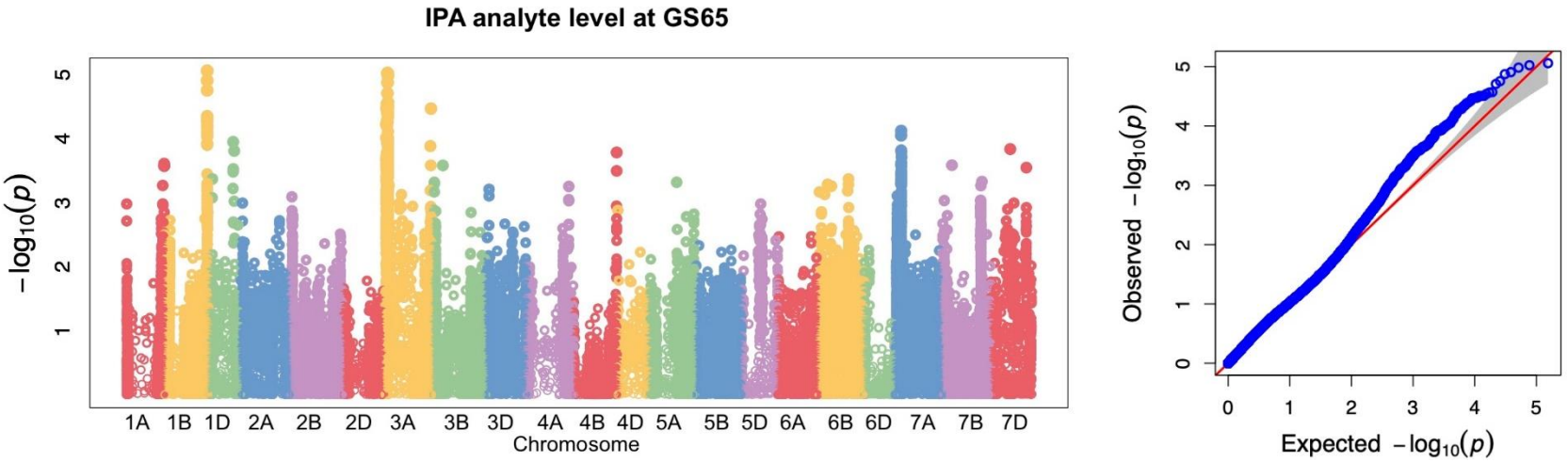

***Figure 5.3**: GWAS results of HiBAP II panel for significant MTAs depicted as a Manhattan plot and QQ plot*

In the Manhattan plots (left) the two –log$_{10}$(P) thresholds shown are the FDR cutoff (green dash line) and the Bonferroni cutoff (green solid line), and in the QQ plots (right) the –log$_{10}$(P) values from the GWAS are plotted against the expected value under the null hypothesis that there's no association with the trait, ***2iP:*** *isopentenyladenine,* ***IPA****: isopentenyladenosine, fruiting efficiency calculated using spike DM at anthesis + 7 days*

0PCA added as a covariate for grain number per m^2, fruiting efficiency, peduncle length, zeatin analyte level at GS65 and zeatin riboside analyte level at GS65

2PCA added as a covariate for grain yield, thousand-grain weight, harvest index and abscisic acid analyte level at GS65

***Table 5.1**: Summary of the marker-trait associations (MTAs) from the genome-wide association study of the HiBAP II panel of 146 lines at anthesis + 7 days and physiological maturity*

*§:0PCA added as a covariate, for all other traits 2PCA used, **Stem PI**: stem partitioning index, **Spike PI**: spike partitioning index, **Lamina PI**: Lamina partitioning index, **Ped L**: stem peduncle length, **Int3 L**: stem internode 3 length, **Spike DM**: dry matter (DM) spike per unit area, **FE**: fruiting efficiency (calculated using spike DM at anthesis + 7 days), **$AGDM_{PM}$**: above ground DM at physiological maturity, **GY**: grain yield, **TGW**: thousand-grain weight, **HI**: harvest index, **GN**: grain number per m^2*

		Significant MTAs ($-log_{10}(P)>6$)			Putative MTAs ($-log_{10}(P)>4$)			Co-located marker
		No.	Location	P value (min, max)	No.	Location	P value (min, max)	
Anthesis + 7 days (GS65+7d)	**Stem PI**	0	-	-	2	5B (1), 7A (1)	$8.5x10^{-5}$, $9.0x10^{-5}$	-
	Spike PI	0	-	-	1	2B (1)	$2.2x10^{-5}$, $2.2x10^{-5}$	HI (2B)
	Lamina PI	0	-	-	7	1B (1), 2B (1), 4A (3), 5B (1), 7B (1)	$8.6x10^{-6}$, $9.3x10^{-5}$	-
	Ped L (cm)§	4	1B (1), 2D (1), 6B (1), 7D (1)	$1.4x10^{-10}$, $6.0x10^{-7}$	12	2A (2), 2B (1), 3A (1), 4A (1), 5A (5), 7A (2)	$1.6x10^{-6}$, $9.7x10^{-5}$	-
	Int 3 L (cm)	0	-	-	1	4A (1)	$9.6x10^{-5}$, $9.6x10^{-5}$	-
	SpikeDM ($g\ m^{-2}$)	0	-	-	3	1B (1), 4A (2)	$5.6x10^{-5}$, $8.4x10^{-5}$	-
	FE_{A+7} (grns g^{-1})§	5	1A (1), 2B (1), 4A (1), 7A (2)	$9.9x10^{-12}$, $2.7x10^{-7}$	3	2A (1), 6A (1), 7A (1)	$1.9x10^{-6}$, $6.6x10^{-5}$	-
Physiological Maturity (GS89)	**$AGDM_{PM}$ ($g\ m^{-2}$)§**	0	-	-	1	6A (1)	$7.3x10^{-5}$, $7.3x10^{-5}$	-
	GY ($g\ m^{-2}$)	9	2B (2), 3A (2), 4A (1), 5A (1), 5B (1), 6B (1), 7B (1)	$3.1x10^{-11}$, $3.1x10^{-7}$	3	1A (2), 2A (1)	$2.0x10^{-5}$, $7.0x10^{-5}$	-
	TGW (g)	5	2A (1), 2B (1), 2D (1), 4A (1), 5B (1)	$2.8x10^{-11}$, $9.8x10^{-7}$	30	2B (1), 3B (26), 5A (1), 5D (1), 7A (1)	$1.0x10^{-6}$, $9.4x10^{-5}$	GN (2B)
	HI	6	1B (1), 2A (1), 2D (1), 3A (1), 6A (2)	$2.6x10^{-11}$, $7.3x10^{-7}$	9	2B (1), 3B (3), 4A (2), 4B (1), 6A (1), 7A (1)	$1.9x10^{-6}$, $9.3x10^{-5}$	Spike PI (2B)
	GN (grains m^{-2})§	7	2B (2), 3A (2), 3D (1), 6A (1), 7A (1)	$2.7x10^{-18}$, $8.6x10^{-7}$	1	1D (1)	$6.8x10^{-6}$, $6.8x10^{-6}$	TGW (2B)

***Table 5.2**: Summary of the spike hormone marker-trait associations (MTAs) from the genome-wide association study of the HiBAP II panel of 146 lines at anthesis*

*§:0PCA added as a covariate, for all other traits 2PCA used, **ABA**: abscisic acid, **GA1**: gibberellin 1, **GA3**: gibberellin 3, **GA4**: gibberellin 4, **GA7**: gibberellin 7, **IAA**: indole-3-acetic acid, **JA**: jasmonic acid, **MEL**: melatonin, **SA**: salicylic acid, **Z**: zeatin, **Zr**: zeatin riboside, **IPA**: isopentenyladenosine, **2iP:** isopentenyladenine*

		Significant MTAs ($-\log_{10}(P)>6$)			Putative MTAs ($-\log_{10}(P)>4$)			Co-located marker
		No.	Location	P value (min, max)	No.	Location	P value (min, max)	
Spike hormone analyte levels (ng/g FW) at Anthesis (GS65)	**ABA**	2	6A (1), 6B (1)	3.2×10^{-10}, 7.8×10^{-8}	6	1B (1), 2D (1), 4A (1), 5A (1), 6B (1), 7A (1)	2.4×10^{-6}, 6.8×10^{-5}	-
	GA1	1	5B (1)	3.1×10^{-7}, 3.1×10^{-7}	24	1B (1), 2D (2), 3B (1), 5B (14), 6B (1), 7A (4), 7D (1)	2.4×10^{-6}, 9.6×10^{-5}	-
	GA3	0	-	-	14	5B (14)	5.4×10^{-6}, 8.2×10^{-5}	-
	GA4	0	-	-	4	2A (1), 2D (1), 5D (1), 6A (1)	1.4×10^{-5}, 9.7×10^{-5}	-
	GA7 §	0	-	-	2	1A (1), 6D (1)	3.7×10^{-5}, 7.4×10^{-5}	-
	IAA	0	-	-	15	2B (1), 2D (1), 5B (11), 7A (1), 7D (1)	2.5×10^{-6}, 9.7×10^{-5}	-
	JA	0	-	-	15	3B (1), 3D (1), 5B (11), 6B (1), 7B (1)	4.4×10^{-6}, 7.7×10^{-5}	-
	SA	0	-	-	2	2D (2)	3.4×10^{-6}, 1.0×10^{-5}	-
	Z§	3	3D (1), 4B (1), 6B (1)	5.4×10^{-12}, 3.0×10^{-8}	6	2A (1), 2B (1), 3B (1), 3D (1), 4A (1), 4B (1)	1.5×10^{-6}, 5.2×10^{-5}	-
	Zr§	4	1B (1), 2B (1), 7A (1), 7B (1)	2.6×10^{-9}, 5.9×10^{-7}	6	2A (1), 2B (1), 5A (1), 6B (1), 7A (1), 7D (1)	1.2×10^{-6}, 9.9×10^{-5}	IPA (1B)
	IPA	0	-	-	32	1B (7), 3A (23), 7A (2)	8.7×10^{-6}, 9.7×10^{-5}	Zr (1B)
	2iP	0	-	-	6	4A (4), 7D (2)	1.3×10^{-5}, 9.2×10^{-5}	-

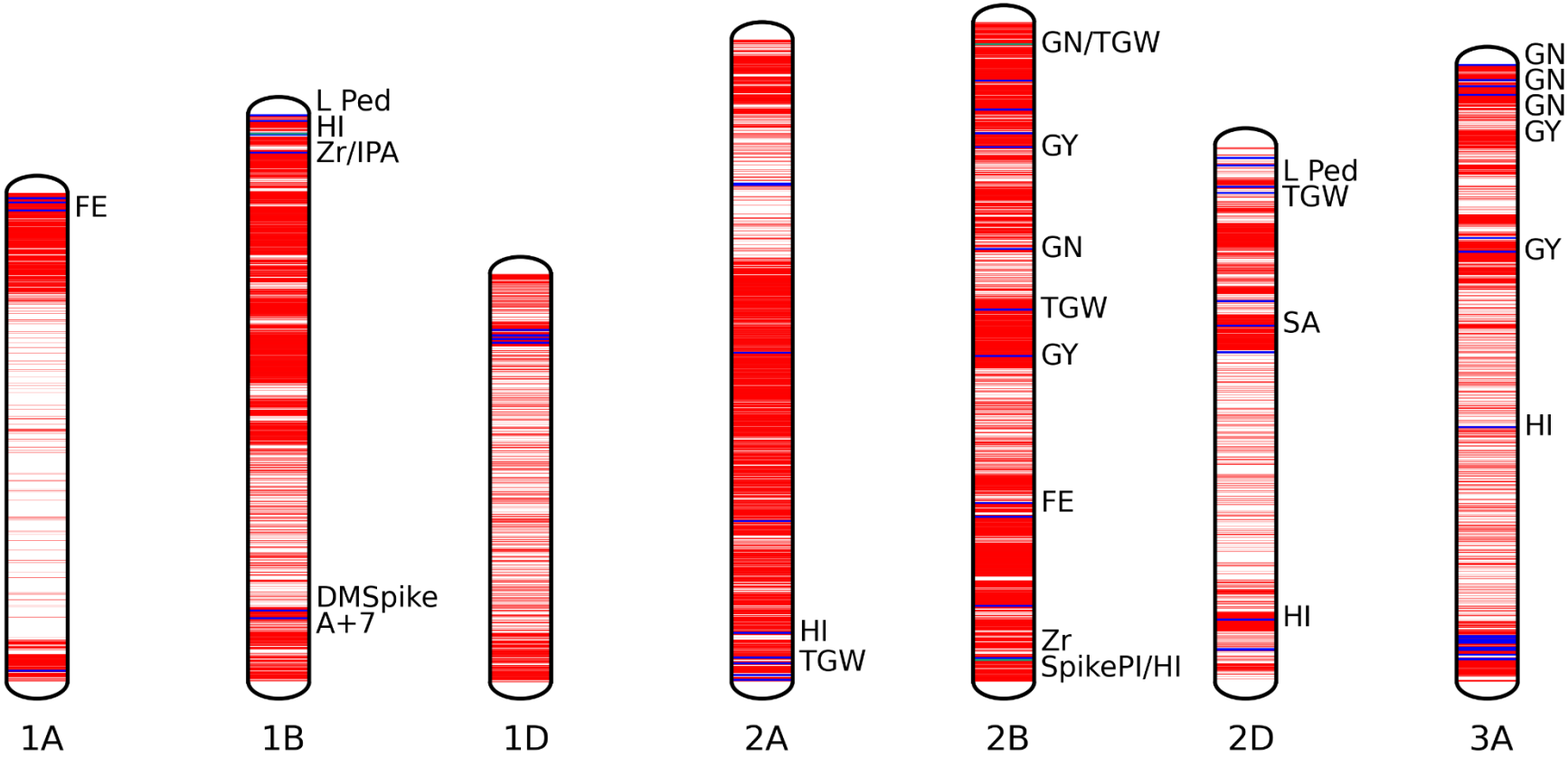
FE
L Ped
HI
Zr/IPA
DMSpike
A+7
HI
TGW
GN/TGW
GY
GN
TGW
GY
FE
Zr
SpikePI/HI
L Ped
TGW
SA
HI
GN
GN
GN
GY
GY
HI
1A
1B
1D
2A
2B
2D
3A

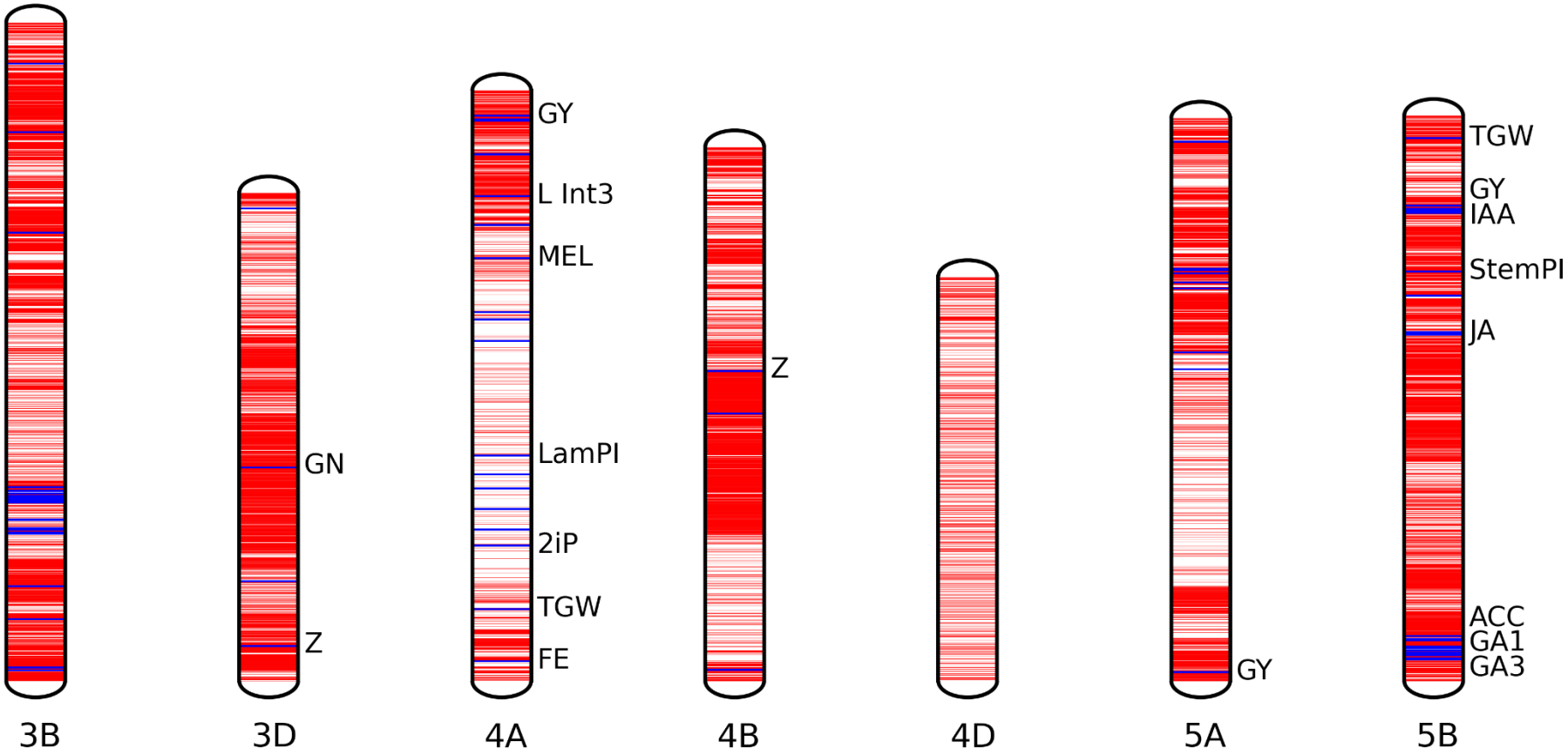
3B
3D
GN
Z
4A
GY
L Int3
MEL
LamPI
2iP
TGW
FE
4B
Z
4D
5A
GY
5B
TGW
GY
IAA
StemPI
JA
ACC
GA1
GA3

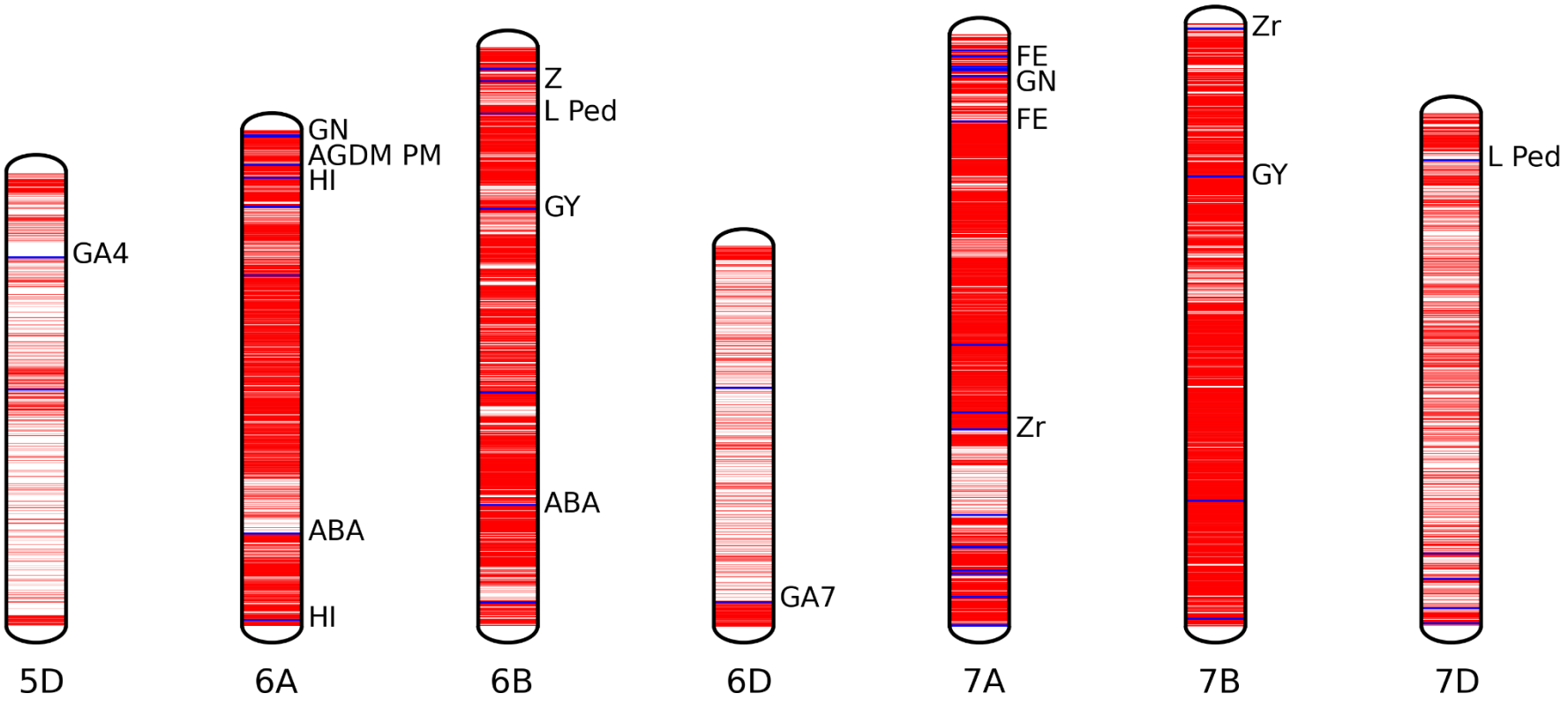

Figure 5.4: *Wheat chromosomal ideogram overlaid with genome-wide association study significant MTA results*

Red lines indicate the location of SNPs, blue lines indicate all putative and significant MTAs, with the highest MTAs for each trait labelled, green lines indicate multi-trait MTAs

Stem PI*: stem partitioning index,* ***Spike PI****: spike partitioning index,* ***Lamina PI****: Lamina partitioning index,* ***L Ped****: stem peduncle length,* ***L Int3****: stem internode 3 length,* ***DMSpike A+7****: DM spike per unit area at anthesis + 7 days,* ***FE****: fruiting efficiency (calculated using spike DM at anthesis + 7 days),* ***2iP:*** *isopentenyladenine,* ***ABA****: abscisic acid,* ***ACC****: 1-aminocyclopropane-1-carboxylic acid,* ***GA1****: gibberellin 1,* ***GA3****: gibberellin 3,* ***GA4****: gibberellin 4,* ***GA7****: gibberellin 7,* ***IAA****: indole-3-acetic acid,* ***IPA****: isopentenyladenosine,* ***JA****: jasmonic acid,* ***MEL****: melatonin,* ***SA****: salicylic acid,* ***Z****: zeatin,* ***Zr****: zeatin riboside,* ***AGDM PM****: above ground DM at physiological maturity,* ***GY****: grain yield,* ***TGW****: thousand-grain weight,* ***HI****: harvest index,* ***GN****: grain number per* m^2

5.3.3 Candidate gene analysis

When searching for candidate genes by using the MTAs from the GWAS, multiple genes close to the SNPs were found. Of the 53 candidate genes listed in Table 5.3, 34 had a gene name associated with them, while the remaining 19 just had an accession name/number. With the genes near MTAs for yield-related traits on chromosome 2B (grain yield, grains per m^2 and thousand-grain weight), the candidate genes were related to grain yield, grain size, number and weight. In the case of peduncle length, most of the candidate genes were associated with shoot system morphology or carbohydrate content. Many of these candidate genes also had days to flowering or days to maturity as an associated trait. Looking in more detail, the marker chr1A-572361729 for FE on chromosome 1A had a candidate gene *NF-YB1* 0.03 Mbp away, which in rice is regulates grain filling and therefore influences yield.

Looking at the spike hormone levels at GS65, the cytokinins such as zeatin and zeatin riboside had candidate genes that were related to yield traits including grain number, grain size and thousand-grain weight (markers chr3D-43783543, chr1B-665661232, chr2B-28422029, chr7B-744404071, Table 5.3). The spike cytokinin traits also had candidate genes that were associated with hormones, for instance, the marker chr1B-665661232 for Zr/IPA on chromosome 1B had a candidate gene with *PIN3*, which in *Arabidopsis* is associated with cytokinin and ethylene sensitivity. In addition, the marker chr7A-244483443 for Zr on chromosome 7A had a candidate gene 0.12 Mbp away *BHLH62*, which in wheat is associated with brassinosteroid sensitivity through regulation by the transcription factor *HY5* in *Arabidopsis thaliana*. Other hormones such as ABA and GA1 had candidate genes *GSH2, ADO2* and *NFYA4* which are associated with stress responses such as oxidative stress tolerance and drought tolerance.

***Table 5.3**: List of potential candidate genes identified from the MTAs in the HiBAP II Panel using KnetMiner*

***Ped L**: stem peduncle length, **FE_{A+7}**: fruiting efficiency (calculated using spike dry matter at anthesis + 7 days), **SPI**: spike partitioning index, **HI**: harvest index, **GY**: grain yield, **GN**: grain number per m^2, **TGW**: thousand-grain weight, **Z**: zeatin, **Zr**: zeatin riboside, **IPA**: isopentenyladenosine, **ABA**: abscisic acid, **GA1**: gibberellin 1*

Trait	Chr	SNP	-Log_{10}(P)	Gene Name	Associated Traits
Ped L	7D	chr7D-580311382	9.85	FIB3	Shoot system morphology
				ATUPS3	Carbohydrate content
				RAN1	Tiller number
				CBSDUF4	Shoot system morphology
				TRAESCS7D02G466200	Days to flowering
FE_{A+7}	1A	chr1A-572361729	11.01	NF-YB1	Grain Yield
				ERF061/EMB2744	Flowering time
FE_{A+7}	2B	chr2B-216790502	10.99	SAP11	Grain weight, shoot system morphology
				COPT4	Flowering time, leaf morphology
SPI /HI	2B	chr2B-26301024	4.66	RBL19	Days to maturity
				TRAESCS2B02G054600	Days to anthesis, root length
				TRAESCS2B02G053700	TGW, Plant height
				TRAESCS2B02G054400	Plant height
HI	2D	chr2D-75260450	10.58	AGL90	Grain weight, Photosynthetic rate, Inflorescence branching
				GPT	Stem elongation, Stomatal opening, ABA sensitivity
				CYP709B2	Flowering time, Shoot system morphology
				TRAESCS2D02G130400	TGW, Grain size and length
HI	3A	chr3A-308957350	9.40	CALS6	Grain yield
				TRAESCS3A02G197700	Flowering time, Plant height
GY	2B	chr2B-395408807	10.51	ZFP10	Grain size
				TRAESCS2B02G286700	Grain number, Grain yield
GN/ TGW	2B	chr2B-774945561	8.63	CDP1	Spikelet fertility, Photosynthetic ability
				TRAESCS2B02G587500	Grain weight, Grain yield
TGW	4A	chr4A-90708744	9.71	HRD3A	Auxin content, Stem elongation, Grain weight
				MYOB3	Fruit morphology, Flowering time
				DRP4C	Shoot system morphology
Z	3D	chr3D-43783543	11.27	OASC	Shoot DM, Grain weight
				RAP	TGW, Grain size and length
Zr/ IPA	1B	chr1B-665661232	6.23	MPK15	Grain size and weight
				PIN3	Cytokinin and ethylene sensitivity
				BIOF	Grain weight, length and size

Trait	Chr	SNP	-Log$_{10}$(P)	Gene Name	Associated Traits
Zr	2B	chr2B-28422029	8.58	ERD6	Grain weight
				NPF2.11/ TRAESCS2B02G057600	Stem elongation, Ethylene sensitivity
				TRAESCS2B02G058400	Grain number
				TRAESCS2B02G059700	Plant height
Zr	7A	chr7A-244483443	7.58	BHLH62	Brassinosteroid sensitivity
				RABA5D	Seedling growth, Grain yield
				RPL32A	Cytokinin content
				EPFL9	Photosynthetic rate
Zr	7B	chr7B-744404071	8.03	CHAT	Plant height, Grain yield
				TRAESCS7B02G491100	TGW, Grain size and length
				TRAESCS7B02G491400	Grain number, Grain yield
				TRAESCS7B02G490900	TGW, Grain size and length
				TRAESCS7B02G491700	Grain number
				TRAESCS7B02G491000	Grain number
ABA	6A	chr6A-115016200	7.11	GSH2	Hypocotyl length, Oxidative stress
				TRAESCS6A02G140300	Grain weight
				TRAESCS6A02G140400	Flowering time, Plant height
ABA	6B	chr6B-150809926	9.49	ADO2	Grain number, Drought tolerance, Stem elongation
				TRAESCS6B02G150200	TGW, Grain size and length
				TRAESCS6B02G149700	Plant height, Grain yield
GA1	5B	chr5B-52610848	6.51	NFYA4	Abscisic acid sensitivity, Drought tolerance, Photosynthetic rate

5.4 Discussion

In the present study, a genome-wide association study was used to dissect genetically grain partitioning traits such as fruiting efficiency, harvest index and spike hormonal levels. Results for these traits in the field experiments are fully described in chapter 3.3, and showed grain yield was strongly correlated with above-ground DM at physiological maturity ($AGDM_{PM}$) and slightly less strongly with harvest index. A trade-off was observed between $AGDM_{PM}$ and HI, so for the yield potential of high biomass genotypes to be exploited, HI must be increased (Foulkes et al., 2011). Two traits that have been suggested to increase grain number per m^2 and HI are spike partitioning index and fruiting efficiency. In the HiBAP II, a higher SPI was associated with a higher HI and spike DM at anthesis + 7 days, as reported elsewhere (Miralles and Slafer, 2007). Although there was no association between SPI and GN, there was a positive association of FE with both HI and GN. For a detailed discussion on the results for FE and SPI, and also the potential trade-off between these traits see chapter 3.4. Plant height, stem PI, peduncle length and internode 3 length were all negatively correlated with HI, and peduncle length was also negatively associated with FE (Table 3.2). In the past, reducing plant height in wheat breeding programmes has increased HI (Acreche et al., 2008), and most modern varieties of wheat are already within the optimum range of 70-100 cm. However, further targeted reductions for specific internodes, internode 3 in particular, could help raise SPI and HI. FE_{Chaff} was positively correlated with the spike cytokinins zeatin riboside, zeatin, IPA and 2iP at anthesis, while grain yield was positively correlated with IPA and 2iP at anthesis. As these traits have extremely complex interactions and are not high-throughput measurements, it is important to identify marker-trait associations through a GWAS in order to enhance harvest index and yield potential.

While GWAS mapping is a useful tool, some drawbacks should be considered. GWAS based on SNPs relies on the pre-existing genetic maps – in this study the IWGSC wheat reference genome RefSeq V1.1 (IWGSC et al., 2018), which means any errors in the mapping could result in errors in the GWAS (Alqudah et al., 2020b). There can also be population structure problems, with spurious relatedness. However, in this study, the lack of deviation from the diagonal line in the QQ plots suggests there were few spurious associations, and therefore both population structure and familial relatedness were well accounted for. The SNPs on the upper right section of the QQ plots are expected to deviate from the diagonal as these SNPs are the markers most likely associated with the trait. For traits with

low heritability value, many markers are required, but the HiBAP II has very high density genotyping through enrichment capture sequencing. Rare alleles are filtered, with individuals with a minor allele of less than 5 % removed. This is because rare alleles lead to a lack of resolution power (Soto-Cerda and Cloutier, 2012). Unfortunately, rare alleles could have relatively large effects on complex traits, so it is important to not dismiss rare alleles in further studies (Alqudah et al., 2020b).

5.4.1 Maker-trait associations

Identification of marker-trait associations, especially for complex traits which are difficult to phenotype in the field, is important for ensuring these traits are deployed in breeding through marker-assisted selection. Grain yield improvement, while essential, is difficult due to the low heritability of grain yield and genotype x environment interactions (Quarrie et al., 2006). Despite the low heritability, previous studies conducting GWAS in wheat have identified genomic regions associated with grain yield and other key yield-related traits (Crossa et al., 2007; Neumann et al., 2011; Hoffstetter et al., 2016; Lozada et al., 2017). In this study on the HiBAP II panel, there were numerous genomic regions highly significantly associated with grain yield across chromosomes 2B, 3A, 4A, 5A, 5B, 6B and 7B. Sehgal et al. (2020) recently conducted a GWAS with 6,461 CIMMYT spring bread wheat lines using 192-plexing on Illumina HiSeq2000 and blasted to the IWGSC wheat reference genome RefSeq V1.1 (IWGSC et al., 2018). In this study, they identified three markers for yield close to the MTAs identified in the HiBAP II for yield on chromosome 4A (chr4A-712872970 and S4A_713064971), 5B (chr5B-599326707 and S5B_513713184) and 7B (chr7B-559714023 and S7B_576927877) (Sehgal et al., 2020). Fifty-eight lines from the HiBAP II were also included in this larger GWAS, and the identification of the same MTA in both studies gives more confidence that these markers are good candidates for grain yield.

As well as looking directly at MTAs for grain yield, it's important also to examine the components that can increase grain yield, such as HI and above-ground biomass (Quarrie et al., 2006). Studies suggest, under optimal conditions, grain yield is limited mainly by grain number and therefore could be improved by targeting fruiting efficiency (Foulkes et al., 2011). The present study identified MTAs for FE, HI, TGW and GN. One marker for GN on chromosome 2B was also found co-locating for TGW, however, this is not expected due to the known trade-off between grain number and grain weight (Ferrante et al., 2012). In chapter 3, it

was shown that there was a large trade-off between GN and TGW (Figure 3.5), so a marker co-locating for these two traits when they are negatively associated suggests this marker may be controlling grain number in the first instance with a pleiotropic effect on grain weight.

A GWA study was performed on the HiBAP I, which shares 50 lines with the HiBAP II and was genotyped using the 35K wheat breeders Axiom Array (Allen et al., 2017). The marker on chromosome 2B in the HiBAP II that was associated with both GN and TGW (chr2B-774945561) is 83 Mbp from an SNP from the HiBAP I associating with GN (AX-94461881) (Molero et al., 2019). Similarly, on chr 6A, the HiBAP II marker (chr6A-522305070) and the HiBAP I marker (AX-94546552) both associated with HI were 35 Mbp apart (Molero et al., 2019). As the two GWA studies were conducted on similar material and grown in the same environment (CIMMYT's Experimental Station, Norman E. Borlaug, CENEB in the Yaqui Valley, near Ciudad Obregon, Sonora, Mexico), it is promising to see confirmation with a second dataset.

Currently, very few studies have included FE as a trait in a genome-wide association study (Guo et al., 2017; Sierra-Gonzalez, 2020). However, a recent investigation by Basile et al. (2019) on 102 Argentinian wheat cultivars with genotyping using the 35k Axiom Array (Allen et al., 2017) and SNPs anchored to the wheat reference genome assembly (IWGSC et al., 2018) found two markers for FE (calculated with chaff dry weight). These FE markers are reasonably close with markers associated with FE in the HiBAP II. On chr 1A, the two markers are 85 Mbp apart (chr1A-572361729 in HiBAP II and chr1A-B32-Hap4 in Basile et al, (2019)) and on chr 2A they are 13 Mbp apart (chr2A-195115685 and chr2A-B30-Hap4). Another study by Gerard et al. (2019) on 96 wheat cultivars and advanced breeding lines from 20 countries where the material was genotyped using the 15K Infinium SNP array (Wang et al., 2014) also found one marker on chromosome 2A for FE (calculated with spike dry weight at anthesis); however, it was located at the other end of chromosome 2A than in the present study (chr2A-195115685 in HiBAP II and Tdurum_contig41912_893 in Gerard et al. (2019)). A third recent paper by Pretini et al. (2020) looking at 102 doubled-haploid lines, genotyped using the iSelect 90K SNP assay (Wang et al., 2014) in which phenotypic data were BLASTed against the wheat genome assembly (IWGSC et al., 2018), found a marker for FE (calculated with chaff dry weight) on chr 1A. However, the marker was 92 Mbp from the HiBAP II marker on chr 1A (chr1A-572361729 in HiBAP II and RAC875_c53185_802 in Pretini et al. (2020)). There was, however, also a

marker on chr 7A which was just 2.5 Mbp away from the HiBAP II marker on 7A (chr7A-628237844 and wsnp_Ku_rep_c113718_96236830). It is promising that despite the limited studies, there are markers with similar positions for FE discovered in different wheat panels, and the increase in number of papers in recent years shows how it is an important trait to understand.

Several other marker studies have identified regions in the wheat chromosome affecting grain number traits. Sakuma et al. (2019) identified locus *Grain Number Increase 1 (GNI1)*, which they showed contributed to floret fertility. One gene lying within the genetic interval harbouring *GN1-A1* (TRIDC2AG055810 on chr 2A, 626823738-626838029 bp) encodes a homeodomain leucine zipper class I transcription factor and reducing the function through mutations resulted in increased grain set per spikelet, grain number and yield. In the HiBAP II, no MTAs for grain number or yield were identified close to *GNI1*. There was one putative MTA for grain yield on chr 2A, but 619 Mbp away. Another gene identified for spikelet number is *TaAPO-A1* (*TraesCS7A01G481600* on chr 7A, 674081462–674082918 bp), the wheat orthologue to *AP01*, a rice gene that positively controls spikelet number (Muqaddasi et al., 2019). A mutation in the F box domain defines two alleles in bread wheat, and a KASP marker developed on this site showed a highly significant association of *TaAPO-A1* with total spikelet number and a weaker but significant association with spike length and grain yield. In the HiBAP II, the closest MTA for grain number on chr 7A is chr7A-684701585, which is 10.6 Mbp away from *TaAPO-A1*. The GWAS performed with the HiBAP II panel did not identify the same markers associated with grain number as in the case of these studies, but instead suggested novel MTAs.

Spike hormone concentrations have not been previously included in GWA studies. In this study, a range of hormones from cytokinins, gibberellins and abscisic acid had significant and putative MTAs. Cytokinin degradation genes *TaCKX2* and *TaCKX6* regulating cytokinin oxidase/dehydrogenase have previously been identified on chromosome 3D in wheat (Zhang et al., 2011; Zhang et al., 2012), and Jablonski et al. (2021) located *TaCKX2* to TraesCS3D02G143300 (chr 3D, 105890418-105896361 bp). The nearest MTA for spike cytokinins and *TaCKX2* in the present study is for marker chr3D-125590342 associated with zeatin concentration, which is 19.7 Mbp away. Therefore, it does not appear any of the cytokinins measured in this GWAS were associated with previously identified cytokinin oxidase/dehydrogenase genes but instead are potentially new markers for genes regulating spike cytokinin levels.

While the MTAs discovered in this study are encouraging, they should be evaluated in the context of the major adaption genes already present in wheat breeding programs. Yields have been increased historically through major genes for adaptation that regulate flowering time, such as the vernalisation sensitivity (*Vrn*) and photoperiod sensitivity (*Ppd*) genes, and genes that regulate plant height such as the *Rht* dwarfing genes (Quarrie et al., 2006). Because these adaption traits have already been optimised in most breeding programs, often in genetic studies the highest P values for MTAs could be linked to pleiotropic effects of these major genes. However, in the case of the HiBAP II, no significant MTAs for plant height or flowering time were found. This may be because the HiBAP II was controlled for both flowering time and plant height in the selection of lines. There were however four significant markers identified for peduncle length (1B, 2D, 6B, 7D) and one putative marker on chr 4A for internode 3 length. *Rht8*, *Rht-B1 and Rht-D1* are located on chr 2D, 4B and 4D, respectively (Neumann et al., 2011). *Rht8* has yet to be mapped onto the IWGSC assembly, but it is possible that the marker for peduncle length on 2D could be linked. The lack of height or flowering time MTAs, and the lack of co-locating markers for internode 3 and peduncle length in the literature, suggests that the MTAs for the yield traits described in this study are novel rather than well-established markers.

5.4.2 Candidate genes

A candidate gene search for the zeatin riboside/IPA MTA on chromosome 1B indicated TRAESCS1B02G445400 was 0.25 Mbp away from the marker chr1B-665661232, which shows homology to (or aligns with) auxin efflux carrier gene *PIN3* in *Arabidopsis thaliana.* There are also two IPA MTAs on chromosome 1B which are +/-0.16 Mbp away from TRAESCS1B02G445400 (Table 5.2). Waldie and Leyser (2018) found that cytokinins can promote PIN3 protein accumulation, and this, in turn, increased auxin transport and shoot branching in *Arabidopsis*. A different study found that short term exogenous cytokinin application upregulated *PIN3* expression, but longer treatments downregulated *PIN3* in root tips of *Arabidopsis* (Ruzicka et al., 2009). They suggested cytokinin might control auxin levels in root meristem cells by modulating auxin transport. Another recent study showed cytokinin downregulated auxin, when Li et al. (2019a) added an exogenous synthetic cytokinin 6-BA in winter wheat, auxin content reduced and the number of fertile florets and number of grains increased. In addition to the proximity of TRAESCS1B02G445400 to the candidate gene in *Arabidopsis*, the neighbouring markers on 1B that are also associating with

TRAESCS1B02G445400, further support that these markers may be associated with the candidate *PIN3* gene. The proximity of multiple markers, along with the previous literature, suggests PIN proteins may be important in wheat for controlling the ratio between auxin and cytokinins, with a high cytokinin: auxin ratio reducing floret abortion.

Two other cytokinin biosynthesis candidate genes for the zeatin riboside MTA on chromosome 7B – TRAESCS7B02G491400 and TRAESCS7B02G491000 (0.17 Mbp and 0.4 Mbp away from the MTA, respectively) are regulated by the transcription factor *PHR1*, which is a phosphate uptake gene expressed with phosphate starvation. Overexpression of *PHR1* in wheat increased phosphate uptake and also improved yield through increasing grain number per spike (Wang et al., 2013). In barley, phosphate deficiency is reported to lead to a decrease in the level of cytokinins in roots, and an increase in root branching (Vysotskaya et al., 2020). Currently, the mechanism by which *PHR1* and spike cytokinin levels may be linked is unclear, but as decreased levels of phosphate lead to a decrease in the level of cytokinin, it can be speculated that cytokinins could act as negative mediators in the phosphate starvation response (Ha and Tran, 2014). Zeatin (the active form of zeatin riboside) at GS49 was positively correlated with grain yield in the field experiments (Table 3.6, chapter 3). In the literature, cytokinins are crucial in promoting cell division, growth and differentiation, as well as delaying leaf senescence, all of which contribute to increasing grain sink strength and/or post-anthesis photosynthetic capacity and therefore yield (Jameson and Song, 2016).

An MTA for a different spike plant hormone, abscisic acid, had a candidate gene 0.25 Mbp away from the marker chr6A-115016200 on chromosome 6A – TRAESCS6A02G140300, which is regulated by *Cruciferin C (CRC),* a gene in *Arabidopsis* that requires ABA for its induction (Suzuki et al., 2001; Kagaya et al., 2005). *CRC* is involved in the regulation of seed storage, and a study by Fujiki et al. (2013) found *CRC* mutant plants had more branching, more flowering and more fruits in *Arabidopsis*. In the HiBAP II in the field, ABA at GS49 was positively associated with fruiting efficiency, and negatively associated with spike DM and TGW (Table 3.6). As *CRC* has been indicated to be important in seed number in *Arabidopsis*, this is consistent with the effects seen in the HiBAP II with ABA associating positively with the grain number traits. While the indication that *CRC*, which requires ABA for its induction, may regulate this candidate gene linked to spike ABA level is interesting, more research is required to understand how TRAESCS6A02G140300 is involved in this process.

Turning to consider FE MTAs, a candidate gene *NF-YB1* was found 0.03 Mbp away from the marker chr1A-572361729 on chromosome 1A. In rice, *NF-YB1* plays an important role in regulating grain filling through regulating sucrose loading to the developing endosperm for starch biosynthesis (Bai et al., 2016). When NF-YB1 was knocked out or down-regulated in rice the grains produced were chalky and defective (Bai et al., 2016). For the sucrose loading effects to be influencing FE, however, they need to occur earlier than grain filling in the pre-anthesis phase when grain number is determined. Therefore, *NF-YB1* may be regulating sucrose loading during the rapid spike growth phase before anthesis, influencing fertile floret number and FE. These results highlight several promising candidate genes for key grain partitioning traits, and further study should be carried out in wheat to validate them in elite backgrounds and assess their suitability for introgression into new cultivars in breeding programmes.

5.4.3 Conclusions

The SNPs identified in this study are important because they are for grain sink strength traits, which are hard to measure in a high-throughput manner in the field, or, in the case of the spike hormones, sampling is also expensive. Being able to identify markers for marker-assisted selection is therefore very important. However, single markers do not inform about the whole genome sequence in the vicinity of the marker that will be linked with it, and so the breeder has to be mindful that even if the gene identified is beneficial for yield, nearby genes could have the opposite effect. Once this has been taken into account, the markers identified in this GWAS, and in particular the markers with promising candidate genes nearby, will be useful to breeders for marker development through the generation of KASP markers, with which to incorporate favourable alleles for the traits into breeding programs through a pyramid crossing scheme (Reynolds et al., 2017), accelerating gains in harvest index and yield potential.

Chapter 6: General Discussion

6.1 Addressing thesis hypotheses

1: Grain yield is correlated with harvest index, above-ground dry matter at maturity and grain number

In the field experiments, genetic variation in grain yield (GY) in the HiBAP II was strongly correlated with above-ground dry matter (DM) at physiological maturity ($AGDM_{PM}$) and slightly less strongly with harvest index (HI) and grain number (GN). However, there was a trade-off between $AGDM_{PM}$ and HI, so the potential of the genotypes which had the highest biomass was not fully exploited. In the glasshouse experiments, GY per plant (GY_P) was strongly associated with GN and AGDM at both physiological maturity and anthesis per plant, but not with HI. Harvest index was not as high in the glasshouse as the field, at a maximum of 0.46 in the glasshouse rather than 0.53 in the field; this is still significantly below the hypothetical limit of ca. 0.64 (Austin, 1980; Foulkes et al., 2011). The lack of association between GY and HI in the glasshouse may be due to the glasshouse results being on a plant scale rather than a population of plants, and the genotypes with more fertile tillers tending to have a lower harvest index but higher GY. Therefore, the hypothesis was confirmed in the field experiments, and partially confirmed in the glasshouse experiments.

2: Increasing grain number is associated with an increase in spike partitioning index (SPI) and fruiting efficiency (FE)

In the field, genetic variation in GN was not associated with spike partitioning index (SPI), which was not expected as previous work in the HiBAP I panel found a positive association between SPI and GN (Sierra-Gonzalez, 2020). However, a lack of association has been observed in other CIMMYT spring wheat germplasm (Rivera-Amado et al., 2019), and could be because of a trade-off between SPI and FE, i.e. more spike DM being allocated to the chaff components in larger spikes rather than developing florets. Unlike spike PI, as expected GN showed a positive association with FE in both the glasshouse and field experiments, indicating FE is an important trait in explaining GN. In the glasshouse, FE_{chaff} explained more of the phenotypic variation in GN per plant than FE_A, which may be again because in the glasshouse results are at the plant level, so assessment of FE_A required two separate plants in different areas of the glasshouse in order to estimate spike biomass and grain number, whereas for FE_{chaff}, chaff biomass and GN are measured on the same plant. It is still suggested that FE calculated at anthesis is a better measurement for field trials, but understandably the chaff weight gives a

more reliable glasshouse measurement. Overall, the hypothesis was confirmed for FE but not for SPI.

3: A trade-off is observed between spike partitioning index and fruiting efficiency

In the field, genetic variation in both SPI and spike DM_{A+7} was negatively associated with FE_{A+7}, as has been reported in previous literature, (Dreccer et al., 2009; Terrile et al., 2017; Sierra-Gonzalez, 2020), suggesting that reducing spike DM_{A+7} may be increasing FE. If reducing spike PI or spike DM_{A+7} increases FE, it may be that plants are unable to allocate enough resources from the rest of the spike to the florets. This may be partly the reason that an increase in grain number did not correlate with an increase in spike PI. Therefore, the hypothesis was supported.

4: Competition for assimilates is observed between spike growth and true-stem internodes 2 and 3 in a stronger way than for the peduncle

In disagreement with the hypothesis that true-stem internodes 2 and 3 would be competing with the spike the most, in the field spike PI was negatively associated with all leaf-sheath internode PIs, but no association was seen with true-stem internode PI. While this result was not consistent with Sierra-Gonzalez et al. (2020) in suggesting the leaf-sheath was the shoot component interacting most strongly with spike growth, the strongest association for the leaf sheaths was for internode 2 leaf sheath, which is suggesting the timing of the strongest competition with spike growth for internode 2 growth is consistent, but the plant organ was different. Therefore, the hypothesis was only partially supported.

5: Genetic variation in spike hormones, particularly cytokinins, is associated with grain number traits in the glasshouse and field

Previous studies have found high levels of cytokinins in the developing grains of cereals (Liu et al., 2013a), and reducing expression of CKX genes in wheat results in an increase in grain number (Li et al., 2018a; Jablonski et al., 2020). In the field, at GS49 isopentenyladenosine (IPA) and zeatin (Z) were positively associated with GY, while isopentenyladenine (2iP) was positively correlated with GN. Z and IPA might be expected also to correlate with GN, however this was not the case. As GY is a complex trait, it is possible in this instance another component of GY was being influenced by cytokinin levels. It is also important to note that in the field, GS49 hormone levels were measured on a subset of 10 lines in one year, therefore repeating this measurement is key to elucidating fully the effect of hormones in the

field. At GS65 in the field zeatin riboside (Zr), IPA and 2iP were all positively associated with FE_{chaff} and GN. Similarly in the glasshouse, Z at GS49 was positively correlated with MS GN and MS FE_{chaff}, while Zr at GS49 was positive with HI and at GS65 positive with FE_{chaff}. As GN is determined pre-anthesis, the cytokinins at GS49 may be expected to correlate with GN rather than GS65. However, the increase of cytokinins from GS49 to GS65 in this study, particularly in the glasshouse experiments, indicates that the positive association with GS65 levels of cytokinin may result from an earlier correlation occuring between GS49 and GS65. While cytokinins generally were associating with yield traits across both the glasshouse and field experiments, the exact cytokinins differed between the glasshouse and the field experiments. Therefore, the hypothesis was generally supported here, with associations between spike cytokinins and grain number traits in both field and glasshouse experiments, even if the exact cytokinins differed.

6: High abscisic acid hormone levels pre-anthesis have a negative association with spike fertility traits determined at anthesis

The overwhelming evidence would suggest that abscisic acid (ABA) has a negative effect on floret development during stem elongation and booting, and to maximise potential grain number in spikes, ABA concentration should be maintained at low levels (Emery et al., 1998; Wang et al., 2001; Liu et al., 2011). In the field experiment at GS49, ABA levels had a negative association with AGDM at both physiological maturity and anthesis + 7 days. This same association was not observed in the glasshouse, but ABA levels were on average lower in the glasshouse (38 ng/g FW) than in the field (71 ng/g FW). Since lower ABA levels have been suggested to maximise potential grain number (Wang et al., 2001), this may explain the lack of negative associations with spike traits in the glasshouse experiments. The hypothesis was partially supported by the present results.

7: A gradient is observed in hormonal concentrations throughout the spike and plant in the glasshouse at both anthesis and booting

In agreement with the hypothesis, for the cytokinins at GS49, there was a significant effect of plant organ position for 2iP, with levels that increased 4-fold from the peduncle to the spike and flag leaf. This would suggest at booting high levels of cytokinins are not required in the peduncle to promote fertile florets. At anthesis, Z was 4 fold higher in the spike than peduncle, and Zr was 2.8 fold higher, suggesting high levels of cytokinins are important in the spike. In disagreement with the hypothesis that there may be a gradient of cytokinin within the spike, there was no effect of spikelet position within the spike on hormones. Other hormones

also showed a gradient throughout the plant, with ABA being half as low in the peduncle than the other organs at both GS49 and GS65. So this hypothesis was supported with regard to the plant organs, but not for the gradient within the spike.

8: Marker-trait associations can be identified for spike hormonal traits and key grain partitioning traits

For the 26 traits analysed, 213 MTAs were identified with a $-\log_{10}$ P value of >4 (putative MTAs), while 46 were identified with a $-\log_{10}$ P value of >6 (significant MTAs). Some of these markers were close to MTAs identified in other GWAS, for example, three markers for yield on chromosomes 4A, 5B and 7B were identified in similar locations in both the HiBAP II and with a large CIMMYT spring bread wheat panel (Sehgal et al., 2020). Therefore, this hypothesis was supported.

9: Co-locating markers will be identified with fruiting efficiency and spike hormone traits

Despite FE and spike hormones positively correlating in the field experiments, there were no co-locating markers between these traits in the GWAS. There was, however, a co-locating marker on chromosome 2B for spike PI and HI, and another on chromosome 1B for two cytokinins IPA and Zr. Therefore, concerning FE, the hypothesis was not supported, but co-locating markers were identified for the spike hormone traits and other yield traits.

10: Candidate genes for key SNPs associating with grain partitioning traits and spike hormonal traits can be identified and confirmed in previous literature

A candidate gene *NF-YB1* was located near a SNP from a FE MTA on chromosome 1A. Three other candidate genes were identified for hormonal traits. A gene for Zr/IPA on chromosome 1B suggested *PIN3* in *Arabidopsis*, which is responsible for auxin transport and regulated by cytokinins, may be a good candidate. A SNP on chromosome 7B for Zr is regulated by transcription factor *PHR1,* which is responsible for phosphate uptake, and may lead to a decrease in the level of cytokinins (Vysotskaya et al., 2020). An ABA candidate gene on chromosome 6A is regulated by *Cruciferin C*, which in *Arabidopsis* requires ABA for its induction (Suzuki et al., 2001; Kagaya et al., 2005). Therefore, the hypothesis that candidate genes would be identified was supported.

6.2 Scaling glasshouse results to the field

In the glasshouse, the traits were studied at the individual plant level, whereas in the field they were studied at the crop level (a population of plants). Therefore, some traits which are measured at a population level in the field such as biomass per m^2 at anthesis often do not correlate well to the biomass of a single plant in the glasshouse (e.g. Figure 6.1a). However single shoot traits which are measured in both the glasshouse and field may scale between the two environments better. For example, FE_{chaff} or stem-internode 3 length (e.g. Figure 6.1b, c). On top of the differing scales, in the field environmental variation is typically greater than in the glasshouse, and therefore the genotype x environment (G x E) interaction in the field is expected to be greater. One of the benefits of performing a glasshouse experiment is therefore potentially a more precise estimation of the genetic variation with a more uniform environmental background. However, it is necessary to consider if the individual plant scale is representative of a field plot. One key difference is the tiller numbers per plant between the glasshouse and field experiments. Due to less shading and inter-shoot competition in the glasshouse, the HiBAP II genotypes produced between 6 to 9 tillers in the glasshouse, whereas in the field there was a maximum of two or three tillers per plant. The different systems also resulted in plant height being reduced in the glasshouse, with a genetic range of 60-80 cm in the glasshouse and 89-121 cm in the field. It also took longer for plants to reach anthesis in the field, with the range being 73-91 days in the field and just 51-60 days in the glasshouse. Some differences between the results in the glasshouse and field experiments may also be due to the high nitrogen supply to the plants in the field (400 kg N ha^{-1}), which is much higher than the standard supply of nitrogen that winter wheat receives in the UK.

The importance of conducting both glasshouse and field experiments was shown when Holmgren et al. (2012) conducted a meta-analysis of field and glasshouse studies to evaluate the effects of drought and irradiance levels on plants. This called for experiments conducted under both field and glasshouse conditions to fully compare how plants respond differently depending on the ecosystem and to investigate the underlying mechanisms. Looking at how traits compared between the main shoot in the glasshouse and populations of fertile shoots in field plots, both stem-internode 3 length and grain yield had a positive correlation amongst genotypes (R^2=0.80, P<0.001, Figure 6.1b and R^2=0.55, P=0.015, Figure 6.1f, respectively). However, other traits only showed a trend between the glasshouse and field values, for example, FE_{chaff} and GN (R^2=0.23 for both, ns, Figure 6.1c, e).

When comparing the spike cytokinin hormones sampled in the glasshouse and field, encouragingly there was a positive association amongst genotypes for several cytokinins such as 2iP and IPA at GS49 and Zr at anthesis. While not all hormones showed a positive association, this would be expected as hormones are very influenced by environmental conditions, which were not completely replicable between the glasshouse and field experiments. Cases where the spike hormone ranges were vastly different, such as Zr at GS49, could be because of the higher radiation intensity the plants received in the field than in the glasshouse. This is the first time to our knowledge that a dataset has compared the same wheat genotypes for spike hormone traits in the glasshouse and field, and it is encouraging to see several of the traits, including spike cytokinins, were scaling to the field level.

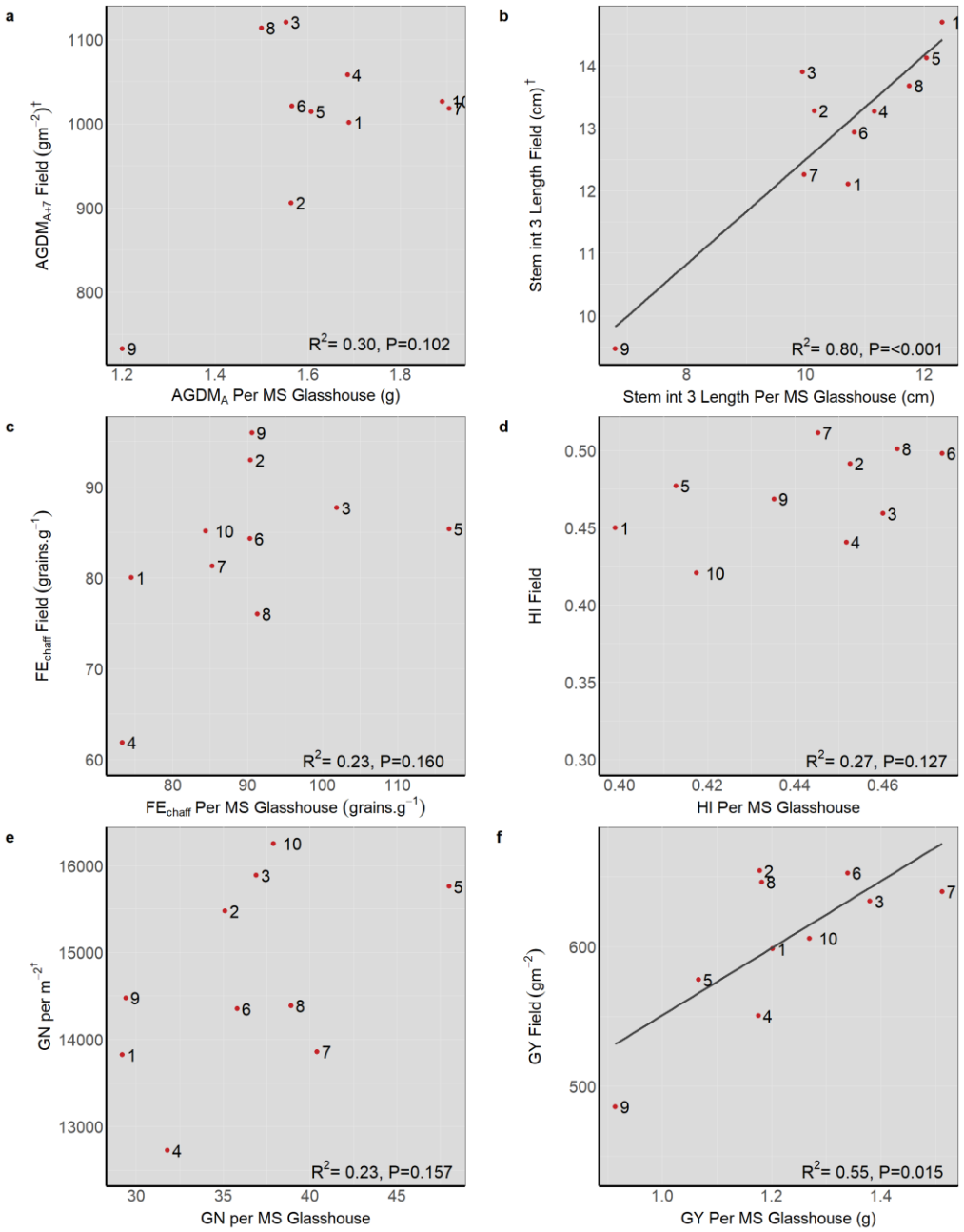

***Figure 6.1**: Linear regressions of yield-related traits among 10 HiBAP II genotypes in the glasshouse experiments for 3 years and field experiments for 2 years*

*Glasshouse: combined means for 2017, 2018, 2019, Field: combined means from 2017-18 and 2018-19, Numbered points are with each genotype, †: DTA added as a covariate if P<0.05, **MS**: main shoot **AGDM$_A$**: above-ground dry matter (DM) at anthesis, **AGDM$_{A+7}$**: above-ground DM at anthesis + 7 days, **int:** internode, **FE$_{chaff}$:** Fruiting efficiency calculated with chaff DM, **HI**: harvest index, **GN**: grain number, **GY**: grain yield, b) y=0.83x+4.1, f) y=240x+310*

6.3 An ideal wheat ideotype for maximising grain sink strength

From the results in this thesis, some key traits which could be suggested in combination could make an ideal wheat ideotype for increasing grain sink strength in high biomass backgrounds, and these are summarised in Table 6.1. The traits were selected to have mainly additive effects, so the spike partitioning index was not included as it has a trade-off with FE and did not positively correlate with GN. GN and HI are suggested as the top-level traits to increase grain yield, as increasing GN results in a stronger grain sink strength, in turn raising HI. GN is negatively associated with TGW, however, this trade-off is not complete, and previous studies have successfully increased both GN and TGW in bi-parental crosses in wheat (Bustos et al., 2013). The next traits which are suggested to be important for the ideal wheat ideotype are FE and spike zeatin riboside level at anthesis. Zeatin riboside is a cytokinin, and higher levels in the HiBAP II were associated most strongly with increased GN, possibly through promotion of cell division, growth and differentiation (Jameson and Song, 2016). Zeatin riboside levels were also positively associated with FE, which is an important trait for explaining grain number and how much spike DM at anthesis is converting to increasing grain number through improved intra-spike partitioning, so that assimilate is delivered to the developing florets rather than spike structural components (Garcia et al., 2014). Reducing the length of stem internode 2 leaf sheath is also suggested to be beneficial to grain sink strength by reallocating assimilates to the spike when it is competing for DM from booting to anthesis. However, in reality, reducing the leaf sheath without also reducing the true-stem may be difficult. Finally, increasing AGDM at anthesis would result in enhanced spike growth and more stem reserves being available for the grains to utilise post-anthesis. However, these reserves need to be able to remobilise to the grains during grain filling to match grain sink strength with additional post-anthesis source capacity in high biomass backgrounds, and should not be invested in areas of the plant which are not beneficial.

Table 6.1: *A ranking of the traits that make up the ideal wheat ideotype for increasing grain sink strength, including the genetic ranges from the HiBAP II field experiments, the suggested mechanism and any trade-offs with other traits*

GN*: grain number per m^2,* ***HI:*** *harvest index,* ***FE_{A+7}:*** *fruiting efficiency calculated with spike DM at anthesis + 7 days,* ***PI:*** *partitioning index,* ***LS:*** *leaf sheath,* ***$AGDM_{A+7}$****: above-ground dry matter (DM) at anthesis + 7 days,* ***$AGDM_{PM}$****: above-ground DM at physiological maturity,* ***GY:*** *grain yield,* ***SPI****: spike partitioning index,* ***TGW****: thousand-grain weight*

Rank	Trait	Field genetic range	Mechanism	Trade-off	References
1	GN	11389-17368 grains m^{-2}	Positively associated with GY, HI, $AGDM_{PM}$ and FE. Increases the grain sink strength through increasing the storage capacity of grains, but larger numbers of smaller grains may result in a trade-off with TGW.	TGW, $AGDM_{A+7}$	Fischer (1985) Slafer and Savin (1994)
2	HI	0.40-0.53	Positively associated with GN, GY and TGW Increasing DM partitioning to, and optimising partitioning within, the spikes is key to increase HI further.	$AGDM_{PM}$	Reynolds et al. (2012) Foulkes et al. (2011)
3	FE_{A+7}	36.0-76.8 grains g^{-1}	Positive association with GN, but no association with GY. The trade-off with SPI may be because plants an unable to allocate enough resources from the rest of the spike to the florets due to restrictions associated with vascular architecture.	TGW, SPI, $AGDM_{A+7}$	Slafer et al. (2015)
4	Zeatin riboside analyte level at GS65	58.5-141.4 ng/g FW	Positive associations in the HiBAP II with FE and GN. Cytokinins are involved with cell division, and previous literature has seen a correlation between cytokinin activity and GN, with a trade-off with TGW, possibly due to accelerated germination of grains resulting in more grains of a smaller size. It is acknowledged that discrepancies between the exact cytokinin have been noted in this study, and so further work to elucidate the best cytokinin at the correct stage is required.	TGW	Jameson and Song (2016) Jablonski et al. (2020)

Rank	Trait	Field genetic range	Mechanism	Trade-off	References
5	Internode 2 Leaf sheath PI	0.027-0.037	Reducing internode 2 leaf sheath PI may help reduce competition between the stem and the spike. In practice reducing LS without decreasing true-stem may be difficult, and leaf sheath may contribute to post-anthesis photosynthesis.	GY, HI, SPI and spike DM_{A+7}	Rivera-Amado et al. (2019) Sierra-Gonzalez et al. (2021)
6	$AGDM_{A+7}$	733-1177 g m^{-2}	$AGDM_{A+7}$ was positively associated with GY, TGW and $AGDM_{PM}$, most likely due to enhanced spike growth and greater accumulation of stem DM reserves available for remobilisation to the grains during grain filling.	GN and FE	Calderini et al. (2021)

6.4 Application of physiological traits in breeding

For a physiological trait to be deployed in plant breeding, it first must be heritable so the trait variation is predominantly due to genetic variation rather than environmental factors. In the HiBAP II, the majority of traits were highly heritable, such as HI, GY, and TGW (H^2=0.83, 0.93 and 0.83, respectively), while some were moderately heritable such as FE_{A+7} and AGDM at anthesis + 7 days ($AGDM_{A+7}$) (H^2= 0.582 and 0.501, respectively). If a trait is heritable, there needs to be a selection tool to deploy it in plant breeding, and this could be either high throughput phenotyping or a molecular marker. Most of the traits measured in the HiBAP II field experiments require destructive growth analysis at anthesis + 7 days and are relatively time-consuming, such as $AGDM_{A+7}$, but this is only feasible on a population containing ca.100-200 genotypes. The internode length traits are not a destructive measurement and there may be scope for developing imaging techniques, e.g. stereoscopy techniques, to process samples more rapidly for these traits, but currently, internode length could be phenotyped on shoots *in situ* on hundreds but not thousands of field plots. Measuring FE with the chaff DM rather than anthesis spike DM removes the requirement for a destructive sampling at anthesis, but it still requires increased processing at physiological maturity. For traits where high throughput phenotyping cannot be developed, such as the spike fertility traits and spike hormones, molecular markers need to be developed.

Ideally, molecular markers need to be within or very close to the gene to be the most useful for marker-assisted selection (MAS). In the case of the candidate genes discovered in the HiBAP II, most of the candidate genes are at least 0.1 Mbp away from the SNP. Therefore, before these could be deployed, further fine mapping of the target area would be required, potentially through developing a backcross population to identify a more precise marker or ideally clone the gene before developing a marker to deploy in breeding. Out of the candidate genes discussed in chapter 5, one of the most promising SNPs for plant breeding is the SNP chr1B-665661232 for spike zeatin riboside on chromosome 1B, which aligns with *PIN3* in *Arabidopsis* and is an auxin export protein controlled by cytokinin levels (Waldie and Leyser, 2018). A second promising SNP is chr1A-572361729, which has an MTA with FE and was 0.03 Mbp away from the candidate gene *NF-YB1*, which is important for regulating sucrose loading in rice (Bai et al., 2016).

The HiBAP II is comprised of genotypes from not only elite backgrounds, but also landrace and synthetic-derivative backgrounds. Breeding programs may have less genetic variation available within their elite germplasm, leading to limited variation

for traits such as FE, spike hormones or stem-internode lengths. Therefore, for these traits, breeders would need to screen wider germplasm using either high throughput phenotyping or marker screens. Relavant wider germplasm for screening could be the A.E. Watkins landrace collection (Wingen et al., 2014), with 700 landraces that cover origins from many Asian and European countries, and have been genotyped previously; the CIMMYT primary synthetics diversity panel (160 genotypes); and the CIMMYT bread wheat diversity panel (370 genotypes).

6.5 Conclusions

Of all the traits considered in the hypotheses, the most promising are FE and the spike hormones. FE has been previously identified as a priority target for increasing GN, and a positive association between FE and GN has been identified in Mediterranean bread wheat cultivars (Acreche et al., 2008), Mexican spring wheat cultivars (Rivera-Amado et al., 2019) and Argentinian spring wheat cultivars (Abbate et al., 1998). However, it is still a relatively new trait, and therefore there are limited studies to date which quantify genetic variation in FE. In recent years FE has been included in genome-wide association studies, and MTAs have been identified on chromosomes 1A, 2A, 2B, 2D, 3B, 4A, 4D, 5A, 5B, 6A, 6B and 7A (Guo et al., 2017; Basile et al., 2019; Gerard et al., 2019). From these studies, an MTA identified by Basile et al. (2019) on chromosome 2A was 13 Mbp away from a FE MTA identified in the HiBAP II. Despite the limited studies, there is therefore growing evidence that FE is an important trait for increasing grain yield, and genomic regions are being identified across the genome which are associated with it.

In the HiBAP II, internode 2 leaf sheath PI showed the strongest competition with the spike at anthesis and associations with grain yield and harvest index. Previous results in the CIMCOG and HiBAP I panels (Rivera-Amado et al., 2019; Sierra-Gonzalez, 2020), reported the true-stem, rather than the leaf sheath, was competing most strongly with the spike, and the inconsistency could be partly due to confounding effects in the variation of plant height in the HiBAP II, which had taller genotypes with more biomass at anthesis + 7 days. Therefore, further studies are required in a high biomass panel with uniform plant height to confirm the present findings.

The data presented on the spike hormonal levels in this thesis are very novel. To our knowledge, quantifying the genetic variation in spike hormonal levels across a panel in the field has not been performed before, and therefore the data of spike

hormonal levels across the HiBAP II panel in the field provides new insights on the role of spike cytokinins in regulating grain sink strength in wheat. The associations observed between the spike hormonal traits and key yield traits, such as cytokinins positively associating with FE and GN, were hypothesised due to earlier research. Previously, the exogenous effects of cytokinins have been studied, e.g. spraying cytokinin during stem elongation resulting in increased GN and GY (Zheng et al., 2016), or the endogenous effects studied through gene expression in transgenic wheat (Zhang et al., 2011). The candidate gene identified on chromosome 1B which aligns with *PIN3* in *Arabidopsis* is also the first suggestion of a candidate gene for *PIN3* being identified in wheat. Two further spike cytokinin IPA MTAs are also associating with the gene, and the known effect of cytokinins to promote PIN3 protein accumulation (Waldie and Leyser, 2018) supports that the markers identified in the genome-wide association study may be associated with the candidate gene *PIN3*.

6.6 Future work

The work in this thesis identified 46 MTAs over 10 traits with a significant $-\log_{10}$ P value of >6. We know the markers are associating with genetic variation within the HiBAP II, but what about different germplasm? To validate the markers across a range of germplasm, first, a KASP marker needs to be developed that can then be validated. This can occur through analysing the association of haplotypic variation for the SNPs with phenotypic expression of the trait, in either bi-parental populations or collections of wider germplasm, such as synthetic wheat and landraces. Priority candidate genes need to be validated, for example, through knocking out or over-expressing the gene, or by testing mutant alleles for the gene in a TILLING (Targeting Induced Local Lesions in Genomes) population and identifying the phenotype of the result. In terms of some of the higher-throughput traits such as stem-internode lengths, these need to be tested across wider germplasm and environments as mentioned above. CIMMYT plant their experiments on a raised-bed system, which tends to favour taller genotypes as they achieve earlier canopy closure in the gap between the beds (Fischer et al., 2005; Fischer et al., 2019). As large proportions of the wheat grown globally is in flat-basin systems, future work should also study the traits with the HiBAP II material in flat-basin systems.

This study has not focused specifically on cross-talk between spike hormones and was not an exhaustive study on all plant hormones. Further studies should identify if different ratios of the hormones reported in this study influence grain number

traits and also quantify the levels of other hormones, for example, by studying the levels of not only *trans*-zeatin but also *cis*-zeatin, which has been indicated to be important in early vegetative shoots and the roots (Gajdosova et al., 2011). We have identified a candidate gene for *PIN3*, indicative of the cross-talk between cytokinin and auxin, however, the effect of the ratio of cytokinin to auxin was not analysed in this study.

This study has indicated that levels of spike hormones such as the cytokinins impact traits differently depending on growth stage. Some of these associations, for example the correlation of cytokinin (Zr and IPA) in the field with grain number at GS65 but not at GS49, require sampling of a larger population and at more frequent timepoints to understand fully the interaction between the effects of the spike hormones on traits and growth stage.

Most of the studies on the effects of hormones on yield-related traits in wheat have quantified the effects of exogenous spraying of hormones. This study has identified several positive associations of grain number traits with spike hormones that have not been previously reported. For example, spike jasmonic acid level at GS49 in the glasshouse was positively associated with spike DM and fertile florets per spike. Previous literature has not reported the effects of jasmonic acid on yield potential, so future studies could investigate the effect of spraying hormones, such as jasmonic acid, on spikes and the resultant yield components. Finally, the effect of spike hormonal traits in other cereals which have yet to be quantified should be studied, and the candidate genes tested through syntenic approaches in these cereals in the future.

Supplementary material

***Table S 1**: List of genotypes in the HiBAP II field experiment*

Ent	GID	Cross names	Origin	Subset
1	7175970	CROC_1/AE.SQUARROSA (205)//BORL95/3/PRL/SARA//TSI/VEE#5/4/FRET2/5/CIRO16	Synthetic derivative	
2	7176779	CIRO16/3/TRCH/SRTU//KACHU	Elite	
3	7174709	CIRO16*2/4/WBLL1/KUKUNA//TACUPETO F2001/3/UP2338*2/VIVITSI	Elite	
4	7174342	TACUPETO F2001/BRAMBLING/5/NAC/TH.AC//3*PVN/3/MIRLO/BUC/4/2*PASTOR*2/6/WAXWING/SRTU//WAXWING/KIRITATI	Elite	
5	7178541	CROC_1/AE.SQUARROSA (205)//BORL95/3/PRL/SARA//TSI/VEE#5/4/FRET2/6/MTRWA92.161/PRINIA/5/SERI*3//RL6010/4*YR/3/PASTOR/4/BAV92	Synthetic derivative	
6	7171118	SAUAL/WHEAR//SAUAL/3/PBW343*2/KUKUNA*2//FRTL/PIFED	Elite	
7	7171238	UP2338*2/VIVITSI/3/FRET2/TUKURU//FRET2/4/MISR 1/5/TUKURU//BAV92/RAYON*2/3/PVN	Elite	
8	7174314	ROLF07/SAUAL//CIRO16/3/ROLF07/SAUAL	Elite	
9	7179800	KAUZ//ALTAR 84/AOS/3/MILAN/KAUZ/4/SAUAL/5/SERI.1B//KAUZ/HEVO/3/AMAD*2/4/KIRITATI/6/KACHU/SAUAL	Elite	1
10	7174351	TACUPETO F2001/BRAMBLING/5/NAC/TH.AC//3*PVN/3/MIRLO/BUC/4/2*PASTOR*2/6/WAXWING/SRTU//WAXWING/KIRITATI	Elite	
11	7047479	TACUPETO F2001/BRAMBLING/5/NAC/TH.AC//3*PVN/3/MIRLO/BUC/4/2*PASTOR*2/6/TRCH/SRTU//KACHU	Elite	1
12	7176624	KACHU/SAUAL/5/SERI.1B//KAUZ/HEVO/3/AMAD*2/4/KIRITATI	Elite	2 (added in Y2)
13	7174421	KACHU/SAUAL/4/VARIS/MISR 2/3/FRET2/KUKUNA//FRET2/5/KACHU/SAUAL	Elite	
14	7176644	KACHU/SAUAL//CIRO16	Elite	
15	7170962	BOKOTA/3/UP2338*2/KKTS*2//YANAC	Elite	
16	7694609	KACHU #1	Elite	
17	6341870	MUCUY	Elite	
18	7048518	MUTUS/DANPHE #1/4/C80.1/3*BATAVIA//2*WBLL1/3/C80.1/3*QT4522//2*PASTOR	Elite	

Ent	GID	Cross names	Origin	Subset
19	7047560	KACHU/SAUAL*2/3/TACUPETO F2001/BRAMBLING//KIRITATI	Elite	
20	7174396	KACHU/SAUAL*2/5/SERI.1B//KAUZ/HEVO/3/AMAD*2/4/KIRITATI	Elite	
21	7176616	KACHU/SAUAL/3/TACUPETO F2001/BRAMBLING//KIRITATI	Elite	
22	7176374	SW2148/2*ROLF07/3/HUW234+LR34/PRINIA*2//SNLG	Elite	
23	7174803	FRET2/KUKUNA//FRET2/3/PARUS/4/FRET2*2/SHAMA*2/5/WBLL1/KUKUNA//TACUPETO F2001/3/UP2338*2/VIVITSI	Elite	
24	7175977	BAJ #1//WAXWING/PIHA	Elite	
25	6175067	NADI #2	Elite	
26	7177745	PFAU/MILAN/5/CHEN/AEGILOPS SQUARROSA (TAUS)//BCN/3/VEE#7/BOW/4/PASTOR/6/CROC_1/AE.SQUARROSA (205)//BORL95/3/PRL/SARA//TSI/VEE#5/4/FRET2/7/CIRO16	Synthetic derivative	
27	7174399	KACHU/SAUAL*2/5/SERI.1B//KAUZ/HEVO/3/AMAD*2/4/KIRITATI	Elite	
28	7177888	HUHWA1/3/2*PRL/2*PASTOR//SUNSTATE	Elite	
29	7175856	HW2045/3/WAXWING/SRTU//WAXWING/KIRITATI/4/KINGBIRD #1//INQALAB 91*2/TUKURU	Elite	
30	7176852	FRET2/KUKUNA//FRET2/3/WHEAR/4/FRET2*2/KUKUNA/7/TUKURU//BAV92/RAYON/6/NG8201/KAUZ/4/SHA7//PRL/VEE#6/3/FASAN/5/MILAN/KAUZ	Elite	
31	7047304	TUKURU//BAV92/RAYON/6/NG8201/KAUZ/4/SHA7//PRL/VEE#6/3/FASAN/5/MILAN/KAUZ/7/SERI.1B//KAUZ/HEVO/3/AMAD*2/4/KIRITATI/8/ATTILA*2/PBW65*2//W485/HD29	Elite	1
32	7174107	WBLL1*2/4/YACO/PBW65/3/KAUZ*2/TRAP//KAUZ/5/KACHU #1/6/MARCHOUCH*4/SAADA/3/2*FRET2/KUKUNA//FRET2/7/WBLL1*2/4/YACO/PBW65/3/KAUZ*2/TRAP//KAUZ/5/KACHU #1	Elite	
33	7177702	KACHU/PAURAQ//PAURAQUE #1	Elite	
34	7044583	CHIR3/4/SIREN//ALTAR 84/AE.SQUARROSA (205)/3/3*BUC/5/PFAU/WEAVER/8/BOW/VEE/5/ND/VG9144//KAL/BB/3/YACO/4/CHIL/6/CASKOR/3/CROC_1/AE.SQUARROSA (224)//OPATA/7/PASTOR//MILAN/KAUZ/3/BAV92	Synthetic derivative	

Ent	GID	Cross names	Origin	Subset
35	7047125	WBLL1/KUKUNA//TACUPETO F2001/3/BAJ #1/4/CIRO16/5/WBLL1/KUKUNA//TACUPETO F2001/3/BAJ #1	Elite	
36	7176556	TUKURU//BAV92/RAYON/6/NG8201/KAUZ/4/SHA7//PRL/VEE#6/3/FASAN/5/MILAN/KAUZ/7/CIRO16	Elite	
37	7173465	KACHU/3/WHEAR//2*PRL/2*PASTOR/4/BOKOTA	Elite	1
38	7046872	MARCHOUCH*4/SAADA/3/2*FRET2/KUKUNA//FRET2/7/TUKURU//BAV92/RAYON/6/NG8201/KAUZ/4/SHA7//PRL/VEE#6/3/FASAN/5/MILAN/KAUZ/8/MARCHOUCH*4/SAADA/3/2*FRET2/KUKUNA//FRET2	Elite	
39	6683244	SHORTENED SR26 TRANSLOCATION//2*WBLL1*2/KKTS/3/BECARD	Elite	
40	7174103	WBLL1*2/SHAMA//KACHU/3/PRL/6/SAUAL/4/CROC_1/AE.SQUARROSA (205)//KAUZ/3/ATTILA/5/SAUAL	Synthetic derivative	
41	7176611	KAUZ//ALTAR 84/AOS/3/MILAN/KAUZ/4/SAUAL/5/SERI.1B//KAUZ/HEVO/3/AMAD*2/4/KIRITATI	Elite	
42	7173767	TILHI/SOKOLL/4/2*ATTILA*2/PBW65//PIHA/3/ATTILA/2*PASTOR	Synthetic derivative	
43	7177692	KACHU*2/6/YAR/AE.SQUARROSA (783)/4/GOV/AZ//MUS/3/SARA/5/MYNA/VUL//JUN	Synthetic derivative	1
44	7174535	SAUAL/MUTUS*2//PICAFLOR #1	Elite	
45	7178542	CROC_1/AE.SQUARROSA (205)//BORL95/3/PRL/SARA//TSI/VEE#5/4/FRET2/6/MTRWA92.161/PRINIA/5/SERI*3//RL6010/4*YR/3/PASTOR/4/BAV92	Synthetic derivative	
46	7046204	COPIO/5/UP2338*2/SHAMA/3/MILAN/KAUZ//CHIL/CHUM18/4/UP2338*2/SHAMA	Elite	
47	7174519	SAUAL/MUTUS*2//CIRO16	Elite	
48	7046390	FRANCOLIN #1/3/PBW343*2/KUKUNA*2//YANAC/4/KINGBIRD #1//INQALAB 91*2/TUKURU	Elite	1
49	7173452	PRL/2*PASTOR//2*CIRO16	Elite	1
50	7178836	WBLL1/KUKUNA//TACUPETO F2001/3/PIHA/4/COPIO	Elite	
51	7178835	WBLL1/KUKUNA//TACUPETO F2001/3/PIHA/4/COPIO	Elite	
52	7179251	KRONSTAD F2004/3/TRCH/SRTU//KACHU/4/CIRO16	Elite	

Ent	GID	Cross names	Origin	Subset
53	7077229	KACHU/SAUAL/4/VARIS/MISR 2/3/FRET2/KUKUNA//FRET2/5/KACHU/SAUAL	Elite	
54	7178785	C80.1/3*BATAVIA//2*WBLL1/5/REH/HARE//2*BCN/3/CROC_1/AE.SQUARROSA (213)//PGO/4/HUITES/6/FRANCOLIN #1/BLOUK #1	Synthetic derivative	
55	7178872	SAAR//PBW343*2/KUKUNA/3/2*CIRO16	Elite	
56	7077414	NGL//2*WHEAR/SOKOLL	Synthetic derivative	
57	7178833	WBLL1/KUKUNA//TACUPETO F2001/3/PIHA/4/WAXWING/KIRITATI*2//YANAC	Elite	
58	7179238	KRONSTAD F2004/5/2*FRET2*2/SHAMA*2/4/BOW/URES//2*WEAVER/3/CROC_1/AE.SQUARROSA (213)//PGO	Synthetic derivative	
59	7077228	KACHU/SAUAL/4/VARIS/MISR 2/3/FRET2/KUKUNA//FRET2/5/KACHU/SAUAL	Elite	
60	7179177	SAAR//PBW343*2/KUKUNA*2/8/NG8201/KAUZ/4/SHA7//PRL/VEE#6/3/FASAN/5/MILAN/KAUZ/6/ACHYUTA/7/PBW343*2/KUKUNA	Elite	1
61	3855011	VOROBEY	Synthetic derivative	1
62	7178834	WBLL1/KUKUNA//TACUPETO F2001/3/PIHA/4/COPIO	Elite	
63	7179063	FRET2/KUKUNA//FRET2/3/TAM200/TUI/4/FRET2*2/SHAMA/5/WBLL1/KUKUNA//TACUPETO F2001/3/UP2338*2/VIVITSI	Elite	
64	7179153	KRONSTAD F2004/5/2*FRET2*2/SHAMA*2/4/BOW/URES//2*WEAVER/3/CROC_1/AE.SQUARROSA (213)//PGO	Synthetic derivative	
65	7178839	WBLL1/KUKUNA//TACUPETO F2001/3/PIHA/4/COPIO	Elite	
66	7179062	FRET2/KUKUNA//FRET2/3/TAM200/TUI/4/FRET2*2/SHAMA/5/WBLL1/KUKUNA//TACUPETO F2001/3/UP2338*2/VIVITSI	Elite	
67	7178937	VARIS/MISR 2/3/FRET2/KUKUNA//FRET2*2/7/TUKURU//BAV92/RAYON/6/NG8201/KAUZ/4/SHA7//PRL/VEE#6/3/FASAN/5/MILAN/KAUZ	Elite	
68	6937974	CHIBIA//PRLII/CM65531/3/MISR 2*2/4/HUW234+LR34/PRINIA//PBW343*2/KUKUNA/3/ROLF07	Elite	

Ent	GID	Cross names	Origin	Subset
69	6332122	CHIPAK	Elite	1
70	6922442	C80.1/3*QT4118//KAUZ/RAYON/3/2*TRCH/7/CMH79A.955/4/AGA/3/4*SN64/CNO67//INIA66/5/NAC/6/RIALTO	Elite-Introgression	
71	5397958	BRBT1*2/KIRITATI	Elite	
72	6179253	WBLL1*2/4/BABAX/LR42//BABAX/3/BABAX/LR42//BABAX	Elite	
73	7129702	BCN/WBLL1//PUB94.15.1.12/WBLL1	Landrace derivative	
74	5995532	WBLL1*2/SHAMA//KACHU #1	Elite	
75	6178005	TECUE #1/2*WAXWING	Elite	
76	5551750	CHEWINK #1	Elite	2
77	6676541	PASTOR//HXL7573/2*BAU/3/WBLL1	Elite	2
78	6692299	SOKOLL/3/PASTOR//HXL7573/2*BAU/4/PARUS/PASTOR	Synthetic derivative	
79	6692410	PAVLOVKA/V15.89C//NAVJ07/3/ROLF07	Elite	
80	6692292	SOKOLL/3/PASTOR//HXL7573/2*BAU/4/ATTILA/PASTOR	Synthetic derivative	
81	5429336	SOKOLL/WBLL1	Synthetic derivative	
82	5865657	CROC_1/AE.SQUARROSA (205)//BORL95/3/PRL/SARA//TSI/VEE#5/4/FRET2	Synthetic derivative	1
83	6056158	MEX94.2.19//SOKOLL/WBLL1	Synthetic+ Landrace derivative	
84	6056057	C80.1/3*QT4118//KAUZ/RAYON/3/2*TRCH	Elite	
85	6056049	WBLL1*2/KURUKU	Elite	
86	7025958	DPW 621-50	Elite	2
87	7034038	MEX94.27.1.20/3/SOKOLL//ATTILA/3*BCN/4/PUB94.15.1.12/WBLL1	Synthetic+ Landrace derivative	1
88	7129720	SOKOLL//PUB94.15.1.12/WBLL1	Synthetic+ Landrace derivative	
89	7129678	SERI/BAV92//PUB94.15.1.12/WBLL1	Landrace derivative	
90	7129674	SERI/BAV92//JANZ	Elite	
91	88517	OR791432/VEE#3.2	Elite	
92	3825355	SOKOLL	Synthetic derivative	2
93	3823821	PASTOR//HXL7573/2*BAU	Elite	
94	6692369	WBLL4//OAX93.24.35/WBLL1/5/CROC_1/AE.SQUARROSA (205)//BORL95/3/PRL/SARA//TSI/VEE#5/4/FRET2	Synthetic+ Landrace derivative	
95	6692380	PUB94.15.1.12/FRTL/5/CROC_1/AE.SQUARROSA (205)//BORL95/3/PRL/SARA//TSI/VEE#5/4/FRET2	Synthetic+ Landrace derivative	1

Ent	GID	Cross names	Origin	Subset
96	6171902	F2SR2-69//YANGLING SHAANXI/PASTOR	Elite	2
97	7129696	BCN/WBLL1//PUB94.15.1.12/WBLL1	Landrace derivative	
98	5343246	CROC_1/AE.SQUARROSA (205)//BORL95/3/PRL/SARA//TSI/VEE#5/4/FRET2	Synthetic derivative	
99	5429403	PASTOR//HXL7573/2*BAU/3/WBLL1	Elite	
100	4755013	KACHU	Elite	
101	6278810	D67.2/PARANA 66.270//AE.SQUARROSA (320)/3/CUNNINGHAM/4/VORB	Synthetic derivative	
102	6056139	SOKOLL/WBLL1	Synthetic derivative	
103	6489623	CMH79A.955/4/AGA/3/4*SN64/CNO67//INIA66/5/NAC/6/RIALTO/7/BCN/WBLL1/8/C80.1/3*QT4118//KAUZ/RAYON/3/2*TRCH	Elite-Introgression	
104	7135887	HE1/2*CNO79//BAV92/3/ROLF07	Elite	1
105	7410999	MEX94.27.1.20/3/SOKOLL//ATTILA/3*BCN/4/PUB94.15.1.12/WBLL1	Synthetic+ Landrace derivative	
106	6489912	C80.1/3*QT4118//KAUZ/RAYON/3/2*TRCH/7/CMH79A.955/4/AGA/3/4*SN64/CNO67//INIA66/5/NAC/6/RIALTO	Elite-Introgression	
107	6175024	TACUPETO F2001/BRAMBLING*2//KACHU	Elite	1
108	7806808	BORLAUG100 F2014	Elite	2
109	6176334	ROLF07*2/5/REH/HARE//2*BCN/3/CROC_1/AE.SQUARROSA (213)//PGO/4/HUITES	Synthetic derivative	
110	6682171	QUAIU*2/KINDE	Elite	
111	6569050	DANPHE #1*2/CHYAK	Elite	
112	6176368	KUTZ	Synthetic derivative	1
113	5390612	SUPER 152	Elite	
114	6415761	FRET2*2/BRAMBLING//BECARD/3/WBLL1*2/BRAMBLING	Elite	2
115	6415882	KIDEA	Elite	2
116	6176829	SAUAL/3/ACHTAR*3//KANZ/KS85-8-4/4/SAUAL	Elite	
117	4982242	JANZ	Elite	2
118	6062418	CMH79A.955/4/AGA/3/4*SN64/CNO67//INIA66/5/NAC	Elite-Introgression	
119	6489593	BCN/RIALTO//ROLF07	Elite	2
120	6000921	SOKOLL//PBW343*2/KUKUNA/3/ATTILA/PASTOR	Synthetic derivative	
121	7129751	CROC_1/AE.SQUARROSA (224)//OPATA/3/PUB94.15.1.12/WBLL1	Synthetic+ Landrace derivative	

Ent	GID	Cross names	Origin	Subset
122	7034028	MEX94.27.1.20/3/SOKOLL//ATTILA/3*BCN/4/PUB94.15.1.12/WBLL1	Synthetic+ Landrace derivative	
123	6177058	PANDORA//WBLL1*2/BRAMBLING	Elite	1
124	6056184	MEX94.2.19/PUB94.15.1.12	Landrace derivative	
125	6384747	VORB//PARUS/PASTOR	Elite	
126	7857856	SERI/BAV92//PUB94.15.1.12/WBLL1	Landrace derivative	
127	7857905	CROC_1/AE.SQUARROSA (205)//BORL95/3/PRL/SARA//TSI/VEE#5/4/FRET2/5/68.111/RGB-U//WARD/3/AE.SQUARROSA (501)	Synthetic derivative	
128	7857929	NAVJ07/3/GARZA/BOY//AE.SQUARROSA (1037)	Synthetic derivative	
129	7857956	WBLL1*2/KUKUNA/5/UP2338*2/SHAMA/3/MILAN/KAUZ//CHIL/CHUM18/4/UP2338*2/SHAMA	Elite	
130	7857960	QUAIU/5/UP2338*2/SHAMA/3/MILAN/KAUZ//CHIL/CHUM18/4/UP2338*2/SHAMA	Elite	2 (added in Y2)
131	6056064	PUB94.15.1.12/WBLL1	Landrace derivative	
132	7129763	C80.1/3*QT4118//KAUZ/RAYON/3/2*TRCH/4/BERKUT/KRICHAUFF	Elite-Introgression	
133	6056169	MEX94.27.1.20/3/SOKOLL//ATTILA/3*BCN	Synthetic+ Landrace derivative	
134	6062417	PUB94.15.1.12/WBLL1	Landrace derivative	
135	7705584	MEX94.27.1.20/3/SOKOLL//ATTILA/3*BCN/4/PUB94.15.1.12/WBLL1	Synthetic+ Landrace derivative	
136	6692326	SOKOLL/3/PASTOR//HXL7573/2*BAU/4/WBLL4//OAX93.24.35/WBLL1	Synthetic+ Landrace derivative	
137	6692395	SOKOLL/WBLL1/5/CROC_1/AE.SQUARROSA (205)//BORL95/3/PRL/SARA//TSI/VEE#5/4/FRET2	Synthetic derivative	
138	7178679	PASTOR//HXL7573/2*BAU/3/SOKOLL/WBLL1/5/CROC_1/AE.SQUARROSA (213)//PGO/3/CMH81.38/2*KAUZ/4/BERKUT/6/W15.92/4/PASTOR//HXL7573/2*BAU/3/WBLL1	Synthetic derivative	
139	6056166	WBLL4//OAX93.24.35/WBLL1	Landrace derivative	1
140	5995318	WBLL1/KUKUNA//TACUPETO F2001/3/BAJ #1	Elite	
141	6692364	WBLL4//OAX93.24.35/WBLL1/5/CROC_1/AE.SQUARROSA (205)//BORL95/3/PRL/SARA//TSI/VEE#5/4/FRET2	Synthetic+ Landrace derivative	

Ent	GID	Cross names	Origin	Subset
142	6680727	WBLL1*2/BRAMBLING/4/BABAX/LR42//BABAX*2/3/SHAMA	Elite	
143	6680863	TRCH*2//ND643/2*WBLL1	Elite	
144	6692366	WBLL4//OAX93.24.35/WBLL1/5/CROC_1/AE.SQUARROSA (205)//BORL95/3/PRL/SARA//TSI/VEE#5/4/FRET2	Synthetic+ Landrace derivative	
145	4097206	SERI*3//RL6010/4*YR/3/PASTOR/4/BAV92	Elite	
146	6691721	BAVIS/3/ATTILA/BAV92//PASTOR/5/CROC_1/AE.SQUARROSA (205)//BORL95/3/PRL/SARA//TSI/VEE#5/4/FRET2	Synthetic derivative	1
147	6692346	SOKOLL/3/PASTOR//HXL7573/2*BAU/5/CROC_1/AE.SQUARROSA (205)//BORL95/3/PRL/SARA//TSI/VEE#5/4/FRET2	Synthetic derivative	
148	7695396	QUAIU/5/UP2338*2/SHAMA/3/MILAN/KAUZ//CHIL/CHUM18/4/UP2338*2/SHAMA	Elite	1
149	7695154	CETA/AE.SQUARROSA (435)/7/2*CHWL86/6/FILIN/IRENA/5/CNDO/R143//ENTE/MEXI_2/3/AEGILOPS SQUARROSA (TAUS)/4/WEAVER	Synthetic derivative	
150	7695191	CETA/AE.SQUARROSA (435)//2*BECARD	Synthetic derivative	

Table S 2*: Fungicide, pesticide and insecticide applications in the field experiments in 2 years*

Date	Product	To Control	Rate
02/01/2018	Buctril	Herbicide	1 L/ha
02/01/2018	Starane	Herbicide	350 ml/ha
29/01/2018	Folicur	Fungicide	1 L/ha
09/02/2018	Lorsban	Insecticide	1 L/ha
01/03/2018	Folicur	Fungicide	1 L/ha
09/01/2019	Admire	Insecticide	1 L/ha
31/01/2019	Lorsban	Insecticide	1 L/ha
06/02/2019	Folicur	Fungicide	1/2 L/ha
13/03/2019	Folicur	Fungicide	1/2 L/ha
14/03/2019	Admire	Insecticide	1 L/ha
14/03/2019	Lorsban	Insecticide	1 L/ha

***Table S 3**: Irrigation dates for 2017-18 and 2018-19 in the field experiments*

Irrigation Dates	
Y1	**Y2**
07/12/2017	23/12/2018
04/01/2018	18/01/2019
01/02/2018	06/02/2019
03/03/2018	01/03/2019
	21/03/2019

***Table S 4:** Phenotypic ranges for 150 HiBAP II genotypes split into groups based on their origin at anthesis +7 days and physiological maturity in the field experiments*

*Combined means for 2017-18 and 2018-19, †: DTA added as a covariate if P<0.05, sig: significance, **DTA**: days from emergence to anthesis, **AGDM$_{A+7}$**: above-ground dry matter (DM) at anthesis + 7 days, **Stem PI**: stem partitioning index, **Spike PI**: spike partitioning index, **Lamina PI**: Lamina partitioning index, **Spike DM**: DM spike per unit area, **FE$_{A+7}$**: fruiting efficiency (calculated using spike DM at anthesis + 7 days), **DTM**: days from emergence to physiological maturity, **AGDM$_{PM}$**: above ground DM at physiological maturity, **GY**: grain yield, **TGW**: thousand-grain weight, **HI**: harvest index, **SM2**: spikes per meter squared, **GN**: grain number per m^2*

		Elite	Landrace	Synthetic	Synthetic + Landrace
Anthesis + 7 days (GS65+7d)	**DTA**	82	85	81	83
	AGDM$_{A+7}$ (g m^{-2})†	1027	1035	1052	1072
	Stem PI†	0.592	0.599	0.591	0.592
	Spike PI†	0.227	0.219	0.229	0.227
	Lamina PI†	0.182	0.182	0.180	0.181
	SpikeDM (g m^{-2})†	272	282	281	293
	FE$_{A+7}$ (grns g^{-1})†	56.5	52.0	53.7	46.1
Physiological Maturity (GS89)	**DTM†**	123	124	123	123
	AGDM$_{PM}$ (g m^{-2})	1331	1371	1362	1348
	GY (g m^{-2})	632	620	632	631
	TGW (g)†	43.2	44.1	44.5	48.6
	HI	0.48	0.45	0.47	0.47
	SM2 (spikesm^{-2})	276	269	287	254
	GN (grainsm^{-2})†	14689	14228	14274	13027

Table S 5: *Fungicide, pesticide and insecticide applications in the glasshouse experiments in all 3 years*

Date	Product	To Control	Rate
08/09/2017	Aphase	Aphids	0.5 g/L
08/09/2017	Amistar	Fungal pathogens	1 ml/L
27/09/2017	Talius	Powdery Mildew	0.25 L/ha
02/10/2017	Spruzit	Aphids	20 ml/L
10/10/2017	Spruzit	Aphids	20 ml/L
11/10/2017	Corbel	Powdery Mildew	0.75 L/ha
23/10/2017	Aphase	Aphids	0.5 g/L
03/11/2017	Folicure	Mildew	1 L/ha
17/11/2017	Chess WG	Aphids	0.6 g/L
11/12/2017	Aphese	Aphids	0.5 g/L
29/06/2018	Amistar Opti	Fungal Pathogens	2 L/ha
10/07/2018	Corbel	Powdery Mildew	1 L/ha
06/08/2018	Corbel	Powdery Mildew	1 L/ha
15/08/2018	Aphase	Aphids	0.5 g/L
03/09/2018	Folicure	Powdery Mildew	1 L/ha
14/09/2018	Aphox	Aphids	0.5 g/L
05/10/2018	Siltra	Powdery Mildew	0.1 ml/m^2
06/11/2018	Corbel	Powdery Mildew	1 L/ha
06/06/2019	Aphox	Aphids	0.5 g/L
06/06/2019	Corbel	Powdery Mildew	1 L/ha
21/06/2019	Aphox	Aphids	0.5 g/L
08/07/2019	Talius	Powdery Mildew	0.25 L/ha
07/08/2019	Chess WG	Aphids	0.6 g/L
07/08/2019	Silwet	Aphids	0.1 L/ha
21/08/2019	Apres	Powdery Mildew	0.3 L/ha

Table S 6*: Linear regressions of hormonal analyte levels plotting GS49 vs. GS65 for 10 HiBAP II genotypes in the glasshouse from cross-year analysis*

ABA*: abscisic acid,* ***GA1****: gibberellin 1,* ***IAA****: indole-3-acetic acid,* ***JA****: jasmonic acid,* ***SA****: salicylic acid,* ***Z****: zeatin,* ***Zr****: zeatin riboside,* ***IPA****: isopentenyladenosine,* ***2iP:*** *isopentenyladenine*

Hormone	R^2 value	P value
ABA	0.5539	0.014
GA1	0.00008	0.981
IAA	0.0043	0.858
JA	0.1406	0.286
SA	0.0069	0.819
Z	0.1565	0.258
Zr	0.0347	0.607
IPA	0.1975	0.198
2iP	0.0611	0.491

***Table S 7**: Significance (p-values) from 1-way ANOVA looking at the genotype significance for each hormone at different growth stages per year for 10 HiBAP II genotypes in the glasshouse*

***ABA**: abscisic acid, **GA1**: gibberellin 1, **IAA**: indole-3-acetic acid, **JA**: jasmonic acid, **SA**: salicylic acid, **Z**: zeatin, **Zr**: zeatin riboside, **IPA**: isopentenyladenosine, **2iP:** isopentenyladenine*

Growth Stage	Hormone	Genotype significance		
		2017	2018	2019
GS49	ABA	0.36	0.058	0.234
	GA1	<0.001	0.017	0.346
	IAA	0.309	<0.001	0.024
	JA	0.006	0.125	0.026
	SA	<0.001	0.014	0.088
	Z	<0.001	0.029	<0.001
	Zr	0.008	<0.001	0.269
	IPA	0.091	0.027	0.057
	2iP	0.06	0.481	0.134
GS65	ABA	0.654	0.127	0.003
	GA1	0.029	0.065	0.619
	IAA	<0.001	0.01	0.494
	JA	0.14	0.092	0.292
	SA	0.002	0.627	0.46
	Z	0.123	0.692	0.611
	Zr	0.249	0.082	0.454
	IPA	0.466	0.638	0.875
	2iP	0.002	0.06	0.082

***Table S 8:** Significance (p-values) from 2-way ANOVA in different spike positions (basal, central and apical) at anthesis (GS65) for 2 spring wheat HiBAP II genotypes in the glasshouse in 2019*

***Z**: zeatin, **Zr**: zeatin riboside, **IPA**: isopentenyladenosine, **ABA**: abscisic acid, **SA**: salicylic acid, **Pos:** position, **Gen:** genotype*

Hormone	Position in Spike Sig	Genotype Sig	Gen x Pos Sig
Z	0.427	0.006	0.673
Zr	0.545	0.265	0.795
IPA	0.788	0.625	0.122
ABA	0.385	0.627	0.405
SA	0.373	0.828	0.528

***Table S 9**: List of the marker-trait associations from the genome-wide association study of the HiBAP II panel of 146 lines at anthesis and maturity in the field*

§:0PCA added as a covariate, for all other traits 2PCA used, highlighted green SNPs are co-locating, -log$_{10}$ (P) values are highlighted red for values >6 and yellow for values >4

***Stem PI**: stem partitioning index, **Spike PI**: spike partitioning index, **Lamina PI**: Lamina partitioning index, **Ped L**: stem peduncle length, **Int3 L**: stem internode 3 length, **Spike DM**: DM spike per unit area, **FE$_{A+7}$**: fruiting efficiency (calculated using spike DM at anthesis + 7 days), **AGDM$_{PM}$**: above ground DM at physiological maturity, **GY**: grain yield, **TGW**: thousand-grain weight, **HI**: harvest index, **GN**: grain number per m^2, **ABA**: abscisic acid, **ACC**: 1-aminocyclopropane-1-carboxylic acid, **GA1**: gibberellin 1, **GA3**: gibberellin 3, **GA4**: gibberellin 4, **GA7**: gibberellin 7, **IAA**: indole-3-acetic acid, **JA**: jasmonic acid, **MEL**: melatonin, **SA**: salicylic acid, **IPA**: isopentenyladenosine, **2iP:** isopentenyladenine, **Z**: zeatin, **Zr**: zeatin riboside*

Trait	SNP	Chr	Position	maf	-log$_{10}$(p)
Stem PI	chr5B-516121264	5B	516121264	26.03 %	4.07
Stem PI	chr7A-64935128	7A	64935128	21.92 %	4.04
Spike PI	chr2B-26301024	2B	26301024	8.22 %	4.66
Lam PI	chr4A-284253489	4A	284253489	14.38 %	5.06
Lam PI	chr1B-86442204	1B	86442204	9.25 %	4.24
Lam PI	chr5B-485909727	5B	485909727	10.62 %	4.19
Lam PI	chr4A-429005550	4A	429005550	13.01 %	4.16
Lam PI	chr2B-666610577	2B	666610577	24.32 %	4.14
Lam PI	chr7B-8990691	7B	8990691	9.59 %	4.11
Lam PI	chr4A-216870231	4A	216870231	8.90 %	4.03
Ped L§	chr7D-580311382	7D	580311382	11.99 %	9.85
Ped L§	chr1B-688238491	1B	688238491	46.92 %	7.12
Ped L§	chr2D-601079519	2D	601079519	20.21 %	6.33
Ped L§	chr6B-638425611	6B	638425611	21.92 %	6.22
Ped L§	chr2A-603558683	2A	603558683	6.85 %	5.81
Ped L§	chr2A-2379434	2A	2379434	43.84 %	5.00
Ped L§	chr5A-414527012	5A	414527012	19.86 %	4.97
Ped L§	chr4A-575154453	4A	575154453	26.37 %	4.96
Ped L§	chr5A-514089000	5A	514089000	26.71 %	4.93
Ped L§	chr7A-709854489	7A	709854489	19.18 %	4.90
Ped L§	chr5A-502826214	5A	502826214	41.44 %	4.74
Ped L§	chr5A-519885350	5A	519885350	27.05 %	4.39
Ped L§	chr7A-717036573	7A	717036573	29.45 %	4.32
Ped L§	chr2B-200072196	2B	200072196	14.73 %	4.17
Ped L§	chr3A-730871846	3A	730871846	28.77 %	4.08
Ped L§	chr5A-517848164	5A	517848164	30.14 %	4.01
Int 3 L	chr4A-611603483	4A	611603483	47.26 %	4.02
Spike DM	chr1B-76957565	1B	76957565	8.22 %	4.25
Spike DM	chr4A-455921170	4A	455921170	9.25 %	4.15
Spike DM	chr4A-191102459	4A	191102459	7.53 %	4.08
FE$_{A+7}$§	chr1A-572361729	1A	572361729	47.95 %	11.01
FE$_{A+7}$§	chr2B-216790502	2B	216790502	27.05 %	10.99
FE$_{A+7}$§	chr7A-628237844	7A	628237844	19.86 %	8.58
FE$_{A+7}$§	chr4A-24979533	4A	24979533	45.55 %	6.88
FE$_{A+7}$§	chr7A-693598468	7A	693598468	32.19 %	6.57

Trait	SNP	Chr	Position	maf	-log10(p)
FE_{A+7}§	chr6A-611325994	6A	611325994	34.59 %	5.73
FE_{A+7}§	chr7A-36327651	7A	36327651	17.12 %	4.37
FE_{A+7}§	chr2A-195115685	2A	195115685	29.45 %	4.18
$AGDM_{PM}$§	chr6A-574118305	6A	574118305	13.36 %	4.14
GY	chr2B-395408807	2B	395408807	32.19 %	10.51
GY	chr2B-649628588	2B	649628588	36.64 %	9.22
GY	chr5B-599326707	5B	599326707	11.30 %	8.80
GY	chr5A-10904434	5A	10904434	37.67 %	7.25
GY	chr7B-559714023	7B	559714023	21.92 %	6.94
GY	chr3A-522497112	3A	522497112	16.78 %	6.84
GY	chr4A-712872970	4A	712872970	22.26 %	6.78
GY	chr3A-713132123	3A	713132123	11.30 %	6.73
GY	chr6B-519553363	6B	519553363	42.81 %	6.51
GY	chr1A-582411013	1A	582411013	7.19 %	4.71
GY	chr2A-7805419	2A	7805419	46.92 %	4.32
GY	chr1A-587488686	1A	587488686	11.99 %	4.16
TGW	chr2A-22572135	2A	22572135	46.58 %	10.56
TGW	chr4A-90708744	4A	90708744	12.67 %	9.71
TGW	chr2D-593803131	2D	593803131	39.38 %	6.77
TGW	chr2B-452277079	2B	452277079	37.33 %	6.48
TGW	chr5B-684433013	5B	684433013	29.11 %	6.01
TGW	chr7A-696449790	7A	696449790	29.79 %	5.99
TGW	chr3B-565381139	3B	565381139	21.92 %	5.71
TGW	chr2B-774945561	2B	774945561	26.03 %	5.05
TGW	chr5A-495105207	5A	495105207	48.29 %	5.05
TGW	chr3B-191023530	3B	191023530	9.93 %	5.01
TGW	chr3B-191188885	3B	191188885	9.93 %	4.85
TGW	chr3B-203564447	3B	203564447	9.25 %	4.78
TGW	chr3B-203157554	3B	203157554	9.59 %	4.61
TGW	chr3B-191139584	3B	191139584	9.59 %	4.61
TGW	chr3B-191158968	3B	191158968	9.59 %	4.61
TGW	chr3B-225951329	3B	225951329	10.27 %	4.46
TGW	chr3B-236185576	3B	236185576	8.56 %	4.38
TGW	chr3B-203146963	3B	203146963	9.93 %	4.38
TGW	chr3B-226481803	3B	226481803	9.59 %	4.33
TGW	chr3B-239620818	3B	239620818	10.62 %	4.32
TGW	chr5D-294228877	5D	294228877	43.49 %	4.31
TGW	chr3B-191093544	3B	191093544	15.07 %	4.25
TGW	chr3B-190883837	3B	190883837	10.27 %	4.19
TGW	chr3B-231343631	3B	231343631	10.27 %	4.19
TGW	chr3B-239407839	3B	239407839	16.10 %	4.17
TGW	chr3B-233303669	3B	233303669	8.56 %	4.17
TGW	chr3B-192417427	3B	192417427	8.56 %	4.17
TGW	chr3B-190913148	3B	190913148	9.93 %	4.14
TGW	chr3B-185728264	3B	185728264	8.56 %	4.13

Trait	SNP	Chr	Position	maf	-log10(p)
TGW	chr3B-187552090	3B	187552090	11.64 %	4.09
TGW	chr3B-228866584	3B	228866584	10.62 %	4.08
TGW	chr3B-229821128	3B	229821128	8.90 %	4.03
TGW	chr3B-230194481	3B	230194481	8.90 %	4.03
TGW	chr3B-244711656	3B	244711656	8.90 %	4.03
TGW	chr3B-224963042	3B	224963042	8.90 %	4.03
HI	chr2D-75260450	2D	75260450	30.82 %	10.58
HI	chr3A-308957350	3A	308957350	17.47 %	9.40
HI	chr6A-557934107	6A	557934107	13.70 %	7.40
HI	chr1B-666054434	1B	666054434	11.99 %	7.32
HI	chr2A-58910704	2A	58910704	44.86 %	6.63
HI	chr6A-7151446	6A	7151446	46.58 %	6.14
HI	chr6A-522305070	6A	522305070	28.42 %	5.73
HI	chr3B-692044049	3B	692044049	16.10 %	5.43
HI	chr7A-69218321	7A	69218321	18.49 %	5.32
HI	chr3B-13552475	3B	13552475	23.63 %	4.35
HI	chr4A-664494265	4A	664494265	39.04 %	4.35
HI	chr3B-77807857	3B	77807857	11.64 %	4.34
HI	chr4B-14178307	4B	14178307	49.32 %	4.22
HI	chr2B-26301024	2B	26301024	8.22 %	4.15
HI	chr4A-663677394	4A	663677394	39.38 %	4.03
GN§	chr3D-269187493	3D	269187493	25.34 %	17.57
GN§	chr6A-609389128	6A	609389128	13.70 %	13.42
GN§	chr3A-749494571	3A	749494571	29.11 %	9.46
GN§	chr2B-774945561	2B	774945561	26.03 %	8.63
GN§	chr7A-684701585	7A	684701585	14.73 %	7.10
GN§	chr3A-713132175	3A	713132175	14.73 %	6.86
GN§	chr2B-526106268	2B	526106268	28.77 %	6.06
GN§	chr1D-411572483	1D	411572483	19.52 %	5.17
ABA	chr6B-150809926	6B	150809926	18.15 %	9.49
ABA	chr6A-115016200	6A	115016200	16.78 %	7.11
ABA	chr2D-636527168	2D	636527168	15.41 %	5.62
ABA	chr5A-393302696	5A	393302696	32.88 %	5.41
ABA	chr1B-681226362	1B	681226362	35.96 %	5.10
ABA	chr7A-692619014	7A	692619014	29.79 %	4.55
ABA	chr6B-290708600	6B	290708600	19.86 %	4.32
ABA	chr4A-706497153	4A	706497153	30.82 %	4.17
ACC	chr5B-56566973	5B	56566973	45.20 %	4.17
GA1	chr5B-52610848	5B	52610848	15.73 %	6.51
GA1	chr5B-51747344	5B	51747344	15.03 %	5.62
GA1	chr5B-51485533	5B	51485533	21.68 %	5.33
GA1	chr2D-38629365	2D	38629365	21.33 %	5.24
GA1	chr5B-51856246	5B	51856246	15.73 %	5.12
GA1	chr6B-29407285	6B	29407285	7.69 %	5.10
GA1	chr5B-51496045	5B	51496045	19.23 %	4.94

Trait	SNP	Chr	Position	maf	-log$_{10}$(p)
GA1	chr7A-1280364	7A	1280364	8.04 %	4.87
GA1	chr2D-39425644	2D	39425644	21.33 %	4.77
GA1	chr5B-52630148	5B	52630148	20.28 %	4.67
GA1	chr5B-51833548	5B	51833548	16.78 %	4.62
GA1	chr7A-343784	7A	343784	7.69 %	4.60
GA1	chr3B-119398811	3B	119398811	33.22 %	4.56
GA1	chr7D-22380303	7D	22380303	23.78 %	4.54
GA1	chr7A-240763	7A	240763	7.69 %	4.50
GA1	chr5B-51413980	5B	51413980	16.08 %	4.41
GA1	chr5B-52335916	5B	52335916	23.08 %	4.39
GA1	chr5B-52319579	5B	52319579	19.58 %	4.28
GA1	chr5B-51270176	5B	51270176	17.13 %	4.26
GA1	chr7A-350234898	7A	350234898	42.66 %	4.21
GA1	chr1B-643043830	1B	643043830	17.83 %	4.15
GA1	chr5B-52462497	5B	52462497	20.28 %	4.10
GA1	chr5B-52291938	5B	52291938	24.13 %	4.08
GA1	chr5B-51553498	5B	51553498	17.13 %	4.07
GA1	chr5B-52717542	5B	52717542	20.28 %	4.02
GA3	chr5B-42282288	5B	42282288	19.86 %	5.27
GA3	chr5B-42154259	5B	42154259	40.41 %	5.10
GA3	chr5B-33190847	5B	33190847	21.58 %	5.07
GA3	chr5B-28155484	5B	28155484	22.95 %	4.56
GA3	chr5B-40897259	5B	40897259	31.16 %	4.54
GA3	chr5B-43436241	5B	43436241	36.64 %	4.46
GA3	chr5B-42369228	5B	42369228	41.10 %	4.43
GA3	chr5B-35174164	5B	35174164	24.32 %	4.34
GA3	chr5B-27257883	5B	27257883	25.00 %	4.29
GA3	chr5B-42093065	5B	42093065	36.30 %	4.26
GA3	chr5B-38164742	5B	38164742	32.19 %	4.21
GA3	chr5B-42872179	5B	42872179	34.59 %	4.16
GA3	chr5B-33045553	5B	33045553	24.32 %	4.15
GA3	chr5B-32644719	5B	32644719	25.34 %	4.09
GA4	chr5D-459322893	5D	459322893	15.07 %	4.84
GA4	chr2D-462364941	2D	462364941	6.16 %	4.66
GA4	chr6A-436385284	6A	436385284	27.40 %	4.14
GA4	chr2A-399497701	2A	399497701	12.33 %	4.01
GA7[§]	chr6D-29877405	6D	29877405	8.68 %	4.43
GA7[§]	chr1A-13006687	1A	13006687	16.32 %	4.13
IAA	chr5B-594869700	5B	594869700	15.07 %	5.60
IAA	chr5B-590072328	5B	590072328	20.21 %	4.86
IAA	chr5B-590808299	5B	590808299	21.23 %	4.66
IAA	chr5B-591070139	5B	591070139	21.58 %	4.63
IAA	chr5B-592865412	5B	592865412	23.29 %	4.31
IAA	chr5B-594651463	5B	594651463	23.97 %	4.31
IAA	chr5B-593300023	5B	593300023	22.26 %	4.30

Trait	SNP	Chr	Position	maf	-log10(p)
IAA	chr7D-90507457	7D	90507457	16.44 %	4.18
IAA	chr2D-627365322	2D	627365322	8.56 %	4.18
IAA	chr7A-138345215	7A	138345215	13.01 %	4.17
IAA	chr5B-590083539	5B	590083539	21.23 %	4.14
IAA	chr5B-592897497	5B	592897497	23.29 %	4.13
IAA	chr5B-593942449	5B	593942449	22.95 %	4.10
IAA	chr2B-730190118	2B	730190118	7.53 %	4.05
IAA	chr5B-595058534	5B	595058534	20.21 %	4.01
SA	chr2D-432763443	2D	432763443	6.51 %	5.47
SA	chr2D-400446413	2D	400446413	11.30 %	4.98
JA	chr5B-439719009	5B	439719009	34.35 %	5.35
JA	chr5B-438501904	5B	438501904	35.50 %	5.31
JA	chr5B-438895756	5B	438895756	33.97 %	5.26
JA	chr5B-438791913	5B	438791913	35.11 %	5.19
JA	chr5B-438462317	5B	438462317	35.50 %	5.00
JA	chr3B-778455882	3B	778455882	10.31 %	4.89
JA	chr5B-438683406	5B	438683406	33.21 %	4.86
JA	chr3D-595698020	3D	595698020	9.92 %	4.62
JA	chr5B-438803500	5B	438803500	31.68 %	4.46
JA	chr6B-693621344	6B	693621344	13.36 %	4.29
JA	chr5B-438911399	5B	438911399	41.60 %	4.28
JA	chr5B-436807472	5B	436807472	37.40 %	4.25
JA	chr5B-438221159	5B	438221159	35.11 %	4.24
JA	chr5B-438640991	5B	438640991	36.26 %	4.20
JA	chr7B-155926926	7B	155926926	15.27 %	4.12
MEL	chr4A-533001275	4A	533001275	6.51 %	4.42
MEL	chr6D-296535126	6D	296535126	42.47 %	4.41
MEL	chr1D-420657745	1D	420657745	9.59 %	4.23
MEL	chr3A-538847511	3A	538847511	5.48 %	4.12
MEL	chr1D-427373247	1D	427373247	8.22 %	4.10
MEL	chr1D-421001469	1D	421001469	9.59 %	4.01
MEL	chr1D-416622739	1D	416622739	8.56 %	4.01
IPA	chr1B-665661232	1B	665661232	13.70 %	5.06
IPA	chr3A-48906355	3A	48906355	15.07 %	5.02
IPA	chr3A-54978281	3A	54978281	22.26 %	4.98
IPA	chr1B-664787813	1B	664787813	12.33 %	4.91
IPA	chr3A-49273614	3A	49273614	16.10 %	4.88
IPA	chr3A-47830170	3A	47830170	17.81 %	4.71
IPA	chr3A-54667262	3A	54667262	15.41 %	4.57
IPA	chr3A-54311084	3A	54311084	17.81 %	4.56
IPA	chr3A-38409236	3A	38409236	21.23 %	4.54
IPA	chr3A-54218347	3A	54218347	20.21 %	4.51
IPA	chr3A-53301382	3A	53301382	17.12 %	4.51
IPA	chr3A-54444945	3A	54444945	21.92 %	4.48
IPA	chr3A-50547810	3A	50547810	15.75 %	4.48

Trait	SNP	Chr	Position	maf	-log$_{10}$(p)
IPA	chr3A-723497849	3A	723497849	11.64 %	4.47
IPA	chr3A-32864065	3A	32864065	25.00 %	4.47
IPA	chr3A-49329726	3A	49329726	19.52 %	4.42
IPA	chr3A-55344072	3A	55344072	21.92 %	4.39
IPA	chr3A-55254240	3A	55254240	19.52 %	4.34
IPA	chr1B-664801923	1B	664801923	11.64 %	4.32
IPA	chr1B-665553185	1B	665553185	8.22 %	4.29
IPA	chr3A-41117748	3A	41117748	13.01 %	4.28
IPA	chr1B-665244628	1B	665244628	7.88 %	4.27
IPA	chr3A-49314230	3A	49314230	16.44 %	4.26
IPA	chr3A-27007837	3A	27007837	23.29 %	4.22
IPA	chr1B-665792290	1B	665792290	21.23 %	4.20
IPA	chr3A-40918077	3A	40918077	15.41 %	4.19
IPA	chr7A-99099447	7A	99099447	30.48 %	4.12
IPA	chr1B-666060076	1B	666060076	17.12 %	4.10
IPA	chr7A-97870856	7A	97870856	27.40 %	4.05
IPA	chr3A-46844503	3A	46844503	15.41 %	4.02
IPA	chr3A-27272934	3A	27272934	25.34 %	4.01
IPA	chr3A-54533090	3A	54533090	14.38 %	4.01
2iP§	chr4A-170484102	4A	170484102	9.25 %	4.89
2iP§	chr7D-58643888	7D	58643888	41.44 %	4.39
2iP§	chr7D-58697197	7D	58697197	41.10 %	4.13
2iP§	chr4A-260446064	4A	260446064	7.88 %	4.06
2iP§	chr4A-465074235	4A	465074235	9.93 %	4.05
2iP§	chr4A-242663063	4A	242663063	10.96 %	4.04
Z§	chr3D-43783543	3D	43783543	18.15 %	11.27
Z§	chr6B-678826779	6B	678826779	34.93 %	9.39
Z§	chr4B-390849013	4B	390849013	17.12 %	7.53
Z§	chr3B-16944639	3B	16944639	18.84 %	5.81
Z§	chr4B-337001468	4B	337001468	17.12 %	5.53
Z§	chr4A-708326528	4A	708326528	41.44 %	5.41
Z§	chr2B-695217140	2B	695217140	41.44 %	5.38
Z§	chr2A-29273709	2A	29273709	9.59 %	4.38
Z§	chr3D-125590342	3D	125590342	21.23 %	4.28
Zr§	chr2B-28422029	2B	28422029	31.51 %	8.58
Zr§	chr7B-744404071	7B	744404071	29.45 %	8.03
Zr§	chr7A-244483443	7A	244483443	39.38 %	7.58
Zr§	chr1B-665661232	1B	665661232	13.70 %	6.23
Zr§	chr7A-266221561	7A	266221561	39.38 %	5.92
Zr§	chr2A-605306165	2A	605306165	11.64 %	5.50
Zr§	chr6B-678804399	6B	678804399	34.25 %	5.14
Zr§	chr2B-91776303	2B	91776303	32.53 %	4.52
Zr§	chr5A-679974451	5A	679974451	48.63 %	4.25
Zr§	chr7D-3415253	7D	3415253	12.33 %	4.00

References

Abbate, P.E., Andrade, F.H., Lazaro, L., Bariffi, J.H., Berardocco, H.G., Inza, V.H., Marturano, F., 1998. Grain yield increase in recent argentine wheat cultivars. Crop Science 38, 1203-1209.

Abbate, P.E., Pontaroli, A.C., Lazaro, L., Gutheim, F., 2013. A method of screening for spike fertility in wheat. Journal of Agricultural Science 151, 322-330.

Acevedo, E., Silva, P., Silva, H., 2002. Wheat growth and physiology. Available online: http://www.fao.org/3/Y4011E/y4011e06.htm [Accessed 23/08/2021].

Acreche, M.M., Briceno-Felix, G., Sanchez, J.A.M., Slafer, G.A., 2008. Physiological bases of genetic gains in Mediterranean bread wheat yield in Spain. European Journal of Agronomy 28, 162-170.

Acreche, M.M., Slafer, G.A., 2009. Grain weight, radiation interception and use efficiency as affected by sink-strength in Mediterranean wheats released from 1940 to 2005. Field Crops Research 110, 98-105.

AHDB, 2021. Wheat Growth Guide. Available online: https://ahdb.org.uk/knowledge-library/wheat-growth-guide [Accessed 23/08/2021].

Aisawi, K.A.B., Reynolds, M.P., Singh, R.P., Foulkes, M.J., 2015. The Physiological Basis of the Genetic Progress in Yield Potential of CIMMYT Spring Wheat Cultivars from 1966 to 2009. Crop Science 55, 1749-1764.

Albajes, R., Cantero-Martinez, C., Capell, T., Christou, P., Farre, A., Galceran, J., Lopez-Gatius, F., Marin, S., Martin-Belloso, O., Motilva, M.J., Nogareda, C., Peman, J., Puy, J., Recasens, J., Romagosa, I., Romero, M.P., Sanchis, V., Savin, R., Slafer, G., Soliva-Fortuny, R., Vinas, I., Voltas, J., 2013. Building bridges: an integrated strategy for sustainable food production throughout the value chain. Molecular Breeding 32, 743-770.

Ali, M.S., Baek, K.H., 2020. Jasmonic Acid Signaling Pathway in Response to Abiotic Stresses in Plants. International Journal of Molecular Sciences 21, 621.

Allen, A.M., Winfield, M.O., Burridge, A.J., Downie, R.C., Benbow, H.R., Barker, G.L.A., Wilkinson, P.A., Coghill, J., Waterfall, C., Davassi, A., Scopes, G., Pirani, A., Webster, T., Brew, F., Bloor, C., Griffiths, S., Bentley, A.R., Alda, M., Jack, P., Phillips, A.L., Edwards, K.J., 2017. Characterization of a Wheat Breeders' Array suitable for high-throughput SNP genotyping of global accessions of hexaploid bread wheat (*Triticum aestivum*). Plant Biotechnology Journal 15, 390-401.

Alonso, M.P., Vanzetti, L.S., Crescente, J.M., Mirabella, N.E., Panelo, J.S., Pontaroli, A.C., 2021. QTL mapping of spike fertility index in bread wheat. Crop Breeding and Applied Biotechnology 21.

Alonso-Blanco, C., Aarts, M.G.M., Bentsink, L., Keurentjes, J.J.B., Reymond, M., Vreugdenhil, D., Koornneef, M., 2009. What Has Natural Variation Taught Us about Plant Development, Physiology, and Adaptation? Plant Cell 21, 1877-1896.

Alqudah, A.M., Haile, J.K., Alomari, D.Z., Pozniak, C.J., Kobiljski, B., Borner, A., 2020a. Genome-wide and SNP network analyses reveal genetic control of spikelet sterility and yield-related traits in wheat. Scientific Reports 10.

Alqudah, A.M., Koppolu, R., Wolde, G.M., Graner, A., Schnurbusch, T., 2016. The Genetic Architecture of Barley Plant Stature. Frontiers in Genetics 7.

Alqudah, A.M., Sallam, A., Baenziger, P.S., Borner, A., 2020b. GWAS: Fast-forwarding gene identification and characterization in temperate Cereals: lessons from Barley - A review. Journal of Advanced Research 22, 119-135.

Alvarado, G., López, M., Vargas, M., Pacheco, Á., Rodríguez, F., Burgueño, J., Crossa, J., 2015. META-R (Multi Environment Trail Analysis with R for Windows) Version 6.04. CIMMYT Research Data & Software Repository Network, Available online: http://hdl.handle.net/11529/10201 [Accessed 17/06/2021].

Amalova, A., Abugalieva, S., Babkenov, A., Babkenova, S., Turuspekov, Y., 2021. Genome-wide association study of yield components in spring wheat collection harvested under two water regimes in Northern Kazakhstan. Peerj 9.

Araus, J.L., Tapia, L., 1987. Photosynthetic gas-exchange characteristics of wheat flag leaf blades and sheaths during grain filling - The case of a spring crop grown under Mediterranean climate conditions. Plant Physiology 85, 667-673.

Ashikari, M., Sakakibara, H., Lin, S.Y., Yamamoto, T., Takashi, T., Nishimura, A., Angeles, E.R., Qian, Q., Kitano, H., Matsuoka, M., 2005. Cytokinin oxidase regulates rice grain production. Science 309, 741-745.

Asseng, S., Kassie, B.T., Labra, M.H., Amador, C., Calderini, D.F., 2017. Simulating the impact of source-sink manipulations in wheat. Field Crops Research 202, 47-56.

Austin, R.B., 1980. Physiological limitations to cereal yields and ways of reducing them by breeding. Pitman Publishing, London, pp. 3-19.

Avalbaev, A.M., Somov, K.A., Yuldashev, R.A., Shakirova, F.M., 2012. Cytokinin oxidase is key enzyme of cytokinin degradation. Biochemistry-Moscow 77, 1354-1361.

Bai, A.N., Lu, X.D., Li, D.Q., Liu, J.X., Liu, C.M., 2016. NF-YB1-regulated expression of sucrose transporters in aleurone facilitates sugar loading to rice endosperm. Cell Research 26, 384-388.

Bancal, P., Soltani, F., 2002. Source–sink partitioning. Do we need Münch? Journal of Experimental Botany 53, 1919-1928.

Barazesh, S., McSteen, P., 2008. Hormonal control of grass inflorescence development. Trends in Plant Science 13, 656-662.

Basile, S.M.L., Ramirez, I.A., Crescente, J.M., Conde, M.B., Demichelis, M., Abbate, P., Rogers, W.J., Pontaroli, A.C., Helguera, M., Vanzetti, L.S., 2019. Haplotype block analysis of an Argentinean hexaploid wheat collection and GWAS for yield components and adaptation. Bmc Plant Biology 19.

Bassil, N.V., Mok, D.W.S., Mok, M.C., 1993. Partial-purification of a cis-trans-isomerase of zeatin from immature seed of Phaselous-vulgaris L. Plant Physiology 102, 867-872.

Benjamini, Y., Yekutieli, D., 2001. The control of the false discovery rate in multiple testing under dependency. Annals of Statistics 29, 1165-1188.

Berry, P.M., Spink, J.H., Foulkes, M.J., Wade, A., 2003. Quantifying the contributions and losses of dry matter from non-surviving shoots in four cultivars of winter wheat. Field Crops Research 80, 111-121.

Blum, A., Sinmena, B., Mayer, J., Golan, G., Shpiler, L., 1994. Stem reserve mobilization supports wheat-grain filling under heat-stress. Australian Journal of Plant Physiology 21, 771-781.

Borras, L., Slafer, G.A., Otegui, M.E., 2004. Seed dry weight response to source-sink manipulations in wheat, maize and soybean: a quantitative reappraisal. Field Crops Research 86, 131-146.

Braun, H.J., Atlin, G., Payne, T., 2010. Multi-location Testing as a Tool to Identify Plant Response to Global Climate Change. Climate Change and Crop Production 1, 115-138.

Brisson, N., Gate, P., Gouache, D., Charmet, G., Oury, F.-X., Huard, F., 2010. Why are wheat yields stagnating in Europe? A comprehensive data analysis for France. Field Crops Research 119, 201-212.

Brocklehurst, P.A., 1977. Factors controlling grain weight in wheat. Nature 266, 348-349.

Brooking, I.R., Kirby, E.J.M., 1981. Interrelationships between stem and ear development in winter-wheat - The effects of a Norin-10 dwarfing gene, GAI-RHT2. Journal of Agricultural Science 97, 373-381.

Bruinsma, J., 2009. The resource outlook to 2050: By how much do land, water and crop yields need to increase by 2050. In: Proc. FAO Expert Meeting on How to Feed the World in 2050, 24–26 June, 2009 Rome.

Bustos, D.V., Hasan, A.K., Reynolds, M.P., Calderini, D.F., 2013. Combining high grain number and weight through a DH-population to improve grain yield potential of wheat in high-yielding environments. Field Crops Research 145, 106-115.

Cai, T., Xu, H.C., Peng, D.L., Yin, Y.P., Yang, W.B., Ni, Y.L., Chen, X.G., Xu, C.L., Yang, D.Q., Cui, Z.Y., Wang, Z.L., 2014. Exogenous hormonal application improves grain yield of wheat by optimizing tiller productivity. Field Crops Research 155, 172-183.

Calderini, D.F., Castillo, F.M., Arenas-M, A., Molero, G., Reynolds, M.P., Craze, M., Bowden, S., Milner, M.J., Wallington, E.J., Dowle, A., Gomez, L.D., McQueen-Mason, S.J., 2021. Overcoming the trade-off between grain weight and number in wheat by the ectopic expression of expansin in developing seeds leads to increased yield potential. New Phytologist 230, 629-640.

Calderini, D.F., Savin, R., Abeledo, L.G., Reynolds, M.P., Slafer, G.A., 2001. The importance of the period immediately preceding anthesis for grain weight determination in wheat. Euphytica 119, 199-204.

Cao, W.X., Wang, Z.L., Dai, T.B., 2000. Changes in levels of endogenous plant hormones during floret development in wheat genotypes of different spike sizes. Acta Botanica Sinica 42, 1026-1032.

Carraro, N., Tisdale-Orr, T.E., Clouse, R.M., Knoller, A.S., Spicer, R., 2012. Diversification and expression of the PIN, AUX/LAX, and ABCB families of putative auxin transporters in Populus. Frontiers in Plant Science 3.

Cassman, K.G., Grassini, P., van Wart, J., 2010. Crop Yield Potential, Yield Trends, and Global Food Security in a Changing Climate. Handbook of Climate Change and Agroecosystems, pp. 37-51.

Chen, L., Zhao, J.Q., Song, J.C., Jameson, P.E., 2020. Cytokinin dehydrogenase: a genetic target for yield improvement in wheat. Plant Biotechnology Journal 18, 614-630.

Colombo, N., Favret, E.A., 1996. The effect of gibberellic acid on male fertility in bread wheat. Euphytica 91, 297-303.

Cortes, L.T., Zhang, Z.W., Yu, J.M., 2021. Status and prospects of genome-wide association studies in plants. Plant Genome 14.

Crespo-Herrera, L.A., Crossa, J., Huerta-Espino, J., Autrique, E., Mondal, S., Velu, G., Vargas, M., Braun, H.J., Singh, R.P., 2017. Genetic Yield Gains In CIMMYT's International Elite Spring Wheat Yield Trials By Modeling The Genotype x Environment Interaction. Crop Science 57, 789-801.

Crossa, J., Burgueno, J., Dreisigacker, S., Vargas, M., Herrera-Foessel, S.A., Lillemo, M., Singh, R.P., Trethowan, R., Warburton, M., Franco, J., Reynolds, M., Crouch, J.H., Ortiz, R., 2007. Association analysis of historical bread wheat germplasm using additive genetic covariance of relatives and population structure. Genetics 177, 1889-1913.

Crossett, A., Lauter, N., Love, T.M., 2010. An Empirical Method for Establishing Positional Confidence Intervals Tailored for Composite Interval Mapping of QTL. Plos One 5.

Cruz-Aguado, J.A., Reyes, F., Rodes, R., Peres, I., Dorado, M., 1999. Effect of source-to-sink ratio on partitioning of dry matter and C-14-photoassimilates in wheat during grain filling. Annals of Botany 83, 655-665.

Darussalam, Cole, M.A., Patrick, J.W., 1998. Auxin control of photoassimilate transport to and within developing grains of wheat. Australian Journal of Plant Physiology 25, 69-77.

Dathe, W., Ronsch, H., Preiss, A., Schade, W., Sembdner, G., Schreiber, K., 1981. Endogenous plant hormones of the broad bean, *Vicia-faba* L (-)-jasmonic acid, a plant growth inhibitor in pericarp. Planta 153, 530-535.

Dave, A., Hernandez, M.L., He, Z.S., Andriotis, V.M.E., Vaistij, F.E., Larson, T.R., Graham, I.A., 2011. 12-Oxo-Phytodienoic Acid Accumulation during Seed Development Represses Seed Germination in *Arabidopsis*. Plant Cell 23, 583-599.

Debruijn, S.M., Vreugdenhil, D., 1992. Abscisic-acid and assimilate partitioning to developing seeds. 1. Does abscisic-acid influence the growth-rate of pea-seeds. Journal of Plant Physiology 140, 201-206.

Dello Ioio, R., Nakamura, K., Moubayidin, L., Perilli, S., Taniguchi, M., Morita, M.T., Aoyama, T., Costantino, P., Sabatini, S., 2008. A Genetic Framework for the Control of Cell Division and Differentiation in the Root Meristem. Science 322, 1380-1384.

Distelfeld, A., Li, C., Dubcovsky, J., 2009. Regulation of flowering in temperate cereals. Current Opinion in Plant Biology 12, 178-184.

Dixon, L.E., Pasquariello, M., Boden, S.A., 2020. TEOSINTE BRANCHED1 regulates height and stem internode length in bread wheat. Journal of Experimental Botany 71, 4742-4750.

Dodig, D., Rancic, D., Radovic, B.V., Zoric, M., Savic, J., Kandic, V., Pecinar, I., Stanojevic, S., Seslija, A., Vassilev, D., Pekic-Quarrie, S., 2017. Response of wheat plants under post-anthesis stress induced by defoliation: II. Contribution of peduncle morpho-anatomical traits and carbon reserves to grain yield. Journal of Agricultural Science 155, 475-493.

Dong, T., Park, Y., Hwang, I., 2015. Abscisic acid: biosynthesis, inactivation, homoeostasis and signalling. Plant Hormone Signalling 58, 29-48.

Dreccer, M.F., van Herwaarden, A.F., Chapman, S.C., 2009. Grain number and grain weight in wheat lines contrasting for stem water soluble carbohydrate concentration. Field Crops Research 112, 43-54.

Dreccer, M.F., Wockner, K.B., Palta, J.A., McIntyre, C.L., Borgognone, M.G., Bourgault, M., Reynolds, M., Miralles, D.J., 2014. More fertile florets and grains per spike can be achieved at higher temperature in wheat lines with high spike biomass and sugar content at booting. Functional Plant Biology 41, 482-495.

Duan, J.Z., Wu, Y.P., Zhou, Y., Ren, X.X., Shao, Y.H., Feng, W., Zhu, Y.J., Wang, Y.H., Guo, T.C., 2018. Grain number responses to preanthesis dry matter and nitrogen in improving wheat yield in the Huang-Huai Plain. Scientific Reports 8.

Duggan, B.L., Richards, R.A., van Herwaarden, A.F., Fettell, N.A., 2005. Agronomic evaluation of a tiller inhibition gene (tin) in wheat. I. Effect on yield, yield components, and grain protein. Australian Journal of Agricultural Research 56, 169-178.

Earl, D.A., Vonholdt, B.M., 2012. STRUCTURE HARVESTER: a website and program for visualizing STRUCTURE output and implementing the Evanno method. Conservation Genetics Resources 4, 359-361.

Ehdaie, B., Alloush, G.A., Madore, M.A., Waines, J.G., 2006a. Genotypic variation for stem reserves and mobilization in wheat: I. postanthesis changes in internode dry matter. Crop Science 46, 735-746.

Ehdaie, B., Alloush, G.A., Madore, M.A., Waines, J.G., 2006b. Genotypic variation for stem reserves and mobilization in wheat: II. Postanthesis changes in internode water-soluble carbohydrates. Crop Science 46, 2093-2103.

Elia, M., Savin, R., Slafer, G.A., 2016. Fruiting efficiency in wheat: physiological aspects and genetic variation among modern cultivars. Field Crops Research 191, 83-90.

Emery, R.J.N., Longnecker, N.E., Atkins, C.A., 1998. Branch development in Lupinus angustifolius L. - II. Relationship with endogenous ABA, IAA and cytokinins in axillary and main stem buds. Journal of Experimental Botany 49, 555-562.

Evans, L.T., Fischer, R.A., 1999. Yield potential: Its definition, measurement, and significance. Crop Science 39, 1544-1551.

Evans, M.L., 1984. Functions of Hormones at the Cellular Level of Organization. In: Scott, T.K. (Ed.), Hormonal Regulation of Development II: The Functions of Hormones from the Level of the Cell to the Whole Plant. Springer Berlin Heidelberg, Berlin, Heidelberg, pp. 23-79.

Evers, J.B., Vos, J., Andrieu, B., Struik, P.C., 2006. Cessation of tillering in spring wheat in relation to light interception and red: Far-red ratio. Annals of Botany 97, 649-658.

FAO, 2017. The future of food and agriculture – Trends and challenges. Rome. Available online: http://www.fao.org/3/i6583e/i6583e.pdf [Accessed 23/08/2021].

FAO, 2019. World Food and Agriculture - Statistical pocketbook 2019. Rome. Available online: http://www.fao.org/3/ca6463en/ca6463en.pdf [Accessed 23/08/2021].

FAOSTAT, 2021. Crop and livestock products data. Rome. Available online: http://www.fao.org/faostat/en [Accessed 23/08/2021].

Feng, J., Shi, Y., Yang, S., Zuo, J., 2017. 3 - Cytokinins. In: Li, J., Li, C., Smith, S.M. (Eds.), Hormone Metabolism and Signaling in Plants. Academic Press, pp. 77-106.

Ferrante, A., Cartelle, J., Savin, R., Slafer, G.A., 2017. Yield determination, interplay between major components and yield stability in a traditional and a contemporary wheat across a wide range of environments. Field Crops Research 203, 114-127.

Ferrante, A., Savin, R., Slafer, G.A., 2012. Differences in yield physiology between modern, well adapted durum wheat cultivars grown under contrasting conditions. Field Crops Research 136, 52-64.

Ferrante, A., Savin, R., Slafer, G.A., 2013. Floret development and grain setting differences between modern durum wheats under contrasting nitrogen availability. Journal of Experimental Botany 64, 169-184.

Ferrante, A., Savin, R., Slafer, G.A., 2015. Relationship between fruiting efficiency and grain weight in durum wheat. Field Crops Research 177, 109-116.

Fischer, R.A., 1985. Number of Kernels in Wheat Crops and the Influence of Solar-radiation and Temperature. Journal of Agricultural Science 105, 447-461.

Fischer, R.A., 2011. Wheat physiology: a review of recent developments. Crop & Pasture Science 62, 95-114.

Fischer, R.A., Byerlee, D., Edmeades, G., 2014. Crop Yields and Global Food Security: Will Yield Increase Continue to Feed the World? 158, 1-634.

Fischer, R.A., Edmeades, G.O., 2010. Breeding and Cereal Yield Progress. Crop Science 50, S85-S98.

Fischer, R.A., Ramos, O.H.M., Monasterio, I.O., Sayre, K.D., 2019. Yield response to plant density, row spacing and raised beds in low latitude spring wheat with ample soil resources: An update. Field Crops Research 232, 95-105.

Fischer, R.A., Sayre, K., Ortiz Monasterio, I., 2005. The effect of raised bed planting on irrigated wheat yield as influenced by variety and row spacing. In: Roth, C.H., Fischer, R.A. & Meisner, C.A (Ed.), Evaluation and performance of permanent raised bed cropping systems in Asia, Australia and Mexico. ACIAR Proceedings No. 121., Griffith, Australia.

Fischer, R.A., Stockman, Y.M., 1980. Kernel number per spike in wheat (Triticum-aestivum L) - responses to preanthesis shading. Australian Journal of Plant Physiology 7, 169-180.

Flohr, B.M., Hunt, J.R., Kirkegaard, J.A., Evans, J.R., Swan, A., Rheinheimer, B., 2018. Genetic gains in NSW wheat cultivars from 1901 to 2014 as revealed from synchronous flowering during the optimum period. European Journal of Agronomy 98, 1-13.

Foulkes, M.J., Reynolds, M.P., 2015. Breeding challenge: improving yield potential. Crop Physiology: Applications for Genetic Improvement and Agronomy, 2nd Edition, 397-421.

Foulkes, M.J., Slafer, G.A., Davies, W.J., Berry, P.M., Sylvester-Bradley, R., Martre, P., Calderini, D.F., Griffiths, S., Reynolds, M.P., 2011. Raising yield potential of wheat. III. Optimizing partitioning to grain while maintaining lodging resistance. Journal of Experimental Botany 62, 469-486.

Frebort, I., Kowalska, M., Hluska, T., Frebortova, J., Galuszka, P., 2011. Evolution of cytokinin biosynthesis and degradation. Journal of Experimental Botany 62, 2431-2452.

Fujiki, Y., Kudo, K., Ono, H., Otsuru, M., Yamaoka, Y., Akita, M., Nishida, I., 2013. Genetic disruption of CRC 12S globulin increases seed oil content and seed yield in *Arabidopsis thaliana*. Plant Biotechnology 30, 327-333.

Gajdosova, S., Spichal, L., Kaminek, M., Hoyerova, K., Novak, O., Dobrev, P.I., Galuszka, P., Klima, P., Gaudinova, A., Zizkova, E., Hanus, J., Dancak, M., Travnicek, B., Pesek, B., Krupicka, M., Vankova, R., Strnad, M., Motyka, V., 2011. Distribution, biological activities, metabolism, and the conceivable function of *cis*-zeatin-type cytokinins in plants. Journal of Experimental Botany 62, 2827-2840.

Gaju, O., DeSilva, J., Carvalho, P., Hawkesford, M.J., Griffiths, S., Greenland, A., Foulkes, M.J., 2016. Leaf photosynthesis and associations with grain yield, biomass and nitrogen-use efficiency in landraces, synthetic-derived lines and cultivars in wheat. Field Crops Research 193, 1-15.

Gaju, O., Reynolds, M.P., Sparkes, D.L., Foulkes, M.J., 2009. Relationships between Large-Spike Phenotype, Grain Number, and Yield Potential in Spring Wheat. Crop Science 49, 961-973.

Gaju, O., Reynolds, M.P., Sparkes, D.L., Mayes, S., Ribas-Vargas, G., Crossa, J., Foulkes, M.J., 2014. Relationships between physiological traits, grain number and yield potential in a wheat DH population of large spike phenotype. Field Crops Research 164, 126-135.

Gale, M.D., Marshall, G.A., 1973. Insensitivity to gibberellin in dwarf wheats Annals of Botany 37, 729-735.

Gale, M.D., Youssefian, S., Russell, G.E., 1985. Chapter 1 - Dwarfing genes in wheat. In: Russell, G.E. (Ed.), Progress in plant breeding. Butterworth-Heinemann, pp. 1-35.

Gallavotti, A., Yang, Y., Schmidt, R.J., Jackson, D., 2008. The relationship between auxin transport and maize branching. Plant Physiology 147, 1913-1923.

Gao, F., Ayele, B.T., 2014. Functional genomics of seed dormancy in wheat: advances and prospects. Frontiers in Plant Science 5.

Garcia, G.A., Serrago, R.A., Gonzalez, F.G., Slafer, G.A., Reynolds, M.P., Miralles, D.J., 2014. Wheat grain number: Identification of favourable physiological traits in an elite doubled-haploid population. Field Crops Research 168, 126-134.

Gardiner, L.J., Joynson, R., Omony, J., Rusholme-Pilcher, R., Olohan, L., Lang, D., Bai, C.H., Hawkesford, M., Salt, D., Spannagl, M., Mayer, K.F.X., Kenny, J., Bevan, M., Hall, N., Hall, A., 2018. Hidden variation in polyploid wheat drives local adaptation. Genome Research 28, 1319-1332.

Gebbing, T., 2003. The enclosed and exposed part of the peduncle of wheat (*Triticum aestivum*) - spatial separation of fructan storage. New Phytologist 159, 245-252.

Geng, J., Li, L.Q., Lv, Q., Zhao, Y., Liu, Y., Zhang, L., Li, X.J., 2017. TaGW2-6A allelic variation contributes to grain size possibly by regulating the expression of cytokinins and starch-related genes in wheat. Planta 246, 1153-1163.

Gerard, G.S., Alqudah, A., Lohwasser, U., Borner, A., Simon, M.R., 2019. Uncovering the Genetic Architecture of Fruiting Efficiency in Bread Wheat: A Viable Alternative to Increase Yield Potential. Crop Science 59, 1853-1869.

Gerard, G.S., Crespo-Herrera, L.A., Crossa, J., Mondal, S., Velu, G., Juliana, P., Huerta-Espino, J., Vargas, M., Rhandawa, M.S., Bhavani, S., Braun, H., Singh, R.P., 2020. Grain yield genetic gains and changes in physiological related traits for CIMMYT's High Rainfall Wheat Screening Nursery tested across international environments. Field Crops Research 249.

Gonzalez, F.G., Miralles, D.J., Slafer, G.A., 2011. Wheat floret survival as related to pre-anthesis spike growth. Journal of Experimental Botany 62, 4889-4901.

Gonzalez, F.G., Slafer, G.A., Miralles, D.J., 2003a. Floret development and spike growth as affected by photoperiod during stem elongation in wheat. Field Crops Research 81, 29-38.

Gonzalez, F.G., Slafer, G.A., Miralles, D.J., 2003b. Grain and floret number in response to photoperiod during stem elongation in fully and slightly vernalized wheats. Field Crops Research 81, 17-27.

Gonzalez-Navarro, O.E., Griffiths, S., Molero, G., Reynolds, M.P., Slafer, G.A., 2016. Variation in developmental patterns among elite wheat lines and relationships with yield, yield components and spike fertility. Field Crops Research 196, 294-304.

Guan, P.F., Lu, L.H., Jia, L.J., Kabir, M.R., Zhang, J.B., Lan, T.Y., Zhao, Y., Xin, M.M., Hu, Z.R., Yao, Y.Y., Ni, Z.F., Sun, Q.X., Peng, H.R., 2018. Global QTL Analysis Identifies Genomic Regions on Chromosomes 4A and 4B Harboring Stable Loci for Yield-Related Traits Across Different Environments in Wheat (*Triticum aestivum* L.). Frontiers in Plant Science 9.

Guo, Z.F., Chen, D.J., Alqudah, A.M., Roder, M.S., Ganal, M.W., Schnurbusch, T., 2017. Genome-wide association analyses of 54 traits identified multiple loci for the determination of floret fertility in wheat. New Phytologist 214, 257-270.

Guo, Z.F., Chen, D.J., Schnurbusch, T., 2018a. Plant and Floret Growth at Distinct Developmental Stages During the Stem Elongation Phase in Wheat. Frontiers in Plant Science 9.

Guo, Z.F., Liu, G.Z., Roder, M.S., Reif, J.C., Ganal, M.W., Schnurbusch, T., 2018b. Genome-wide association analyses of plant growth traits during the stem elongation phase in wheat. Plant Biotechnology Journal 16, 2042-2052.

Ha, S., Tran, L.S., 2014. Understanding plant responses to phosphorus starvation for improvement of plant tolerance to phosphorus deficiency by biotechnological approaches. Critical Reviews in Biotechnology 34, 16-30.

Haas, M., Schreiber, M., Mascher, M., 2019. Domestication and crop evolution of wheat and barley: Genes, genomics, and future directions. Journal of Integrative Plant Biology 61, 204-225.

Hanif, M., Langer, R.H.M., 1972. The Vascular System of the Spikelet in Wheat (*Triticum aestivum*). Annals of Botany 36, 721-727.

Harrison, C.J., 2017. Auxin transport in the evolution of branching forms. New Phytologist 215, 545-551.

Hassani-Pak, K., Singh, A., Brandizi, M., Hearnshaw, J., Parsons, J.D., Amberkar, S., Phillips, A.L., Doonan, J.H., Rawlings, C., KnetMiner: a comprehensive approach for supporting evidence-based gene discovery and complex trait analysis across species. Plant Biotechnology Journal.

Hassani-Pak, K., Singh, A., Brandizi, M., Hearnshaw, J., Parsons, J.D., Amberkar, S., Phillips, A.L., Doonan, J.H., Rawlings, C., 2021. KnetMiner: a comprehensive approach for supporting evidence-based gene discovery and complex trait analysis across species. Plant Biotechnology Journal.

Hawkesford, M.J., Araus, J.L., Park, R., Calderini, D., Miralles, D., Shen, T.M., Zhang, J.P., Parry, M.A.J., 2013. Prospects of doubling global wheat yields. Food and Energy Security 2, 34-48.

Hedden, P., 2003. The genes of the Green Revolution. Trends in Genetics 19, 5-9.

Hedden, P., 2020. The Current Status of Research on Gibberellin Biosynthesis. Plant and Cell Physiology 61, 1832-1849.

Hedden, P., Sponsel, V., 2015. A Century of Gibberellin Research. Journal of Plant Growth Regulation 34, 740-760.

Hedden, P., Thomas, S.G., 2012. Gibberellin biosynthesis and its regulation. Biochemical Journal 444, 11-25.

Heffner, E.L., Lorenz, A.J., Jannink, J.L., Sorrells, M.E., 2010. Plant Breeding with Genomic Selection: Gain per Unit Time and Cost. Crop Science 50, 1681-1690.

Heffner, E.L., Sorrells, M.E., Jannink, J.L., 2009. Genomic Selection for Crop Improvement. Crop Science 49, 1-12.

Hess, J.R., Carman, J.G., Banowetz, G.M., 2002. Hormones in wheat kernels during embryony. Journal of Plant Physiology 159, 379-386.

Hirose, N., Takei, K., Kuroha, T., Kamada-Nobusada, T., Hayashi, H., Sakakibara, H., 2008. Regulation of cytokinin biosynthesis, compartmentalization and translocation. Journal of Experimental Botany 59, 75-83.

Hoffstetter, A., Cabrera, A., Sneller, C., 2016. Identifying Quantitative Trait Loci for Economic Traits in an Elite Soft Red Winter Wheat Population. Crop Science 56, 547-558.

Holmgren, M., Gomez-Aparicio, L., Quero, J.L., Valladares, F., 2012. Non-linear effects of drought under shade: reconciling physiological and ecological models in plant communities. Oecologia 169, 293-305.

Holubova, K., Hensel, G., Vojta, P., Tarkowski, P., Bergougnoux, V., Galuszka, P., 2018. Modification of Barley Plant Productivity Through Regulation of Cytokinin Content by Reverse-Genetics Approaches. Frontiers in Plant Science 9.

Huang, S., Cerny, R.E., Qi, Y.L., Bhat, D., Aydt, C.M., Hanson, D.D., Malloy, K.P., Ness, L.A., 2003. Transgenic studies on the involvement of cytokinin and gibberellin in male development. Plant Physiology 131, 1270-1282.

Huang, Y.Y., Yang, W.L., Pei, Z., Guo, X.L., Liu, D.C., Sun, J.Z., Zhang, A.M., 2012. The genes for gibberellin biosynthesis in wheat. Functional & Integrative Genomics 12, 199-206.

Hunter, J.D., 2007. Matplotlib: A 2D graphics environment. Computing in Science & Engineering 9, 90-95.

Imriz, G., 2020. The action of methyl jasmonate on the growth of Fusarium culmorum causing organism of foot and root rot disease in wheat. Fresenius Environmental Bulletin 29, 11017-11023.

IWGSC, Appels, R., Eversole, K., Stein, N., Feuillet, C., Keller, B., Rogers, J., Pozniak, C.J., Choulet, F., Distelfeld, A., Poland, J., Ronen, G., Sharpe, A.G., Barad, O., Baruch, K., Keeble-Gagnère, G., Mascher, M., Ben-Zvi, G., Josselin, A.-A., Himmelbach, A., Balfourier, F., Gutierrez-Gonzalez, J., Hayden, M., Koh, C., Muehlbauer, G., Pasam, R.K., Paux, E., Rigault, P., Tibbits, J., Tiwari, V., Spannagl, M., Lang, D., Gundlach, H., Haberer, G., Mayer, K.F.X., Ormanbekova, D., Prade, V., Šimková, H., Wicker, T., Swarbreck, D., Rimbert, H., Felder, M., Guilhot, N., Kaithakottil, G., Keilwagen, J., Leroy, P., Lux, T., Twardziok, S., Venturini, L., Juhász, A., Abrouk, M., Fischer, I., Uauy, C., Borrill, P., Ramirez-Gonzalez, R.H., Arnaud, D., Chalabi, S., Chalhoub, B., Cory, A., Datla, R., Davey,

M.W., Jacobs, J., Robinson, S.J., Steuernagel, B., van Ex, F., Wulff, B.B.H., Benhamed, M., Bendahmane, A., Concia, L., Latrasse, D., Bartoš, J., Bellec, A., Berges, H., Doležel, J., Frenkel, Z., Gill, B., Korol, A., Letellier, T., Olsen, O.-A., Singh, K., Valárik, M., van der Vossen, E., Vautrin, S., Weining, S., Fahima, T., Glikson, V., Raats, D., Číhalíková, J., Toegelová, H., Vrána, J., Sourdille, P., Darrier, B., Barabaschi, D., Cattivelli, L., Hernandez, P., Galvez, S., Budak, H., Jones, J.D.G., Witek, K., Yu, G., Small, I., Melonek, J., Zhou, R., Belova, T., Kanyuka, K., King, R., Nilsen, K., Walkowiak, S., Cuthbert, R., Knox, R., Wiebe, K., Xiang, D., Rohde, A., Golds, T., Čížková, J., Akpinar, B.A., Biyiklioglu, S., Gao, L., N'Daiye, A., Kubaláková, M., Šafář, J., Alfama, F., Adam-Blondon, A.-F., Flores, R., Guerche, C., Loaec, M., Quesneville, H., Condie, J., Ens, J., Maclachlan, R., Tan, Y., Alberti, A., Aury, J.-M., Barbe, V., Couloux, A., Cruaud, C., Labadie, K., Mangenot, S., Wincker, P., Kaur, G., Luo, M., Sehgal, S., Chhuneja, P., Gupta, O.P., Jindal, S., Kaur, P., Malik, P., Sharma, P., Yadav, B., Singh, N.K., Khurana, J.P., Chaudhary, C., Khurana, P., Kumar, V., Mahato, A., Mathur, S., Sevanthi, A., Sharma, N., Tomar, R.S., Holušová, K., Plíhal, O., Clark, M.D., Heavens, D., Kettleborough, G., Wright, J., Balcárková, B., Hu, Y., Salina, E., Ravin, N., Skryabin, K., Beletsky, A., Kadnikov, V., Mardanov, A., Nesterov, M., Rakitin, A., Sergeeva, E., Handa, H., Kanamori, H., Katagiri, S., Kobayashi, F., Nasuda, S., Tanaka, T., Wu, J., Cattonaro, F., Jiumeng, M., Kugler, K., Pfeifer, M., Sandve, S., Xun, X., Zhan, B., Batley, J., Bayer, P.E., Edwards, D., Hayashi, S., Tulpová, Z., Visendi, P., Cui, L., Du, X., Feng, K., Nie, X., Tong, W., Wang, L., 2018. Shifting the limits in wheat research and breeding using a fully annotated reference genome. Science 361, eaar7191.

Jablonski, B., Ogonowska, H., Szala, K., Bajguz, A., Orczyk, W., Nadolska-Orczyk, A., 2020. Silencing of TaCKX1 Mediates Expression of Other TaCKX Genes to Increase Yield Parameters in Wheat. International Journal of Molecular Sciences 21.

Jablonski, B., Szala, K., Przyborowski, M., Bajguz, A., Chmur, M., Gasparis, S., Orczyk, W., Nadolska-Orczyk, A., 2021. TaCKX2.2 Genes Coordinate Expression of Other TaCKX Family Members, Regulate Phytohormone Content and Yield-Related Traits of Wheat. International Journal of Molecular Sciences 22.

Jacobsen, J.V., Barrero, J.M., Hughes, T., Julkowska, M., Taylor, J.M., Xu, Q., Gubler, F., 2013. Roles for blue light, jasmonate and nitric oxide in the regulation of dormancy and germination in wheat grain (*Triticum aestivum* L.). Planta 238, 121-138.

Jafarzadeh, J., Bonnett, D., Jannink, J.L., Akdemir, D., Dreisigacker, S., Sorrells, M.E., 2016. Breeding Value of Primary Synthetic Wheat Genotypes for Grain Yield. Plos One 11.

Jaiswal, V., Gahlaut, V., Mathur, S., Agarwal, P., Khandelwal, M.K., Khurana, J.P., Tyagi, A.K., Balyan, H.S., Gupta, P.K., 2015. Identification of Novel SNP in Promoter Sequence of TaGW2-6A Associated with Grain Weight and Other Agronomic Traits in Wheat (*Triticum aestivum* L.). Plos One 10.

Jameson, P.E., 2017. Cytokinins. In: Thomas, B., Murray, B.G., Murphy, D.J. (Eds.), Encyclopedia of Applied Plant Sciences (Second Edition). Academic Press, Oxford, pp. 391-402.

Jameson, P.E., McWha, J.A., Wright, G.J., 1982. Cytokinins and changes in their activity during the development of grains of wheat (Triticum-aestivum L.). Zeitschrift Fur Pflanzenphysiologie 106, 27-36.

Jameson, P.E., Song, J.C., 2016. Cytokinin: a key driver of seed yield. Journal of Experimental Botany 67, 593-606.

Jameson, P.E., Song, J.C., 2020. Will cytokinins underpin the second 'Green Revolution'? Journal of Experimental Botany 71, 6872-6875.

Janda, K., Hideg, E., Szalai, G., Kovacs, L., Janda, T., 2012. Salicylic acid may indirectly influence the photosynthetic electron transport. Journal of Plant Physiology 169, 971-978.

Jansen, R.C., 2007. Quantitative Trait Loci in Inbred Lines. Handbook of Statistical Genetics, pp. 587-622.

Javadipour, Z., Balouchi, H., Dehnavi, M.M., Yadavi, A., 2019. Roles of methyl jasmonate in improving growth and yield of two varieties of bread wheat (*Triticum aestivum*) under different irrigation regimes. Agricultural Water Management 222, 336-345.

Jones, R.J., Schreiber, B.M.N., 1997. Role and function of cytokinin oxidase in plants. Plant Growth Regulation 23, 123-134.

Joynson, R., Molero, G., Coombes, B., Gardiner, L.J., Rivera-Amado, C., Pinera-Chavez, F.J., Evans, J.R., Furbank, R.T., Reynolds, M.P., Hall, A., 2021. Uncovering candidate genes involved in photosynthetic capacity using unexplored genetic variation in Spring Wheat. Plant Biotechnology Journal 19.

Juliana, P., Singh, R.P., Braun, H.J., Huerta-Espino, J., Crespo-Herrera, L., Govindan, V., Mondal, S., Poland, J., Shrestha, S., 2020. Genomic Selection for Grain Yield in the CIMMYT Wheat Breeding Program-Status and Perspectives. Frontiers in Plant Science 11.

Kagaya, Y., Okuda, R., Ban, A., Toyoshima, R., Tsutsumida, K., Usui, H., Yamamoto, A., Hattori, T., 2005. Indirect ABA-dependent regulation of seed storage protein genes by FUSCA3 transcription factor in *Arabidopsis*. Plant and Cell Physiology 46, 300-311.

Kang, H.M., Zaitlen, N.A., Wade, C.M., Kirby, A., Heckerman, D., Daly, M.J., Eskin, E., 2008. Efficient control of population structure in model organism association mapping. Genetics 178, 1709-1723.

Kasahara, H., 2016. Current aspects of auxin biosynthesis in plants. Bioscience Biotechnology and Biochemistry 80, 34-42.

Kasembe, J.N.R., 1967. Phenotypic Restoration of Fertility in a Male-Sterile Mutant by Treatment with Gibberellic Acid. Nature 215, 668-&.

Kebrom, T.H., Spielmeyer, W., Finnegan, E.J., 2013. Grasses provide new insights into regulation of shoot branching. Trends in Plant Science 18, 41-48.

Kirby, E.J.M., Appleyard, M., 1984. Cereal development guide. National Agricultural Centre, Arable Unit, Kenilworth.

Knox, J.P., Wareing, P.F., 1984. Apical Dominance in Phaseolus vulgaris L. Journal of Experimental Botany 35, 239-244.

Koch, T., Bandemer, K., Boland, W., 1997. Biosynthesis of *cis*-jasmone: A pathway for the inactivation and the disposal of the plant stress hormone jasmonic acid to the gas phase? Helvetica Chimica Acta 80, 838-850.

Korasick, D.A., Enders, T.A., Strader, L.C., 2013. Auxin biosynthesis and storage forms. Journal of Experimental Botany 64, 2541-2555.

Kudo, T., Makita, N., Kojima, M., Tokunaga, H., Sakakibara, H., 2012. Cytokinin Activity of *cis*-Zeatin and Phenotypic Alterations Induced by Overexpression of Putative *cis*-Zeatin-O-glucosyltransferase in Rice. Plant Physiology 160, 319-331.

Kumar, J., Pratap, A., Solanki, R.K., Gupta, D.S., Goyal, A., Chaturvedi, S.K., Nadarajan, N., Kumar, S., 2012. Genomic resources for improving food legume crops. Journal of Agricultural Science 150, 289-318.

Larsson, E., Vivian-Smith, A., Offringa, R., Sundberg, E., 2017. Auxin Homeostasis in *Arabidopsis* Ovules Is Anther-Dependent at Maturation and Changes Dynamically upon Fertilization. Frontiers in Plant Science 8.

Lazaro, L., Abbate, P.E., 2012. Cultivar effects on relationship between grain number and photothermal quotient or spike dry weight in wheat. Journal of Agricultural Science 150, 442-459.

Lee, B.T., Martin, P., Bangerth, F., 1988. Phytohormone levels in the florets of a single wheat spikelet during pre-anthesis development and relationships to grain set. Journal of Experimental Botany 39, 927-933.

Lefevere, H., Bauters, L., Gheysen, G., 2020. Salicylic Acid Biosynthesis in Plants. Frontiers in Plant Science 11.

Leopold, A.C., Nooden, L.D., 1984. Hormonal Regulatory Systems in Plants In: Scott, T.K. (Ed.), Hormonal Regulation of Development II: The Functions of Hormones from the Level of the Cell to the Whole Plant. Springer Berlin, Heidelberg, pp. 4-17.

Li, S.N., Song, M., Duan, J.Z., Yang, J.H., Zhu, Y.J., Zhou, S.M., 2019a. Regulation of Spraying 6-BA in the Late Jointing Stage on the Fertile Floret Development and Grain Setting in Winter Wheat. Agronomy-Basel 9.

Li, T., Liu, H.W., Mai, C.Y., Yu, G.J., Li, H.L., Meng, L.Z., Jian, D.W., Yang, L., Zhou, Y., Zhang, H.J., Li, H.J., 2019b. Variation in allelic frequencies at loci associated with kernel weight and their effects on kernel weight-related traits in winter wheat. Crop Journal 7, 30-37.

Li, Y.L., Song, G.Q., Gao, J., Zhang, S.J., Zhang, R.Z., Li, W., Chen, M.L., Liu, M., Xia, X.C., Risacher, T., Li, G.Y., 2018a. Enhancement of grain number per spike by RNA interference of cytokinin oxidase 2 gene in bread wheat. Hereditas 155.

Li, Y.P., Fu, X., Zhao, M.C., Zhang, W., Li, B., An, D.G., Li, J.M., Zhang, A.M., Liu, R.Y., Liu, X.G., 2018b. A Genome-wide View of Transcriptome Dynamics During Early Spike Development in Bread Wheat. Scientific Reports 8.

Liu, J., Feng, B., Xu, Z.B., Fan, X.L., Jiang, F., Jin, X.F., Cao, J., Wang, F., Liu, Q., Yang, L., Wang, T., 2018. A genome-wide association study of wheat yield and quality-related traits in southwest China. Molecular Breeding 38.

Liu, X., Li, R., Chang, X., Jing, R., 2013a. Mapping QTLs for seedling root traits in a doubled haploid wheat population under different water regimes. Euphytica 189, 51-66.

Liu, X.L., Huang, M., Fan, B., Buckler, E.S., Zhang, Z.W., 2016. Iterative Usage of Fixed and Random Effect Models for Powerful and Efficient Genome-Wide Association Studies. Plos Genetics 12.

Liu, Y., Gu, D.D., Wu, W., Wen, X.X., Liao, Y.C., 2013b. The Relationship between Polyamines and Hormones in the Regulation of Wheat Grain Filling. Plos One 8.

Liu, Y., Wang, Q.S., Ding, Y.F., Li, G.H., Xu, J.X., Wang, S.H., 2011. Effects of external ABA, GA(3) and NAA on the tiller bud outgrowth of rice is related to changes in endogenous hormones. Plant Growth Regulation 65, 247-254.

Lo Valvo, P.J., Miralles, D.J., Serrago, R.A., 2018. Genetic progress in Argentine bread wheat varieties released between 1918 and 2011: Changes in physiological and numerical yield components. Field Crops Research 221, 314-321.

Lopes, M.S., Dreisigacker, S., Pena, R.J., Sukumaran, S., Reynolds, M.P., 2015. Genetic characterization of the wheat association mapping initiative (WAMI) panel for dissection of complex traits in spring wheat. Theoretical and Applied Genetics 128, 453-464.

Lopez-Cruz, M., Crossa, J., Bonnett, D., Dreisigacker, S., Poland, J., Jannink, J.L., Singh, R.P., Autrique, E., de los Campos, G., 2015. Increased Prediction Accuracy in Wheat Breeding Trials Using a Marker x Environment Interaction Genomic Selection Model. G3-Genes Genomes Genetics 5, 569-582.

Lorenz, A.J., Smith, K.P., 2015. Adding Genetically Distant Individuals to Training Populations Reduces Genomic Prediction Accuracy in Barley. Crop Science 55, 2657-2667.

Lovelock, D.A., Sola, I., Marschollek, S., Donald, C.E., Rusak, G., van Pee, K.H., Ludwig-Muller, J., Cahill, D.M., 2016. Analysis of salicylic acid-dependent pathways in *Arabidopsis thaliana* following infection with Plasmodiophora brassicae and the influence of salicylic acid on disease. Molecular Plant Pathology 17, 1237-1251.

Lozada, D.N., Mason, R.E., Babar, M.A., Carver, B.F., Guedira, G.B., Merrill, K., Arguello, M.N., Acuna, A., Vieira, L., Holder, A., Addison, C., Moon, D.E., Miller, R.G., Dreisigacker, S., 2017. Association mapping reveals loci associated with multiple traits that affect grain yield and adaptation in soft winter wheat. Euphytica 213.

Lu, J., Chang, C., Zhang, H.P., Wang, S.X., Sun, G.L., Xiao, S.H., Ma, C.X., 2015. Identification of a Novel Allele of TaCKX6a02 Associated with Grain Size, Filling Rate and Weight of Common Wheat. Plos One 10.

Lê, S., Josse, J., Husson, F., 2008. FactoMineR: An R Package for Multivariate Analysis. Journal of Statistical Software **25**, 1-18.

Mackay, I., Horwell, A., Garner, J., White, J., McKee, J., Philpott, H., 2011. Reanalyses of the historical series of UK variety trials to quantify the contributions of genetic and environmental factors to trends and variability in yield over time. Theoretical and Applied Genetics 122, 225-238.

Macmillan, J., Takahashi, N., 1968. Proposed Procedure for the Allocation of Trivial Names to the Gibberellins. Nature 217, 170-171.

Marciniak, K., Przedniczek, K., 2019. Comprehensive Insight into Gibberellin- and Jasmonate-Mediated Stamen Development. Genes 10.

McCarty, D.R., 1995. Genetic-control and integration of maturation and germination pathways in seed development Annual Review of Plant Physiology and Plant Molecular Biology 46, 71-93.

McWha, J.A., 1975. Changes in abscisic-acid levels in developing grains of wheat (Triticum-aestivum-L). Journal of Experimental Botany 26, 823-827.

Millet, E., 1986. Relationships between floret size and grain weight in aneuploid lines of homoeologous group-5 chromosomes of common wheat (*Triticum aestivum* L.) cv. Chinese Spring. Canadian Journal of Genetics and Cytology 28, 497-501.

Minchin, P.E.H., Thorpe, M.R., Farrar, J.F., 1993. A simple mechanistic model of phloem transport which explains skin priority Journal of Experimental Botany 44, 947-955.

Mirabella, N.E., Abbate, P.E., Ramirez, I.A., Pontaroli, A.C., 2016. Genetic variation for wheat spike fertility in cultivars and early breeding materials. Journal of Agricultural Science 154, 13-22.

Miralles, D.J., Richards, R.A., Slafer, G.A., 2000. Duration of the stem elongation period influences the number of fertile florets in wheat and barley. Australian Journal of Plant Physiology 27, 931-940.

Miralles, D.J., Slafer, G.A., 1997. Radiation interception and radiation use efficiency of near-isogenic wheat lines with different height. Euphytica 97, 201-208.

Miralles, D.J., Slafer, G.A., 2007. Sink limitations to yield in wheat: how could it be reduced? Journal of Agricultural Science 145, 139-149.

Molero, G., Joynson, R., Pinera-Chavez, F.J., Gardiner, L.J., Rivera-Amado, C., Hall, A., Reynolds, M.P., 2019. Elucidating the genetic basis of biomass accumulation and radiation use efficiency in spring wheat and its role in yield potential. Plant Biotechnology Journal 17, 1276-1288.

Muqaddasi, Q.H., Brassac, J., Koppolu, R., Plieske, J., Ganal, M.W., Roder, M.S., 2019. TaAPO-A1, an ortholog of rice ABERRANT PANICLE ORGANIZATION 1, is associated with total spikelet number per spike in elite European hexaploid winter wheat (*Triticum aestivum* L.) varieties. Scientific Reports 9.

Müller, M., Munné-Bosch, S., 2011. Rapid and sensitive hormonal profiling of complex plant samples by liquid chromatography coupled to electrospray ionization tandem mass spectrometry. Plant Methods 7, 37.

Nadeem, M.A., Nawaz, M.A., Shahid, M.Q., Dogan, Y., Comertpay, G., Yildiz, M., Hatipoglu, R., Ahmad, F., Alsaleh, A., Labhane, N., Ozkan, H., Chung, G.W., Baloch, F.S., 2018. DNA molecular markers in plant breeding: current status and recent advancements in genomic selection and genome editing. Biotechnology & Biotechnological Equipment 32, 261-285.

Nakajima, M., Yamaguchi, I., Kizawa, S., Murofushi, N., Takahashi, N., 1991. Semi-quantification of GA1 and GA4 in male-sterile anthers of rice by radioimmunoassay. Plant and Cell Physiology 32, 511-513.

Nambara, E., Marion-Poll, A., 2005. Abscisic acid biosynthesis and catabolism. Annual Review of Plant Biology 56, 165-185.

Naylor, A.W., 1984. Functions of Hormones at the Organ Level of Organization. In: Scott, T.K. (Ed.), Hormonal Regulation of Development II: The Functions of Hormones from the Level of the Cell to the Whole Plant. Springer Berlin Heidelberg, Berlin, Heidelberg, pp. 172-218.

Neumann, K., Kobiljski, B., Dencic, S., Varshney, R.K., Borner, A., 2011. Genome-wide association mapping: a case study in bread wheat (*Triticum aestivum* L.). Molecular Breeding 27, 37-58.

Nordstrom, A., Tarkowski, P., Tarkowska, D., Norbaek, R., Astot, C., Dolezal, K., Sandberg, G., 2004. Auxin regulation of cytokinin biosynthesis in *Arabidopsis thaliana*: A factor of potential importance for auxin-cytokinin-regulated development. Proceedings of the National Academy of Sciences of the United States of America 101, 8039-8044.

Ober, E.S., Setter, T.L., Madison, J.T., Thompson, J.F., Shapiro, P.S., 1991. Influence of water deficit on maize endosperm development - Enzyme-activities and RNA transcripts of starch and zein synthesis, abscisic-acid and cell-division. Plant Physiology 97, 154-164.

Okada, K., Ueda, J., Komaki, M.K., Bell, C.J., Shimura, Y., 1991. Requirement of the auxin polar transport-system in early stages of *Arabidopsis* floral bud formation. Plant Cell 3, 677-684.

Parker, C.W., Badenochjones, J., Letham, D.S., 1989. Radioimmunoassay for quantifying the cytokinins *cis*-zeatin and *cis*-zeatin ziboside and its applications to xylem sap samples. Journal of Plant Growth Regulation 8, 93-105.

Pask, A., Pietragalla, J., Mullan, D., Reynolds, M., 2012. Physiological breeding II: A field guide to wheat phenotyping, CIMMYT, Mexico.

Pei, Z.M., Ghassemian, M., Kwak, C.M., McCourt, P., Schroeder, J.I., 1998. Role of farnesyltransferase in ABA regulation of guard cell anion channels and plant water loss. Science 282, 287-290.

Peltonen-Sainio, P., Kangas, A., Salo, Y., Jauhiainen, L., 2007. Grain number dominates grain weight in temperate cereal yield determination: Evidence based on 30 years of multi-location trials. Field Crops Research 100, 179-188.

Peng, Y.J., Yang, J.F., Li, X., Zhang, Y.L., 2021. Salicylic Acid: Biosynthesis and Signaling. In: Merchant, S.S. (Ed.), Annual Review of Plant Biology, Vol 72, 2021, pp. 761-791.

Phinney, B.O., West, C.A., Ritzel, M., Neely, P.M., 1957. Evidence for gibberellin-like substances from flowering plants. Proceedings of the National Academy of Sciences of the United States of America 43, 398-404.

Picciarelli, P., Ceccarelli, N., Paolicchi, F., Calistri, G., 2001. Endogenous auxins and embryogenesis in Phaseolus coccineus. Australian Journal of Plant Physiology 28, 73-78.

Pigolev, A., Miroshnichenko, D., Dolgov, S., Savchenko, T., 2021. Regulation of Sixth Seminal Root Formation by Jasmonate in *Triticum aestivum* L. Plants-Basel 10.

Pinera-Chavez, F.J., Berry, P.M., Foulkes, M.J., Jesson, M.A., Reynolds, M.P., 2016a. Avoiding lodging in irrigated spring wheat. I. Stem and root structural requirements. Field Crops Research 196, 325-336.

Pinera-Chavez, F.J., Berry, P.M., Foulkes, M.J., Molero, G., Reynolds, M.P., 2016b. Avoiding lodging in irrigated spring wheat. II. Genetic variation of stem and root structural properties. Field Crops Research 196, 64-74.

Pretini, N., Vanzetti, L.S., Terrile, II, Borner, A., Plieske, J., Ganal, M., Roder, M., Gonzalez, F.G., 2020. Identification and validation of QTL for spike fertile floret and fruiting efficiencies in hexaploid wheat (*Triticum aestivum* L.). Theoretical and Applied Genetics 133, 2655-2671.

Pritchard, J.K., Stephens, M., Donnelly, P., 2000. Inference of population structure using multilocus genotype data. Genetics 155, 945-959.

Python Core Team, 2020. Python: A dynamic, open source programming language. Python Software Foundation. Available online: https://www.python.org/ [Accessed 21/08/2021].

Qin, F.F., Du, F.L., Xu, R.Y., Xu, Q.C., Tian, C.M., Li, F.M., Wang, F.H., 2009. Photosynthesis in different parts of a wheat plant. Journal of Food Agriculture & Environment 7, 399-404.

Qiu, X., Xu, Y.H., Xiong, B., Dai, L., Huang, S.J., Dong, T.T., Sun, G.C., Liao, L., Deng, Q.X., Wang, X., Zhu, J., Wang, Z.H., 2020. Effects of exogenous methyl jasmonate on the synthesis of endogenous jasmonates and the regulation of photosynthesis in citrus. Physiologia Plantarum 170, 398-414.

Quarrie, S.A., Quarrie, S.P., Radosevic, R., Rancic, D., Kaminska, A., Barnes, J.D., Leverington, M., Ceoloni, C., Dodig, D., 2006. Dissecting a wheat QTL for yield present in a range of environments: from the QTL to candidate genes. Journal of Experimental Botany 57, 2627-2637.

R Core Team, 2020. A language and environment for statistical computing. R Foundation for Statistical Computing. R Foundation for Statistical Computing Vienna, Austria. Available online: https://www.R-project.org/ [Accessed 23/08/2021].

Rashad, R.T., 2020. Effect of Soaking Seeds in Some Growth Regulators on Wheat Grown in Sandy Soil. Egyptian Journal of Soil Science 60, 99-108.

Rasheed, A., Xia, X.C., Mahmood, T., Quraishi, U.M., Aziz, A., Bux, H., Mahmood, Z., Mirza, J.I., Mujeeb-Kazi, A., He, Z.H., 2016. Comparison of Economically

Important Loci in Landraces and Improved Wheat Cultivars from Pakistan. Crop Science 56, 287-301.

Rasmussen, R.D., Hole, D., Hess, J.R., Carman, J.G., 1997. Wheat kernel dormancy and plus abscisic acid level following exposure to fluridone. Journal of Plant Physiology 150, 440-445.

Reale, L., Rosati, A., Tedeschini, E., Ferri, V., Cerri, M., Ghitarrini, S., Timorato, V., Ayano, B.E., Porfiri, O., Frenguelli, G., Ferranti, F., Benincasa, P., 2017. Ovary Size in Wheat (*Triticum aestivum* L.) is Related to Cell Number. Crop Science 57, 914-925.

Reynolds, M., Atkin, O.K., Bennett, M., Cooper, M., Dodd, I.C., Foulkes, M.J., Frohberg, C., Hammer, G., Henderson, I.R., Huang, B.R., Korzun, V., McCouch, S.R., Messina, C.D., Pogson, B.J., Slafer, G.A., Taylor, N.L., Wittich, P.E., 2021. Feature Review Addressing Research Bottlenecks to Crop Productivity. Trends in Plant Science 26, 607-630.

Reynolds, M., Dreccer, F., Trethowan, R., 2007. Drought-adaptive traits derived from wheat wild relatives and landraces. Journal of Experimental Botany 58, 177-186.

Reynolds, M., Foulkes, J., Furbank, R., Griffiths, S., King, J., Murchie, E., Parry, M., Slafer, G., 2012. Achieving yield gains in wheat. Plant Cell and Environment 35, 1799-1823.

Reynolds, M., Foulkes, M.J., Slafer, G.A., Berry, P., Parry, M.A.J., Snape, J.W., Angus, W.J., 2009. Raising yield potential in wheat. Journal of Experimental Botany 60, 1899-1918.

Reynolds, M.P., Delgado, M.I., Gutierrez-Rodriguez, M., Larque-Saavedra, A., 2000. Photosynthesis of wheat in a warm, irrigated environment - I: Genetic diversity and crop productivity. Field Crops Research 66, 37-50.

Reynolds, M.P., Pask, A.J.D., Hoppitt, W.J.E., Sonder, K., Sukumaran, S., Molero, G., Joshi, A.K., 2017. Strategic crossing of biomass and harvest index-source and sink-achieves genetic gains in wheat. Euphytica 213.

Reynolds, M.P., Pellegrineschi, A., Skovmand, B., 2005. Sink-limitation to yield and biomass: a summary of some investigations in spring wheat. Annals of Applied Biology 146, 39-49.

Richards, R.A., 1992. The effect of dwarfing genes in spring wheat in dry environments. 1 Agronomic characteristics Australian Journal of Agricultural Research 43, 517-527.

Rivera-Amado, A.C., 2016. Identifying physiological traits to optimize assimilate partitioning and spike fertility for yield potential in wheat (*Triticum aestivum* L.) genotypes.

Rivera-Amado, C., Molero, G., Trujillo-Negrellos, E., Reynolds, M., Foulkes, J., 2020. Estimating Organ Contribution to Grain Filling and Potential for Source Upregulation in Wheat Cultivars with a Contrasting Source-Sink Balance. Agronomy-Basel 10.

Rivera-Amado, C., Trujillo-Negrellos, E., Molero, G., Reynolds, M.P., Sylvester-Bradley, R., Foulkes, M.J., 2019. Optimizing dry-matter partitioning for increased spike growth, grain number and harvest index in spring wheat. Field Crops Research 240, 154-167.

Robertsen, C.D., Hjortshoj, R.L., Janss, L.L., 2019. Genomic Selection in Cereal Breeding. Agronomy 9, 95.

Rodríguez-Gacio, M.d.C., Matilla-Vázquez, M.A., Matilla, A.J., 2009. Seed dormancy and ABA signaling. Plant Signaling & Behavior 4, 1035-1048.

Ruan, J.J., Zhou, Y.X., Zhou, M.L., Yan, J., Khurshid, M., Weng, W.F., Cheng, J.P., Zhang, K.X., 2019. Jasmonic Acid Signaling Pathway in Plants. International Journal of Molecular Sciences 20.

Rustgi, S., Shafqat, M.N., Kumar, N., Baenziger, P.S., Ali, M.L., Dweikat, I., Campbell, B.T., Gill, K.S., 2013. Genetic Dissection of Yield and Its Component Traits Using High-Density Composite Map of Wheat Chromosome 3A: Bridging Gaps between QTLs and Underlying Genes. Plos One 8.

Ruzicka, K., Simaskova, M., Duclercq, J., Petrasek, J., Zazimalova, E., Simon, S., Friml, J., Van Montagu, M.C.E., Benkova, E., 2009. Cytokinin regulates root meristem activity via modulation of the polar auxin transport. Proceedings of the National Academy of Sciences of the United States of America 106, 4284-4289.

Sadras, V.O., Lawson, C., 2011. Genetic gain in yield and associated changes in phenotype, trait plasticity and competitive ability of South Australian wheat varieties released between 1958 and 2007. Crop & Pasture Science 62, 533-549.

Sahu, G.K., Kar, M., Sabat, S.C., 2002. Electron transport activities of isolated thylakoids from wheat plants grown in salicylic acid. Plant Biology 4, 321-328.

Sakuma, S., Golan, G., Guo, Z.F., Ogawa, T., Tagiri, A., Sugimoto, K., Bernhardt, N., Brassac, J., Mascher, M., Hensel, G., Ohnishi, S., Jinno, H., Yamashita, Y., Ayalon, I., Peleg, Z., Schnurbusch, T., Komatsuda, T., 2019. Unleashing floret fertility in wheat through the mutation of a homeobox gene. Proceedings of the National Academy of Sciences of the United States of America 116, 5182-5187.

Sayre, K., Hobbs, P., 2004. The Raised-Bed System of Cultivation for Irrigated Production Conditions. pp. 337-355.

Sayre, K.D., Rajaram, S., Fischer, R.A., 1997. Yield potential progress in short bread wheats in northwest Mexico. Crop Science 37, 36-42.

Schafer, M., Brutting, C., Meza-Canales, I.D., Grosskinsky, D.K., Vankova, R., Baldwin, I.T., Meldau, S., 2015. The role of *cis*-zeatin-type cytokinins in plant growth regulation and mediating responses to environmental interactions. Journal of Experimental Botany 66, 4873-4884.

Schmitz, R.Y., Skoog, F., Playtis, A.J., Leonard, N.J., 1972. Cytokinins - Synthesis and biological-activity of geometric and position isomers of zeatin. Plant Physiology 50, 702-705.

Sedaghat, M., Tahmasebi-Sarvestani, Z., Emam, Y., Mokhtassi-Bidgoli, A., 2017. Physiological and antioxidant responses of winter wheat cultivars to strigolactone and salicylic acid in drought. Plant Physiology and Biochemistry 119, 59-69.

Sehgal, D., Mondal, S., Crespo-Herrera, L., Velu, G., Juliana, P., Huerta-Espino, J., Shrestha, S., Poland, J., Singh, R., Dreisigacker, S., 2020. Haplotype-Based, Genome-Wide Association Study Reveals Stable Genomic Regions for Grain Yield in CIMMYT Spring Bread Wheat. Frontiers in Genetics 11.

Sehgal, D., Singh, R., Rajpal, V.R., 2016. Quantitative Trait Loci Mapping in Plants: Concepts and Approaches. Molecular Breeding for Sustainable Crop Improvement, Vol 2 11, 31-59.

Serrago, R.A., Miralles, D.J., Slafer, G.A., 2008. Floret fertility in wheat as affected by photoperiod during stem elongation and removal of spikelets at booting. European Journal of Agronomy 28, 301-308.

Shakirova, F.M., Sakhabutdinova, A.R., Bezrukova, M.V., Fatkhutdinova, R.A., Fatkhutdinova, D.R., 2003. Changes in the hormonal status of wheat seedlings induced by salicylic acid and salinity. Plant Science 164, 317-322.

Sharma, R.C., Crossa, J., Velu, G., Huerta-Espino, J., Vargas, M., Payne, T.S., Singh, R.P., 2012. Genetic Gains for Grain Yield in CIMMYT Spring Bread Wheat across International Environments. Crop Science 52, 1522-1533.

Shearman, V., Sylvester-Bradley, R., Scott, R., Foulkes, M., 2005. Physiological processes associated with wheat yield progress in the UK. Crop Science 45, 175-185.

Shettel, N.L., Balke, N.E., 1983. Plant Growth Response to Several Allelopathic Chemicals. Weed Science 31, 293-298.

Shimizu-Sato, S., Mori, H., 2001. Control of outgrowth and dormancy in axillary buds. Plant Physiology 127, 1405-1413.

Shorinola, O., Kaye, R., Golan, G., Peleg, Z., Kepinski, S., Uauy, C., 2019. Genetic Screening for Mutants with Altered Seminal Root Numbers in Hexaploid Wheat Using a High-Throughput Root Phenotyping Platform. G3-Genes Genomes Genetics 9, 2799-2809.

Sidak, Z., 1967. Rectangular Confidence Regions for the Means of Multivariate Normal Distributions. Journal of the American Statistical Association 62, 626-633.

Siddique, K.H.M., Kirby, E.J.M., Perry, M.W., 1989. Ear: Stem ratio in old and modern wheat varieties; relationship with improvement in number of grains per ear and yield. Field Crops Research 21, 59-78.

Sierra-Gonzalez, A., 2020. Genetic analysis of physiological traits to increase grain partitioning in high biomass cultivars in wheat (*Triticum aestivum L.*).

Sierra-Gonzalez, A., Molero, G., Rivera-Amado, C., Babar, M.A., Reynolds, M.P., Foulkes, M.J., 2021. Exploring genetic diversity for grain partitioning traits to enhance yield in a high biomass spring wheat panel. Field Crops Research 260.

Simaskova, M., O'Brien, J.A., Khan, M., Van Noorden, G., Otvos, K., Vieten, A., De Clercq, I., Van Haperen, J.M.A., Cuesta, C., Hoyerova, K., Vanneste, S., Marhavy, P., Wabnik, K., Van Breusegem, F., Nowack, M., Murphy, A., Friml, J., Weijers, D., Beeckman, T., Benkova, E., 2015. Cytokinin response factors regulate PIN-FORMED auxin transporters. Nature Communications 6.

Sitbon, F., Hennion, S., Sundberg, B., Little, C.H.A., Olsson, O., Sandberg, G., 1992. Transgenic tobacco plants coexpressing the agrobacterium tumefaciens iaaM and iaaH genes display altered growth and indoleacetic-acid metabolism Plant Physiology 99, 1062-1069.

Slafer, G.A., Andrade, F.H., 1993. Physiological attributes related to the generation of grain-yield in bread wheat cultivars released at different eras. Field Crops Research 31, 351-367.

Slafer, G.A., Andrade, F.H., Satorre, E.H., 1990. Genetic-improvement effects on pre-anthesis physiological attributes related to wheat grain-yield. Field Crops Research 23, 255-263.

Slafer, G.A., Elia, M., Savin, R., Garcia, G.A., Terrile, II, Ferrante, A., Miralles, D.J., Gonzalez, F.G., 2015. Fruiting efficiency: an alternative trait to further rise wheat yield. Food and Energy Security 4, 92-109.

Slafer, G.A., Rawson, H.M., 1994. Sensitivity of wheat phasic development to major environmental factors - A re-examination of some assumptions made by physiologists and modelers Australian Journal of Plant Physiology 21, 393-426.

Slafer, G.A., Savin, R., 1994. Source-sink relationships and grain mass at different positions within the spike in wheat. Field Crops Research 37, 39-49.

Song, Q.F., Zhang, G.L., Zhu, X.G., 2013. Optimal crop canopy architecture to maximise canopy photosynthetic CO2 uptake under elevated CO2 - a theoretical study using a mechanistic model of canopy photosynthesis. Functional Plant Biology 40, 109-124.

Soto-Cerda, B.J., Cloutier, S., 2012. Association Mapping in Plant Genomes. Genetic Diversity in Plants, 29-54.

Spichal, L., 2012. Cytokinins - recent news and views of evolutionally old molecules. Functional Plant Biology 39, 267-284.

Sreenivasulu, N., Schnurbusch, T., 2012. A genetic playground for enhancing grain number in cereals. Trends in Plant Science 17, 91-101.

Stowe, B.B., Yamaki, T., 1957. The history and physiological action of the gibberellins. Annual Review of Plant Physiology and Plant Molecular Biology 8, 181-216.

Sukhikh, I.S., Vavilova, V.J., Blinov, A.G., Goncharov, N.P., 2021. Diversity and Phenotypical Effect of Allelic Variants of *Rht* Dwarfing Genes in Wheat. Russian Journal of Genetics 57, 127-138.

Suzuki, M., Kao, C.Y., Cocciolone, S., McCarty, D.R., 2001. Maize VP1 complements *Arabidopsis* abi3 and confers a novel ABA/auxin interaction in roots. Plant Journal 28, 409-418.

Suzuki, Y., Kurogochi, S., Murofushi, N., Ota, Y., Takahashi, N., 1981. Seasonal Changes of GA1, GA19 and Abscisic Acid in Three Rice Cultivars. Plant and Cell Physiology 22, 1085-1093.

Tang, Y., Horikoshi, M., Li, W.X., 2016. ggfortify: Unified Interface to Visualize Statistical Results of Popular R Packages. R Journal 8, 474-485.

Tang, Y.L., Wu, X.L., Li, C.S., Yang, W.Y., Huang, M.B., Ma, X.L., Li, S.Z., 2017. Yield, growth, canopy traits and photosynthesis in high-yielding, synthetic hexaploid-derived wheats cultivars compared with non-synthetic wheats. Crop & Pasture Science 68, 115-125.

Tanimoto, E., 2012. Tall or short? Slender or thick? A plant strategy for regulating elongation growth of roots by low concentrations of gibberellin. Annals of botany 110, 373-381.

Terrile, II, Miralles, D.J., Gonzalez, F.G., 2017. Fruiting efficiency in wheat (Triticum aestivum L): Trait response to different growing conditions and its relation to spike dry weight at anthesis and grain weight at harvest. Field Crops Research 201, 86-96.

Travaglia, C., Reinoso, H., Cohen, A., Luna, C., Tommasino, E., Castillo, C., Bottini, R., 2010. Exogenous ABA Increases Yield in Field-Grown Wheat with Moderate Water Restriction. Journal of Plant Growth Regulation 29, 366-374.

Uzunova, A.N., Popova, L.P., 2000. Effect of salicylic acid on leaf anatomy and chloroplast ultrastructure of barley plants. Photosynthetica 38, 243-250.

Van de Velde, K., Thomas, S.G., Heyse, F., Kaspar, R., Van Der Straeten, D., Rohde, A., 2021. N-terminal truncated RHT-1 proteins generated by translational reinitiation cause semi-dwarfing of wheat Green Revolution alleles. Molecular Plant 14, 679-687.

VSN International, 2021. GenStat for Windows 21st Edition. VSN International, Hemel Hempstead, UK. Available at: https://vsni.co.uk/software/genstat [Accessed 18/09/2021].

Vysotskaya, L., Akhiyarova, G., Feoktistova, A., Akhtyamova, Z., Korobova, A., Ivanov, I., Dodd, I., Kuluev, B., Kudoyarova, G., 2020. Effects of Phosphate Shortage on Root Growth and Hormone Content of Barley Depend on Capacity of the Roots to Accumulate ABA. Plants 9, 1722.

Waddington, S.R., Cartwright, P.M., Wall, P.C., 1983. A quantitative scale of spike initial and pistil development in barley and wheat. Annals of Botany 51, 119-130.

Waldie, T., Leyser, O., 2018. Cytokinin Targets Auxin Transport to Promote Shoot Branching. Plant Physiology 177, 803-818.

Walker-Simmons, M., Sesing, J., 1990. Temperature effects on embryonic abscisic-acid levels during development of wheat-grain dormancy. Journal of Plant Growth Regulation 9, 51-56.

Walkowiak, S., Gao, L.L., Monat, C., Haberer, G., Kassa, M.T., Brinton, J., Ramirez-Gonzalez, R.H., Kolodziej, M.C., Delorean, E., Thambugala, D., Klymiuk, V., Byrns, B., Gundlach, H., Bandi, V., Siri, J.N., Nilsen, K., Aquino, C., Himmelbach, A., Copetti, D., Ban, T., Venturini, L., Bevan, M., Clavijo, B., Koo, D.H., Ens, J., Wiebe, K., N'Diaye, A., Fritz, A.K., Gutwin, C., Fiebig, A., Fosker, C., Fu, B.X., Accinelli, G.G., Gardner, K.A., Fradgley, N., Gutierrez-Gonzalez, J., Halstead-Nussloch, G., Hatakeyama, M., Koh, C.S., Deek, J., Costamagna, A.C., Fobert, P., Heavens, D., Kanamori, H., Kawaura, K., Kobayashi, F., Krasileva, K., Kuo, T., McKenzie, N., Murata, K., Nabeka, Y., Paape, T., Padmarasu, S., Percival-Alwyn, L., Kagale, S., Scholz, U., Sese, J., Juliana, P., Singh, R., Shimizu-Inatsugi,

R., Swarbreck, D., Cockram, J., Budak, H., Tameshige, T., Tanaka, T., Tsuji, H., Wright, J., Wu, J.Z., Steuernagel, B., Small, I., Cloutier, S., Keeble-Gagnere, G., Muehlbauer, G., Tibbets, J., Nasuda, S., Melonek, J., Hucl, P.J., Sharpe, A.G., Clark, M., Legg, E., Bharti, A., Langridge, P., Hall, A., Uauy, C., Mascher, M., Krattinger, S.G., Handa, H., Shimizu, K.K., Distelfeld, A., Chalmers, K., Keller, B., Mayer, K.F.X., Poland, J., Stein, N., McCartney, C.A., Spannagl, M., Wicker, T., Pozniak, C.J., 2020. Multiple wheat genomes reveal global variation in modern breeding. Nature 588, 277-283.

Wang, J., Sun, J.H., Miao, J., Guo, J.K., Shi, Z.L., He, M.Q., Chen, Y., Zhao, X.Q., Li, B., Han, F.P., Tong, Y.P., Li, Z.S., 2013. A phosphate starvation response regulator Ta-PHR1 is involved in phosphate signalling and increases grain yield in wheat. Annals of Botany 111, 1139-1153.

Wang, J., Zhang, Z., 2021. GAPIT Version 3: Boosting Power and Accuracy for Genomic Association and Prediction. Genomics, Proteomics & Bioinformatics.

Wang, S.C., Wong, D.B., Forrest, K., Allen, A., Chao, S.M., Huang, B.E., Maccaferri, M., Salvi, S., Milner, S.G., Cattivelli, L., Mastrangelo, A.M., Whan, A., Stephen, S., Barker, G., Wieseke, R., Plieske, J., Lillemo, M., Mather, D., Appels, R., Dolferus, R., Brown-Guedira, G., Korol, A., Akhunova, A.R., Feuillet, C., Salse, J., Morgante, M., Pozniak, C., Luo, M.C., Dvorak, J., Morell, M., Dubcovsky, J., Ganal, M., Tuberosa, R., Lawley, C., Mikoulitch, I., Cavanagh, C., Edwards, K.J., Hayden, M., Akhunov, E., Int Wheat Genome, S., 2014. Characterization of polyploid wheat genomic diversity using a high-density 90 000 single nucleotide polymorphism array. Plant Biotechnology Journal 12, 787-796.

Wang, Z.L., Cao, W.X., Dai, T.B., Zhou, Q., 2001. Effects of exogenous hormones on floret development and grain set in wheat. Plant Growth Regulation 35, 225-231.

Wang, Z.L., Mambelli, S., Setter, T.L., 2002. Abscisic acid catabolism in maize kernels in response to water deficit at early endosperm development. Annals of Botany 90, 623-630.

Wasternack, C., Hause, B., 2013. Jasmonates: biosynthesis, perception, signal transduction and action in plant stress response, growth and development. An update to the 2007 review in Annals of Botany. Annals of Botany 111, 1021-1058.

Wickham, H., 2016. ggplot2: Elegant Graphics for Data Analysis. Springer-Verlag, New York.

Wilen, R.W., Ewan, B.E., Gusta, L.V., 1994. Interaction of abscisic-acid and jasmonic acid on the inhibition of seed-germination and the induction of freezing tolerance. Canadian Journal of Botany-Revue Canadienne De Botanique 72, 1009-1017.

Wilkinson, S., Kudoyarova, G.R., Veselov, D.S., Arkhipova, T.N., Davies, W.J., 2012. Plant hormone interactions: innovative targets for crop breeding and management. Journal of Experimental Botany 63, 3499-3509.

Williams, R.H., Cartwright, P.M., 1980. The effect of applications of a synthetic cytokinin on shoot dominance and grain-yield in spring barley. Annals of Botany 46, 445-452.

Winfield, M.O., Allen, A.M., Burridge, A.J., Barker, G.L.A., Benbow, H.R., Wilkinson, P.A., Coghill, J., Waterfall, C., Davassi, A., Scopes, G., Pirani, A., Webster, T., Brew, F., Bloor, C., King, J., West, C., Griffiths, S., King, I., Bentley, A.R., Edwards, K.J., 2016. High-density SNP genotyping array for hexaploid wheat and its secondary and tertiary gene pool. Plant Biotechnology Journal 14, 1195-1206.

Wingen, L.U., Orford, S., Goram, R., Leverington-Waite, M., Bilham, L., Patsiou, T.S., Ambrose, M., Dicks, J., Griffiths, S., 2014. Establishing the A. E. Watkins landrace cultivar collection as a resource for systematic gene discovery in bread wheat. Theoretical and Applied Genetics 127, 1831-1842.

Wrigley, C.W., Batey, I.L., 2012. 7 - Assessing grain quality. In: Cauvain, S.P. (Ed.), Breadmaking (Second Edition). Woodhead Publishing, pp. 149-187.

Xu, H.C., Cai, T., Wang, Z.L., He, M.R., 2015. Physiological basis for the differences of productive capacity among tillers in winter wheat. Journal of Integrative Agriculture 14, 1958-1970.

Xu, Q., Truong, T.T., Barrero, J.M., Jacobsen, J.V., Hocart, C.H., Gubler, F., 2016. A role for jasmonates in the release of dormancy by cold stratification in wheat. Journal of Experimental Botany 67, 3497-3508.

Xue, Q.W., Soundararajan, M., Weiss, A., Arkebauer, T.J., Baenziger, P.S., 2002. Genotypic variation of gas exchange parameters and carbon isotope discrimination in winter wheat. Journal of Plant Physiology 159, 891-898.

Yang, J.C., Peng, S.B., Visperas, R.M., Sanico, A.L., Zhu, Q.S., Gu, S.L., 2000. Grain filling pattern and cytokinin content in the grains and roots of rice plants. Plant Growth Regulation 30, 261-270.

Yildirim, M., Koc, M., Akinci, C., Barutcular, C., 2013. Variations in morphological and physiological traits of bread wheat diallel crosses under timely and late sowing conditions. Field Crops Research 140, 9-17.

Youssef, H.M., Eggert, K., Kopplu, R., Alqudah, A.M., Poursarebani, N., Fazeli, A., Sakuma, S., Tagiri, A., Rutten, T., Govind, G., Lundqvist, U., Graner, A., Komatsuda, T., Sreenivasulu, N., Schnurbusch, T., 2017. VRS2 regulates hormone-mediated inflorescence patterning in barley. Nature Genetics 49, 157-161.

Zadoks, J.C., Chang, T.T., Konzak, C.F., 1974. Decimal code for growth stages of cereals. Weed Research 14, 415-421.

Zeng, Z.R., Morgan, J.M., King, R.W., 1985. Regulation of grain number in wheat - genotype difference and responses to applied abscisic-acid and to high-temperature. Australian Journal of Plant Physiology 12, 609-619.

Zhang, D.B., Yuan, Z., 2014. Molecular Control of Grass Inflorescence Development. Annual Review of Plant Biology, Vol 65 65, 553-+.

Zhang, J.P., Liu, W.H., Yang, X.M., Gao, A.N., Li, X.Q., Wu, X.Y., Li, L.H., 2011. Isolation and characterization of two putative cytokinin oxidase genes related to grain number per spike phenotype in wheat. Molecular Biology Reports 38, 2337-2347.

Zhang, L., Zhao, Y.L., Gao, L.F., Zhao, G.Y., Zhou, R.H., Zhang, B.S., Jia, J.Z., 2012. TaCKX6-D1, the ortholog of rice OsCKX2, is associated with grain weight in hexaploid wheat. New Phytologist 195, 574-584.

Zhang, X., Wang, T., Li, C., 2005. Different responses of two contrasting wheat genotypes to abscisic acid application. Biologia Plantarum 49, 613-616.

Zheng, C.F., Zhu, Y.J., Wang, C.Y., Guo, T.C., 2016. Wheat Grain Yield Increase in Response to Pre-Anthesis Foliar Application of 6-Benzylaminopurine Is Dependent on Floret Development. Plos One 11.